Università degli Studi della Calabria

Facoltà di Farmacia e Scienze della Nutrizione e della Salute
Dipartimento Farmaco-Biologico (MED/04 PATOLOGIA GENERALE)

Dottorato di Ricerca in "Biochimica Cellulare ed Attività dei Farmaci in Oncologia" (XIX ciclo)

ERα reduces breast cancer cells motility upon cell adhesion on Fibronectin and Collagen IV and regulates α5β1 integrin expression

Docente Tutor
Ch.mo Prof. Diego SISCI

Coordinatore
Ch.mo Prof. Sebastiano ANDO'

Dottoranda
D.ssa Emilia MIDDEA
Emilia Middea

Anno Accademico 2005-2006

INDEX

Summary

The expression of estrogen receptor alpha (ERα) is generally associated with a less invasive and aggressive phenotype in breast carcinoma. In an attempt to understand the role of ERα in regulating breast cancer cells invasiveness, we have demonstrated that cell adhesion on Fibronectin (Fn) and type IV Collagen (Col) induces ERα-mediated transcription and reduces cell migration in MCF-7 and in MDA-MB-231 cell lines expressing ERα. Analysis of deleted mutants of ERα indicates that the transcriptional activation function (AF)-1 is required for ERα-mediated transcription as well as for the inhibition of cell migration induced by cell adhesion on extracellular matrix (ECM) proteins. In addition, the nuclear localization signal region and some serine residues in the AF-1 of the ERα are required for the regulation of cell invasiveness as we have observed in HeLa cells. It is worth noting that c-Src activation is coincident with adhesion of cells to ECM proteins and that the inhibition of c-Src activity by PP2 or the expression of a dominant-negative c-Src abolishes ERα-mediated transcription and partially reverts the inhibition of cell invasiveness in ERα-positive cancer cells. These findings address the integrated role of ECM proteins and ERα in influencing breast cancer cell motility through a mechanism that involves c-Src and it seems not to be related to a specific cell type.

Furthermore, to explain the mechanisms by which ERα regulates cell adhesion, we have evaluated the expression of α5β1 integrin, prevalently expressed in stationary cells, in response to 17β-estradiol (E2). Here we show that E2 increases the expression of integrin α5β1 through ERα, which interacts with the regulatory region of α5 gene. We evidenced an enhanced binding of Sp1 protein to a GC-rich Sp1 region located

upstream to an ERE half-site in the 5'-flanking region of the *α5* gene. Estrogen responsiveness of *α5* gene promoter defines a general mechanism of regulation not strictly linked to the cell type, as we observed in HeLa cells. Our data provides fundamental insight into the molecular mechanisms underlying the negative modulation of the invasive process in ERα positive cancer cells.

Introduction

Several clinical studies have demonstrated that estrogen receptor alpha (ERα)-positive tumors have lower metastatic potential than ERα-negative tumors (Fraker et al., 1984; Osborne et al., 1985; McGuire, 1986; Price et al., 1990). Many reports correlate ERα expression to lower matrigel invasiveness and to a reduced metastatic potential of breast cancer cell lines (Liotta et al., 1991; Thompson et al., 1992; Rochefort et al., 1998); however, the molecular mechanisms that define this process are still unclear. The interaction of cells with the extracellular matrix (ECM) influences many aspects of cell behavior, including growth, morphology, migratory properties and differentiation (Hynes, 1990; Clark and Brugge, 1995; Giancotti and Ruoslahti, 1999). The adhesion to ECM is mediated by integrin receptors that are reported to control growth factor signaling pathways. Specifically, cells adherent to ECM show an enhanced activation of the p42 and p44 forms of the mitogen-activated protein kinase (MAPK) (Miyamoto et al., 1996; Lin et al., 1997; Renshaw et al., 1997; Aplin and Juliano, 1999). In addition, binding of the integrin receptor with ECM proteins causes a direct transient activation of MAP kinase in the absence of growth factors (Chen et al., 1994; Schlaepfer et al., 1994; Zhu and Assoian, 1995). The transcriptional activation function (AF)-1 of the N-terminal ERα is a target of various protein kinases such as MAPK, PI3-k, Akt and c-Src, which are activated by growth factor pathways, either in the presence or in the absence of 17β-estradiol (E2) (Power et al., 1991; Chalbos et al., 1993; Aronica et al., 1994; Kato et al., 1994; Couse et al., 1995; Ignar-Trowbridge et al., 1995; Bunone et al., 1996; Weigel, 1996; Joel et al., 1998). c-Src is also one of the first protein kinases activated by cell adhesion to ECM (Guan, 1997; Schlaepfer et al., 1997; Schaller et al., 1999) and it has been shown to play a significant role in several phases of outside–in

signaling in many cell types (Kaplan et al., 1995; Lowell et al., 1996; Suen et al., 1999). The overexpression and activation of Src family kinases have been identified in a range of human cancers (Irby and Yeatman, 2000) and these have been indicated to contribute not only to the growth and survival of breast cancer cells but also to increase their metastatic potential (Summy and Gallick, 2003). In this study, we have tested the hypothesis that cell adhesion on ECM modulates ERα transcriptional activity, producing a reduction of cell migration. Our results show that estrogen receptor activation function 1 (AF-1)/ERα is an effector of the adhesion protein signals. Cell adhesion on Fibronectin (Fn) and type IV collagen (Col) induces the transcriptional activation of ERα and the reduction of cell migration in MCF-7 cells, as well as in MDA-MB-231 and in HeLa cells both engineered to express ERα. In addition, we have found that c-Src is essential for ERα activation in response to cell adhesion. Focusing on the relationship between c-Src activity and ERα expression in breast cancer cells, we have shown that the transactivation of ERα upon cell adhesion on ECM proteins counteracts the action of c- Src on cell motility and invasiveness in cancerous cells.

On the other hand it has well documented how E2/ERα up-regulates genes which reduce cell invasiveness like α1antichymotrypsin (Confort, C. et al., 1995) and down-regulates genes involved in the enzymatic remodeling and degradation of ECM proteins like metalloproteinase-9 (Crowe, D.L., and Brown, T.N., 1999) and Collagenase type IV (Abbas Abidi, S.M. et al.,1997).

Cell adhesion to ECM is mainly mediated by integrins which mostly control the physical strength of cell substratum attachment (Lynch, L., et al., 2005). Several studies have demonstrated that variations in integrin cell surface expression levels (Keely, P.J. et al., 1995), or in adsorbed concentration of its substratum, or its ligand (DiMilla, P.A.

et al., 1993), or in the integrin-ligand affinity (Huttenlocher, A. et al.,1996), could affect the adhesion strength and a speed of cell movement (Lynch, L., et al., 2005).

A role of E2/ERα on integrin expression rises from physiological circumstances consistent with the evidence that α5β1 increases more than 2 times in breast tissues between puberty and sexual maturity and drops dramatically after ovariectomy (Woodward, T.L. et al., 2001). So, we assume that E2 dependence still producing lesser invasiveness and methastatic potential, may rise by a specific modulatory role of E2 on integrin expression which mostly regulate the adhesion of tumor cells to substrates. Fibronectin (Fn)-mediated attachment and signaling in cells occurs in response to Fn binding to cell surface integrins. Fn has been demonstrated to bind to different Fn specific integrins including α4β1, α5β1, αvβ1 β3, and αvβ6 (Yang, J.T. et al., 1999). However previous studies have shown that α4 subunit is not present in mammary cells (Delcommenne, M., and Streuli, C.H., 1995). Furthermore immunoistochemical analysis revealed little or not αv protein in mammary epithelia and in myoepithelia cells (Woodward, T.L. et al., 2000) at any stage of development examined. Other authors reported that α5 subunit appears to be the key receptor for Fn and α5 knockout mice most closely resemble Fn knockout mice (Yang, J.T. et al., 1999; Watt, F.M., and Hodivala, K.J., 1994). Besides, only the β1 subunit protein has been demonstrated to form an heterodimer with the α5 subunit, so the immunohistochemical detection of α5 subunit, has been reported to mean that the α5β1 integrin was also detected herein.

In the present study we elucidated the molecular mechanism by which E2/ERα signaling up-regulates the expression of α5 integrin subunit either in MCF-7 or HeLa cells ectopically expressing ERα. This event appears to occur through the functional interaction of E2/ERα on Sp1 protein at the site -420/-370 up-stream ATG and very

likely address a general modulatory mechanism induced by E2 not tightly linked to cell type investigated.

Results

Cell adhesion on Fn or Col induces ERα translocation into the nuclear compartment

First, we determined whether cell adhesion on either Fn or Col may infuence ERα expression. MCF-7 cells, serum-starved for 24 h, were plated onto Fn-, Col- and P-Lys- (negative control) coated dishes and incubated for 30 min, 1 h, 4 h and 8 h. Equal amounts of cytosolic and total (nuclear + cytosolic) protein lysates were resolved by SDS–PAGE and analysed by Western blot for ERα detection. Figure 1b shows a significant decrease of ERα content in the cytosol 30 min to 4 h after cell adhesion on Fn and Col with respect to the control reported in Figure 1a. No substantial changes in total ERα content were observed in our time course study (Figure 1b). These results support the conclusion that cell adhesion on either Fn or Col induced a translocation of ERα into the nuclear compartment. The observed compartmentalization of ERα was confirmed by immunocytochemistry using MCF-7 cells maintained in a serum-free medium for 96 h, then detached, plated onto Fn-, Col- and P-Lys-coated slides and incubated for 2 h (Figure 1c). No signal was detected in the control cells (P-Lys); this may be due to the binding of ERα with chaperon proteins that possibly mask the epitope for the ERα antibody

Fn and Col induce estrogen-responsive element (ERE) transcription

Since Fn and Col were able to translocate ERα into the nuclear compartment, we evaluated their ability to induce ERα-mediated transcription. MCF-7 cells were transfected with the ERE responsive reporter plasmid (XETL) and the pRL-Tk plasmid expressing Renilla luciferase, as an internal control. The cells were then serum starved for 24 h and exposed to E2, Fn, Col or P-Lys before luciferase assays. Figure 2a shows

a significant increase in ERE-mediated transcription induced by both Fn and Col in the absence of ER ligand.

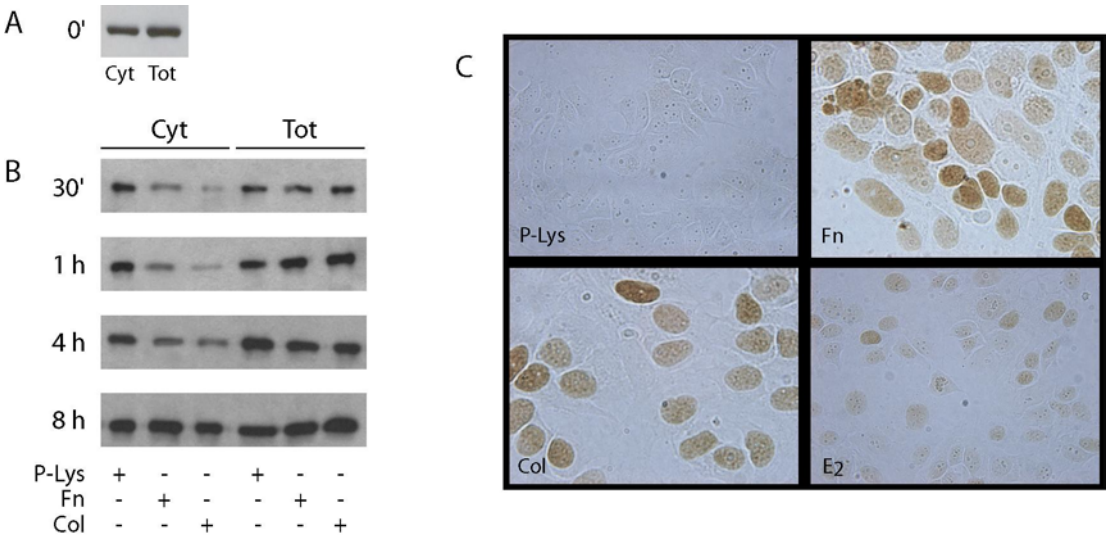

Figure 1. ***Cell adhesion on Fn or Col induces ERα translocation into the nuclear compartment.*** (A) MCF-7 cells serum-starved for 24 h were detached and an aliquot was lysed and used as control (time 0); (B) a further aliquot was plated in PRF-SFM on P-Lys- (2 μg/cm^2), Fn- (30 μg/ml) or Col- (30 μg/ml) coated dishes. After 30 min, 1 h, 4 h and 8 h of incubation, cytosolic (Cyt) and total (cytosolic and nuclear) (Tot) protein lysates were subjected to Western blotting with an anti-ERα monoclonal antibody. These results are representative of five independent experiments. (C) MCF-7 cells serum starved for 96 h were detached and plated in PRF-SFM on PLys- (2 μg/cm^2), Fn- (30 μg/ml) and Col- (30 μg/ml) coated slides or plated on culture-treated slide and incubated with E2 (10 nM). After 2 h, cells were fixed, probed with anti-ERα antibody and stained as described in Materials and methods

In contrast, P-Lys failed to induce ERα-mediated transcription, showing that the observed effect is specifically due to the integrin substrates. The same results were obtained in MDA-MB-231 cells transiently expressing ERα and the reporter gene, suggesting that the Fn/Col-induced transcriptional activation is specifically mediated by ERα (Figure 2c).

A slight but significant increase in luciferase expression was observed in wild-type MDA-MB-231 treated with both Fn and Col (Figure 2b), probably due to the

expression of ERβ (Lazennec et al., 2001), as we detected in the present study (data not shown). The antiestrogen ICI reversed this upregulatory effect induced by both ECM proteins in all the experimental conditions and in both cell lines. In addition, no substantial differences were observed in luciferase expression when transfected MCF-7 and MDA-MB-231 were plated onto both Fn- and Col coated dishes (data not shown).

Figure 2. ***Fn and Col activate ERE-mediated transcription***.
MCF-7 (a) and MDA-MB-231 (b) cells were transfected with 0.3 μg/well of pSG5 and 0.6 μg/well of XETL by calcium phosphate method. MDA-MB-231 were also cotransfected with 0.3 μg/well HeG0 and 0.6 μg/well of XETL (c). Cells were incubated in the transfection cocktail for 6 h, serum starved for an additional 24 h and then incubated for 16 h in PRF-SFM (untreated) or in PRF-SFM containing either 10 nM estradiol (E2), 30 μg/ml Fn, 30 μg/ml Col or 15 μg/ml P-Lys. The same treatments were also carried out in the presence of 100 nM ICI 182,780. Firefly luciferase activity was internally normalized to R. luciferase and expressed as fold of increase with respect to the PRF-SFM (untreated) sample. Results represent the mean ± s.d. of at least five independent experiments. ★ $P< 0.001$ vs PRF-SFM; ■ $P< 0.05$ vs PRF-SFM; ◆◆ $P< 0.001$ vs the homologues samples without ICI 182,780

ERE-mediated transcription induced by Fn and Col upregulates pS2 and cathepsin D mRNA

Owing to their ability to induce ERE-mediated transcription, Fn and Col were assessed for their capacity to regulate the expression of endogenous ERα-specific target genes as pS2 (Figure 3a) and cathepsin D (Figure 3b).

The results show the ability of Fn and Col, but not of P-Lys, to upregulate both pS2 and cathepsin D mRNAs.

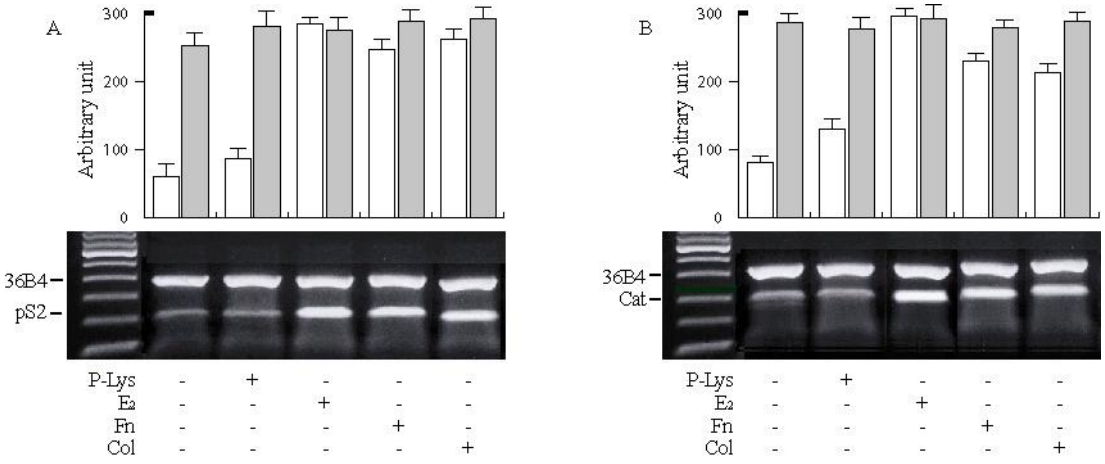

Figure 3. ***Adhesion of breast cancer cells on Fn and Col upregulates pS2 and cathepsin D mRNA levels.*** Semiquantitative RT–PCR of pS2 mRNA (**A**) and cathepsin D (**B**).
Serum-starved MCF-7 cells were detached and plated, in PRF-SFM, on dishes previously coated with 2 μg/cm^2 P-Lys, 30 μg/ml Fn (Fn), 30 μg/ml or plated on uncoated dishes and treated with 10 nM estradiol (E2).
The 36B4 mRNA levels were determined in the same amplification tube as control. The quantitative representation of three independent experiments expressing the optical density of pS2 (□) and 36B4 (▣) RT–PCR products (a) and of cathepsin D (□) and 36B4 (▣) RT–PCR products (b) is reported in the histograms

Fn and Col induce ERE-mediated transcription through AF-1 activation

Subsequently, we questioned which functional domain of ERα was affected by the adhesion protein signals. To exclude the influence of specific factors present in breast cancer cells, we transiently cotransfected HeLa cells with the reporter plasmid

XETL and with either HeG0 (data not shown) or HE15 (Figure 4a) or HE19 (Figure 4b) coding for the carboxyl-terminal and amino-terminal truncated receptor, respectively. The treatment with either E2 or Fn and Col leads to an increase of luciferase activity in HeLa cells expressing ERα corresponding to that observed in MCF-7 (data not shown). Both ECM proteins induced ERE-mediated transcription only in HeLa cells transiently expressing the AF-1/DBD domains of ERα (Figure 4a), while the treatment with E2 gave a significant increase of ERE-mediated transcription when the AF-2/DBD domains of ERα were expressed (Figure 4b). ICI abolished the upregulatory effects induced by Fn, Col and E2, while 4-OH tamoxifen (4OH-Tam) treatment was able to negatively interfere only with E2-induced activation in cells expressing either ERα (data not shown) or the AF-2/ DBD domains of ERα. In summary, these data demonstrate that either Fn or Col is able to activate ERα by targeting the AF-1 domain.

Fn and Col activate ERa through c-Src

On the basis of previous findings demonstrating that c- Src is activated by Fn (Schlaepfer et al., 1997) and that ERα is activated in its AF-1 domain by signals transduced from c-Src (Feng et al., 2001), we questioned whether c-Src might be involved in ERα activation induced by cell adhesion/treatment to Fn and Col. We investigated the role of c-Src in MCF-7 cells transfected with pcDNA3 as control vector, c-Src(+) and c-Src(-) (dominant negative of c-Src) (Figure 5a).

Figure 4. ***Fn and Col induce ligand-independent transcriptional activation of the ERα.***
HeLa cells were transfected with 0.3 μg/well HE15 and 0.6 μg/well XETL (a) or with 0.3 μg/well HE19 and 0.6 μg/well XETL (b). At 6 h after transfection cocktail addition, cells were shifted in PRF-SFM for 24 h and then incubated for 16 h in PRF-SFM containing either 15 μg/ml P-Lys, 10 nM estradiol (E2), 30 μg/ml Fn or 30 μg/ml Col. The same treatments were also carried out in the presence of 100 nM 4-OH Tam and 100 nM ICI 182,780. Firefly luciferase activity was internally normalized to R. luciferase and expressed as fold of increase with respect to the PRF-SFM (untreated) samples. Results represent the mean ± s.d. of five independent experiments. ★★ $P<0.001$ and ★ $P<0.01$ vs PRF-SFM (untreated); ◆◆ $P<0.005$ vs the homologues samples without 4-OH Tam and ICI 182,780

The overexpression of c-Src potentiates ERα transactivation both in basal condition as well as upon E2, Fn and Col exposure. The expression of the dominant-negative c-Src as well as the treatment with PP2-abrogated EREmediated transcription induced by both Fn and Col, however, only attenuated the response to E2. Altogether, these data suggest that c-Src is required for ERα activation by signals derived from cell

adhesion to ECM. Under the same experimental conditions, we evaluated the autophosphorylation of c-Src and the phosphorylation of the exogenous substrate enolase (Figure 5b) after 5 min of exposure. The indicated time was chosen after a time course study (here not reported) performed at 0, 5, 10 and 20 min displaying the maximal enzymatic activity at 5 min. The results provide evidence that both E2, Fn and Col activate c-Src, while either the expression of a dominant-negative c-Src or the presence of PP2 strongly reduces both the autophosphorylation of c-Src and the phosphorylation of enolase.

E2, Fn and Col reduce cell motility

Since previous studies have shown that ERα expression leads to a lower matrigel invasiveness and to a reduced metastatic potential in breast cancer cells (Rochefort et al., 1998; Platet et al., 2000), we investigated whether the activation of ERα by both ECM proteins was correlated with the motility of breast cancer cells. MCF- 7, MDA-MB-231 and HeLa cells were used to evaluate cell invasion on Transwell chambers previously coated with Fn, Col or P-Lys and incubated overnight in PRFSFM or in PRF-SFM containing E2. In agreement with previous studies (Rochefort et al., 1998), E2 treatment produced a marked reduction of cell migration in MCF- 7 (Figure 6a) as well as in both MDA-MB-231 (data not shown) and HeLa cells expressing ERα (Figure 6b). Similar inhibition was observed after cell adhesion to either Fn or Col. To further clarify the contribution of the two ERα/AF domains in regulating cell motility, HeLa cells were transfected with either the AF-1- or AF- 2-deleted constructs and plated onto transwells coated with both ECM proteins. Cells

expressing the AF-1/ DBD domains (Figure 6c) showed a strong reduction of cell invasion induced by both ECM proteins and reversed by ICI (data not shown).

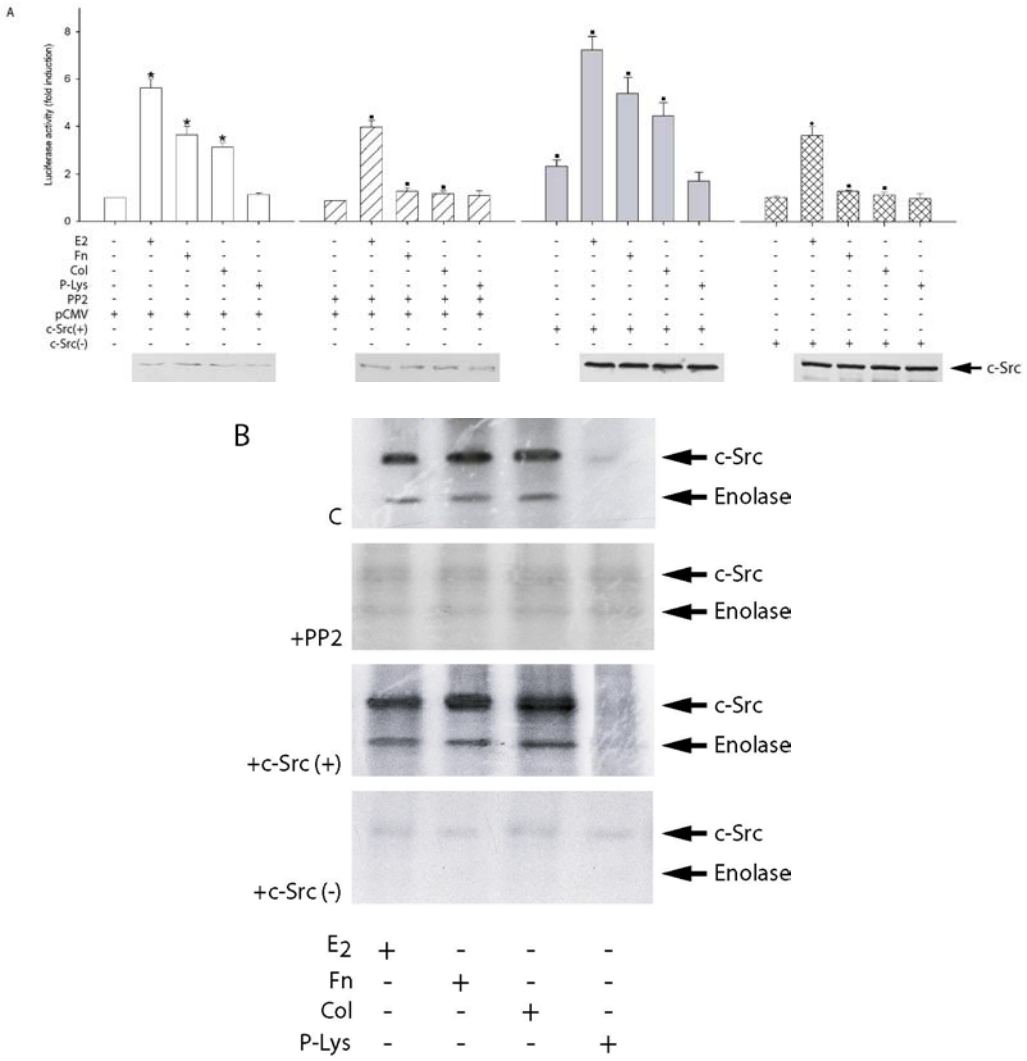

Figure 5. ***Fn and Col activate unliganded-ERα through c-Src***. (a) MCF-7 cells were cotransfected with calcium phosphate precipitation method using 0.5 μg/well of XETL and 0.5 μg/well of pCMV empty vector or 0.5 μg/well of XETL plasmid with 0.5 μg/well of c-Src (+) or 0.5 μg/well of c-Src (-). At 6 h after transfection, cells were serum starved for 24 h and then incubated for 16 h in PRF-SFM (untreated) or PRF-SFM containing either 10 nM estradiol (E2), 30 μg/ml Fn, 30 μg/ml Col or 15 μg/ml P-Lys. The same treatments were also carried out in the presence of 3 μM of PP2. Firefly luciferase activity was internally normalized to R. luciferase and expressed as fold of increase with respect to the PRF-SFM (untreated) sample. Results represent the mean ± s.d. of five independent experiments. The inset pictures present the expression of c-Src and were assessed by Western blotting as described in Materials and methods using 30 μg of total cell lysates. (b) MCF-7 cells, transfected and treated as before for 5 min, were lysed and immunoprecipitated with an anti c-Src antibody/protein A/G complex and assayed for c-Src-kinase activity using acid-treated enolase as described in Materials and methods. These results are representative of three independent experiments. ★ $P < 0.001$ vs the PRF-SFM (untreated); ■ $P < 0.01$ vs the homologues samples without PP2 and cSrc(-); ◆ $P < 0.05$ vs the homologues samples without PP2 and cSrc (-)

In contrast, only E2 treatment reduced cell migration when the AF-2/DBD domains of the ERα were expressed (Figure 6d).

JCP-06-0415.R1(20952)

JOURNAL OF CELLULAR PHYSIOLOGY 9999:1–9 (2007)

Fas Ligand Expression in TM4 Sertoli Cells is Enhanced by Estradiol "In situ" Production

STEFANIA CATALANO,[1] PIETRO RIZZA,[1] GUOWEI GU,[1] INES BARONE,[1] CINZIA GIORDANO,[2] STEFANIA MARSICO,[1] IVAN CASABURI,[1] EMILIA MIDDEA,[1] MARILENA LANZINO,[1] MICHELE PELLEGRINO,[1] AND SEBASTIANO ANDÒ[2]*

[1]Department of Pharmaco-Biology, University of Calabria 87036 Arcavacata di Rende (CS), Calabria, Italy

[2]Department of Cell Biology Faculty of Pharmacy, University of Calabria 87036 Arcavacata di Rende (CS), Calabria, Italy

The testis is an immunologically privileged site of the body where Sertoli cells work on to favor local immune tolerance by testicular autoantigens segregation and immunosuppressive factors secretion. Fas/Fas Ligand (FasL) system, expressed prevalently in Sertoli cells, has been considered to be one of the central mechanisms in testis immunological homeostasis. In different cell lines it has been reported that the proapoptotic protein FasL is regulated by 17-β estradiol (E2). Thus, using as experimental model mouse Sertoli cells TM4, which conserve a large spectrum of functional features present in native Sertoli cells, like aromatase activity, we investigated if estradiol "in situ" production may influence FasL expression. Our results demonstrate that an aromatizable androgen like androst-4-ene-3,17-dione (Δ4) enhanced FasL mRNA, protein content and promoter activity in TM4 cells. The treatment with N^6,2′-*O*-dibutyryladenosine-3′-5′-cyclic monophosphate [$(Bu)_2$cAMP] (simulating FSH action), that is well known to stimulate aromatase activity in Sertoli cells, amplified Δ4 induced FasL expression. Functional studies of mutagenesis, electrophoretic mobility shift (EMSA) and chromatin immunoprecipitation (ChIP) assays revealed that the Sp-1 motif on FasL promoter was required for E2 enhanced FasL expression in TM4 cells. These data let us to recruit FasL among those genes whose expression is up-regulated by E2 through a direct interaction of ERα with Sp-1 protein. Finally, evidence that an aromatizable androgen is able to increase FasL expression suggests that E2 production by aromatase activity may contribute to maintain the immunoprivilege status of Sertoli cells. J. Cell. Physiol. 9999: 1–9, 2007. © 2006 Wiley-Liss, Inc.

The immunoprivilege of male gonad lies on blood-testis barrier, prevalently maintained by Sertoli cell functions. This physical barrier between the general circulation and testicular tissue probably conceals antigens from the immune system and prevents effector cell access (Filippini et al., 2001; Bart et al., 2002; Ferguson et al., 2002). This immune protective function together with the secretion of hormonal and nutritive factors produced by Sertoli cells, under FSH control, substain germ cells functional maturation along all spermatogenesis process (Griswold et al., 1988; De Cesaris et al., 1992).

The Fas/FasL system was first identified in T cells (Suda et al., 1993; Lynch et al., 1995) where it plays a key role in eliminating T cell populations following antigenic stimulation and clonal proliferation. This system is also functional in the testis (Bellgrau et al., 1995; Sanberg et al., 1996) and in a variety of other tissues in which these proteins are constitutively expressed to maintain their immunoprivilege, such as eyes (Griffith et al., 1995), placenta (Guller, 1997; Uckman et al., 1997) and brain (Saas et al., 1997).

FasL is a type II trans-membrane protein that belongs to the tumor necrosis factor (TNF) family of cytokines and induces apoptosis in cells expressing Fas receptors (Suda et al., 1993). Fas (CD95, APO-1) is a transmembrane receptor protein, sharing a high degree of homology with the tumor necrosis factor/nerve growth factor receptor family (TNF/NGF-Rs) (Watanabe-Fukunaga et al., 1992, Nagata and Goldstein, 1995). It is characterized by an intracellular domain called "death domain" responsible for the activation of the intracellular signaling pathway following Fas-FasL interaction (Nagata and Goldstein, 1995).

The Fas/FasL expression during testicular development and its cell specific localization within the testis is still a matter of debate, but it is generally assumed that FasL is predominantly expressed in Sertoli cells (Suda et al., 1993; Bellgrau et al., 1995; French et al., 1996; Lee et al., 1997; Francavilla et al., 2000; D'Abrizio et al., 2004).

Among the different factors influencing FasL, it has been reported that 17-β estradiol (E2) is able to regulate the expression of this proapoptotic protein in human endometrial cells (Selam et al., 2001) and human ovarian tissue (Sapi et al., 2002). Moreover, estrogen treatment increases FasL expression in monocytes through the interaction of estrogen receptor with FasL promoter (Mor et al., 2003).

It has been well established that the estrogens biosynthesis, in the testis, is catalyzed by the enzyme complex referred to as aromatase cytochrome P450, which aromatizes the A ring of C19 androgens to the phenolic A ring of C18 estrogens (Armstrong and Dorrington, 1977; Van der Molen et al., 1981). The enzyme aromatase is composed of two polypeptides: an ubiquitous non-specific flavoprotein NADPH-cytochrome P450 reductase and a specific form of cytochrome P450

Stefania Catalano and Pietro Rizza contributed equally to this work.

Contract grant sponsor: PRIN-MIUR; Contract grant number: 2004067227.

*Correspondence to: Sebastiano Andò, Department of Cell Biology University of Calabria, Arcavacata di Rende (CS) Calabria 87036, Italy. E-mail: sebastiano.ando@unical.it

Received 22 June 2006; Accepted 24 October 2006

Published online in Wiley InterScience (www.interscience.wiley.com.), 00 Month 2006.
DOI: 10.1002/jcp.20952

(P450arom encoded by the CYP 19 gene) (Simpson et al., 1994). In the testis an age-related change has been observed in the cellular localization of the aromatization event, primarily in Sertoli cells in immature animals, but located in Leydig and germ cells in adults (Levallet et al., 1998; Andò et al., 2001). Besides, the synthesis of estrogens is regulated at the level of the aromatizing enzyme system by Follicole-Stimulating Hormone (FSH) and cyclic AMP (Dorrington and Armstrong, 1975).

In the mouse Sertoli cell line TM4 we previously demonstrated P450arom immunocytochemical localization together with its enzymatic activity (Catalano et al., 2003).

In the present study, we investigated if an aromatizable androgen like androst-4-ene-3,17-dione (Δ4), after its conversion to E2, can modulate FasL expression in TM4 cells.

Our results demonstrate that estradiol "in situ" production enhanced FasL mRNA, protein content and promoter activity.

Many transcription factors have been reported to regulate FasL promoter by DNA-protein interaction upon diverse biological signals in different cells and tissues (Latinis et al., 1997; Kasihatla et al., 1998; Matsui et al., 1998; Mittelstadt and Ashwell, 1998; Kavurma et al., 2001; Kirschhoff et al., 2002; Kavurma and Khachigian, 2003).

Functional studies of mutagenesis, electrophoretic mobility shift analysis and ChIP assay lead us to demonstrate that the up-regulatory effects induced by E2 on FasL expression are mediated by a direct interaction of Estrogen Receptor alpha (ERα) with Sp-1 protein.

MATERIALS AND METHODS

Materials

Dulbecco's Modified Eagle's Medium/Nutrient Mixture F-12 Ham (DMEM/F12), Triazol Reagent and 100 bp DNA ladder by Invitrogen (Carlsbad, CA), L-Glutamine, penicillin, horse serum, Eagle's non-essential amino acids, calf serum (CS), streptomycin, bovine serum albumine (BSA), phosphate-buffered saline (PBS) were purchased from Eurobio (Les Ullis Cedex, France). FuGENE 6, Sephadex G50 spin columns and poly (dI-dC) by Roche (Indianapolis, IN). GoTaq DNA polymerase, T4 polynucleotide Kinase, TNT master mix, Dual luciferase kit, Sp-1 human recombinant protein and TK renilla luciferase plasmid were provided by Promega (Madison, WI). The RETROscript kit and DNase I were purchased from Ambion (Austin, TX). Aprotinin, leupeptin, phenylmethylsulfonyl fluoride (PMSF), sodium orthovanadate, androst-4-ene-3,17-dione (Δ4), 7α,19α-dimethyl-19-nortestosterone (miboleron), formaldehyde, NP-40, proteinase K, tRNA, Tamoxifen (Tam), N^6,2′-*O*-dibutyryladenosine-3′-5′-cyclic monophosphate [$(Bu)_2$cAMP] and 1,3,5-Tris(4-Hydroxyphenyl)-4-propyl-1H-pyrazole (PPT) by Sigma (Milan, Italy). Antibodies against ERα, ERβ, β-actin, Sp-1, and polymerase II (N20) were provided by Santa Cruz Biotechnology (Santa Cruz, CA) whereas anti-FasL antibody by BD biosciences (San Josè, CA). ECL System and [γ^{32}P]ATP were purchased by Amersham Pharmacia (Buckinghamshire, UK). Letrozole was provided by Novartis Pharma AG (Basel, Switzerland), Mithramycin by ICN Biomedicals, (Shelton, CT). Salmon sperm DNA/protein A agarose by UBI (Chicago, IL). Diarylpropionitrile (DPN) and ICI 182,780 were purchased from Tocris chemical (Bristol, UK). ABI Prism 7000 Sequence Detection System, TaqMan Ribosomal RNA Reagent kit, TaqMan Ribosomal RNA Control Reagent kit and SYBR Green Universal PCR Master Mix by Biosystems (Forster City, CA).

Cell cultures

The TM4 cell line, derived from the testis of immature BALB/c mice, was originally characterized based on its morphology, hormone responsiveness, and metabolism of steroids (Mather, 1980). This cell line was obtained from the American Type Culture Collection (ATCC) (Manassas, VA) and cultured in DMEM-F12 containing 2.5% fetal CS, 5% horse serum, 1 mg/ml penicillin–streptomycin. Human uterin cervix adenocarcinoma (HeLa) cells were obtained from the ATCC. HeLa cells were cultured in DMEM/F12 containing 5% CS, 1% L-Glutamine, 1% Eagle's non essential amino acids and 1 mg/ml penicillin–streptomycin.

Western blot analysis

TM4 cells were grown in 10 cm dishes to 70–80% confluence and lysed in 500 μl of 50 mM Hepes (pH 7.5), 150 mM NaCl, 1.5 mM $MgCl_2$, 1 mM EGTA, 10% glycerol, 1% Triton X-100, a mixture of protease inhibitors (Aprotinin, PMSF and Na-orthovanadate). Equal amounts of total proteins were resolved on a 11% SDS-polyacrylamide gel and then electroblotted onto a nitrocellulose membrane. Blots were incubated overnight at 4°C with: (1) mouse monoclonal ERα antibody, (2) rabbit polyclonal ERβ ??antibody, (3) mouse monoclonal FasL antibody, (4) mouse monoclonal β-actin antibody. The antigen-antibody complex was detected by incubation of membranes 1 h at room temperature with peroxidase-coupled goat anti-rabbit IgG or goat anti-mouse IgG and revealed using the ECL System. Blots were then exposed to film and bands of interest were quantified by densitometer (Mod 620 BioRad[Q2]). The results obtained as optical density arbitrary values were transformed to percentages of the control (percent control) taking the samples from cells not treated as 100%.

Real-time RTPCR

Total cellular RNA was extracted from TM4 cells using "TRIAZOL Reagent" as suggested by the manufacturer. All RNA was treated with DNase I and purity and integrity of the RNA were confirmed spectroscopically and by gel electrophoresis prior to use. Two micrograms of total RNA was reverse transcribed in a final volume of 50 μl using a RETROscript kit as suggested by the manufacturer. cDNA was diluted 1:5 in nuclease free water, aliquoted and stored at −20°C. The cDNAs obtained were further amplified for FasL gene using the following primers: forward 5′-CGAGGAGTGTGGCCCATTT-3′ and reverse 5′-GGTTCCATATGTGTCTTCCCATTC-3′.

PCR reactions were performed in the ABI Prism 7000 Sequence Detection System, using 0.1 μM of each primer, in a total volume of 30 μL reaction mixture following the manufacturer's recommendations. SYBR Green Universal PCR Master Mix for the dissociation protocol was used for FasL and 18S. Negative control contained water instead of first-strand cDNA. Each sample was normalized on the basis of its 18S ribosomal RNA content. The 18S quantification was performed using a TaqMan Ribosomal RNA Reagent kit following the method provided in the TaqMan Ribosomal RNA Control Reagent kit. The relative FasL gene expression levels were normalized to a calibrator that was chosen to be the basal, untreated sample. Final results were expressed as n-fold differences in FasL gene expression relative to 18S rRNA and calibrator, calculated following the ΔΔCt method, as follows:

$$\text{n} - \text{fold} = 2^{-(\Delta Ct_{\text{sample}} - \Delta Ct_{\text{calibrator}})}$$

where ΔCt values of the sample and calibrator were determined by subtracting the average Ct value of the 18S rRNA reference gene from the average Ct value of the different genes analyzed.

Transfection assay

Transient transfection experiments were performed using pGL_2 vectors containing different deleted segments of human FasL gene promoter (p-2365: −2365/−2; p-318: −318/−2; p-237: −237/−2) ligated to a luciferase reporter gene (kindly provided by Dr. Paya, Department of Immunology, Mayo Clinic Rochester, Minnesota, USA). Deletion of Sp-1 sequence in FasL gene promoter was generated by PCR using as template p-318 construct. The resulting plasmid encoding the human Fas-L gene promoter containing the desired deletion was designed p-280 Sp-1 and the sequence was confirmed by nucleotide sequence analysis.

FuGENE 6 was used as recommended by the manufacturer to transfect TM4 cells plated in 3.5 cm^2 wells with pGL_2 FasL promoter constructs (0.5 μg/well).

Another set of experiments was performed in HeLa cells cotransfecting p-318 FasL promoter (−318/−2) (0.5 μg/well) and the wild-type human ERα expression vector (HEGO) (0.5 μg/well) (Tora et al., 1989) or pCMV5-hERβ, containing human ERβ gene (0.5 μg/well) (a gift from JA Gustafsson).

Empty vectors were used to ensure that DNA concentrations were constant in each transfection. TK renilla luciferase plasmid (25 ng/well) was used to normalize the efficiency of the transfection. Twenty-four hours after transfection, the medium was changed and TM4 cells were treated in serum free medium (SFM) in the presence of Δ4, $(Bu)_2$cAMP, mibolerone, letrozole, PPT and DPN. HeLa cells, 24 h after transfection, were treated in the presence or absence of E2 for 24 h.

The firefly and renilla luciferase activities were measured using Dual Luciferase Kit. The firefly luciferase data for each sample were normalized on the basis of transfection efficiency measured by renilla luciferase activity.

Electrophoretic mobility shift assay (EMSA)

Nuclear extracts were prepared from TM4 as previously described (Andrews and Faller, 1991). Briefly, TM4 cells plated into 60 mm dishes were scraped into 1.5 ml of cold PBS. Cells were pelleted for 10 sec and resuspended in 400 μl cold buffer A (10 mM HEPES-KOH pH 7.9 at 4°C, 1.5 mM $MgCl_2$, 10 mM KCl, 0.5 mM dithiothreitol, 0.2 mM PMSF, 1 mM leupeptin) by flicking the tube. The cells were allowed to swell on ice for 10 min and then vortexed for 10 sec. Samples were then centrifuged for 10 sec and the supernatant fraction discarded. The pellet was resuspended in 50 μl of cold Buffer B (20 mM HEPES-KOH pH 7.9, 25% glycerol, 1.5 mM $MgCl_2$, 420 mM NaCl, 0.2 mM EDTA, 0.5 mM dithiothreitol, 0.2 mM PMSF, 1 mM leupeptin) and incubated on ice for 20 min for high-salt extraction. Cellular debris was removed by centrifugation for 2 min at 4°C and the supernatant fraction (containing DNA binding proteins) was stored at −70°C. The yield was determined by Bradford method (Bradford, 1976). The probe was generated by annealing single stranded oligonucleotides and labeled with [γ^{32}P] ATP and T4 polynucleotide kinase, and then purified using Sephadex G50 spin columns. The DNA sequences used as probe or as cold competitor are the following (the nucleotide motifs of interest are underlined and mutations are shown as lowercase letters): Sp1 5′-AAATTGTGGGCGGAAACTTCCAGGGG-3′, mutated Sp-1 5′-AAATTGTGttCGGAAACTTCCAGGGG-3′. Oligonucleotides were synthesized by Sigma Genosys. The protein binding reactions were carried out in 20 μl of buffer (20 mM HEPES pH 8, 1 mM EDTA, 50 mM KCl, 10 mM DTT, 10% glicerol, 1 mg/ml BSA, 50 μg/ml poli dI/dC) with 50,000 cpm of labeled probe, 10 μg of TM4 nuclear protein and 5 μg of poly (dI-dC). The above-mentioned mixture was incubated at room temperature for 20 min in the presence or absence of unlabeled competitor oligonucleotide. For experiments involving Sp-1, ERα and ERβ antibodies, the reaction mixture was incubated with these antibodies at 4°C for 12 h. For in vitro mithramycin treatment, mithramycin (100 nM) was incubated with the labeled probe for 30 min at 4°C before the addition of nuclear extract. As positive controls we used Sp-1 human recombinant protein (1 μl) and in vitro transcribed and translated ERα protein (1 μl) synthesized using T7 polymerase in the rabbit reticulocyte lysate system as direct by the manufacturer. The entire reaction mixture was electrophoresed through a 6% polyacrylamide gel in 0.25 X Tris borate-EDTA for 3 h at 150 V. Gel was dried and subjected to autoradiography at −70°C.

Chromatin immunoprecipitation (ChIP)

According to the ChIP assay procedure previously described (Shang et al., 2000), TM4 cells were grown in 60 mm dishes to 50–60% confluence, shifted to SFM for 24 h and then treated with E2 (100 nM), ICI 182,780 (10 μM), E2 + ICI for 1 h. Thereafter, the cells were washed twice with PBS and cross-linked with 1% formaldehyde at 37°C for 10 min. Next, cells were washed twice with PBS at 4°C, collected and resuspended in 200 μl of lysis buffer (1% SDS, 10 mM EDTA, 50 mM Tris-HCl pH 8.1) and left on ice for 10 min. Then, cells were sonicated four times for 10 sec at 30% of maximal power (Sonics, Vibra Cell 500W) and collected by centrifugation at 4°C for 10 min at 14,000 rpm. The supernatants were diluted in 1.3 ml of IP buffer (0.01% SDS, 1.1% Triton X-100, 1.2 mM EDTA, 16.7 mM Tris-HCl pH 8.1, 16.7 mM NaCl) and immunocleared with 80 μl of sonicated salmon sperm DNA/protein A agarose for 1 h at 4°C. The precleared chromatin was immunoprecipitated with a specific anti-Sp-1, anti ERα and anti polymerase II antibodies and with a normal mouse serum IgG (Nms) as negative control. At this point, 60 μl of salmon sperm DNA/protein A agarose were added and precipitation was further continued for 2 h at 4°C. After pelleting, precipitates were washed sequentially for 5 min with the following buffers: Wash A (0.1% SDS, 1% Triton X-100, 2 mM EDTA, 20 mM Tris-HCl pH 8.1, 150 mM NaCl), Wash B (0.1% SDS, 1% Triton X-100, 2 mM EDTA, 20 mM Tris-HCl pH 8.1, 500 mM NaCl), and Wash C (0.25 M LiCl, 1% NP-40, 1% sodium deoxycholate, 1 mM EDTA, 10 mM Tris-HCl pH 8.1), and then twice with TE buffer (10 mM Tris, 1 mM EDTA). The immunocomplexes were eluated with elution buffer (1% SDS, 0.1 M $NaHCO_3$), reverse crosslinked by heating at 65°C and digested with proteinase K (0.5 mg/ml) at 45°C for 1 h. DNA was obtained by phenol/chloroform/isoamyl alcohol extraction. Two microliters of 10 mg/ml yeast tRNA were added to each sample and DNA was precipitated with 70% EtOH for 24 h at −20°C, and then washed with 95% EtOH and resuspended in 20 μl of TE buffer. One microlitre of each sample was used for PCR amplification with the following primers flanking Sp-1 sequence present in the Fas-L promoter region: 5′-GCAACTGAGGCCTTGAAGGC-3′ (forward) and 5′-GCAGCTGGTGAGTCAGGCCAG-3′ (reverse). The PCR conditions were 1 min at 94°C, 1 min at 65°C, and 2 min at 72°C. The amplification products obtained in 25 cycles were analyzed in a 2% agarose gel and visualized by ethidium bromide staining.

Statistical analysis

Each datum point represents the mean ± SE of three different experiments. Data were analyzed by ANOVA test using the STATPAC computer program.

RESULTS

Estradiol "in situ" production, by aromatase activity, enhances FasL expression in TM4 cell line

In TM4 cells, which exibit a spectrum of features in common with native Sertoli cells, like the presence of aromatase activity, we investigated if an aromatizable androgen Δ4, through its conversion into E2, may influence FasL mRNA and protein content by Real-time RT-PCR and Western blot analysis. Since aromatase expression and activity, in Sertoli cells, is under FSH control (Dorrington and Armstrong, 1975) we also evaluated the treatment with $(Bu)_2$cAMP (simulating FSH action) on FasL expression.

As shown in Figure 1A the treatment with Δ4 (100 nM) for 24 h resulted in an increase of FasL mRNA expression more than 1.9-fold. The simultaneous treatment with $(Bu)_2$cAMP (1 mM) and Δ4, further enhanced FasL mRNA expression compared with Δ4 treatment alone (2.4-fold), suggesting that $(Bu)_2$cAMP stimulates E2 "in situ" production by its action on aromatase activity. These up-regulatory effects were reversed by addition of the aromatase inhibitor letrozole (1 μM) (90%), while no significant difference was observed in the presence of a non-aromatizable androgen mibolerone (100 nM) with or without $(Bu)_2$cAMP.

Next, we performed Western blot analysis using a monoclonal antibody anti FasL. We detected a band of

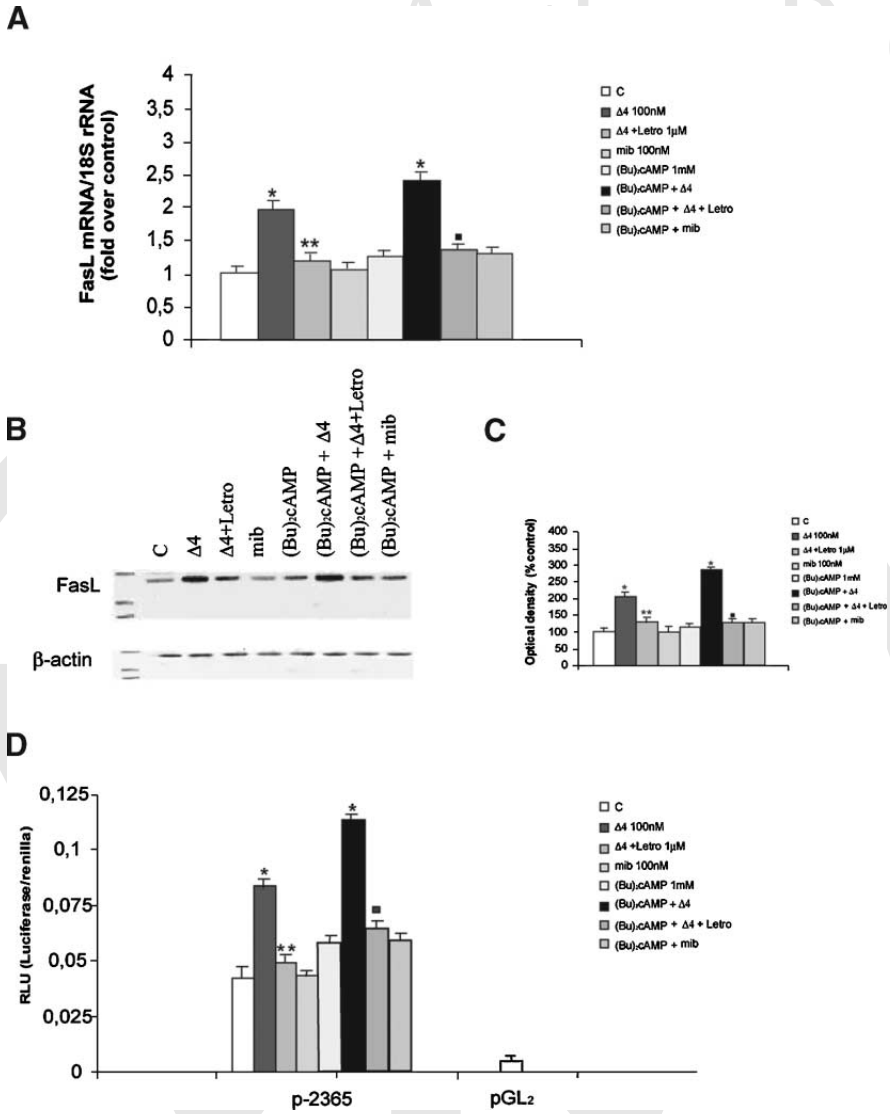

Fig. 1. Effects of Δ4 on FasL expression. **A**: Total RNA was obtained from TM4 cells untreated (control, C) or treated for 24 h with Δ4 (100 nM) mibolerone (mib 100 nM), $(Bu)_2$cAMP (1 mM), $(Bu)_2$cAMP + Δ4 and $(Bu)_2$cAMP + mib. One micromolar of aromatase inhibitor letrozole (Letro) was used. Real time RT-PCR was performed to analyze mRNA levels of FasL. Data represent the mean ± SE of values from three separate RNA samples. Each sample was normalized to its 18S ribosomal RNA content. Final results are expressed as n-fold differences of gene expression relative to calibrator (control) calculated with the ΔΔCt method as indicated in the "Material and Methods" section. $^*P < 0.01$ compared to control. $^{**}P < 0.01$ compared to Δ_4 treated samples; ■ $P < 0.01$ compared to $(Bu)_2$cAMP + Δ4 treated samples. **B**: Immunoblot of FasL from TM4 cells treated in the absence (C) or in the presence of the above-mentioned treatments. **C**: The histograms represent the mean ± SE of three separate experiments in which band intensities were evaluated in term of optical density arbitrary units and expressed as percentage of the control assumed as 100%. $^*P < 0.01$ compared to control; $^{**}P < 0.01$ compared to Δ_4 treated samples; ■ $P < 0.01$ compared to $(Bu)_2$cAMP + Δ4 treated samples. **D**: Transcriptional activity of TM4 cells transfected with p-2365 construct is shown. TM4 cells were treated in the absence (C) or in the presence of Δ4 (100 nM), mibolerone (mib 100 nM), $(Bu)_2$cAMP (1 mM), $(Bu)_2$cAMP + Δ4 and $(Bu)_2$cAMP + mib. One micromolar of aromatase inhibitor letrozole was used. The values represent the means ± SE of three different experiments. In each experiment, the activities of the transfected plasmids were assayed in triplicate transfections. pGL_2: basal activity measured in cells transfected with pGL_2 basal vector. $^*P < 0.01$ compared to control. $^{**}P < 0.01$ compared to Δ4 treated samples; ■ $P < 0.01$ compared to $(Bu)_2$cAMP + Δ4 treated samples.

37 kDa which intensity was increased upon Δ4 treatment. Exposure to $(Bu)_2$cAMP combined with Δ4 enhanced the effect induced by Δ4 alone. The addition of letrozole reversed these up-regulatory effects (Fig. 1B,C).

To evaluate whether E2 "in situ" production was able to activate FasL promoter we transiently transfected TM4 cells with vector containing human FasL promoter fused to the luciferase reporter gene. The treatment for 24 h with Δ4 or Δ4 + $(Bu)_2$cAMP displayed a significant increase of the basal promoter activity that was reversed by letrozole (Fig. 1D).

Effects of Δ4 on expression of human FasL promoter/luciferase reporter gene constructs in TM4 cells

To delimit the *cis*-elements involved in FasL transcriptional activation by Δ4, we transiently transfected TM4 cells with plasmids containing different deleted segments of human FasL promoter. Schematic representation of constructs is shown in Figure 2A. Transfected cells were untreated (C) or treated with 100 nM of Δ4 and 1 μM of letrozole.

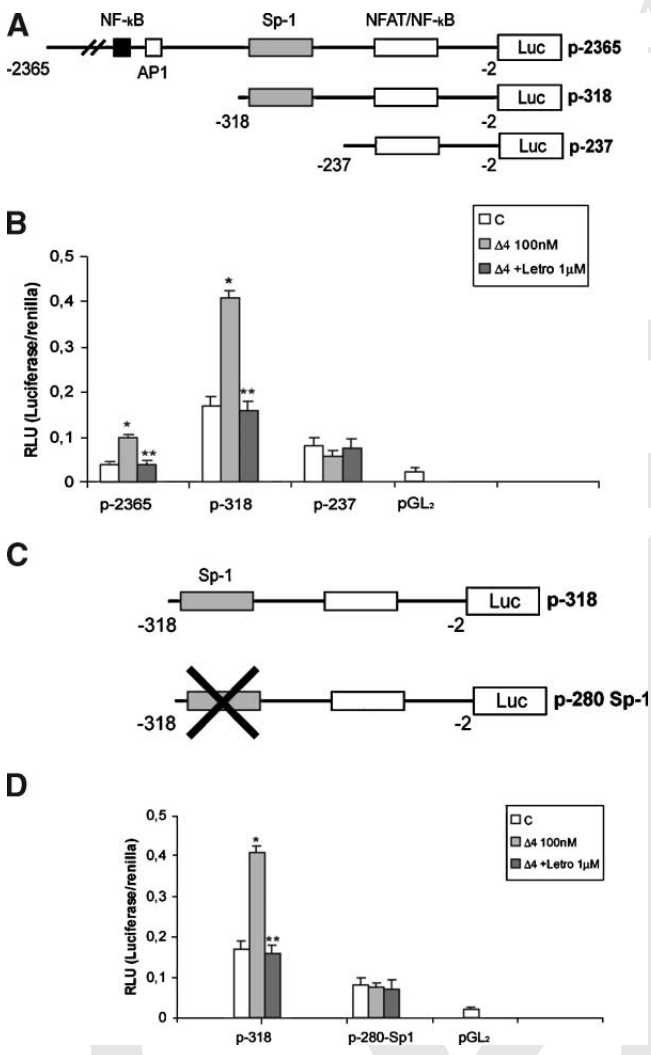

Fig. 2. Effects of estradiol "in situ" production on expression of human FasLpromoter/luciferase reporter gene construts in TM4 cells. **A**: Schematic map of the FasL promoter fragments used in this study. All of the promoter constructs contain the same 3′ boundary (−2). The 5′ boundaries of the promoter fragments varied from −237 to −2,365. Each fragment was subcloned into the pGL_2 vector. **B**: Transcriptional activity of TM4 cells with promoter constructs is shown. TM4 cells were treated in the absence (C) or in the presence of Δ4 (100 nM), and Δ4 + letrozole (1 μM) for 24 h. The values represent the means ± SE of three different experiments. In each experiment, the activities of the transfected plasmids were assayed in triplicate transfections. pGL_2: basal activity measured in cells transfected with pGL_2 basal vector. $^*P < 0.01$ compared to control; $^{**}P < 0.01$ compared to Δ4 treated samples. **C**: Schematic representation of the p-318 and p-280 Sp-1 constructs. The deletion of Sp-1 sequence is present in p-280 Sp-1 construct containing the region from −318 to −2 of FasL promoter gene. Each fragment was subcloned into the pGL2 vector. **D**: Transcriptional activity of TM4 cells with p-280 Sp-1 construct is shown. TM4 cells were treated in the absence (C) or in the presence of Δ4 (100 nM), and Δ4 + letrozole (1 μM) for 24 h. The values represent the mean ± SE of three different experiments. In each experiment, the activities of the transfected plasmids were assayed in triplicate transfections. $^*P < 0.01$ compared to control; $^{**}P < 0.01$ compared to Δ4-treated samples.

p-318 plasmid showed a higher basal activity when compared with the other plasmids (p-2365, p-237) (Fig. 2B) suggesting the presence of a DNA sequences upstream from −318 to which transcription factors with repressor activity bind. These data well fit with previous results demonstrating that FasL gene promoter region, located between −318 and −237, plays a major role in promoting basal transcription in TM4 Sertoli cells (McClure et al., 1999).

In TM4 cells transfected with p-2365 and p-318 plasmids the treatment with Δ4 induced a significant increase of the basal promoter activity that was completely reversed by letrozole. In contrast, Δ4 was unable to activate p-237 construct eliciting, in the region from −318 to −237, the presence of *cis*-element involved in estrogen responsiveness. In fact, this region contains Sp-1 site, a potential target of ER. In order to explore the role of the Sp-1 binding site in the regulation of FasL expression by Δ4, functional experiments were performed using the Sp-1 deleted plasmid (p-280 Sp-1). Luciferase assay revealed that the inducibility by Δ4 on FasL promoter was totally lost (Fig. 2D). These results suggest that the up-regulatory effects of estradiol production by aromatase activity require Sp-1 sequence motif.

ERβ is not involved in E2-modulating FasL expression

Before exploring more closely the possible interaction between E2/ER complex to Sp-1 and the role of this binding in modulating FasL expression, we set out to determine which functional ER(s) isoform was present in TM4 cells. By Western blotting analysis, we demonstrated in TM4 protein extracts the presence of both ER(s) (Fig. 3A, lane 2), As positive control, the breast cancer cell line MCF-7 (ERα positive) and human prostate cancer cell line LNCaP (ERβ positive) were used (Fig. 3A, lane 1).

In the presence of the two different ER antagonists ICI 182,780 (10 μM) and tamoxifen (10 μM) (Tam) the up-regulation of E2 on FasL expression was abrogated demonstrating that this effect was specifically dependent by ER (Fig. 3B,C).

To specify which isoforms of ER were mainly involved in FasL transactivation, we cotransfected HeLa cells (ER negative) with p-318 FasL promoter and the wild type human ERα or ERβ expression vector. The treatment with E2 (100 nM) for 24 h showed an increased transcriptional activation of FasL promoter only in cells cotransfected with ERα (Fig. 3D).

Finally, to demonstrate further the direct involvement of ERα in FasL transactivation we used 100 nM of the selective agonists of ERα [1,3,5-Tris(4-Hydroxyphenyl)-4-propyl-1H-pyrazole (PPT)] and ERβ [diarylpropionitrile (DPN)] in TM4 cells transiently transfected with p-318 FasL promoter. The treatment with PPT showed an increase of FasL promoter activity while no change was observed in the presence of DPN (Fig. 3E).

Effects of 17-β estradiol treatment on Sp1 DNA binding activity in TM4 cells

On the basis of the evidences that the up-regulatory effects of E2 on FasL require the crucial presence of Sp-1-RE, EMSA was performed using synthetic oligodeoxyribonucleotides corresponding to the putative Sp-1 binding site. In the presence of TM4 nuclear extracts (10 μg) we observed the formation of a specific complex (Fig. 4A, lane 1), which was abrogated by a 100-fold molar excess of unlabeled probe (Fig. 4A, lane 2). This inhibition was not observed when a mutated Sp-1 oligonucleotide was used as competitor (Fig. 4A, lane 3). E2-treatment induced a strong increase in Sp-1 DNA binding activity (Fig. 4A, lane 4) compared with basal levels. In the presence of ICI 182,780 the Sp-1 DNA binding activity was drastically reduced (Fig. 4A, lane 5). The addition of mithramycin (100 nM), that binds to

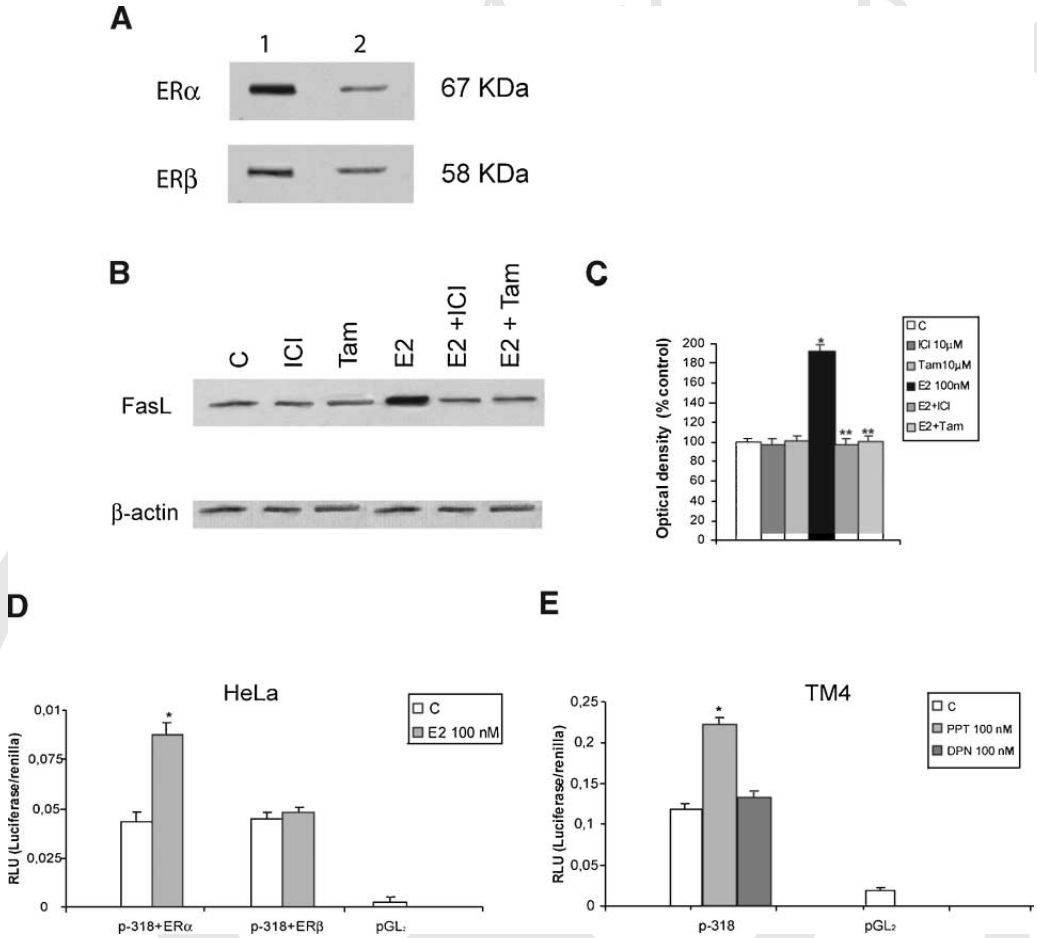

Fig. 3. 17β-Estradiol enhances FasL transcriptional activity through ERα. **A**: Lysates from TM4 cells were used to evaluate by Western blot analysis the expression of ERα and ERβ (lane 2). The human breast cancer cell line MCF-7 and human prostate cancer cell line LNCaP were used as positive control for ERα and ERβ respectively (lane 1). **B**,**C**: Immunoblot of FasL from TM4 cells treated in the absence (C) or in the presence of E2 (100 nM) for 24 h. The pure anti-estrogen ICI 182,780 (10 μM) and tamoxifen (Tam 10 μM) were used. The histograms represent the means ± SE of three separate experiments in which band intensities were evaluated in term of optical density arbitrary units and expressed as percentage of the control assumed as 100%. $^{*}P < 0.01$ compared to control; $^{**}P < 0.01$ compared to E2 treated samples. **D**: HeLa cells were transiently cotransfected with p-318 FasL promoter construct (−318/−2) and ERα or ERβ plasmids. The cells were untreated (C) or treated with E2 (100 nM) for 24 h. The values represent the means ± SE of three different experiments. In each experiment, the activities of the transfected plasmids were assayed in triplicate transfections. $^{*}P < 0.01$ compared to control. **E**: TM4 cells transfected with p-318 FasL promoter construct were untreated (C) or treated with PPT (100 nM) and DPN (100 nM) for 24 h. $^{*}P < 0.01$ compared to control.

GC boxes and prevents sequential Sp-1 binding, decreased the binding of E2 treated TM4 nuclear extracts on Sp-1 DNA sequence (Fig. 4A, lane 6). In a cell free system we observed in the presence of Sp-1 reconbinant protein a single band that causes the same shift respect to the complex revealed in TM4 nuclear extracts (Fig. 4A, lane 7) which was abrogated by 100-fold molar excess of unlabeled probe (Fig. 4A, lane 8). Transcribed and translated in vitro ERα protein did not bind directly to Sp-1 probe (Fig. 4A, lane 9). When the nuclear extracts from TM4 cells treated with E2 were incubated with either anti-Sp-1 or anti-ERα antibody, the original band DNA-protein complex was immunodepleted (Fig. 4B, lanes 3 and 4), whereas anti-ERβ antibody gave no effects (lane 5).

Taken together these results suggest that ERα is recruited by Sp-1 in our DNA binding complex.

17-β Estradiol enhances recruitment of Sp-1/ERα to the promoter region of FasL gene in TM4 cells

Interaction of ERα and Sp-1 with the FasL gene promoter was also investigated using a ChIP assay. After sonication and immunoprecipitation by anti ERα or anti Sp-1 antibodies, PCR was used to determine binding of ERα/Sp-1 protein to the −317 to −2 DNA region of the FasL gene promoter. Our results indicated that treatment with E2 induced an increased recruitment of Sp-1/ERα complex to the FasL promoter. The latter event was reduced in the presence of E2 + ICI. The enhanced recruitment of Sp-1/ERα was correlated with greater association of polymerase II to the FasL regulatory region (Fig. 5A). No PCR product was observed using DNA immunoprecipitated with normal mouse serum IgG.

DISCUSSION

In testis, Fas/FasL interaction has been thought to play an important role in the establishment of immunoprivilege.

Several reports have demonstrated that Sertoli cells through FasL may trigger apoptotic cell death of sensitive lymphoid cells, which express on their cell surface Fas receptor. This has provided new insights into the concepts of tolerance and immunoprivilege (Bellgrau et al., 1995; Sanberg et al., 1996; Ferguson and Griffith, 1997). For instance, testis grafts from mice

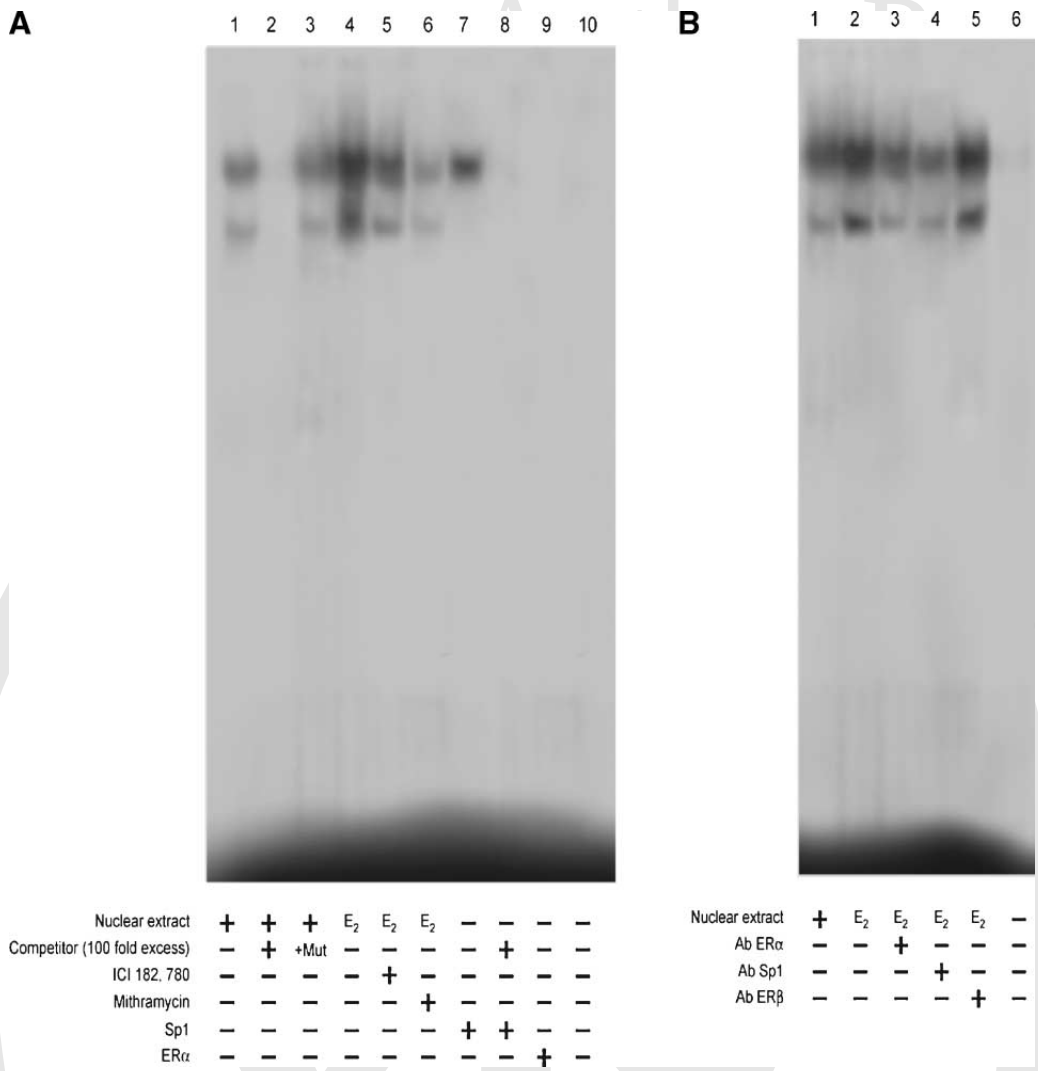

Fig. 4. Electrophoretic mobility shift assay of the Sp-1 binding site in the FasL promoter region. **A**: Nuclear extracts from TM4 cells were incubated with a double-stranded Sp1-specific consensus sequence probe labeled with [γ-^{32}P] ATP and subjected to electrophoresis in a 6% polyacrilamide gel (**lane 1**). Competition experiments were perfomed adding as competitor a 100-fold molar excess of unlabeled probe (**lanes 2** and **8**) or a 100-fold molar excess of unlabeled oligonucleotide containing a mutated Sp-1 (**lane 3**). Nuclear extracts were obtained from TM4 cells treated with 100 nM of E2 (**lane 4**), E2 + ICI 182,780 (10 μM) (**lane 5**), E2 + mithramycin (100 nM) (**lane 6**) for 24 h. As control we used human Sp-1 recombinant protein and transcribed and translated in vitro ERα protein (**lane 7** and **9**). **Lane 10** contains probe alone. **B**: Anti-ERα, anti Sp-1 and anti-ERβ antibodies (**lanes 3–5**) were incubated with E2-treated TM4 nuclear extracts. Lane 6 contains probe alone.

expressing FasL survived when transplanted into allogeneic animals. On the contrary, grafts derived from "gld" mice, which lack functional FasL, were rejected (Bellgrau et al., 1995).

In the present report, for the first time, we have provided evidences that, in TM4 cell line, an aromatizable androgen Δ4 induces a strong increase in FasL mRNA, protein content and promoter activity. These effects are reversed by addition of letrozole, an aromatase inhibitor, addressing how E2 "in situ" production by aromatase activity plays a crucial role in modulating the immunoprivileged status of these somatic cells. A further support to the specificity of the above described results raises from the evidence that no noticeable effect was produced by mibolerone, a non-aromatizable steroid.

It is well known that postnatal development and function of testicular Sertoli cells is regulated primarily by FSH, a glycoprotein hormone secreted by the pituitary gland (Dorrington and Armstrong, 1975). In the prepubertal testis, FSH is required for Sertoli cells proliferation to achieve the adult number of these cells (Griswold, 1998). This proliferative stage of Sertoli cells development is also characterized by the presence of FSH-dependent cytochrome P450 aromatase activity (Carreau et al., 2003; Sharpe et al., 2003). In our recent work (Catalano et al., 2003) we have documented in TM4 cell line a strong dose-dependent stimulation of aromatase activity induced by $(Bu)_2$cAMP similar to that described previously in immature Sertoli cells (Andò et al., 2001). In the present study it is worth to emphasize that FSH induced an increased FasL expression through the enhancement of aromatase activity.

To elucidate the molecular mechanism involved in Δ4 enhanced FasL expression, we transiently transfected TM4 cells with different constructs containing deleted segments of the human FasL promoter.

A maximal constitutive reporter gene activity was observed with p-318 construct, containing the region between −318 and −2 bp from the transcriptional start

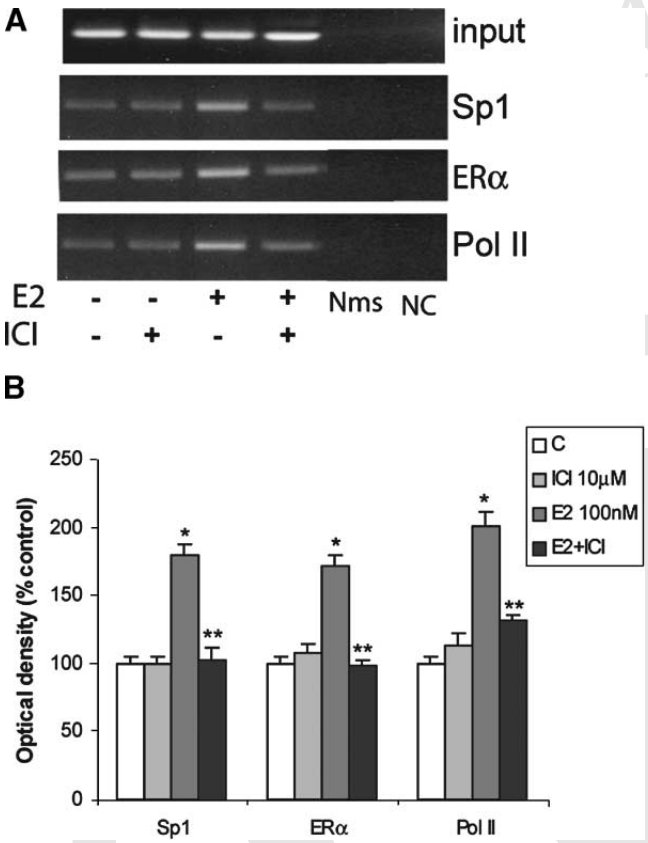

Fig. 5. 17β-Estradiol increases Sp-1/ERα recruitement to FasL promoter. **A**: Soluble precleared chromatin was obtained from TM4 cells treated for 1 h with 100 nM E2, 10 μM ICI and E2 + ICI or left untreated (C) and immunoprecipitated (IP) with an anti-Sp-1, anti ERα, anti polymerase II antibodies and with a normal mouse serum (Nms) as negative control. The FasL promoter sequences containing Sp-1 were detected by PCR with specific primers, as described in "Materials and Methods". To control input DNA, FasL promoter was amplified from 30 μl of initial preparations of soluble chromatin (before immunoprecipitations). PCR products obtained at 25 cycles are shown. Sample without the addition of DNA was used as negative control (NC). This experiment was repeated three times with similar results. **B**: The histograms represent the means ± SE of three separate experiments in which band intensities were evaluated in term of optical density arbitrary units and expressed as percentage of the control assumed as 100%. $^{*}P < 0.01$ compared to control; $^{**}P < 0.01$ compared to E2-treated samples.

site of the human FasL promoter. This is in agreement with previous results demonstrating that FasL gene promoter region from 318 to −237 bp plays a major role in promoting basal transcription in TM4 cells (McClure et al., 1999). Moreover, the induced activation by Δ4 was not observed in cells transfected with p-237 construct (−237 to −2) suggesting that the region between −318 and −237 bp contains elements that mediate the potentiating effects of estrogen on FasL expression.

A broadening number of transactivating factors has been identified as regulators of FasL gene expression (Kavurma and Khachigian, 2003), as nuclear factor in activated T cells (NF-AT) (Latinis et al., 1997), nuclear factor-kappa B (NF-KB) (Matsui et al., 1998), activator protein-1 (AP-1) (Kasihatla et al., 1998), interferon regulatory factor-1 (IFN-1) (Kirschhoff et al., 2002), early growth response factor (Egr) (Mittelstadt and Ashwell, 1998) and specificity protein-1 (Sp-1) (Kavurma et al., 2001).

Sp-1 is involved in the transcriptional regulation of many genes and has also been identified to be important in the regulation of FasL gene expression and apoptosis. Indeed, this transcription factor is able to activate FasL promoter via a distinct recognition element, and inducible FasL promoter activation is abrogated by expression of the dominant-negative mutant form of Sp-1 (Kavurma et al., 2001). In addition, it has been recently demonstrated that nuclear extracts of TM4 Sertoli cells contain high levels of Sp-1 and Sp-3 that specifically bind to the GGGCGG consensus sequence present in the FasL gene, and overexpression of Sp-1 but not Sp-3 is able to increase the basal transcription of the FasL promoter (McClure et al., 1999).

The latter observation fits with our functional studies demonstrating that Sp-1 is a crucial effector of estradiol signal in enhancing FasL gene expression. For instance, it is well known that ERs can transactivate gene promoters without directly binding to DNA but instead through interaction with other DNA-bound factors in promoter regions lacking TATA box. This has been most extensively investigated in relationship to protein complexes involving Sp-1 and ERα at GC boxes, which are classic binding sites for members of the Sp-1 family of transcription factors. Sp-1 protein plays an important role in the regulation of mammalian and viral genes, and recent results have shown that E2 responsiveness of c-fos, cathepsin D, retinoic acid receptor α1 and insulin-like grow factor-binding protein 4 gene expression in breast cancer cells is linked to specific GC rich promoter sequences that bind ER/Sp-1 complex in which only Sp-1 protein binds DNA (Krishnan et al., 1994; Cowley et al., 1997; Porter et al., 1997; Sun et al., 1998; Qin et al., 1998; Saville et al., 2000).

In our work, the interaction between ERα and Sp-1 is clearly evidenced by gel mobility shift analysis and chromatin immunoprecipitation assay. Besides, the functional assays performed in ER-negative HeLa cells showed that ERα and not ERβ mediates the estrogen-induced increase in FasL gene expression. The specificity of ERα to induce transcription of FasL in TM4 was demonstrated using selective agonists for the ER subtypes. For instance we evidenced that only PPT was able to enhance FasL promoter activity.

Our results stemming from functional analysis, EMSA and ChiP assays led us to recruit FasL among those genes whose expression is upregulated by E2 through a direct interaction of ERα with Sp-1 protein.

In conclusion, the present study demonstrates that aromatizable steroids, normally present in the testicular milieu, through their conversion into E2 by aromatase activity, are able to increase FasL expression in TM4 Sertoli cells. The aromatase enzyme assures that estrogens through a short autocrine loop maintain Sertoli cells proliferation before their terminal differentiation. Thus, we propose that at the latter crucial maturative stage, FasL may achieve an intracellular content sufficient to protect Sertoli cells from any injury induced by Fas expressing immunocells, then potentiating the immunoprivileged condition of the testis.

ACKNOWLEDGMENTS

We thank Dr C.V. Paya for providing us with the pGL2 promoter FasL (p-2365, p-318, p-237) and Dr Domenico Sturino for English revision of the manuscript.

LITERATURE CITED

Andrews NC, Faller DV. 1991. A rapid micropreparation technique for extraction of DNA-binding proteins from limiting numbers of mammalian cells. Nucleic Acids Res 19:2499.

Andò S, Sirianni R, Forastieri P, Casaburi I, Lanzino M, Rago V, Giordano F, Giordano C, Carpino A, Pezzi V. 2001. Aromatase expression in prepubertal Sertoli cells: Effect of thyroid hormone. Mol Cell Endocrinol 178:11–21.
Armstrong DT, Dorrington JH. 1977. Estrogen biosynthesis in ovaries and testes. Adv Sex Horm Res 32:17–258.
Bart J, Green HJ, van der Graaf WT, Hollema H, Hendrikse NH, Vaanburg W, Sleijfer DT, de Vries EG. 2002. An oncological view on the blood-testis barrier. Lancet Oncol 3:357–363.
Bellgrau D, Gold D, Selawry H, Moore J, Franzusoff A, Duke RC. 1995. A role for CD95 ligand in preventing graft rejection. Nature 377:630–632.
Bradford MM. 1976. A rapid and sensitive method for quantitation of microgram quantities of protein utilizing the principle of protein-dye binding. Anal Biochem 72:248–254.
Carreau S, Lambard S, Delalande C, Denis-Galeraud I, Bilinska B, Bourguiba S. 2003. Aromatase expression and role of estrogens in male gonad: A review. Reprod Biol Endocrinol 1:35.
Catalano S, Pezzi V, Chimento A, Giordano C, Carpino A, Young M, McPhaul MJ, Andò S. 2003. Triiodothyronine decreases the activity of the proximal promoter (PII) of the Aromatase gene in the mouse Sertoli cell line TM4. Mol Endocrinol 17:923–934.
Cowley SM, Hoare S, Mosselman S, Parker MG. 1997. Estrogen receptor alpha and beta form heterodimers on DNA. J Biol Chem 272:19858–19862.
D'Abrizio P, Baldini E, Russo PF, Biordi L, Graziano FM, Rucci N, Properzi G, Francavilla S, Ulisse S. 2004. Ontogenesis and cell specific localizzation of Fas ligand expression in the rat testis. Int J Androl 27:304–310.
De Cesaris P, Filippini A, Cervelli C, Riccioli A, Muci S, Storace G, Stefanini M, Riparo E. 1992. Immunosuppressive molecules produced by Sertoli cells cultured in vitro: Biological effects on lymphocytes. Biochem Biophys Res Commun 186:1639–1646.
Dorrington JH, Armstrong DT. 1975. Follicle-stimulating hormone stimulates estradiol-17 β synthesis in cultured Sertoli cells. Cell Biol 72:2677–2681.
Ferguson TA, Griffith TS. 1997. A vision of cell death: Insight into immune privilege. Immunol Rey 156:167–184.
Ferguson TA, Green DR, Griffith TS. 2002. Cell death and immune privilege. Int Rev Immunol 21:153–172.
Filippini A, Riccioli A, Padula F, Lauretti P, D'Alessio A, De Cesaris P, Gandini L, Lenzi A, Riparo E. 2001. Control and impairment of immune privilege in the testis and semen. Human Reprod Update 7:444–449.
Francavilla S, D'Abrizio P, Rucci N, Silvano G, Properzi G, Straface E, Cordeschi G, Necozione S, Gnessi L, Arizzi M, Ulisse S. 2000. Fas and Fas ligand expression in fetal and adult human testis with normal or deranged spermatogenesis. J Clin Endocrinol Metab 85:2692–2700.
French LE, Hahne M, Viard I, Radlgruber G, Zanone R, Becker K, Muller C, Tschopp J. 1996. Fas and Fas ligand in embryos and adult mice: Ligand expression in several immune-privileged tissues and coexpression in adult tissues characterized by apoptotic cell turnover. J Cell Biol 133:335–343.
Griffith TS, Brunner T, Fletcher SM, Green DR, Ferguson TA. 1995. Fas ligand-induced apoptosis as a mechanism of immune privilege. Nature 270:1189–1192.
Griswold MD. 1998. The central role of Sertoli cells in spermatogenesis. Semin Cell Dev Biol 9:411–416.
Griswold MD, Morales C, Sylvester SR. 1988. Molecular biology of the Sertoli cell. Oxf Rev Reprod Biol 10:124–161.
Guller S. 1997. Role of Fas ligand in conferring immune privilege to non-lymphoid cells. Ann NY Acad Sci 828:268–272.
Kasihatla S, Brunner T, Genestier L, Echeverri F, Mahboubi A, Green DR. 1998. DNA damaging agents induce expression of Fas lignd and subsequent apoptosis in T lynphocytes via the actiation of NF-kB and AP-1. Mol Cell 1:543–551.
Kavurma MM, Khachigian LM. 2003. Signaling and transcriptional control of FasL gene expression. Cell Death Differ 10:36–44.
Kavurma MM, Santiago FS, Bonfoco E, Khachigian LM. 2001. Sp-1 phosphorylation regulates apoptosis via extracellular FasL-Fas engagement. J Biol Chem 276:4964–4971.
Kirschhoff S, Sebens T, Baumann S, Krueger A, Zawatzky R, Li-Webber M, Meini E, Neipel F, Fieckenstein B[Q3], Krammer PH. 2002. Viral IFN-regulatory factors inhibit activation-induced cell death via two positive regulatory IFN-regulatory factor 1-dependent domains in the CD95 ligand promoter. J Immunol 168:1226–1234.
Krishnan V, Wang X, Safe S. 1994. Estrogen receptor-Sp1 complexes mediate estrogen-induced cathepsin D gene expression in MCF-7 human breast cancer cells. J Biol Chem 269:15912–15917.
Latinis KM, Norian LA, Eliason SL, Koretzky GA. 1997. Two NFAT transcription factor binding sites partecipate in the regulation of CD95 (Fas) ligand expression in activated human T cells. J Biol Chem 272:31427–31434.
Lee J, Richburg JH, Younkin SC, Boekelheide K. 1997. The Fas system is a key regulator of germ cell apoptosis in testis. Endocrinology 138:2081–2088.
Levallet J, Bilinska B, Mittre H, Genissel C, Fresnel J, Carreau S. 1998. Expression and immunolocalization of functional cytochrome P450 aromatase in mature rat tesicular cells. Biol Reprod 58:919–926.
Lynch DH, Ramsdell F, Alderson MR. 1995. Fas and FasL in the homeostatic regulation of immune responses. Immunol Today 16:569–574.
Mather J. 1980. Establishment and characterization of two distinct mouse testicular epithelial cell lines. Biol Reprod 23:243–252.
Matsui K, Fine A, Zhu B, Marshak-Rothstein A, Ju ST. 1998. Identification of two NF-kappa B sites in mouse CD95 ligand (Fas ligand) promoter: Funcional anlaysis in T cell hybridoma. J Immunol 161:3469–3473.
McClure RF, Heppelmann CJ, Paya CV. 1999. Constitutive Fas ligand gene transcription in Sertoli cells is regulated by Sp1. J Biol Chem 274:7756–7762.
Mittelstadt PR, Ashwell JD[Q4]. 1998. Cyclosporin A-sensitive transcription factor Egr-3 regulates Fas ligand expression. Mol Cell Biol 18:3744–3751.
Mor G, Sapi E, Abrahams VM, Rutherford T, Song J, Hao XY, Muzaffar S, Kohen F. 2003. Interaction of the estrogen receptors with the Fas ligand promoter in human monocytes. J Immunol 170:114–122.
Nagata S, Goldstein P. 1995. The Fas death factor. Science 267:1449–1456.
Porter W, Saville B, Holvik D, Safe S. 1997. Funcional synergy between the transcription factor Sp-1 and the estrogen receptor. Mol Endocrinol 11:1569–1580.
Qin C, Singh P, Safe S. 1998. Transcriptional activation of insulin-like growth factor binding protein 4 by 17β-estradiol in MCF-7 cells: Role of estrogen receptor-Sp1 complexes. Endocrinology 140:2501–2508.
Saas P, Walker P, Hahne M, Quiquerez AL, Schnuriger V, Perrin G, French L, Meir EGV, deTribolet N, Tschopp J, Dietrich PY. 1997. Fas ligand expression by astrocytoma in vivo: Maintaining immune privilege in the brain? J Clin Invest 99:1173–1178.
Sanberg PR, Borlongan CV, Saporta S, Cameron DF. 1996. Testis-derived Sertoli cells survive and provide localized immunoprotection for xenografts in rat brain. Nat Biotechnol 114:1692–1695.
Sapi E, Brown WD, Aschkenazi S, Lim C, Munoz[Q5] A, Kacinski BM, Rutherford T, Mor G. 2002. Regulation of Fas ligand expression by estrogen in normal ovary. J Soc Gynerol Investig 9:243–250.
Saville B, Wormke M, Wang F, Nguyen T, Enmark E, Kuiper G, Gustafsson JA, Safe S. 2000. Ligand-, cell-, and estrogen receptor subtype (α/β)- dependent activation at GC-rich (Sp-1) promoter elements. J Biol Chem 275:5379–5387.
Selam B, Kayisli UA, Mulayim N, Arici A. 2001. Regulation of Fas ligand expression by estradiol and progesterone in human endometrium. Biol Reprod 65:979–985.
Shang Y, Hu X, DiRenzo J, Lazar MA, Brown H. 2000. Cofactor dynamics and sufficiency in estrogen receptor-regulated transcription. Cell 103:843–852.
Sharpe RM, McKinnell C, Kivlin C, Fisher JS. 2003. Proliferation and functional maturation of Sertoli cells, and their relevance to disorders of testis function in adulthood. Reproduction 125:769–784.
Simpson ER, Mahendroo MS, Means GD, Kilgore MW, Hinshelwood MM, Graham-Lorence S, Amameh B, lto Y, Fisher CR, Mandelson CR, Bulun SE. 1994. Aromatase cytocrome P450, the enzyme responsible for estrogen biosynthesis. Endocr Rev 15:342–355.
Suda T, Takahashi T, Goldstein P, Nagata S. 1993. Molecular cloning and expression of the Fas ligand, a novel member of the tumor necrosis factor family. Cell 75:1169–1178.
Sun G, Porter W, Safe S. 1998. Estrogen-induced retinoic acid receptor α1 gene expression: Role of estrogen receptor-Sp1 complex. Mol Endocrinol 12:882–890.
Tora L, Mullick A, Metger D, Ponglikitmongkol M, Park I, Chambon P. 1989. The cloned human oestrogen receptor contains a mutation which alters its hormone binding properties. EMBO J 88:1981–1986.
Uckman D, Steele A, Cherry Wang BY, Chamizo W, Koutsonikolis A, Gilbert-Barness E, Good RA. 1997. Trophoblasts express Fas ligand: A proposed mechanism for immune privilege in placenta and maternal invasion. Mol Hum Reprod 3:655–662.
Van der Molen HJ, Brinkmann AO, De Jong FH, Rommeerts FF. 1981. Testicular oestrogens. J Endocrinol 89:33P–46P.
Watanabe-Fukunaga R, Brannan CI, Itoh N, Yonehara S, Copeland NG, Jenkins NA, Nagata S. 1992. The cDNA structure, expression, and chromosomal assignment of the mouse Fas antigen. J Immunol 148:1274–1279.

Q1: Please check the affiliations.

Q2: Please provide the complete locaiton.

Q3: Please check the first name.

Q4: Please check the first name.

Q5: Please check the change made in author name.

C1

REPRINT BILLING DEPARTMENT · 111 RIVER STREET · HOBOKEN, NJ 07030
FAX: (201) 748-7670
E-MAIL: reprints@wiley.com

PREPUBLICATION REPRINT ORDER FORM

Please complete this form even if you are not ordering reprints. This form **MUST** be returned with your corrected proofs and original manuscript. Your reprints will be shipped approximately 4 weeks after publication. Reprints ordered after printing will be substantially more expensive.

JOURNAL ***JOURNAL OF CELLULAR PHYSIOLOGY*** VOLUME _____ ISSUE _____
TITLE OF MANUSCRIPT _____
MS. NO. _____ NO. OF PAGES _____ AUTHOR(S) _____

No. of Pages	100 Reprints	200 Reprints	300 Reprints	400 Reprints	500 Reprints
	$	$	$	$	$
1-4	**336**	**501**	**694**	**890**	**1052**
5-8	**469**	**703**	**987**	**1251**	**1477**
9-12	**594**	**923**	**1234**	**1565**	**1850**
13-16	**714**	**1156**	**1527**	**1901**	**2273**
17-20	**794**	**1340**	**1775**	**2212**	**2648**
21-24	**911**	**1529**	**2031**	**2536**	**3037**
25-28	**1004**	**1707**	**2267**	**2828**	**3388**
29-32	**1108**	**1894**	**2515**	**3135**	**3755**
33-36	**1219**	**2092**	**2773**	**3456**	**4143**
37-40	**1329**	**2290**	**3033**	**3776**	**4528**

**REPRINTS ARE ONLY AVAILABLE IN LOTS OF 100. IF YOU WISH TO ORDER MORE THAN 500 REPRINTS, PLEASE CONTACT OUR REPRINTS DEPARTMENT AT (201) 748-6353 FOR A PRICE QUOTE.

☐ Please send me _____ reprints of the above article at $ _____

Please add appropriate State and Local Tax (Tax Exempt No._____) $ _____
for United States orders only.

Please add 5% Postage and Handling $ _____

TOTAL AMOUNT OF ORDER** $ _____

***International orders must be paid in currency and drawn on a U.S. bank*

Please check one: ☐ Check enclosed ☐ Bill me ☐ Credit Card
If credit card order, charge to: ☐ American Express ☐ Visa ☐ MasterCard

Credit Card No _____ Signature _____ Exp. Date _____

BILL TO:
Name _____
Institution _____
Address _____
_____
Purchase Order No. _____

SHIP TO: (Please, no P.O. Box numbers)
Name _____
Institution _____
Address _____
_____
Phone _____ Fax _____
E-mail _____

WILEY
Publishers Since 1807

111 River Street
Hoboken, NJ 07030

COPYRIGHT TRANSFER AGREEMENT

Date:

To:

Production/Contribution ID#_____ Publisher/Editorial office use only

Re: Manuscript entitled_____
_____ (the "Contribution")
for publication in ***JOURNAL OF CELLULAR PHYSIOLOGY***_____ (the "Journal") published by Wiley-Liss, Inc., a subsidiary of John Wiley & Sons, Inc. ("Wiley").

Dear Contributor(s):

Thank you for submitting your Contribution for publication. In order to expedite the publishing process and enable Wiley to disseminate your work to the fullest extent, we need to have this Copyright Transfer Agreement signed and returned to us as soon as possible. If the Contribution is not accepted for publication this Agreement shall be null and void.

A. COPYRIGHT

1. The Contributor assigns to Wiley, during the full term of copyright and any extensions or renewals of that term, all copyright in and to the Contribution, including but not limited to the right to publish, republish, transmit, sell, distribute and otherwise use the Contribution and the material contained therein in electronic and print editions of the Journal and in derivative works throughout the world, in all languages and in all media of expression now known or later developed, and to license or permit others to do so.

2. Reproduction, posting, transmission or other distribution or use of the Contribution or any material contained therein, in any medium as permitted hereunder, requires a citation to the Journal and an appropriate credit to Wiley as Publisher, suitable in form and content as follows: (Title of Article, Author, Journal Title and Volume/Issue Copyright © [year] Wiley-Liss, Inc. or copyright owner as specified in the Journal.)

B. RETAINED RIGHTS

Notwithstanding the above, the Contributor or, if applicable, the Contributor's Employer, retains all proprietary rights other than copyright, such as patent rights, in any process, procedure or article of manufacture described in the Contribution, and the right to make oral presentations of material from the Contribution.

C. OTHER RIGHTS OF CONTRIBUTOR

Wiley grants back to the Contributor the following:

1. The right to share with colleagues print or electronic "preprints" of the unpublished Contribution, in form and content as accepted by Wiley for publication in the Journal. Such preprints may be posted as electronic files on the Contributor's own website for personal or professional use, or on the Contributor's internal university or corporate networks/intranet, or secure external website at the Contributor's institution, but not for commercial sale or for any systematic external distribution by a third party (e.g., a listserve or database connected to a public access server). Prior to publication, the Contributor must include the following notice on the preprint: "This is a preprint of an article accepted for publication in [Journal title] © copyright (year) (copyright owner as specified in the Journal)". After publication of the Contribution by Wiley, the preprint notice should be amended to read as follows: "This is a preprint of an article published in [include the complete citation information for the final version of the Contribution as published in the print edition of the Journal]", and should provide an electronic link to the Journal's WWW site, located at the following Wiley URL: http://www.interscience.Wiley.com/. The Contributor agrees not to update the preprint or replace it with the published version of the Contribution.

2. The right, without charge, to photocopy or to transmit online or to download, print out and distribute to a colleague a copy of the published Contribution in whole or in part, for the Contributor's personal or professional use, for the advancement of scholarly or scientific research or study, or for corporate informational purposes in accordance with Paragraph D.2 below.

3. The right to republish, without charge, in print format, all or part of the material from the published Contribution in a book written or edited by the Contributor.

4. The right to use selected figures and tables, and selected text (up to 250 words, exclusive of the abstract) from the Contribution, for the Contributor's own teaching purposes, or for incorporation within another work by the Contributor that is made part of an edited work published (in print or electronic format) by a third party, or for presentation in electronic format on an internal computer network or external website of the Contributor or the Contributor's employer.

5. The right to include the Contribution in a compilation for classroom use (course packs) to be distributed to students at the Contributor's institution free of charge or to be stored in electronic format in datarooms for access by students at the Contributor's institution as part of their course work (sometimes called "electronic reserve rooms") and for in-house training programs at the Contributor's employer.

D. CONTRIBUTIONS OWNED BY EMPLOYER

1. If the Contribution was written by the Contributor in the course of the Contributor's employment (as a "work-made-for-hire" in the course of employment), the Contribution is owned by the company/employer which must sign this Agreement (in addition to the Contributor's signature), in the space provided below. In such case, the company/employer hereby assigns to Wiley, during the full term of copyright, all copyright in and to the Contribution for the full term of copyright throughout the world as specified in paragraph A above.

2. In addition to the rights specified as retained in paragraph B above and the rights granted back to the Contributor pursuant to paragraph C above, Wiley hereby grants back, without charge, to such company/employer, its subsidiaries and divisions, the right to make copies of and distribute the published Contribution internally in print format or electronically on the Company's internal network. Upon payment of the Publisher's reprint fee, the institution may distribute (but not resell) print copies of the published Contribution externally. Although copies so made shall not be available for individual re-sale, they may be included by the company/employer as part of an information package included with software or other products offered for sale or license. Posting of the published Contribution by the institution on a public access website may only be done with Wiley's written permission, and payment of any applicable fee(s).

E. GOVERNMENT CONTRACTS

In the case of a Contribution prepared under U.S. Government contract or grant, the U.S. Government may reproduce, without charge, all or portions of the Contribution and may authorize others to do so, for official U.S. Government purposes only, if the U.S. Government contract or grant so requires. (U.S. Government Employees: see note at end).

F. COPYRIGHT NOTICE

The Contributor and the company/employer agree that any and all copies of the Contribution or any part thereof distributed or posted by them in print or electronic format as permitted herein will include the notice of copyright as stipulated in the Journal and a full citation to the Journal as published by Wiley.

G. CONTRIBUTOR'S REPRESENTATIONS

The Contributor represents that the Contribution is the Contributor's original work. If the Contribution was prepared jointly, the Contributor agrees to inform the co-Contributors of the terms of this Agreement and to obtain their signature to this Agreement or their written permission to sign on their behalf. The Contribution is submitted only to this Journal and has not been published before, except for "preprints" as permitted above. (If excerpts from copyrighted works owned by third parties are included, the Contributor will obtain written permission from the copyright owners for all uses as set forth in Wiley's permissions form or in the Journal's Instructions for Contributors, and show credit to the sources in the Contribution.) The Contributor also warrants that the Contribution contains no libelous or unlawful statements, does not infringe on the rights or privacy of others, or contain material or instructions that might cause harm or injury.

CHECK ONE:

[____]Contributor-owned work

_____ _____
Contributor's signature Date

_____
Type or print name and title

_____ _____
Co-contributor's signature Date

_____
Type or print name and title

ATTACH ADDITIONAL SIGNATURE PAGE AS NECESSARY

[____]Company/Institution-owned work (made-for-hire in the course of employment)

_____ _____
Company or Institution (Employer-for-Hire) Date

_____ _____
Authorized signature of Employer Date

[____]**U.S. Government work**

Note to U.S. Government Employees

A Contribution prepared by a U.S. federal government employee as part of the employee's official duties, or which is an official U.S. Government publication is called a "U.S. Government work," and is in the public domain in the United States. In such case, the employee may cross out Paragraph A.1 but must sign and return this Agreement. If the Contribution was not prepared as part of the employee's duties or is not an official U.S. Government publication, it is not a U.S. Government work.

[____]**U.K. Government work (Crown Copyright)**

Note to U.K. Government Employees

The rights in a Contribution prepared by an employee of a U.K. government department, agency or other Crown body as part of his/her official duties, or which is an official government publication, belong to the Crown. In such case, the Publisher will forward the relevant form to the Employee for signature.

Human sperm express a functional androgen receptor: effects on PI3K/AKT pathway.

SAVERIA AQUILA[1,3*], MARIAELENA GENTILE[2*], EMILIA MIDDEA[1,3], STEFANIA CATALANO[1], STEFANIA MARSICO[1,3], MARILENA LANZINO[1,3], IVAN CASABURI[1], INES BARONE[1,3], PAOLA CUTUGNO[1] AND SEBASTIANO ANDÒ[2]

[1]Dept. Pharmaco-Biology (Faculty of Pharmacy), [2]Dept. Cellular Biology (Faculty of Biological Sciences, [3]Centro Sanitario - University of Calabria 87036 Arcavacata di Rende (COSENZA) ITALY.

Short title: Androgen receptor in human sperm

Summary sentence: In human sperm androgen receptor is able to modulate PI3K/AKT pathway on the basis of the androgen levels.

Key words: androgen receptor, androgens, human sperm, male reproduction, PI3K/AKT.

Corresponding address: Prof. Sebastiano Andò

Faculty of Pharmacy-University of Calabria

Arcavacata di Rende (CS) 87030 - ITALY

TEL: +39 0984 496201

FAX: +39 0984 496203

E-mail: sebastiano.ando@unical.it

E-mail: aquisav@libero.it

FOOTNOTES: This work was supported by PRIN 2004 Prot. N. 0067227, AIRC - 2003 and MURST and Ex 60% -2005. Saveria Aquila[1*] and Mariaelena Gentile[2*] contributed equally to this work.

ABSTRACT

Results from mice lacking the androgen receptor (AR) showed that it is critical for the proper development and function of the testes. The aim of this study was to investigate whether a functional AR is present in human sperm. By using RT-PCR and Western blot AR expression was demonstrated. by immunocytochemistry the AR was located at the head region. Dihydrotestosterone, in a dose-dependent manner, leads to the rapid phosphorylation of the AR on tyrosine, serine and threonine residues which was reduced by the AR antagonist OH-Flutamide. The effects of AR on PI3K/AKT pathway depend on androgen concentrations. Specifically, 0.1 and 1 nM dihydrotestosterone stimulated PI3K activity, while 10 nM dihydrotestosterone produced a decrease of PI3K activity, p-AKT S473 and p-BCL2 in the presence of an enhanced PTEN phosphorylation. In addition, 10 nM DHT was able to induce the cleavage of caspases 8, 9 and 3 which was reversed either by casodex or OH-Flutamide, confirming that the effect is mediated by the AR. By using wortmannin, a specific PI3K inhibitor, the cleavage of caspase 3 was reproduced confirming that in sperm the PI3K/AKT pathway is involved in caspase activation.

In conclusion, human sperm express a functional AR that has the ability to modulate the PI3K/AKT pathway influencing sperm cell physiology.

INTRODUCTION

A functional androgen receptor (AR) is required for male embryonic sexual differentiation, pubertal development and regulation of spermatogenesis in mammals. The role of AR during spermatogenesis has been the subject of intense interest for many years (1). Several findings have shown that AR function is required for the completion of meiosis and the transition of spermatocytes to haploid round spermatids (2). Studies of androgen withdrawal and disruption of AR activity, either by surgical, chemical or genetic means, have demonstrated that spermatogenesis rarely proceeds beyond meiosis. In all of these model systems, very few round and even fewer

elongated spermatids are observed as clearly demonstrated in a previous study (3). However, the mechanisms by which androgens regulate male fertility are not fully understood and the sites of androgen action within the male reproductive system are not yet resolved. Whereas few studies have raised the intriguing possibility that some germ cells may exhibit immunoreactive AR (4, 5), other reports point to Sertoli cells or Leydig cells or peritubular/myoid cells as the exclusive androgen target cells in the testis (6, 7, 8, 9). Recently, the presence of the AR in human sperm was demonstrated by Western blot and by immunofluorescence assay (10).

It is generally accepted that androgens bind to intracellular androgen receptors resulting in mRNA and protein synthesis (11). Nevertheless, rapid responses to androgens have been observed in different tissues that cannot be explained by involvement of mRNA and protein synthesis (12, 13). These rapid, nongenomic effects are also seen for other steroid hormones (14) and their importance as a complementary route for cell regulation has recently become evident. Different nuclear receptors (15, 16) were found to be present in human spermatozoa, regulating cellular processes through nongenomic mechanisms. This may represent the exclusive modality of action in spermatozoa since they are apparently transcriptionally inactive cells.

In addition to stimulating cell growth, androgens and/or AR play important roles in the promotion of cell apoptosis (17, 18, 19, 20). The term *apoptosis* defines programmed cell death, which is executed by the activation of caspases, a family of cytoplasmic cysteine proteases (21) through two major pathways: the intrinsic and the extrinsic. The intrinsic pathway involves the cell sensing stress that triggers mitochondria-dependent processes, resulting in cytochrome *c* release and activation of caspase 9 (22). The extrinsic pathway involves the final cleavage of caspase 8 (23). Both caspases 8 and 9 can be directly regulated through protein phosphorylation from AKT (24, 25). The PI3K signaling pathway is an important intracellular mediator of cell survival and antiapoptotic signals (26). PI3K activation leads to production of 3'-phosphoinositide second messengers, such as phosphatidylinositol 3,4,5-trisphosphate, which activate a variety of

downstream cell survival signals. Accumulation of phosphatidylinositol 3,4,5-trisphosphate at the membrane recruits a number of signaling proteins containing pleckstrin homology domains, including protein kinase B (also known as AKT). On recruitment, AKT becomes phosphorylated and activated and exerts its antiapoptotic activity through inactivation of proapoptotic proteins. In addition, the PI3K pathway has also been shown to be negatively regulated by Phosphatase and tensin homologue (PTEN), a lipid phosphatase that cleaves the D3 phosphate of the second messenger phosphatidylinositol 3,4,5-trisphosphate (27, 28). Recently in fibroblasts, it has been demonstrated that AR mediates androgen nongenomic function and that androgen activates PI3K/AKT through the formation of a triple complex between AR, the regulatory subunit p85 of PI3K (PIK3R1) and SRC tyrosine kinase. Indeed, this interaction is dependent on androgen concentration, particularly high androgen concentration which dissociates the AR-SRC tyrosine kinase-PI3K complex (29).

The functional impact of programmed cell death in human sperm is poorly understood (30). Up to now it has been unclear whether apoptosis in ejaculated spermatozoa takes place in a similar way as in somatic cells or whether spermatozoa, which are thought to have a transcriptionally inactive nucleus, undergo abortive forms of this process (30). However, sperm constitutively express proteins required to execute apoptosis. Active caspases were observed predominantly in the postacrosomal region (caspases 8, 1, and 3) and caspase 9 was particularly localized in the midpiece, associated with mitochondria (31). Moreover, a wide spectrum of cell cytoskeletal proteins and membrane components are also targets of caspase 3 (31) and the proper regulation of the caspase cascade plays an important role both in sperm differentiation and testicular maturity (32). In addition, caspases have been implicated in the pathogenesis of multiple andrological pathologies such as impaired spermatogenesis, decreased sperm motility, increased levels of sperm DNA fragmentation, testicular torsion, varicocele and immunological infertility (32). Further studies

are needed to evaluate the full significance of caspases activation in spermatozoa. A direct link between AR and sperm survival has not been investigated previously.

In the present study we have demonstrated the presence of AR in sperm. It emerges from our data that low androgen concentrations stimulate PI3K activity that is inhibited at higher levels. It should be mentioned that in the latter circumstance increases in PTEN phosphorylation and caspases 8, 9 and 3 cleavages were evident.

MATERIALS AND METHODS

Chemicals

PMN Cell Isolation Medium was from BIOSPA (Milan, Italy). Total RNA Isolation System kit, enzymes, buffers, nucleotides 100 bp ladder used for RT-PCR were purchased from Promega (Milan, Italy). Moloney Murine Leukemia Virus (M-MLV) was from Gibco BRL - Life Technologies Italia (Milan, Italy). Oligonucleotide primers and TA Cloning kit were made by Invitrogen (Milan, Italy). Gel band purification kit was from Amersham Pharmacia Biotech (Buckinghamshire, UK). DMEM-F12 medium, BSA protein standard, Laemmli sample buffer, prestained molecular weight markers, Percoll (colloidal PVP coated silica for cell separation), Sodium bicarbonate, Sodium lactate, Sodium pyruvate, Dimethyl Sulfoxide (DMSO), anti-rabbit IgG FITC conjugated, Earle's balanced salt solution, Hoechst 33342, steroids and all other chemicals were purchased from Sigma Chemical (Milan, Italy). Acrylamide bisacrylamide was from Labtek Eurobio (Milan, Italy). Triton X-100, Eosin Y was from Farmitalia Carlo Erba (Milan, Italy). ECL Plus Western blotting detection system, Hybond^{TM} ECL^{TM}, [γ-^{32}P]ATP, Hepes Sodium Salt were purchased from Amersham Pharmacia Biotech (Buckinghamshire, UK). Goat polyclonal actin antibody (1-19), monoclonal mouse anti-AR (AR 441) and anti- PIK3R1 antibodies, monoclonal anti-p-tyrosine (PY99), normal mouse serum, peroxidase-coupled anti-rabbit and anti-goat, Protein A/G-agarose plus were from Santa Cruz Biotechnology (Heidelberg, Germany). Monoclonal mouse anti-p-SRC tyrosine kinase was from Oncogene (Milan, Italy). Polyclonal rabbit

anti-p-serine, anti-p-threonine, anti-p-AKT1/AKT2/AKT3 S473, anti-p-BCL2, anti-p-PTEN, anti-caspase 8, anti-caspase 9 and anti-caspase 3 antibodies were from Cell Signaling (Milan, Italy). Casodex (Cax) was from Astra Zeneca (Milan, Italy) and Hydroxy-flutamide (OH-Flut) was from Schering (Milan, Italy). The specific caspases inhibitor Z-VAD-FMK (ZVF) was from R&D Systems (Milan, Italy). PCR 2.1 vector was from Promega (Milan, Italy) and the sequencing was by MWG AG Biotech (Ebersberg, Germany).

Semen samples and spermatozoa preparations

Semen specimens from normozoospermic men were obtained after 3 days of sexual abstinence. The samples were ejaculated into sterile containers and left for at least 30 minutes (min) in order to completely liquefy before being processed. Sperm from ejaculates with normal parameters of semen volume, sperm count, motility, vitality and morphology, according to the WHO Laboratory Manual (33), were included in this study. In each experiment, three normal samples were pooled. Spermatozoa preparation was performed as previously described (34). Briefly, after liquefaction, normal semen samples were pooled and subjected to centrifugation (800 *g*) on a discontinuous Percoll density gradient (80:40 % v:v) (33). The 80 % Percoll fraction was examined using an optical microscope equipped with a x100 oil objective to ensure that a pure sample of sperm was obtained. An independent observer, who observed several fields for each slide, inspected the cells. Percoll-purified sperm were washed with unsupplemented Earle's medium and were incubated in the same medium (uncapacitating medium) for 30 min at 37 °C and 5 % CO_2, without (control) or with treatments (experimental). Some samples were incubated in capacitating medium (Earle's balanced salt solution medium supplemented with 600 mg BSA /100 ml and 200 mg sodium bicarbonate /100 ml). When the cells were treated with the inhibitors Cax, OH-Flut and ZVF, a pre-treatment of 15 min was performed. The study was approved by the local medical-ethical committees and all participants gave their informed consent.

RNA isolation and Reverse Transcriptase- Polymerase Chain Reaction (RT-PCR)

Total RNA was isolated from human ejaculated spermatozoa and purified as previously described (34). Before RT-PCR, RNA was incubated with ribonuclease-free deoxyribonuclease (DNAse) I in single-strength reaction buffer at 37 °C for 15 min. This was followed by heat inactivation of DNAse I at 65 °C for 10 min. Five micrograms of DNAse-treated RNA samples were reverse transcribed by 200 IU M-MLV reverse transcriptase in a reaction vol of 20 µl (0.4 µg oligo-dT, 0.5 m_M deoxy-NTP and 24 IU RNAsin) for 30 min at 37 °C, followed by heat denaturation for 5 min at 95 °C. PCR amplification of cDNA was performed with 2 U of Taq DNA polymerase, 50 pmol primer pair for *AR*. These primers were chosen to amplify the region of the DNA binding domain plus the hinge region of the *AR*. Contamination by leucocytes and germ cells in the sperm preparations was assessed by amplifying *PTPRC* and *KIT* transcripts respectively. The applied PCR primers and the expected lengths of the resulting PCR products are shown in Table 1. PCR was carried for 40 cycles using the following parameters: 95°C/1 min, 55°C/1 min, 72°C/2 min for *AR*; 95°C/1 min, 52°C/1 min, 72°C/2 min for *KIT*; 95°C/1 min, 55°C/1 min, 72°C/2 min for *PTPRC*. For all PCR amplifications, negative (reverse transcription-PCR performed without M-MLV reverse transcriptase) and positive controls (LnCap for *AR*, human testis for *KIT* and human leucocytes for *PTPRC*) were included. The PCR-amplified products were subjected to electrophoresis in 2 % agarose gels stained with ethidium bromide and visualised under UV transillumination.

Gel extraction and DNA sequence analysis

The *AR* RT-PCR product was extracted from the agarose gel by using a gel band purification kit, the purified DNAs was subcloned into PCR 2.1 vector and then sequenced.

Western blot analysis of sperm proteins

Sperm samples washed twice with Earle's balanced salt solution (uncapacitating medium), were incubated for 30 min without or with the treatments indicated in the figures. During Western blot analysis, sperm samples were processed as previously described (34). The negative control was performed using a sperm lysate that was immunodepleted of AR (i.e. preincubation of lysates with

anti-AR antibody for 1 hour (h) at room temperature and immunoprecipitated with Protein A/G-agarose) (16). As internal controls, all membranes were subsequently stripped (glycine 0.2 M, pH 2.6 for 30 min at room temperature) of the first antibody and reprobed with anti-actin antibody. As a positive control LnCap (prostate cancer cell line) was used.

The intensity of bands representing relevant proteins was measured by Scion Image laser densitometry scanning program.

Immunofluorescence assay

Sperm cells, were rinsed three times with 0.5 mM Tris-HCl buffer, pH 7.5 and were fixed using absolute methanol for 7 min at –20 °C. AR staining was carried out, after blocking with normal human serum (10 %), using the monoclonal anti-human AR (1:200) as primary antibody and an anti-mouse IgG FITC-conjugated (1:100) as secondary antibody. To stain DNA in living cells, Hoechst 33342 (Hoechst) was added at a final concentration of 10 μg/ml. The specificity of AR was tested by using normal mouse serum instead the primary antibody (Fig. 2 D); sperm cells incubated without the primary antibody were also used as negative controls (data not shown). The cellular localization of AR and Hoecst was studied with Bio-Rad MRC 1024 confocal microscope connected to a Zeiss Axiovert 135 M inverted microscope with 600 magnification. The fluorophores were imaged separately to ensure no excitation/emission wavelength overlap, scoring a minimum of 200 spermatozoa per slide.

Immunoprecipitation of sperm proteins

Spermatozoa were washed in Earle's balanced salt solution and centrifuged at 800 x *g* for 20 min. Sperm were resuspended in the same uncapacitating medium and incubated without (control, UC) or in the presence of DHT at increasing concentrations (0.1 nM, 1 nM, 10 nM, 100 nM) for 30 min. Other samples were pretreated for 15 min with 10 μM OH-Flut. In order to evaluate the rapid effect of DHT on AR, spermatozoa were incubated in the unsupplemented Earle's medium at 37 °C and 5 % CO_2 at different times (5 min, 30 min, 1 h). To avoid non-specific binding, sperm lysates

were incubated for 2 h with protein A/G-agarose beads at 4 °C and centrifuged at 12,000 x *g* for 5 min. The supernatants (each containing 600 µg total protein) were then incubated overnight with 10 µl anti-AR and 500 µl HNTG (IP) buffer (50 mM HEPES, pH 7.4; 50 mM NaCl; 0.1% Triton X-100; 10% glycerol; 1 mM phenylmethylsulfonylfluoride; 10 µg/ml leupeptin; 10 µg/ml aprotinin; 2 µg/ml pepstatin). Immune complexes were recovered by incubation with protein A/G-agarose. The beads containing bound proteins were washed three times by centrifugation in immunoprecipitation buffer, then denaturated by boiling in Laemmli sample buffer and analyzed by Western blot to identify the coprecipitating effector proteins. Immunoprecipitation using normal mouse serum was used as negative control. Membranes were stripped of bound antibodies by incubation in glycine (0.2 M, pH 2.6) for 30 min at room temperature. Before reprobing with the different indicated antibodies, stripped membranes were washed extensively in TBS-T and placed in blocking buffer (TBS-T containing 5% milk) overnight.

Evaluation of sperm viability

Viability was assessed by using Eosin Y method. Spermatozoa were washed in uncapacitating medium and centrifuged at 800 x *g* for 20 min. To test androgen effects on sperm viability, spermatozoa were incubated in unsupplemented Earle's medium at 37 °C and 5 % CO_2 without (control, UC) or in the presence of dihydrotestosterone (DHT) at increasing concentrations (0.1 nM, 10 nM, 100 nM) or 10 nM testosterone (T) for 2 h. In a different set of experiments, sperm were incubated in unsupplemented Earle's medium at 37 °C and 5 % CO_2 without (UC) or in the presence of 10 nM DHT or T at different times (0 min, 10 min, 30 min, 2 h, 6 h and 24 h). Some samples were pre-treated for 15 min with 10 µM OH-Flut. 10 µl of Eosin Y (0.5 % in PBS) were mixed with an equal volume of sperm sample on a microscope slide. The stained dead cells and live cells that excluded the dye, were scored among a total of 200 cells and by an independent observer. Further, viability was evaluated before and after pooling the samples.

PI3K activity

Spermatozoa were washed in Earle's balanced salt solution and centrifuged at 800 x *g* for 20 min. Sperm were resuspended in the same uncapacitating medium and in different tubes containing no androgens (control, UC), T or DHT at the indicated concentrations for 30 min. Some samples were resuspended in capacitating medium (Earle's balanced salt solution medium supplemented with 600 mg BSA / 100 ml and 200 mg sodium bicarbonate / 100 ml). Some samples were pretreated for 15 min with 10 µM OH-Flut alone or each combined with increasing (0.1 nM, 1nM, 10 nM, 100 nM) DHT. The negative control was performed using a sperm lysate, where p110 catalyzing subunit of PI3K was previously removed by preincubation with the respective antibody (1 h at room temperature) and subsequently immunoprecipitated with protein A/G-agarose. The PIK3R1 was precipitated from 500 µg of sperm lysates. The immunoprecipitates were washed once with cold PBS, twice with 0.5 M LiCl, 0.1 M Tris (pH 7.4) and finally with 10 mM Tris, 100 mM NaCl, 1 mM EDTA. The presence of PI3K activity in immunoprecipitates was determined by incubating the beads with reaction buffer containing 10 mM HEPES (pH 7.4), 10 mM $MgCl_2$, 50 µM ATP, 20 µCi [γ-^{32}P] ATP, and 10 µg L-α-phosphatidylinositol-4,5-bis phosphate (PI-4,5-P_2) for 20 min at 37 °C. The reactions were stopped by adding 100 µl of 1 M HCl. Phospholipids were extracted with 200 µl $CHCl_3$/methanol. Phase separation was facilitated by centrifugation at 5000 rpm for 2 min in a tabletop centrifuge. The labelled products of the kinase reaction, the PI phosphates, in the lower chloroform phase were spotted onto *trans*-1,2-diaminocyclohexane-*N*,*N*,*N*',*N*'-tetraacetic acid–treated silica gel 60 thin-layer chromatography plates state running solvent used for TLC. Radioactive spots were visualized by autoradiography.

DNA laddering

DNA laddering was determined by gel electrophoresis. Spermatozoa were washed in Earle's balanced salt solution and centrifuged at 800 x *g* for 20 min, then were resuspended in the same uncapacitating medium and in different tubes containing no androgens (control, UC), T or DHT or

estrogen (E) or progesterone (PRG) or wortmannin (W) at the indicated concentrations for 30 min. Some samples were resuspended in capacitating medium (CAP). Some samples were pretreated for 15 min with 10 µM Cax or 10 µM OH-Flut or ZVF alone or each combined with 10 nM DHT. After incubation cells were pelletted at 800 x *g* for 10 minutes. The samples were resuspended in 0.5 ml of extraction buffer (50 mM Trios-HCl pH 8, 10mM EDTA, O.5% SDS) for 20 minutes in rotation at 4 °C. DNA was extracted with phenol/chloroform for 3 times and once with chloroform. The aqueous phase was used to precipitate acids nucleic with 0.1 volumes or of 3 M sodium acetate and 2.5 volumes cold EtOH overnight at -20 °C. The DNA pellet was resuspended in 15 µl of H_2O treated with RNAse A for 30 minutes at 37 °C. The absorbance of the DNA solution at 260 and 280 nm was determined by spectrophotometry. The extracted DNA (2 µg/lane) was subjected to electrophoresis on 1.5 % agarose gels. The gels were stained with ethidium bromide and then photographed.

STATISTICAL ANALYSIS

The experiments for RT-PCR, Immunofluorescence and Immunoprecipitation assays were repeated on at least four independent occasions, Western blot analysis was performed in at least six independent experiments, PI3K activity was performed in at least four independent experiments. The data obtained from viability (six replicate experiments using duplicate determinations) were presented as the mean ± SEM. Statistical analysis was performed using analysis of variance (ANOVA) followed by Newman-Keuls testing to determine differences in means. $p<0.05$ was considered as statistically significant.

RESULTS

AR mRNA and protein were detected in human sperm

To determine whether mRNA for *AR* is present in human ejaculated spermatozoa, RNA isolated from percoll-purified sperm samples from normal men was subjected to reverse PCR. The

nucleotide sequence of *AR* was deduced from the cDNA sequence of the human *AR* gene and our primers amplified a region from 1648 to 2055 bp corresponding to the DNA binding domain plus the hinge region of the AR. RT-PCR amplification of *AR* in human sperm revealed the expected PCR product size of 400 bp. This product was sequenced and found identical to the classical human *AR*. No detectable levels of mRNA coding either *PTPRC*, a specific marker of leucocytes, or *KIT*, a specific marker of germ cells, were found in the same semen samples (Fig 1 A), thus ruling out any potential contamination.

The presence of AR protein in human ejaculated spermatozoa was investigated by Western blot using a monoclonal antibody raised against the epitope mapping at the 299-316 aa in the N-terminus of AR from human origin (Fig. 1B). The antibody revealed in sperm two protein bands with molecular weights of approximately 110 kDa and 85-87 kDa, the latter expressed to a greater extent. The negative control (N) was performed as described in *Materials and method*.

Immunolocalization of AR in human sperm

Using an immunofluorescence technique, we identified a positive signal for AR in human spermatozoa (Fig. 2A). No immunoreaction was detected either by replacing the anti-AR antibody by normal mouse serum (Fig. 2D) or when the primary antibody was omitted (data not shown), demonstrating the immunostaining specificity. AR immunoreactivity was specifically compartmentalized at the sperm head (Fig. 2A), where the DNA is packaged as it can be seen in Fig. 2B in which the DNA is stained by Hoechst. Fig. 2C shows the merged images of A and B.

AR is phosphorylated in human sperm

It was reported that the function of AR is strongly correlated with the phosphorylation status (35) which is rapidly enhanced upon androgen exposure and it is able to activate signal transduction pathways. AR immunoprecipitates were blotted with three different antibodies: anti-p-tyrosine, anti-p-threonine and anti-p-serine. As shown in Fig. 3, two major AR antibody reactive proteins corresponding to the 85-87 and 110 kDa were observed. To determine if the changes in phosphorylation status of AR under androgen treatments may occur in ejaculated sperm, these were

exposed for 30 min to varying concentrations of DHT (0.1 nM to 10 nM). We observed that the AR phosphorylation was enhanced in a dose related manner (Fig. 3 A) and was significantly reduced by OH-Flut, an AR antagonist. To investigate if the enhanced phosphorylation status may represent an early event we performed a time course study at the following times: 0 min, 5 min, 30 min, 1 h. The time course revealed that AR phosphorylation occurred rapidly as they were observed from time 0 to 5 min and then dropped significantly after 1 h (Fig. 3 B). Moreover, all three phospho-antibodies demonstrated a prevalence for phosphorylation of the 110 kDa isoform.

Androgens effect on sperm viability

To evaluate sperm viability under androgen treatment we performed different sets of experiments. Sperm were incubated in the presence of 10 nM T or 10 nM DHT at the indicated times (Fig. 4 A). Other samples were incubated in uncapacitating medium for 2 hours in the absence or presence of different T or DHT concentrations (0.1 nM to 100 nM). As shown in Fig. 4 B the majority of cells remained viable in the control at 2 h. Cell viability significantly decreased with 10 and 100 nM T or DHT. Interestingly, the effect of androgen was reversed by using OH-Flut, addressing an AR mediated effect. It deserves to be mentioned that 100 nM androgen concentration is much higher than that commonly found circulating *in vivo* in man while about 3 nM is detected in the seminal plasma (36).

Androgen action on PI3K activity, p-AKT, p-BCL2 and pPTEN is mediated by AR

As shown in Fig. 5A low androgen concentration induced PI3K activity, while concentrations from 10 to 100 nM reduced the enzymatic activity. Both 10 nM T and to a greater extent 10 nM DHT treatments decreased PI3K activity and this effect was reversed by OH-Flut (Fig. 5 A). Concomitantly, we obtained the reduction of the downstream p-AKT S473 (Fig. 5 B) and of p-BCL2 (Fig. 5 C), a known antiapoptotic protein (37). Specifically, DHT and not testosterone has a significant inhibitory effect on p-AKT S473 levels. Further, androgens

significantly increased the phosphorylation of PTEN, a specific inhibitor of PI3K (Fig. 5 D). All the above mentioned effects were reversed by two known antiandrogens, Cax and OH-Flut, that were added alone or combined with 10 nM DHT, indicating that the effects of androgens are mediated by the classic AR in sperm. Recently, it was found that estradiol (E) enhances sperm survival signaling (14). Therefore, we aimed to evaluate in sperm if a functional interaction exists between androgen and estrogen on PI3K activity. In sperm samples incubated with 100 nM E combined with increasing (0.1 nM, 1 nM and 10 nM) DHT concentrations, the estradiol-induced PI3K activity progressively decreases (Fig. 5 E).

Androgens induce AR, PIK3R1 and phospho-SRC tyrosine kinase coimmunoprecipitation in human sperm

It was reported that a triple complex between AR, PIK3R1, and SRC tyrosine kinase is required for androgen-stimulated PI3K/AKT activation (38, 29), therefore we investigated if it also occurs in sperm. At the 0.1 nM DHT concentration, phospho-SRC tyrosine kinase coimmunoprecipitated with the two proteins immunodetected by the C-19 anti-AR antibody in sperm that migrated at 110 and 85-87 kDa. Remarkably, no association of phospho-SRC tyrosine kinase with AR occurred at the 100 nM DHT concentration. Fig. 6 shows immunocomplexes blotted with anti-AR (A) or phospho-SRC tyrosine kinase (B) or anti- PIK3R1 (C) antibodies. The possibility that androgen treatment could modify the AR level was excluded since the same amount of AR was detected by immunoblot of sperm lysates, irrespective of DHT concentration.

Our results demonstrated that, in contrast to the 100 nM DHT concentration, the 0.1 nM concentration increases coimmunoprecipitation of phospho-SRC tyrosine kinase and PI3-kinase with AR. These data may explain the mechanism through which high DHT concentration reduced PI3k activity.

Androgens effects on caspases are mediated by AR

On the basis of the abovementioned results we sought to evaluate androgen action on the caspases family (31), since these proteins are involved in cell death. Particularly, caspase 3 which is the main effector of both caspases 8 and 9, executes the final disassembly of the cell by cleaving a variety of cell structure proteins and generating DNA strand breaks. Our study revealed the caspases 8, 9 and 3 activation upon 30 min of 10 nM T or 10 nM DHT treatments. The DHT effect was reversed by both AR antagonists, 10 μM Cax or 10 μM OH-Flut (Fig. 7A). Notably, the effect on caspases is specific for androgen as it was not observed with estradiol or progesterone treatments. Particularly, progesterone treatment was performed because of the similarity in structure between Progesterone Receptor and AR. The cleavage of caspase 3 was increased by androgens in a dose-dependent manner (Fig. 7C). In the presence of wortmannin, a specific inhibitor of PI3K activity, the cleavage of caspase 3 was also observed, addressing a regulatory role of PI3K in caspase activation in sperm. Furthermore, in order to demonstrate a specific effect on caspase activation an additional control experiment was included showing that activation of caspases by androgens can be inhibited with a specific caspases inhibitor such as ZVK**.** All these data were confirmed by DNA laddering assay (Fig. 7B and Fig. 7D).

DISCUSSION

Androgens and AR have been shown to play critical roles in testis function (39). AR has been detected in Sertoli, Leydig, peritubular myoid, and spermatid cells (round and elongated) (4, 5, 6). The currently prevailing view is that sperm does not contain AR and this stems from previous studies reporting that no AR immunostaining of germ cells was observed both in rat and in human testis (6). However, several studies reported that in spermatozoa the binding capacity of androgens was greater than that of estrogens or progesterone (40, 41) and recently AR was shown to be present in sperm by Western Blot and Immunofluorescence assays (10).

In this study we have demonstrated the presence of AR in human sperm at different levels: mRNA expression, protein expression and immunolocalization. By RT-PCR we amplified a gene

region corresponding to the DNA binding domain plus the hinge region of the human AR. This product was sequenced and found to be identical to the classical human *AR*. As it concerns the presence of mRNAs in mammalian ejaculated spermatozoa, originally it was hypothesized that these transcripts were carried over from earlier stages of spermatogenesis, however new reports re-evaluate the significance of mRNA in these cells (42, 43) and the issue is currently under investigation.

To date, multiple isoforms of the AR have been described and among them two proteins were well characterized: AR-B and AR-A (44). They are believed to be derived from the same gene and differ only in the NH_2-terminal transactivation domain (44). Our antibody against an epitope (aminoacids 299–311) that is common to both the AR-A and AR-B isoforms detected two protein bands: one of 85-87 kDa and another one approximately of 110 kDa. Both, the AR-B and AR-A isoforms are expressed in a variety of fetal and adult (male and female) human tissues and especially in reproductive tissues (45). The B form migrates with an apparent mass of 110 kDa and constitutes more than 80% of the immunoreactive receptor in most cell types. The A form of the AR migrates with an apparent mass of 87 kDa. It was identified as an NH_2-terminally (from 1 to 187 aa) truncated protein of AR-B and it was first described in human genital skin fibroblasts. The detection of two distinct forms of the AR raised a number of issues. AR-A is expressed at low levels in many androgen-responsive tissues; however, it appears to have functions similar to those of the full-length AR-B isoform. Functional activities of cDNAs containing the two isoforms, were assessed using cotransfection assays that employed two models of androgen-responsive genes (MMTV-luciferase and PRE2-tk-luciferase) in response to mibolerone, a potent androgen agonist, in three different cell lines (46). These studies demonstrated subtle differences in the activities of the A and B isoforms, which depended on the promoter and cell context. Additional studies failed to reveal any major differences in the responses of the AR-A and AR-B isoforms to a variety of androgen agonists and antagonists, suggesting that the previously reported functional defect of the AR-A is due principally to its level of expression. When assays of AR function are performed under conditions in which

levels of expression of the two isoforms are equivalent, the AR-A and AR-B possess similar functional activities. The ratio of AR-B:AR-A may vary among tissues and at different stages of development. However, it is unknown whether these isoforms have divergent biologic signal transduction capacities in humans, therefore we cannot predict what is the physiological correlate of a low AR-B:AR-A ratio as observed in sperm.

By immunohistochemical assays we have demonstrated that AR protein is detectable in the sperm head. Solakidi *et al*. (10) reported AR prevalently localized in the midpiece region and the labelling pattern was similar to that of ERα. The apparent discrepancy between the latter finding and ours may be due to the different methods to process samples.

An increasing body of evidence suggests that androgens and other steroid hormones can exert rapid, nongenomic effects (12, 14). Different nuclear receptors such as progesterone receptor (15), estrogen receptor α and estrogen receptor β (16) were found to be present in human ejaculated spermatozoa, regulating cellular processes through nongenomic mechanisms. All these findings strengthen the importance of the nuclear receptors in nongenomic signalling (14) which may represent their exclusive modality of action in spermatozoa since they are apparently transcriptionally inactive cells. Here we have demonstrated that in human ejaculated sperm short exposure to androgens produces an increase in AR phosphorylation in a dose-dependent manner, while the antagonist OH-Flut significantly reduces this effect. Furthermore, we observed the most prominent phosphorylation on the 110 kDa band which is the less expressed isoform in sperm. It is known that the function of nuclear receptors is strongly correlated with their phosphorylation status rather than the level of total receptor proteins. The 110 kDa isoform exhibits a major length of the N-terminal domain which is an important effector of the cell signalling (44, 45) This may explain why the phosphorylated status of the 110 kDa appears much more pronunced than the smaller isoform. From these findings it emerges that in sperm the 110 kDa is the most involved isoform in mediating AR trafficking signals.

On the basis of our data androgens are able to modulate sperm survival depending on their concentration. To investigate the molecular mechanism involved in these effects we evaluated their action on the PI3K/AKT pathway, since it represents the main cell survival pathway and it was identified in sperm (16). 0.1 nM and 1 nM androgens induced PI3K activity which was reduced by higher concentrations (10 nM and 100 nM). 10 nM DHT was able to reduce the PI3K downstream signalling, while phosphorylation of PTEN, a proapoptotic marker which inhibits the PI3K pathway, was enhanced. To gain further insight into the mechanism involved in the PI3K/AKT modulation by AR, we investigated the association between AR/PIK3R1/p-SRC tyrosine kinase as it was reported depending on androgen concentration in somatic cells (38, 29). In our study high androgen concentrations (10 nM and 100 nM) produce a detachment of SRC tyrosine kinase from the PIK3R1 /AR complex, confirming that the triple complex is needed to the PI3K pathway activation. Furthermore, sperm treatment with wortmannin, a specific PI3K/AKT inhibitor, induced caspase 3 cleavage showing that the PI3K/AKT pathway is involved in the modulation of the caspases activity. The sperm death under high androgens (10 nM T, 10 nM and 100 nM DHT) was confirmed both by DNA laddering and cleavage of caspases 8, 9 and 3. In addition, increasing androgen concentrations were able to counteract estradiol-induced PI3K activity already previously documented (16).

It is well established that in men intratesticular testosterone levels are approximately 800 nM (47), while they are ranging from 16 to 20 nM in serum (47, 36). The androgenic milieu in seminal plasma is dependent on circulating androgen levels and no longer intratesticular levels (48, 49). The biologically active amount of T, represented by its free fraction, is mostly converted in the genital tract in DHT by 5 alpha-reductase which is particularly expressed in the epydidimus and in the adnexal glands (50). A careful evaluation of the total androgenic milieu in seminal plasma, prevalently represented by the two most important androgens T and DHT, reveals the presence of about 1 nM of T and 2 nM of DHT and their ratio is about T/DHT 0.61 (49). Therefore, the seminal androgenic milieu, prevalently represented by the total molar concentration

of T plus DHT corresponds to about 3 nM. The effects induced by the dose of 10 nM DHT were opposite to those induced by the lower dose of androgens. On the other hand, the same opposite pattern of androgen effects according to the doses tested on PI3K pathway was previously documented in other cellular type (29).

From all these findings, it emerges that an excess of androgens in the local hormonal milieu through a PI3K activity inhibition, may negatively interfere in the sperm survival. Concluding, in human sperm AR is able to modulate PI3K/AKT pathway on the basis of the androgen levels. Further work will be required to more fully elucidate the role that AR plays in male fertility.

REFERENCES

1. Collins LL, Lee HJ, Chen YT, Chang M, Hsu HY, Yeh S, Chang C. The androgen receptor in spermatogenesis. Cytogenet Genome Res 2003;103:299-301.
2. De Gendt K, Swinnen JV, Saunders PT, Schoonjans L, Dewerchin M, Devos A, Tan K, Atanassova N, Claessens F, Lecureuil C, Heyns W, Carmeliet P, Guillou F, Sharpe RM, Verhoeven G. A Sertoli cell-selective knockout of the androgen receptor causes spermatogenic arrest in meiosis. Proc Natl Acad Sci 2004; 101:1327-1332.
3. Yeh S, Tsai MY, Xu Q, Mu XM, Lardy H, Huang KE, Lin H, Yeh SD, Altuwaijri S, Zhou X, Xing L, Boyce BF, Hung MC, Zhang S, Gan L, Chang C. Generation and characterization of androgen receptor knockout (ARKO) mice: an in vivo model for the study of androgen functions in selective tissues. Proc Natl Acad Sci U S A 2002; 99:13498-13503. Erratum in: Proc Natl Acad Sci U S A 2002; 12;99:15245. Hung Min-Chi [corrected to Hung Mien-Chie].

4. Kimura N, Mizokami A, Oonuma T, Sasano H, Nagura H. Immunocytochemical localization of androgen receptor with polyclonal antibody in paraffin-embedded human tissues. J Histochem Cytochem 1993; 41:671–678.
5. Vornberger W, Prins G, Musto NA, Suarez-Quian CA. Androgen receptor distribution in rat testis: new implications for androgen regulation of spermatogenesis. Endocrinology 1994; 134:2307–2316.
6. Suarez-Quian CA, Martinez-Garcia F, Nistal M, Regadera J. Androgen receptor distribution in adult human testis. J Clin Endocrinol Metab 1999; 84:350-358.
7. Ruizeveld de Winter JA, Trapman J, Vermey M, Mulder E, Zegers ND, van der Kwast TH. Androgen receptor expression in human tissues: an immunohistochemical study. J Histochem Cytochem 1991; 39:927–936.
8. Iwamura M, Abrahamsson P-A, Benning CM, Cockett AT, Di Sant'Agnese PA. Androgen receptor immunostaining and its tissue distribution in formalin fixed, paraffin-embedded sections after microwave treatment. J Histochem Cytochem 1994; 42:783–788.
9. Goyal HO, Bartol FF, Wiley AA, Neff CW. Immunolocalization of receptors for androgen and estrogen in male caprine reproductive tissues: unique distribution of estrogen receptors in efferent ductule epithelium. Biol Reprod 1996; 56:90–101.
10. Solakidi S, Psarra AM, Nikolaropoulos S, Sekeris CE. Estrogen receptors {alpha} and {beta} (ER{alpha} and ER{beta}) and androgen receptor (AR) in human sperm: localization of ER{beta} and AR in mitochondria of the midpiece. Hum Reprod 2005; 20:3481-3487.
11. McPhaul M J, Young M. Complexities of androgen action. J Am Acad Dermatol 2001; 45:S87-S94.
12. Peterziel H, Mink S, Schonert A, Becker M, Klocker H, Cato AC. Rapid signalling by androgen receptor in prostate cancer cells. Oncogene 1999; 18:6322-6329.

13. Castoria G, Lombardi M, Barone MV, Bilancio A, Di Domenico M, De Falco A, Varricchio L, Bottero D, Nanayakkara M, Migliaccio A, Auricchio F. Rapid signalling pathway activation by androgens in epithelial and stromal cells. Steroids 2004; 69:517-522.
14. Cato ACB, Nestl A, Mink S. Rapid actions of steroid receptors in cellular signaling pathways. Sci STKE 2002; 138:RE9.
15. Calogero AE, Burrello N, Barone N, Palermo I, Grasso U, D'Agata R. Effects of progesterone on sperm function: mechanisms of action. Hum Reprod 2000; 15:28-45.
16. Aquila S, Sisci D, Gentile ME, Middea E, Catalano S, Carpino A, Rago V, Andò S. Estrogen Receptor (ER) α and ER β Are Both Expressed in Human Ejaculated Spermatozoa: Evidence of Their Direct Interaction with Phosphatidylinositol-3-OH Kinase/Akt Pathway. J Clin Endoc Metab 2004; 89:1443-1451.
17. Olsen NJ, Viselli SM, Fan J, Kovacs WJ. Androgens Accelerate Thymocyte Apoptosis. Endocrinology 1998; 139:748-752.
18. King KJ, Nicholson HD, Assinder SJ. Effect of increasing ratio of estrogen: androgen on proliferation of normal human prostate stromal and epithelial cells, and the malignant cell line LNCaP. Prostate 2006; 66:105-114.
19. Heisler LE, Evangelou A, Lew AM, Trachtenberg J, Elsholtz HP, Brown TJ. Androgen-dependent cell cycle arrest and apoptotic death in PC-3 prostatic cell cultures expressing a full-length human androgen receptor. Mol Cell Endocrinol 1997; 126:59-73.
20. Shetty G, Wilson G, Hardy MP, Niu E, Huhtaniemi I, Meistrich ML. Inhibition of recovery of spermatogenesis in irradiated rats by different androgens. Endocrinology 2002;143:3385-3396.
21. Cohen GM. Caspases - the executioners of apoptosis. Biochem J 1997; 326:1-16.
22. Olson M, Kornbluth S. Mitochondria in apoptosis and human disease. Curr Mol Med 2001; 1:91-122.

23. Schulze-Osthoff K, Ferrari D, Los M, Wesselborg S, Peter ME. Apoptosis signaling by death receptors. Eur J Biochem 1998; 254:439-459.
24. Shim D, Kang HY, Jeon BW, Kang SS, Chang SI, Kim HY. Protein kinase B inhibits apoptosis induced by actinomycin D in ECV304 cells through phosphorylation of caspase 8. Arch Biochem Biophys 2004; 425:214-220.
25. Cardone MH, Roy N, Stennicke HR, Salvesen GS, Franke TF, Stanbridge E, Frisch S, Reed JC. Regulation of cell death protease caspase-9 by phosphorylation. Science 1998; 282:1318-1321.
26. Parsons R. Human cancer, PTEN and the PI-3 kinase pathway. Semin Cell Dev Biol 2004; 15:171–176.
27. Maehama T, Dixon JE. The tumor suppressor, PTEN/MMAC1, dephosphorylates the lipid second messenger, phosphatidylinositol 3,4,5-trisphosphate. J Biol Chem 1998; 273:13375–13388.
28. Wu X, Senechal K, Neshat MS, Whang YE, Sawyers CL. The PTEN/MMAC1 tumor suppressor phosphatase functions as a negative regulator of the phosphoinositide 3-kinase/AKT pathway. Proc Natl Acad Sci U S A 1998; 95:15587–15591.
29. Castoria G, Lombardi M, Barone MV, Bilancio A, Di Domenico M, Bottero D, Vitale F, Migliaccio A, Auricchio F. Androgen-stimulated DNA synthesis and cytoskeletal changes in fibroblasts by a nontranscriptional receptor action. J Cell Biol 2003; 161:547-556.
30. Sakkas D, Seli E, Bizzaro D, Tarozzi N, Manicardi GC. Abnormal spermatozoa in the ejaculate: abortive apoptosis and faulty nuclear remodelling during spermatogenesis. Reprod Biomed Online 2003; 7:428-432.
31. Paasch U, Grunewald S, Agarwal A, Glandera HJ. Activation pattern of caspases in human spermatozoa. Fertil Steril 2004; 81:802-809.

32. Said TM, Paasch U, Glander HJ, Agarwal A. Role of caspases in male infertility. Hum Reprod Update 2004; 10:39-51.
33. World Health Organization. WHO laboratory manual for the examination of human semen and sperm-cervical mucus interactions. 4th ed Cambridge, UK: Cambridge University Press 1999.
34. Aquila S, Sisci D, Gentile ME, Middea E, Siciliano L, Andò S. Human ejaculated spermatozoa contain active P450 aromatase. J Clin Endocrinol Metab 2002; 87:3385-3390.
35. Wang LG, Liu XM, Kreis W, Budman DR. Phosphorylation/dephosphorylation of androgen receptor as a determinant of androgen agonistic or antagonistic activity. Biochem Biophys Res Commun 1999; 259:21-28.
36. Luboshitzky R, Kaplan-Zverling M, Shen-Orr Z, Nave R, Herer P. Seminal plasma androgen/oestrogen balance in infertile men. Int J Androl 2002; 25:345-351.
37. Ito T, Deng X, Carr BK, May WS. Bcl-2 phosphorylation required for anti-apoptosis function. J Biol Chem 1997; 272:11671–11673.
38. Sun M, Yang L, Feldman RI, Sun XM, Bhalla KN, Jove R, Nicosia SV, Cheng JQ. Activation of phosphatidylinositol 3-kinase/Akt pathway by androgen through interaction of PIK3R1, androgen receptor, and Src. J Biol Chem 2003; 278:42992-43000.
39. Collins LL, Lee HJ, Chen YT, Chang M, Hsu HY, Yeh S, Chang C. The androgen receptor in spermatogenesis. Cytogenet Genome Res 2003; 103:299-301.
40. Cheng CY, Boettcher B, Rose RJ, Kay DJ, Tinneberg HR. The binding of sex steroids to human spermatozoa. An autoradiographic study. Int J Androl 1981; 4:1-17.
41. Hyne RV, Boettcher B. The selective binding of steroids by human spermatozoa. Contraception 1977; 15:163-174.

42. Miller D, Ostermeier GC, Krawetz SA. The controversy, potential and roles of spermatozoal RNA. Trends Mol Med 2005; 11:156-163.
43. Ando S, Aquila S. Arguments raised by the recent discovery that insulin and leptin are expressed in and secreted by human ejaculated spermatozoa. Mol Cell Endocrinol 2005; 245:1-6.
44. Wilson CM, McPhaul MJ. A and B forms of the androgen receptor are expressed in a variety of human tissues. Mol Cell Endocrinol 1996; 120:51-57.
45. Wilson CM, McPhaul MJ. A and B forms of the androgen receptor are present in human genital skin fibroblasts. Proc Natl Acad Sci USA 1994; 91:1234–1238.
46. Gao T, McPhaul MJ. Functional activities of the A and B forms of the human androgen receptor in response to androgen receptor agonists and antagonists. Mol Endocrinol 1998;12:654-663.
47. Coviello AD, Bremner WJ, Matsumoto AM, Herbst KL, Amory JK, Anawalt BD, Yan X, Brown TR, Wright WW, Zirkin BR, Jarow JP. Intratesticular testosterone concentrations comparable with serum levels are not sufficient to maintain normal sperm production in men receiving a hormonal contraceptive regimen. J Androl 2004; 25:931-938.
48. Kuwahara M. The effects of ligation of vas deferens, corpus epididymidis and vasa efferentia on the testicular function in rats.Tohoku J Exp Med 1976; 120:251-257.
49. Ando S, Giacchetto C, Beraldi E, Panno ML, Carpino A, Sposato G, Lombardi A. Testosterone and dihydrotestosterone seminal plasma levels in varicocele patients. Andrologia 1983;15:374-379.
50. Steers WD. 5alpha-reductase activity in the prostate. Urology 2001; 58:17-24

Acknowledgments

Our special thank to Domenico Sturino (Faculty of Pharmacy, University of Calabria – Italy) for the English review of the manuscript and to Dr. Vincenzo Cunsolo (Biogemina SAS, Catania – Italy).

FIGURE LEGENDS

FIG 1 *AR* expression in human ejaculated spermatozoa

A: Reverse transcription-PCR analysis of human *AR* gene, *KIT* and *PTPRC* in percolled human ejaculated spermatozoa (S1), negative control (no M-MLV reverse transcriptase added) (-), positive control (LnCap, prostate cancer cell; T, human testis and L, human leucocytes), marker (M). Arrows indicate the expected size of the PCR products; **B:** Western blot of AR protein by using a monoclonal antibody raised against the epitope 299-316 of the AR from human origin: Extracts of percolled sperm, were subjected to electrophoresis on 10% SDS-Polyacrylamide gels, blotted onto nitrocellulose membranes and probed with the above mentioned antibody. Expression of the receptors in three samples of ejaculated spermatozoa from normal men (S1, S2, S3). LNCap cells were used as positive control. (N), negative control performed as described in *Materials and method*. The experiments were repeated at least four times and the autoradiographs of the figure show the results of one representative experiment.

FIG 2 Immunolocalization of AR in human ejaculated spermatozoa

Spermatozoa were extensively washed and incubated in the unsupplemented Earle's medium for 30 min at 37 °C and 5 % CO_2 . Spermatozoa were then fixed and analyzed by immunostaining as detailed in *Materials and Methods*. (A) AR localization in sperm; (B) Staining with Hoechst of spermatozoa nuclei; (C) Overlapping images of A/B; (D) Sperm cells incubated replacing the anti-AR antibody by normal mouse IgG were utilized as negative control. The pictures shown are representative examples of experiments that were performed at least four times with reproducible results.

FIG 3 AR is phosphorylated in human sperm

AR phosphorylation was determined by immunoprecipitation using an AR specific antibody. The immunoprecipitates were blotted with three different antibody: anti-p-tyrosine (pTyrAR), anti-p-threonine (pThrAR) and anti-p-serine (pSerAR). **A**: Sperm were incubated without (control, UC) or in the presence of DHT at increasing concentrations (0.1 nM, 1 nM, 10 nM) for 30 min. Some samples were pre-treated for 15 min with 10 µM OH-Flut. The autoradiographs presented are representative examples of experiments that were performed at least four times with repetitive results. Molecular weight markers are indicated on the right of the blot. The histograms indicated on the right of each blot are the quantitative representation after densitometry of data (mean ± S.D.) of four independent experiments. •$P < 0.05$, ••$P < 0.01$ DHT-treated *vs* untreated cells and *$p<0.05$ 10 nM DHT *vs* 0.1 nM DHT. **B**: Time course of sperm incubated without (control, UC) or in the presence of 10 nM DHT. Six hundred micrograms of sperm lysates were immunoprecipitated using anti-AR and then blotted with specific antibodies raised to anti-p-tyrosine, anti-p-serine, anti-p-threonine, anti-AR. Immunoprecipitation by using normal mouse serum was used as negative control (N). The autoradiographs presented are representative examples of experiments that were performed at least four times with repetitive results. Molecular weight markers are indicated on the right of the blot. The histograms indicated on the right of each blot are the quantitative representation after densitometry of data (mean ± S.D.) of four independent experiments. $P < 0.05$, ••$P < 0.01$ DHT-treated *vs* untreated cells.

FIG 4 Effect of androgen on sperm viability

Viability was assessed by using Eosin Y as described in *Materials and Method*. **A**: Time course of sperm incubated in the unsupplemented Earle's medium at 37 °C and 5 % CO_2 without (UC) or in the presence of 10 nM T or 10 nM DHT. **B**: Sperm were incubated without (UC) or in the presence of T or DHT at increasing concentrations (0.1 nM, 10 nM, 100 nM) for 2 h. Some samples were pretreated for 15 min with 10 µM OH-Flut and then treated with 10 nM T or DHT. All experiments

were repeated at least six independent times with duplicate samples, and the values represent the mean ± SEM. •P < 0.05, ••P < 0.01, •••P < 0.005 versus control.

FIG 5 Androgens action on PI3K activity, p-AKT , p-BCL2 and pPTEN is mediated by AR

Washed pooled sperm from normal samples were incubated in the unsupplemented Earle's medium at 37 °C and 5 % CO_2, in the absence (UC) or in the presence of 10 nM T or in the presence of DHT at increasing concentrations (0.1 nM, 1 nM, 10 nM, 100 nM) for 30 min. 500 µg of sperm lysates were used for PI3K activity in sperm incubated at the indicated DHT concentatrions in the absence or in the presence of 10 µM OH-Flut (**A**). The autoradiograph presented is representative example of experiments that were performed at least four times with repetitive results. The histograms indicated on the bottom of the figure are the quantitative representation after densitometry of data (mean ± S.D.) of four independent experiments. ••P < 0.01 T and DHT-treated *vs* untreated cells, **p<0.01 10 nM and 100 nM DHT *vs* 0.1 nM and 1 nM DHT, ◆◆ p<0.01 and ◆ p<0.05 10 µM OH-Flut plus DHT-treated *vs* DHT treated cells. 50 µg of sperm lysates were used for western blot analysis of p-AKT S473 (**B**), p-BCL2 (**C**) and p-PTEN (**D**). The autoradiographs presented are representative examples of experiments that were performed at least six times with repetitive results. The histograms indicated on the right of each blot are the quantitative representation after densitometry of data (mean ± S.D.) of six independent experiments. ••P < 0.01 Capacitated (CAP) or DHT-treated *vs* untreated cells, •P < 0.05 T-treated *vs* untreated cells, ◆ p<0.05 10 and ◆◆ p<0.01 µM OH-Flut plus DHT or Cax plus DHT-treated *vs* DHT treated cells. **E**: PI3K activity of sperm incubated with estradiol (E) and/or DHT at the indicated increasing concentrations. The negative controls were performed using a sperm lysate, where p110 catalyzing subunit of PI3K was previously removed by preincubation with the respective antibody (1 h at room temperature) and subsequently immunoprecipitated with protein A/G-agarose (N). The autoradiographs presented are representative examples of experiments that were performed at least four times with repetitive

results. The histograms indicated on the bottom of the figure are the quantitative representation after densitometry of data (mean ± S.D.) of four independent experiments. ●●P < 0.01 DHT- and E-treated *vs* untreated cells, ◆ p<0.05 10, ◆◆ p<0.01 and ◆◆◆ p<0.001 E plus DHT-treated vs DHT-trated cells.

Fig 6 AR, PIK3R1 and phospho-SRC tyrosine kinase coimmunoprecipitate in human sperm.

Washed spermatozoa from normal samples were incubated in the unsupplemented Earle's medium for 30 min at 37 °C and 5% CO_2, without (UC) or in the presence of DHT at increasing concentrations (0.1 nM, 1 nM, 10 nM, 100 nM). 700 µg of sperm lysates were immunoprecipitated using anti-AR antibody and then blotted with specific antibodies raised to AR (A), p-SRC tyrosine kinase (B) and PIK3R1 (C). LnCap lysates were used as positive control (lane 1); Immunoprecipitation by using normal mouse serum was used as negative control (N). The autoradiographs presented are representative examples of experiments that were performed at least four times with repetitive results. Molecular weight markers are indicated *on the left* of the blot.

Fig 7 Androgens effects on caspases are mediated by AR

A: Washed pooled sperm from normal samples were incubated in the unsupplemented Earle's medium at 37 °C and 5 % CO_2 (UC) in the presence of 10 nM T or 10 nM DHT or 100 nM E for 30 min. Some samples were washed with the unsupplemented Earle's medium and incubated in capacitating medium (CAP). Some samples were treated with Cax or Flut or ZVF each alone or combined with 10 nM DHT. The sperm were lysed and subjected to western blot analysis. 70 µg of sperm lysates were used for western blot analysis of caspase 8, caspase 9 and caspase 3. **B:** DNA laddering was performed in sperm treated as indicated. **C:** Effect of increasing DHT concentrations (0.1 nM to 100 nM), 100 nM PRG and 10 µM wortmanninn (W) on caspase 3 cleavage. The experiments were repeated at least six times and the autoradiographs of the figure show the results of one representative experiment. **D:** DNA laddering was performed in sperm treated as indicated.

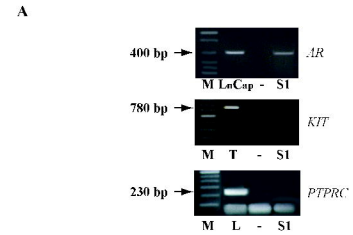
A
400 bp
AR
M LnCap - S1
780 bp
KIT
M T - S1
230 bp
PTPRC
M L - S1
B
110 kDa
85- 87 kDa
AR
LnCap N S1 S2 S3

Fig. 1

A

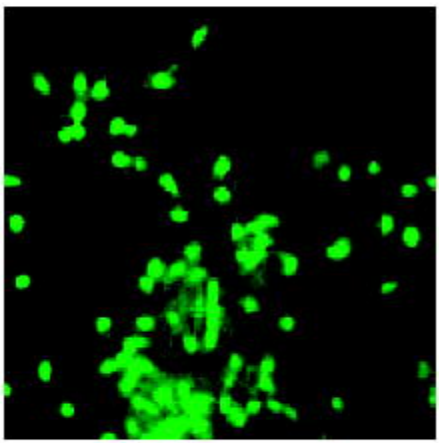

B

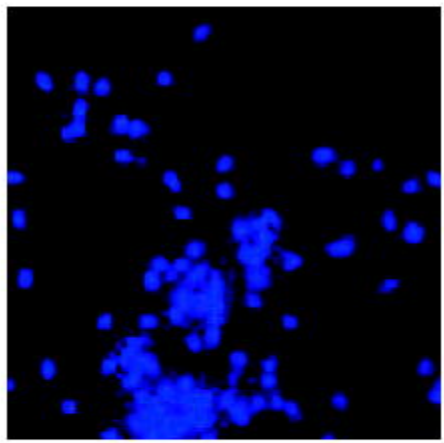

C

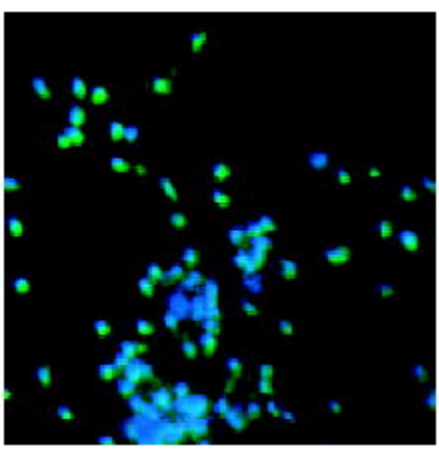

D

Fig. 2

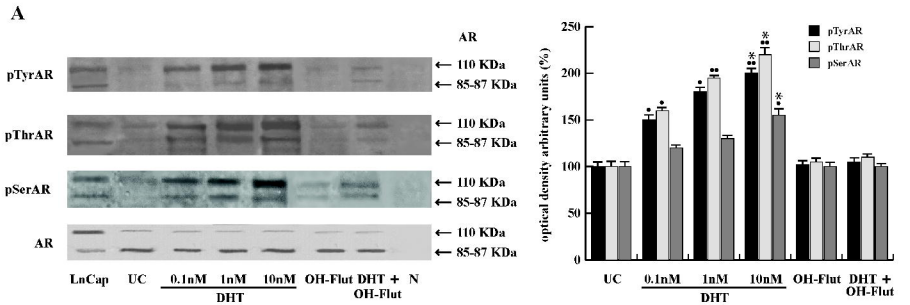
A
AR
pTyrAR
pThrAR
pSerAR
AR
← 110 KDa
← 85-87 KDa
LnCap
UC
0.1nM
1nM
10nM
DHT
OH-Flut
DHT + OH-Flut
N
optical density arbitrary units (%)
pTyrAR
pThrAR
pSerAR
250
200
150
100
50
0
UC
0.1nM
1nM
10nM
DHT
OH-Flut
DHT + OH-Flut

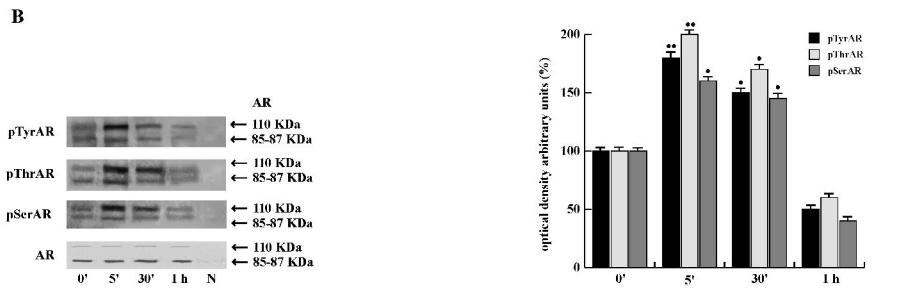
B
AR
pTyrAR
pThrAR
pSerAR
AR
← 110 KDa
← 85-87 KDa
0'
5'
30'
1 h
N
optical density arbitrary units (%)
pTyrAR
pThrAR
pSerAR
200
150
100
50
0
0'
5'
30'
1 h

Fig. 3

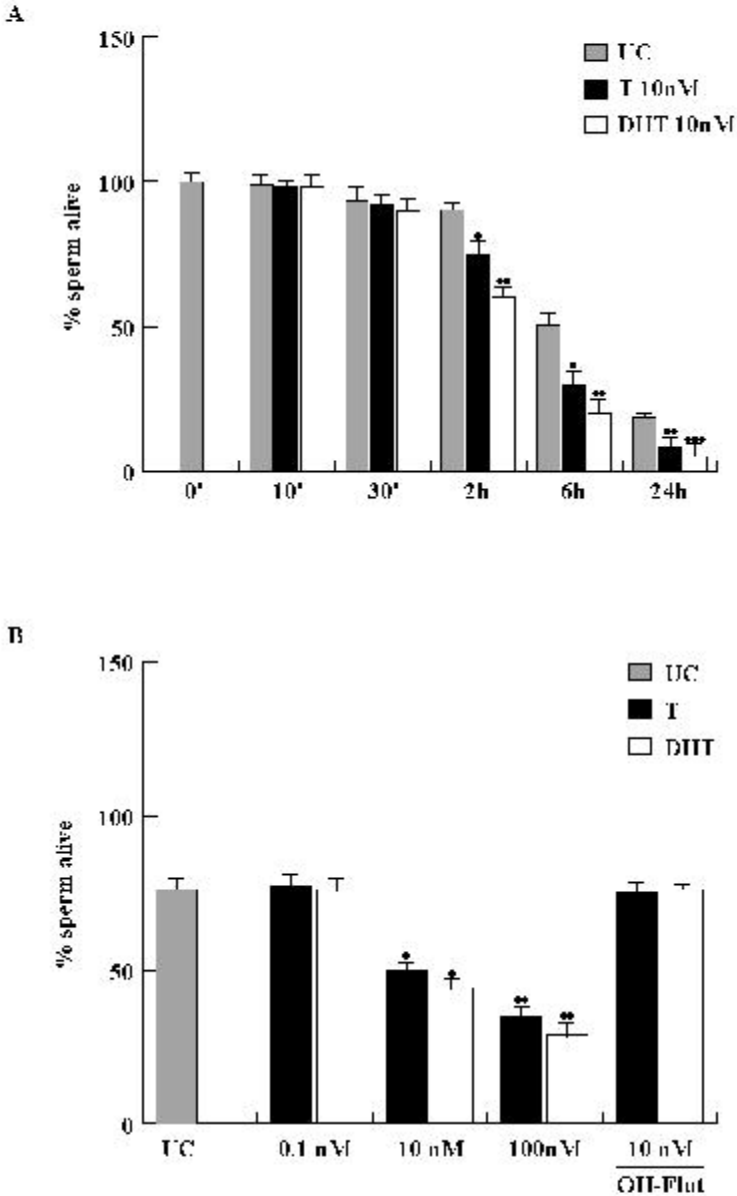
A
150
100
50
0
% sperm alive
UC
T 10nM
DHT 10nM
0'
10'
30'
2h
6h
24h
B
150
100
50
0
% sperm alive
UC
T
DHT
UC
0.1 nM
10 nM
100nM
10 nM
OH-Flut

Fig. 4

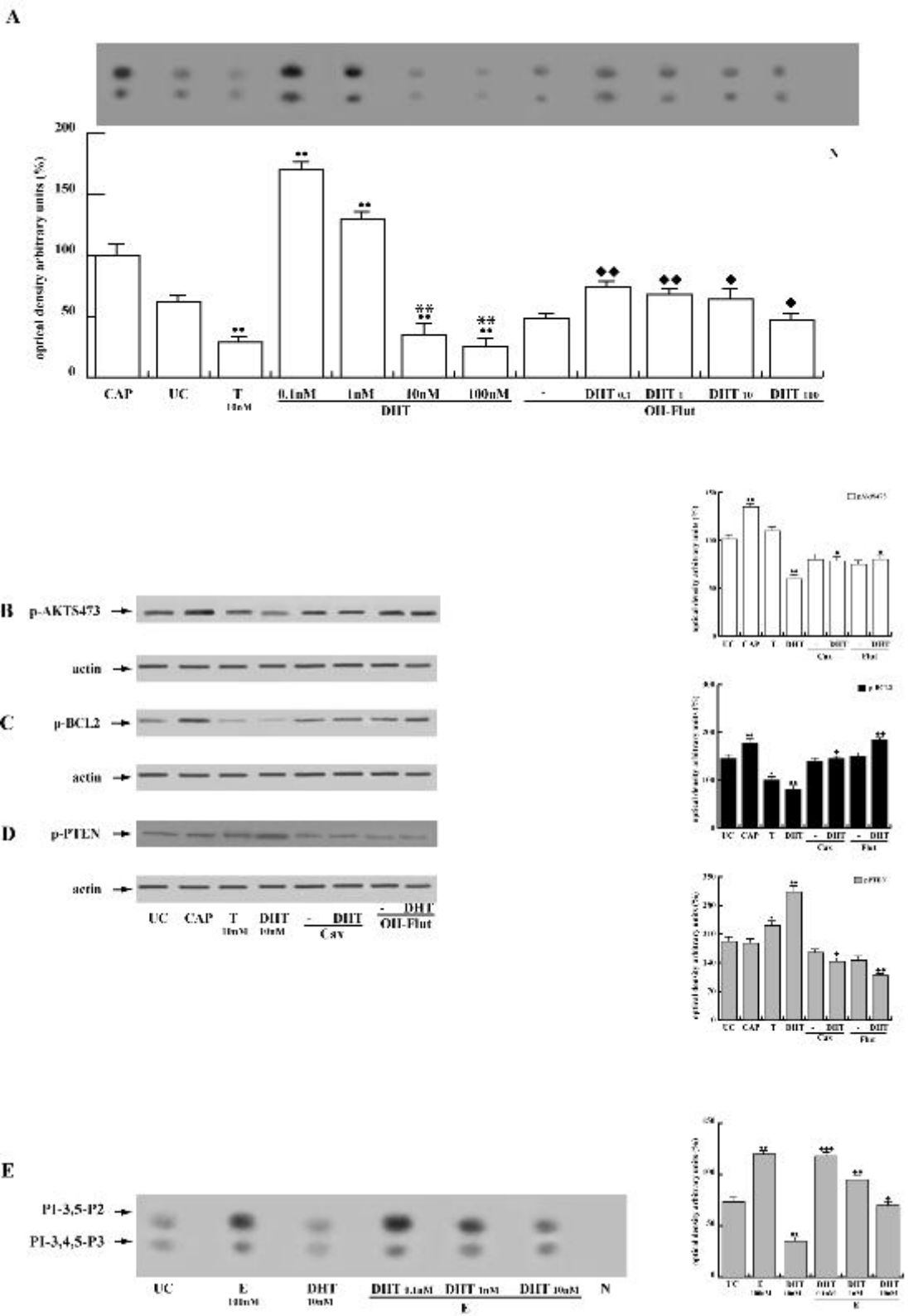
A
optical density arbitrary units (%)
200
150
100
50
0
CAP
UC
T
10nM
0.1nM
1nM
10nM
100nM
DHT
-
DHT 0.1
DHT 1
DHT 10
DHT 100
OH-Flut
N
B
p-AKTS473
actin
C
p-BCL2
actin
D
p-PTEN
actin
UC
CAP
T
10nM
DHT
10nM
-
DHT
Cav
-
DHT
OH-Flut
E
PI-3,5-P2
PI-3,4,5-P3
UC
E
100nM
DHT
10nM
DHT 0.1nM
DHT 1nM
DHT 10nM
N
E

Fig. 5

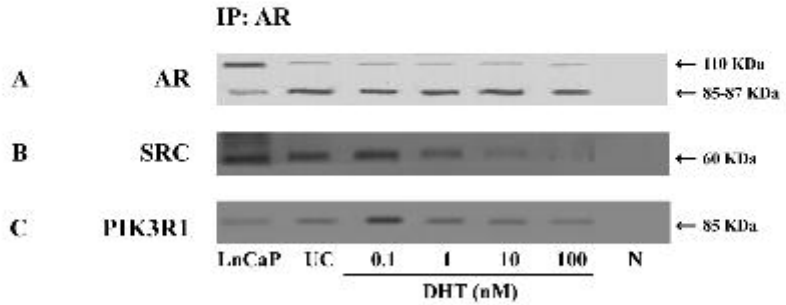
IP: AR
A
AR
← 110 KDa
← 85-87 KDa
B
SRC
← 60 KDa
C
PIK3R1
← 85 KDa
LnCaP
UC
0.1
1
10
100
N
DHT (nM)

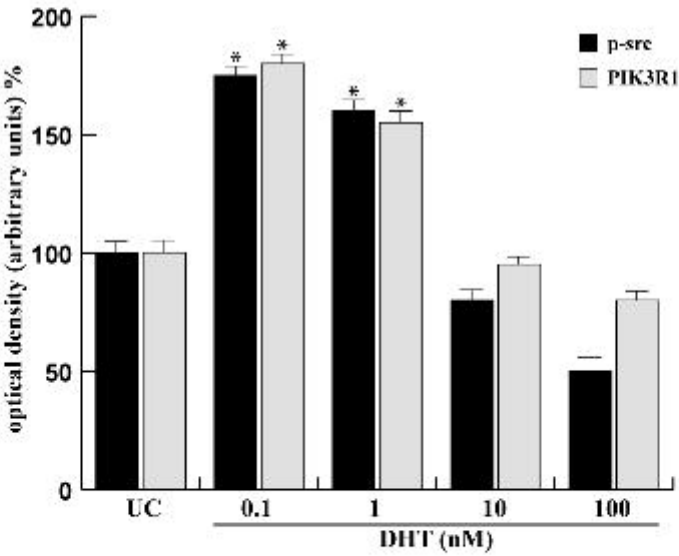
optical density (arbitrary units) %
200
150
100
50
0
p-src
PIK3R1
*
UC
0.1
1
10
100
DHT (nM)

Fig. 6

A

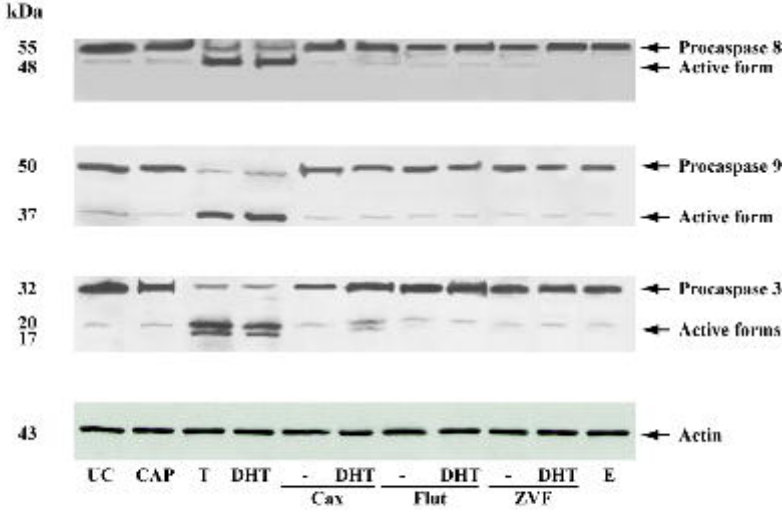
kDa
55
48
Procaspase 8
Active form
50
37
Procaspase 9
Active form
32
20
17
Procaspase 3
Active forms
43
Actin
UC CAP T DHT - DHT - DHT - DHT E
Cax
Flut
ZVF

B

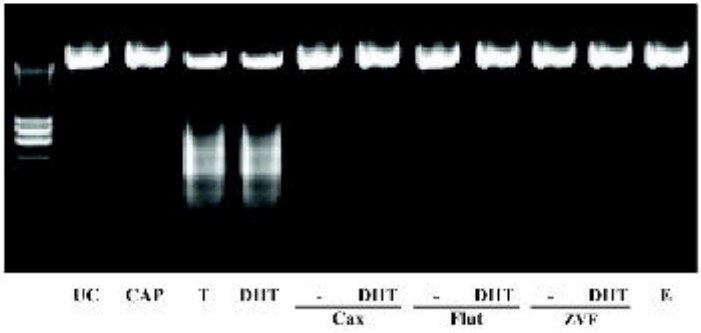
UC CAP T DHT - DHT - DHT - DHT E
Cax
Flut
ZVF

C

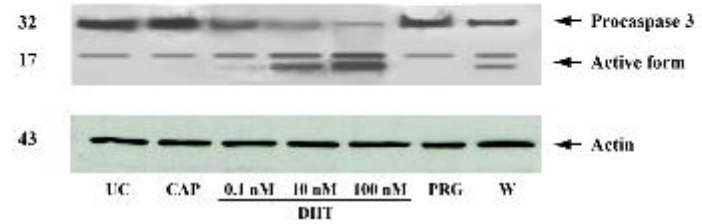
32
17
Procaspase 3
Active form
43
Actin
UC CAP 0.1 nM 10 nM 100 nM PRG W
DHT

D

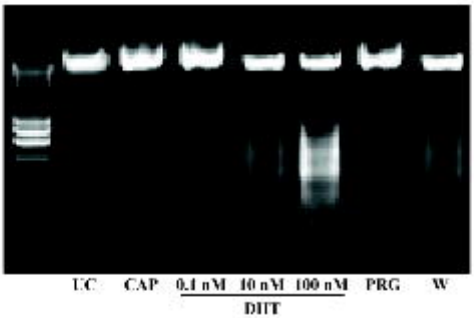
UC CAP 0.1 nM 10 nM 100 nM PRG W
DHT

Fig. 7

Table 1 Oligonucleotide sequences used for RT-PCR

Gene	Sequence (5' - 3')	Size of PCR product (bp)
AR	5' - TGCCCATTGACTATTACTTTCC - 3' 5' - TGTCCAGCACACACTACACC - 3'	400
KIT	5' - AGTACATGGACATGAAACCTGG - 3' 5' - GATTCTGCTCAGACATCGTCG - 3'	780
PTPRC	5' - CAATAGCTACTACTCCATCTAAGCCA - 3' 5' - ATGTCTTATCAGGAGCAGTACATG - 3'	230

JOURNAL OF CELLULAR PHYSIOLOGY 209:977–986 (2006)

Peroxisome Proliferator-Activated Receptor (PPAR)γ Is Expressed By Human Spermatozoa: Its Potential Role on the Sperm Physiology

SAVERIA AQUILA,[1,4] DANIELA BONOFIGLIO,[1] MARIAELENA GENTILE,[2,4] EMILIA MIDDEA,[1,4] SABRINA GABRIELE,[1] MARIA BELMONTE,[1] STEFANIA CATALANO,[1,4] MICHELE PELLEGRINO,[2] AND SEBASTIANO ANDÒ[3,4]*

[1]*Department of Pharmaco-Biology, University of Calabria, Arcavacata di Rende (Cosenza), Italy*
[2]*Department of Cellular Biology, University of Calabria, Arcavacata di Rende (Cosenza), Italy*
[3]*Faculty of Pharmacy, University of Calabria, Arcavacata di Rende (Cosenza), Italy*
[4]*Centro Sanitario, University of Calabria, Arcavacata di Rende (Cosenza), Italy*

The peroxisome proliferation-activated receptor gamma (PPARγ) is mainly expressed in the adipose tissue and integrates the control of energy, lipid, and glucose homeostasis. The present study, by means of RT-PCR, Western blot, and immunofluorescence techniques, demonstrates that human sperm express the PPARγ. The functionality of the receptor was evidenced by 15-deoxy-12,14-prostaglandin J_2 (PGJ2) and rosiglitazone (BRL) PPARγ-agonists that were tested on capacitation, acrosome reaction, and motility. Both treatments also increase AKT phosphorylations and influence glucose and lipid metabolism in sperm. The specificity of PGJ2 and BRL effects through PPARγ on human sperm was confirmed by an irreversible PPARγ antagonist, GW9662. Our findings provide evidence that human sperm express a functional PPARγ whose activation influences sperm physiology. In conclusion, the presence of PPARγ in male gamete broadens the field of action of this nuclear receptor, bringing us to look towards sperm as an endocrine mobile unit independent of the systemic regulation. J. Cell. Physiol. 209: 977–986, 2006. © 2006 Wiley-Liss, Inc.

The peroxisome proliferator-activated receptor gamma (PPARγ) is member of the nuclear receptor superfamily that integrates the control of energy, lipid, and glucose homeostasis (Rangwala and Lazar, 2004; Kota et al., 2005). Like all nuclear receptors, PPARγ has a modular structure that comprises: the N-terminal A/B domain, harboring a ligand-independent transcriptional activation function (AF-1), the DNA-binding domain, which contains two zinc fingers, and the C-terminal region, containing the ligand-binding domain and the ligand-dependent activation domain AF-2. The principal site of expression of PPARγ is the adipose tissue (Gurnell, 2005), but this receptor is also present, albeit at lower levels, in many other tissues and cell types such as epithelial cells (Pan et al., 2005), B- and T-cells (Kostadinova et al., 2005), macrophages (Genolet et al., 2004), endothelial cells (Nicol et al., 2005), neutrophils (Standiford et al., 2005 and references therein), and smooth muscle cells (Wang et al., 2006).

The activity of PPARγ is governed by the binding to small lipophilic ligands. Endogenous ligands include a versatile array of compounds such as polyunsaturated fatty acids and eicosanoids derived from nutrition or metabolic pathways and comprising the prostaglandin D2 metabolite 15-deoxy-12,14-prostaglandin J_2 (PGJ2) (Kobayashi et al., 2005). PPARγ is also activated by synthetic compounds termed thiazolidinediones (TZDs), class of insulin-sensitizing agents that are used to treat type II diabetes (Petersen et al., 2000). Uncertainty surrounds, despite intensive investigation and years of clinical use of TZDs, the mechanisms by which activation of PPARγ promotes insulin sensitivity. In addition to their anti-hyperglycemic effects, these compounds also dramatically reduce circulating levels of triglycerides and non-esterified free fatty acids. To date, much still remains unclear and unknown about the specific target tissues of TZDs. Adipose tissue is one likely target, and other candidate sites for TZD action include skeletal muscle, liver and pancreatic beta cells, and tissue-specific conditional knockouts of PPARγ are now being used to address all these questions (Kintscher and Law, 2005 and references therein). However, the function of PPARγ is not restricted to adipogenesis and insulin sensitization. In peripheral monocytes and macrophages, PPARγ-agonists are reported to inhibit the production of inflammatory cytokines (Skolnik et al., 2002). PPARγ ligands can also induce differentiation and apoptosis in breast (Yee et al., 2003), prostate cancer (Xu et al., 2003), and non-small cell lung cancer (Chang and Szabo, 2000).

The mechanisms controlling the interaction between energy balance and reproduction are the subject of intensive investigations and compelling evidence demonstrates a close link between energy status and reproductive function (Quandt, 1984; Moschos et al., 2002). The integrated control of those systems is

Saveria Aquila and Daniela Bonofiglio equally contributed to this work.

Contract grant sponsor: PRIN 2004 Prot. N. 0067227, AIRC–2004, MURST and Ex 60% -2005.

*Correspondence to: Sebastiano Andò, Faculty of Pharmacy, University of Calabria, Arcavacata di Rende (Cosenza) 87036, Italy. E-mail: sebastiano.ando@unical.it

Received 9 May 2006; Accepted 30 June 2006

DOI: 10.1002/jcp.20807

probably a multi-faceted phenomenon conducted by an array of signals governing energy homeostasis, metabolism, and fertility. Interestingly, it was documented that augmented insulin sensitivity may improve ovulatory function and fertility in women with polycystic ovary syndrome (Seli and Duleba, 2002). In mice, the loss of the PPARγ gene in oocytes and granulosa cells resulted in impaired fertility (Cui et al., 2002).

The energy homeostasis depends on very well tuned machinery balancing energy storage and expenditure. The transcriptional regulation, affecting the levels of expression of key proteins is the most effective mechanism on a longer time scale, however it is now quite clear that some transcriptional factors as nuclear receptors, in addition to their classic genomic action, also regulate cellular processes through their non-genomic mechanism (Cato et al., 2002). Different nuclear receptors such as progesterone receptor (Shah et al., 2005), estrogen receptor α, and estrogen receptor β (Aquila et al., 2004) were found to be present in human-ejaculated spermatozoa, regulating cellular processes through their non-genomic mechanisms. All these findings strengthen the importance of the nuclear receptors non-genomic signaling, which may represent their exclusive modality of action in spermatozoa as they are apparently transcriptional inactive cells. Sperm functionalities need to be rapidly activated to accommodate dynamic changes in the surrounding milieu. These mechanisms would enable the sperm to use tools which are already present and which get functionally activated or repressed.

The significance of PPARγ in male fertility is not yet been investigated and no published reports are available on the impact of PPARγ agonists on male fertility. In the current study, we showed the expression of PPARγ in human sperm providing a unique approach to study lipid and glucose metabolism at molecular level in the male gamete.

MATERIALS AND METHODS

Chemicals

PMN Cell Isolation Medium was from BIOSPA (Milan, Italy). Total RNA Isolation System kit, enzymes, buffers, nucleotides 100-bp ladder used for RT-PCR were purchased from Promega (Milan, Italy). Moloney Murine Leukemia Virus (M-MLV) was from Gibco BRL—Life Technologies Italia (Milan, Italy). Oligonucleotide primers were made by Invitrogen (Milan, Italy). BSA protein standard, Laemmli sample buffer, pre-stained molecular weight markers, Percoll (colloidal PVP coated silica for cell separation), Sodium bicarbonate, Sodium lactate, Sodium pyruvate, Dimethyl Sulfoxide (DMSO), Earle's balanced salt solution, 15-deoxy-12,14-prostaglandin J_2 (PGJ2), the irreversible PPARγ antagonist GW9662 (GW), and all other chemicals were purchased from Sigma Chemical (Milan, Italy). Acrylamide bisacrylamide was from Labtek Eurobio (Milan, Italy). Triton X-100, Eosin Y was from Farmitalia Carlo Erba (Milan, Italy). Gel band purification kit, ECL Plus Western blotting detection system, Hybond^{TM} ECL^{TM}, [-^{32}P]ATP, HEPES Sodium Salt were purchased from Amersham Pharmacia Biotech (Buckinghamshire, UK). Triglycerides assay kit and Cholesterol-oxidase (CHOD)–peroxidase (POD) enzymatic colorimetric kit were from Inter-Medical (Biogemina Sas, Catania, Italy). Goat polyclonal actin antibody (I–19), polyclonal rabbit anti-PPARγ antibody, polyclonal rabbit anti-phosphotyrosine antibody (PY99), rabbit anti-p-Akt1/Akt2/Akt3 S473 antibody, total anti-Akt1/Akt2 antibody, peroxidase-coupled anti-rabbit and anti-goat, anti-rabbit IgG FITC-conjugated, Protein A/G-agarose plus were from Santa Cruz Biotechnology (Heidelberg, Germany). BRL49653 (BRL) was a kind gift from GlaxoSmithKline (West Sussex, UK).

Semen samples and spermatozoa preparations

Human semen was collected, according to the WHO-recommended procedure by masturbation from men undergoing semen analysis for couple infertility in our laboratory. Sperm samples with normal parameters of semen volume, sperm count, motility, vitality, and morphology, according to the WHO Laboratory Manual (World Health Organization, 1999), were included in this study. In each experiment, three normal samples were pooled. Washed pooled sperm were subjected to the treatments and incubated for the indicated times. Then, samples were centrifuged and the upper phase was used to determinate the cholesterol levels, while the pellet containing sperm was used for RT-PCR or lysed to perform Western blots, triglycerides assay, acyl-CoA dehydrogenase assay, G6PDH activity. At the beginning, prior the centrifugation, several aliquots were used to perform sperm motility, viability, and acrosin activity. Spermatozoa preparations were performed as previously described (Aquila et al., 2002). The study was approved by the local medical–ethical committees and all participants gave their informed consent.

Processing of ejaculated sperm

After liquefaction, normal semen samples were pooled and subjected to centrifugation (800*g*) on a discontinuous Percoll density gradient (80:40% v:v) (World Health Organization, 1999). The 80% Percoll fraction was examined using an optical microscope equipped with a 100× oil objective to ensure that a pure sample of sperm was obtained. An independent observer, who observed several fields for each slide, inspected the cells. Percoll-purified sperm were washed with unsupplemented Earle's medium and were incubated in the same medium (uncapacitating medium) for 30 min at 37°C and 5% CO_2, without (control) or with treatments (experimental). Some samples were incubated in capacitating medium (Earle's balanced salt solution medium supplemented with 600 mg BSA/100 ml and 200 mg sodium bicarbonate/100 ml). When the cells were treated with an inhibitor, a pre-treatment of 15 min was performed and subsequently the sperm were incubated with the substances reported in the manuscript for 30 min.

Evaluation of sperm motility and viability

Sperm motility was assessed by means of light microscopy examining an aliquot of each sperm sample in absence (NC) or in the presence of increasing BRL or PGJ2 (1 to 20 μM) and/or 10 μM GW alone or combined with 10 μM BRL or 10 μM PGJ2. Sperm motility was expressed as percentage of total motile sperm. Viability was assessed by red-eosin exclusion test using Eosin Y to evaluate potential toxic effects of the treatments. A blinded observer scored 200 cells for stain uptake (dead cells) or exclusion (live cells). Viability was evaluated before and after pooling the samples and there were no adverse effects among the different treatments on human sperm viability.

RNA isolation, reverse transcriptase-polymerase chain reaction (RT-PCR)

Total RNA was isolated from human-ejaculated spermatozoa purified as previously described (Aquila et al., 2002). Before RT-PCR, RNA was incubated with ribonuclease-free deoxyribonuclease (Dnase) I in single-strength reaction buffer at 37°C for 15 min. This was followed by heat inactivation of Dnase I at 65°C for 10 min. Two micrograms of Dnase-treated RNA samples were reverse transcribed by 200 IU M-MLV reverse transcriptase in a reaction volume of 20 μl (0.4 μg oligo-dT, 0.5 mM deoxy-NTP and 24 IU Rnasin) for 30 min at 37°C, followed by heat denaturation for 5 min at 95°C. PCR amplification of complementary DNA (cDNA) was performed with 2 U of Taq DNA polymerase, 50 pmol primer pair in 10 mM Tris-HCL (pH 9.0) containing 0.1% Triton X-100, 50 mM KCl, 1.5 mM $MgCl_2$, and 0.25 mM each dNTP. PCR amplification of cDNA was performed with 2 U of Taq DNA polymerase, 50 pmol primer pair for PPARγ. Contamination by leucocytes and germ cells in our sperm cells preparations was assessed by amplifying CD45 and c-kit transcripts respectively. The applied PCR primers and the expected lengths of the resulting PCR products are shown in Table 1. The cycle profiles used are

TABLE 1. Oligonucleotide sequences used for RT-PCR

Gene	Sequenze (5′–3′)	Size of PCR product (bp)
PPARγ	5′–GAGTTCATGCTTGTCAAGGATGC–3′ 5′–CGATATCACTGGAGATCTCGCC–3′	233
c-kit	5′–AGTACATGGACATGAAACCTGG–3′ 5′–GATTCTGCTCAGACATCGTCG–3′	780
CD45	5′–CAATAGCTACTACTCCATCTAAGCCA–3′ 5′–ATGTCTTATCAGGAGCAGTACATG–3′	230

described in Table 2. For all PCR amplifications, negative (reverse transcription-PCR performed without M-MLV reverse transcriptase) and positive controls were included (MCF7 breast cancer cells for PPARγ (Elstner et al., 1998), human germ cells for c-Kit, and human leucocytes for CD45). The PCR-amplified products were subjected to electrophoresis in 2% agarose gels stained with ethidium bromide and visualized under UV transillumination.

Gel extraction and DNA sequence analysis

The PPARγ RT-PCR product was extracted from the agarose gel by using a gel band purification kit, the purified DNA was subcloned into PCR 2.1 vector and then sequenced by MWG AG Biotech (Ebersberg, Germany).

Western blot analysis of sperm proteins

Sperm samples, washed twice with Earle's balanced salt solution (uncapacitating medium), were incubated without or with the indicated treatments, and then centrifuged for 5 min at 5,000*g*. The pellet was resuspended in lysis buffer as previously described (Aquila et al., 2002). Equal amounts of protein (70 μg) were boiled for 5 min, separated by 10% polyacrylamide gel electrophoresis, transferred to nitrocellulose sheets, and probed with an appropriate dilution of the indicated antibody. The bound of the secondary antibody was revealed with the ECL Plus Western blotting detection system according to the manufacturer's instructions. The negative control was performed using a sperm lysate that was immunodepleted of PPARγ (Aquila et al., 2004) (i.e., pre-incubate lysate with anti-PPARγ antibody, 1 h at room temperature, and immunoprecipitate with Protein A/G-agarose).

As internal control, all membranes were subsequently stripped (glycine 0.2 M, pH 2.6 for 30 min at room temperature) of the first antibody and reprobed with anti-β actin or total Akt1/2 antibodies.

Immunofluorescence assay

Sperm cells, recovered from Percoll gradient, were rinsed three times with 0.5 mM Tris-HCl buffer, pH 7.5 and fixed with absolute methanol for 7 min at −20°C. PPARγ staining was carried out, after blocking with normal horse serum (10%), using a rabbit polyclonal anti-human PPARγ as primary antibody and an anti-rabbit IgG FITC-conjugated (1:100) as secondary antibody. Sperm cells incubated without the primary antibody or with normal rabbit serum instead of the primary antibody were utilized as the negative controls. The slides were examined under a fluorescence microscope (Olympus BX41, Milan Italy), and a minimum of 200 spermatozoa for slide were scored.

TABLE 2. Cycling conditions for the different sets of pairs

Gene	Cycle profile	No. of cycles
PPARγ	Denaturation: 95°C/1 min Annealing: 60°C/1 min Extention: 72°C/2 min	40
c-kit	Denaturation: 95°C/1 min Annealing: 52°C/1 min Extention: 72°C/2 min	40
CD45	Denaturation: 95°C/1 min Annealing: 55°C/1 min Extention: 72°C/2 min	40

Measurement of cholesterol in the sperm culture medium

Cholesterol was measured in duplicate by a CHOD–POD enzymatic colorimetric method according to manufacturer's instructions in the incubation medium from human spermatozoa. Sperm samples, washed twice with uncapacitating medium, were incubated in the same medium (control) or in capacitating medium for 30 min at 37°C and 5% CO_2. Some samples were incubated in the presence of increasing PGJ2 concentrations (1 to 20 μM). Other samples were incubated in the presence of 10 μM GW alone or combined with 10 μM PGJ2. At the end of the sperm incubation, the culture media were recovered by centrifugation, lyophilized and subsequently dissolved in 1 ml of buffer reaction. The samples were incubated for 10 min at room temperature, then the cholesterol content was measured spectrophotometrically at 505 nm. Cholesterol standard used was 200 mg/dl. The limit of sensitivity for the assay was 0.05 mg/dl. Inter- and intraassay variations were 0.04% and 0.03%, respectively. Cholesterol results are presented as mg per 10×10^6 number of spermatozoa.

Acrosin activity assay

Acrosin activity was assessed by the method of Kennedy et al. (1989). Percoll-purified sperms were washed in Earle's medium and centrifuged at 800*g* for 20 min. Sperms were resuspended (final concentration of 10×10^6 sperms/ml) in different tubes containing no treatment (control) or the indicated treatments (experimental). Then 1 ml of substrate–detergent mixture (23 mmol/L BAPNA in DMSO and 0.01% Triton X-100 in 0.055 mol/L NaCl, 0.055 mol/L HEPES at pH 8.0, respectively) for 3 h at room temperature was added. Aliquots (50 μl) were removed at 0 and 3 h, and the percentages of viable cells were determined. No significant differences were detected between the control and experimental conditions. After incubation, 0.5 mol/L benzamidine was added (0.1 ml) to each of the tubes and then centrifuged at 1,000*g* for 30 min. The supernatants were collected and the acrosin activity measured spectrophotometrically at 410 nm. In this assay, the total acrosin activity is defined as the amount of the active (non-zymogen) acrosin associated with sperm plus the amount of active acrosin that is obtained by proacrosin activable. The acrosin activity was expressed as $\mu IU/10^6$ sperms. Quantification of acrosin activity was performed as previously described (Aquila et al., 2003).

Triglycerides assay

Triglycerides were measured in duplicate by a GPO–POD enzymatic colorimetric method according to manufacturer's instructions in sperm lysates. Sperm samples, washed twice with uncapacitating medium, were incubated in the same medium (control) or in capacitating medium for 30 min at 37°C and 5% CO_2. Other samples were incubated in the presence of the indicated treatments. At the end of the sperm incubation, 10 μl of lysate was added to the 1 ml of buffer reaction and incubated for 10 min at room temperature. Then the triglycerides content was measured spectrophotometrically at 505 nm. Data are presented as $\mu g/10^6$ sperms.

Assay of acyl-CoA dehydrogenase activity

Assay of acyl-CoA dehydrogenase was performed on sperm incubated in the presence of the indicated treatments, using a modification of the method described by Lehman et al. (1990). In brief, after lysis, 70 μg of sperm protein was added to buffer containing 20 mM Mops, 0.5 mM EDTA, and 100 μM FAD^+ at pH 7.2. Reduction of FAD^+ to FADH was read at 340 nm upon addition of octanoyl-CoA (100 μM) every 20 sec for 1.5 min. Data are expressed in nmol/min/mg protein. The enzymatic activity was determined with three control media: one without octanoyl-CoA as substrate, one without the co-enzyme (FAD^+), and the third without either substrate or co-enzyme (data not shown). Every experiment was performed six times, in duplicate within each experiment.

Glucose-6-phosphate dehydrogenase (G6PDH) activity

The conversion of $NADP^+$ to NADPH, catalyzed by G6PDH, was measured by the increase of absorbance at 340 nm. Sperm

samples, washed twice with uncapacitating medium, were incubated in the same medium (control) for 30 min at 37°C and 5% CO_2. Some samples were treated with increasing concentration of BRL or with 3.3 nM insulin, or 10 μM GW alone or combined with 10 μM BRL. Other samples were treated with 10 μM BRL plus 3.3 nM insulin or 10 μM GW plus 10 μM BRL and 3.3 nM insulin. After incubation, 50 μl of sperm extracts were loaded into individual cuvettes containing buffer (100 mM triethanolamine, 100 mM $MgCl_2$, 10 mg/ml glucose-6-phosphate, 10 mg/ml $NADP^+$, pH 7.6) for spectrophotometric determination. The absorbance of samples was read at 340 nm every 20 sec for 1.5 min. Data are expressed in nmol/min/10^6 sperms. The enzymatic activity was determined with three control media: one without glucose-6-phosphate as substrate, one without the co-enzyme ($NADP^+$), and the third without either substrate or co-enzyme (data not shown). Every experiment was performed eight times, in duplicate within each experiment.

STATISTICAL ANALYSIS

The experiments for RT-PCR were repeated on at least three independent occasions, whereas Western blot analysis was performed in at least six independent experiments. The data obtained from motility, viability (six replicate experiments using duplicate determinations), CHOD–POD enzymatic colorimetric method, Triglycerides Assay, acyl-CoA dehydrogenase activity (six replicate experiments using duplicate determinations), G6PDH (eight replicate experiments using duplicate determinations) were presented as the mean ± SD. The differences in mean values were calculated using analysis of variance (ANOVA) with a significance level of $P < 0.05$.

RESULTS

Expression of PPARγ in human sperm

RT-PCR and western blot. To determine whether mRNA for PPARγ is present in human-ejaculated spermatozoa, RNA isolated from percoll-separated sperm of normal men was subjected to reverse PCR. The primer sequences were based on the human PPARγ gene sequence and the RT-PCR amplification revealed the expected PCR product size of 233 bp of the coding region of the human PPARγ cDNA (Fig. 1A). This product was sequenced and found to be corresponding to the classical human PPARγ. No detectable levels of mRNA coding either CD45, a specific marker of human leucocytes, or c-kit, a specific marker of human germ cells, were found in the same semen samples (Fig. 1A), ruling out any potential contamination. In addition, the RT-PCR products were not a result of any DNA contamination as the RNA samples were subjected to DNAse treatment before RT-PCR.

The presence of PPARγ protein in human-ejaculated sperm was investigated by Western blot using an antibody raised against the carboxyl-terminus of the human PPARγ protein (Fig. 1B). One immunoreactive band, corresponding to the molecular mass values of 70 kDa, was observed at the same mobility of the MCF-7 extract, used as positive control. The negative control (lane 2) was performed using a sperm lysate, where PPARγ was previously removed by pre-incubation with the respective antibody (1 h at room temperature) and subsequently immunoprecipitated with protein A/G-agarose.

Immunolocalization. Using a immunofluorescence technique and the same antibody used for Western blot, we obtained a positive signal for PPARγ in human spermatozoa. In the majority of population of uncapacitated sperm, immunoreactivity is predominantly compartmentalized to the subacrosomial region and the midpiece while the tail is almost completely unstained (Fig. 2A). No fluorescent signal was obtained when primary antibody was omitted (Fig. 2B) or when the normal rabbit IgG was used instead of the primary antibody (Fig. 2C), thus further confirming the specificity of the antibody binding.

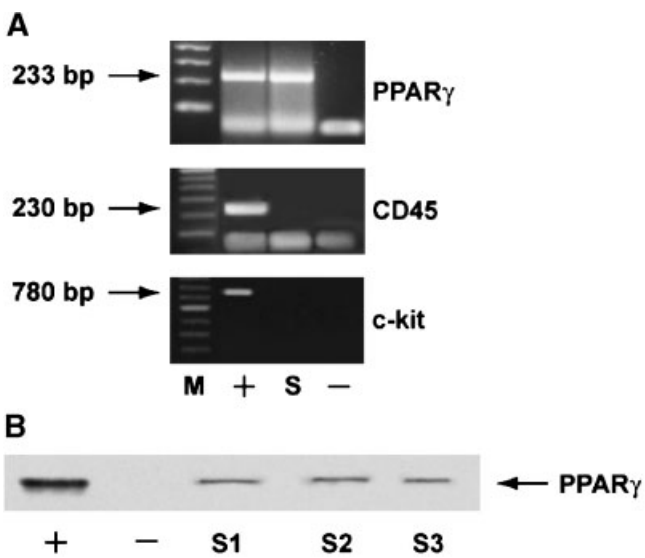

Fig. 1. PPARγ expression in human-ejaculated spermatozoa. **A**: Reverse transcription-PCR analysis of human PPARγ, CD45, and c-Kit genes in percolled human spermatozoa (S), negative control (no M-MLV reverse transcriptase added) (−), positive controls (MCF7 breast cancer cells for PPARγ, human germ cells for c-Kit and human leucocytes for CD45) (+), marker (lane M). Arrows indicated the expected size of the PCR products. **B**: Western blot of PPARγ protein in human sperm, expression in three samples of ejaculated spermatozoa from normal men (S1, S2, S3). MCF-7 extract was used as control (+). The negative control (see Materials and Methods, is represented in lane 2 (−). The experiments were repeated at least three times for RT-PCR, six times for Western blot and the autoradiographs of the figure show the results of one representative experiment.

PPARγ-agonists influence on capacitation, acrosome reaction and motility is PPARγ-mediated

We first investigated whether PPARγ-agonists are able to influence the sperm extratesticular maturation evaluating their action on both capacitation and acrosome reaction. Further, in all the experiments we used both a natural PPARγ-ligand, PGJ2 (1, 10, and 20 μM) and a synthetic ligand BRL (1, 10, and 20 μM), obtaining similar results, therefore in the text, we reported the data relative to the natural PPARγ-ligand.

Sperm membrane cholesterol efflux contributes to one signaling mechanism that controls sperm capacitation (Travis and Kopf, 2002) and it has been demonstrated that it initiates signaling events leading to tyrosine phosphorylation of sperm proteins, also representative of the capacitation status (Visconti et al., 1995). Washed sperm were treated with increasing concentration of PGJ2 (1, 10, and 20 μM) and incubated under uncapacitating conditions (*see Materials and Methods*). At the end of incubation, the samples were centrifuged, the upper phase was used to determinate the cholesterol levels, while the sperm were lysed to evaluate protein tyrosine phosphorylation. Our results showed a significant increase in both tyrosine phosphorylation (Fig. 3A) and cholesterol efflux (Fig. 3B) upon 1 to 20 μM PGJ2 treatment. Both processes were inhibited by using the specific PPARγ-antagonist GW suggesting an involvement of this receptor in the induction of capacitation.

Acrosin activity, performed in the same experimental conditions, showed an increase by PGJ2 reversed by GW

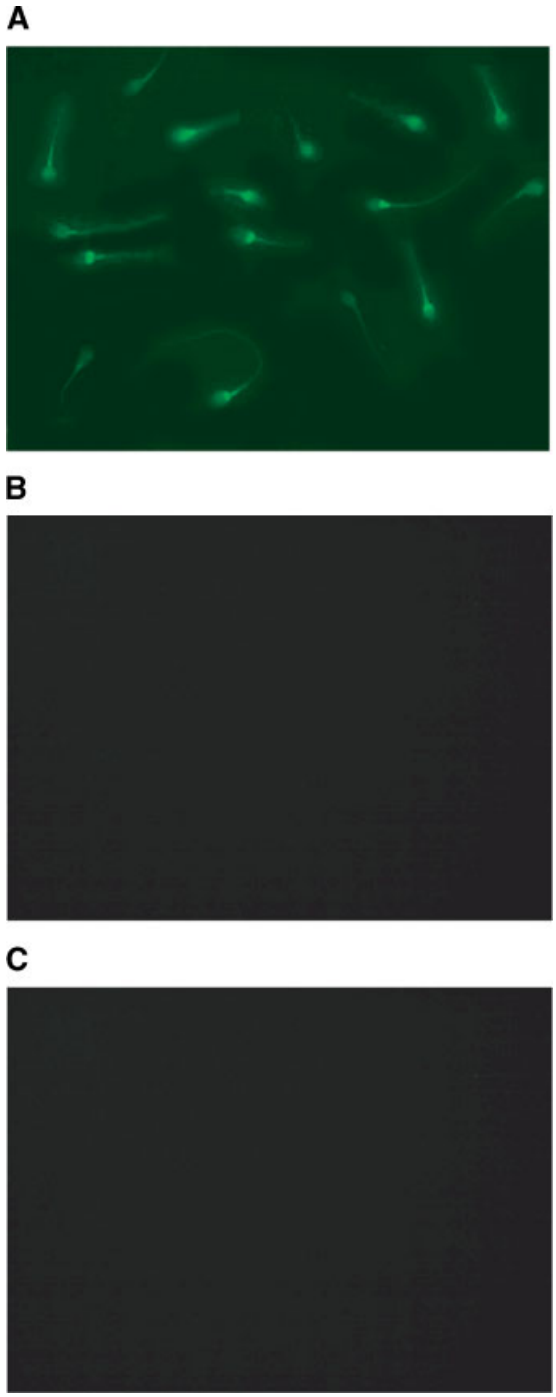

Fig. 2. Immunolocalization of PPARγ in human-ejaculated spermatozoa. **A**: PPARγ immunolocalization; (**B**) Sperm cells incubated without the primary antibody were utilized as negative control. **C**: Sperm cells incubated replacing the anti-PPARγ antibody by normal rabbit serum were utilized as negative control. The pictures shown are representative examples of experiments that were performed at least three times with reproducible results.

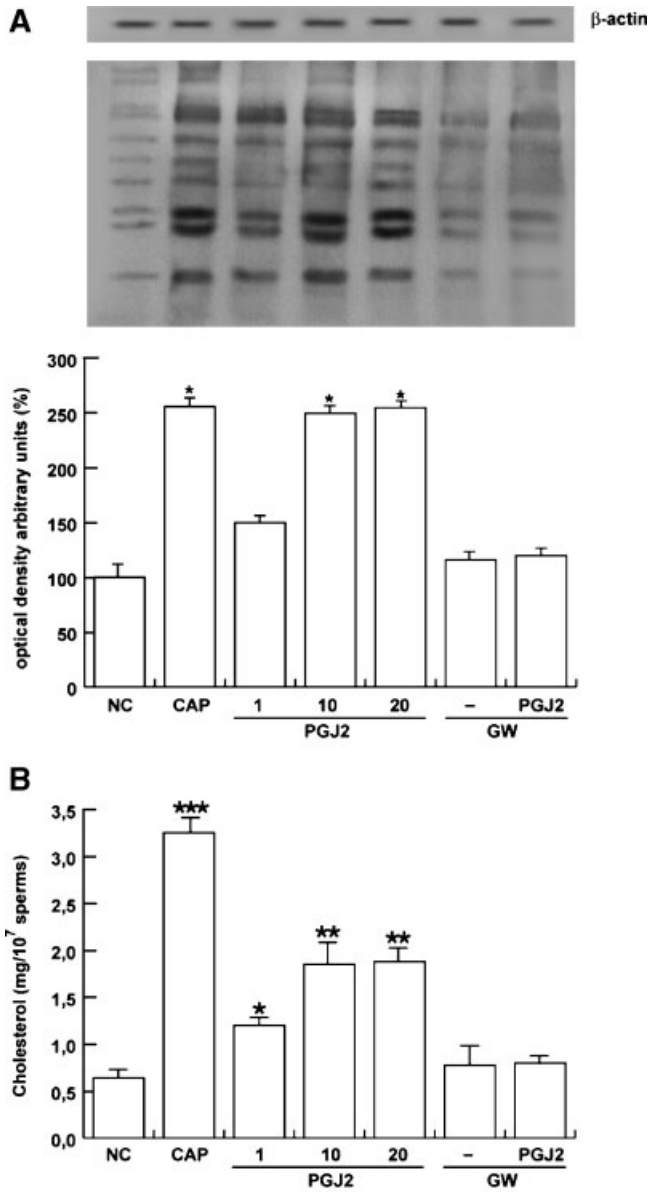

Fig. 3. PGJ2 effects on tyrosine phosphorylation of sperm proteins and cholesterol efflux are PPARγ-mediated. Washed spermatozoa were incubated in the unsupplemented Earle's medium for 30 min at 37°C and 5% CO_2, in the absence (NC) or in the presence of increasing concentration of PGJ2 (1, 10, 20 μM) or with 10 μM GW alone or combined with 10 μM PGJ2. Other samples were incubated in capacitating medium (CAP). **A**: Sperm lysates (70 μg) were used for Western blot analysis of protein tyrosine phosphorylation. On the bottom, quantitative representation after densitometry. **B**: Cholesterol in culture medium from human-ejaculated spermatozoa was measured by enzymatic colorimetric assay. Columns are mean ± SD of six independent experiments performed in duplicate. Data are expressed in mg/10^7 sperms. $^*P < 0.05$ versus control, $^{**}P < 0.01$ versus control; $^{***}P < 0.001$ versus control.

(Fig. 4A). BRL also significantly induced sperm motility (data not shown). The PGJ2-induced effects on sperm motility were antagonized by the specific GW antagonist while the antagonist alone had no significant effect (Fig. 4B).

PPARγ affects lipid metabolism in human sperm

The favorable metabolic effects of PPARγ-agonists are supposedly related to the PPARγ-driven changes in lipid metabolism. Owing to the critical role that PPARγ plays in lipid metabolism, we evaluated both the intracellular level of triglycerides and the β-oxidation of the fatty acids under PPARγ-agonists in sperm.

Stimulation with BRL induced a significant decrease in sperm triglycerides levels however GW didn't reverse the effect addressing a PPARγ-independent event (Fig. 5A). While in the samples treated with PGJ2, GW is able to block the PPARγ-agonist effect (Fig. 5B). As it concerns the β-oxidation of the fatty acids, a dose-dependent increase under PGJ2 treatment was

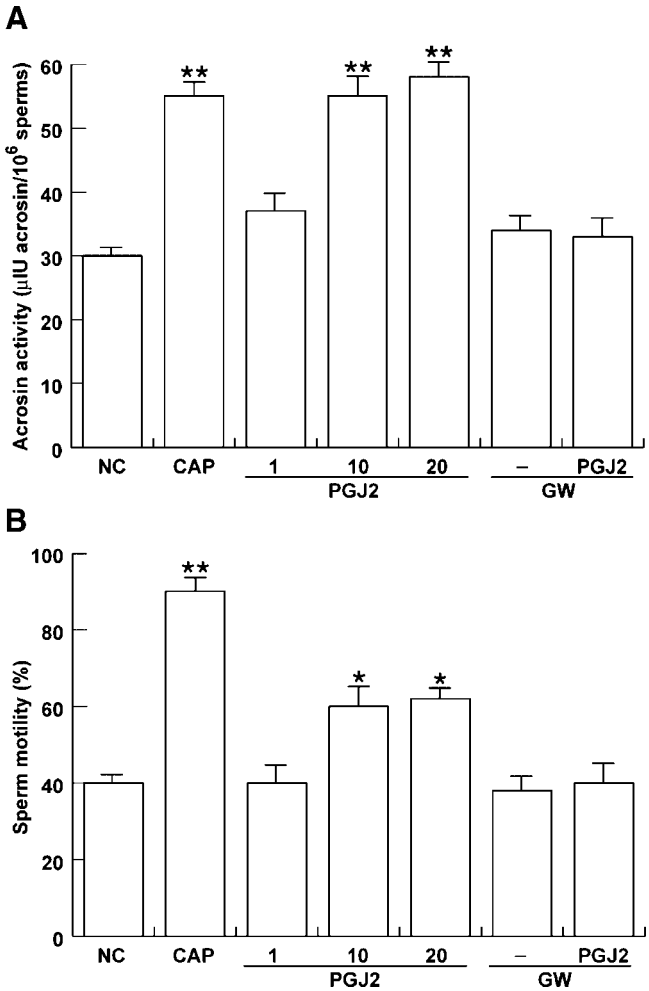

Fig. 4. PGJ2 effects on acrosin activity and sperm motility are PPARγ-mediated. Washed spermatozoa were incubated in the unsupplemented Earle's medium for 30 min at 37°C and 5% CO_2, in the absence (NC) or in the presence of increasing concentration of PGJ2 (1, 10, 20 μM) or with 10 μM GW alone or combined with 10 μM PGJ2. Other samples were incubated in capacitating medium (CAP). **A**: Acrosin activity was assessed as reported in Materials and Methods. **B**: Sperm motility was expressed as percentage of total motile sperm. Columns are mean ± SD of six independent experiments performed in duplicate. $^{*}P < 0.05$ versus control; $^{**}P < 0.01$ versus control.

observed (Fig. 5C) and GW was able to reverse PGJ2-induced effect.

PPARγ-agonist activates PI3K/Akt pathway in human sperm

PPARγ activation has been reported to regulate components of the PI3K signaling cascade in various cell types (Bonofiglio et al., 2005). We speculated that PPARγ may be involved in the control of some sperm functions, perhaps by influencing the activity of PI3K. Therefore, we examined the effects of PPARγ-agonist treatment on PI3K-mediated signaling by evaluating the phosphorylation of the major downstream signal transducer, AKT, since its phosphorylation has been correlated with its activity (Datta et al., 1999).

Increasing doses of BRL (1, 10, and 20 μM) resulted in a significant increase in the AKT phosphorylation (Fig. 6). To address whether PPARγ-agonist stimulation of AKT was specifically mediated through PPARγ, we treated sperm with 10 μM GW in the presence or absence of 10 μM BRL. BRL-stimulatory effect was reduced by

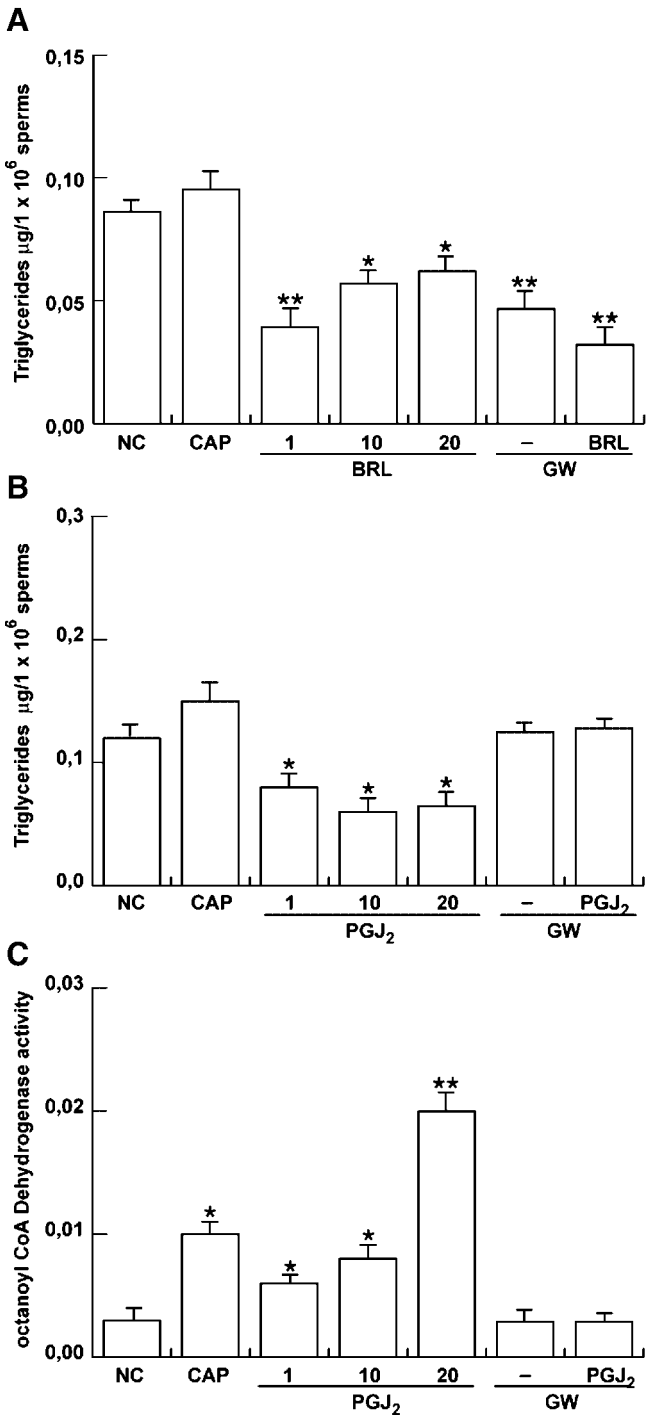

Fig. 5. PPARγ-agonists influence lipid metabolism in sperm. **A**: Sperm samples, washed twice with uncapacitating medium were incubated in the same medium (NC) or in capacitating medium (CAP) for 30 min at 37°C and 5% CO_2. Other samples were incubated in the presence of increasing BRL concentrations (1, 10, 20 μM) or in the presence of 10 μM GW alone, or combined with 10 μM BRL. **B**: Sperm samples were incubated with PGJ2 instead of BRL. Data are presented as μg/10^6 sperms. **C**: Assay of acyl-CoA dehydrogenase was performed on sperm lysates (see Materials and Methods) in the same experimental conditions above mentioned. Columns are mean ± SD of six independent experiments performed in duplicate. Data are presented as nmol/min/mg protein. Columns are mean ± SD. $^{*}P < 0.05$ versus control; $^{**}P < 0.01$ versus control.

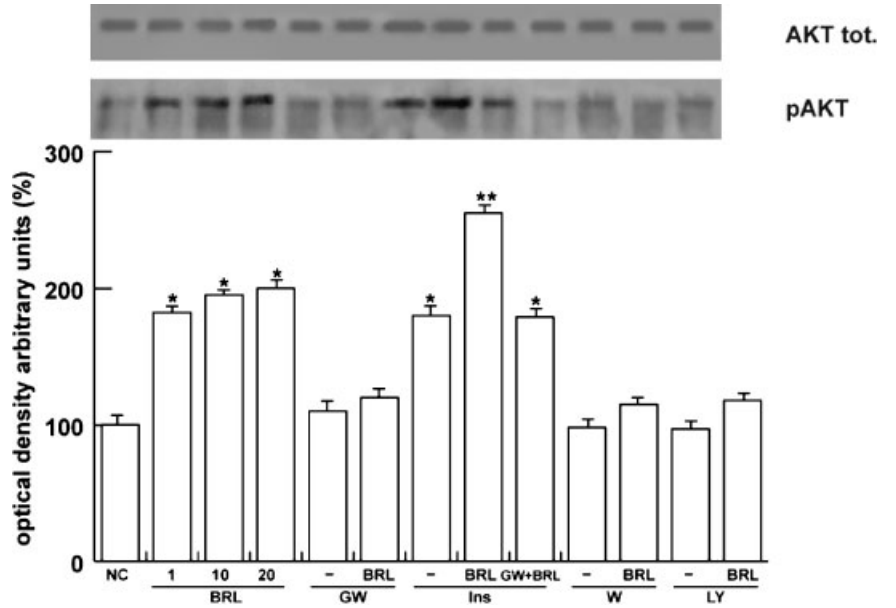

Fig. 6. BRL increases insulin-induced AKT phosphorylation in human sperm. Washed spermatozoa were incubated in the unsupplemented Earle's medium for 30 min at 37°C and 5% CO_2, in the absence (NC) or in the presence of increasing BRL (1, 10, 20 μM). Some samples were incubated in the presence of 10 μM GW alone or combined with 10 μM BRL, in the presence of 3.3 nM Ins alone or combined with 10 μM BRL or combined with 10 μBRL plus 3.3 nM insulin (Ins), in the presence of 10 μM worthmannin (W) alone or combined with 10 μM BRL, in the presence of 10 μM LY294002 (LY) alone or combined with 10 μM BRL. In the upper part, is reported total AKT. On the bottom, is reported the densitometric evaluation. The autoradiographs presented are representative examples of experiments that were performed at least four times with repetitive results. *$P < 0.01$ versus control, **$P < 0.001$ versus control.

GW. We also tested the effects of PI3K inhibitors, 10 μM wortmannin, and 10 μM LY294002, confirming that the action of PPARγ on AKT is through PI3K activation.

AKT plays multifunction roles in insulin action and its activation has been shown to be dependent on PI3K (Datta et al., 1999). In addition, we recently showed that in sperm insulin activates PI3K pathway (Aquila et al., 2005b), therefore we aimed to investigate the interrelation between insulin and PPARγ. It was also reported that BRL is an insulin-sensitizing agent since it belongs to TZDs (Petersen et al., 2000). Insulin alone induced a significant increase in AKT phosphorylation according to our previous data (Aquila et al., 2005b). In the presence of BRL, insulin displayed greater stimulatory effect. Therefore BRL increased PI3K activation induced by insulin (Fig. 6), suggesting an insulin-sensitizing action also in sperm. All these treatments were also used in combination with GW showing an involvement of PPARγ in BRL action.

PPARγ affects glucose metabolism through the pentose phosphate pathway (PPP) in human sperm

Given the beneficial effects of PPARγ ligands in therapies aimed at lowering glucose levels in type 2 diabetes, a role of PPARγ in glucose metabolism has been explored (Lenhard et al., 1997). An important metabolic response to insulin in the regulation of glucose homeostasis is related to the G6PDH activity (Stumpo and Kletzien, 1984), while the effect of PPARγ action on this enzymatic activity was never investigated. In our previous study, we demonstrated that insulin regulate in autocrine fashion sperm G6PDH activity (Aquila et al., 2005a). Thus, we speculated that in sperm, insulin and PPARγ are possibly interrelated and relevant on glucose metabolism through the PPP.

As shown in Figure 7, 10 μM BRL activates G6PDH activity and insulin in a higher extent. In the presence of BRL, insulin action was further enhanced and this effect was reversed by GW. Our results address a regulatory role of PPARγ in sperm glucose metabolism and worthy evidence an insulin-sensitizing effect by BRL.

DISCUSSION

Lipid and carbohydrate homeostasis in higher organisms is under the control of an integrated system that has the capacity to rapidly respond to metabolic changes. The PPARγ is a nuclear fatty acid receptor that has been implicated in energy homeostasis and in many pathological processes (Knouff and Auwerx, 2004). Specifically, it modulates lipid homeostasis in

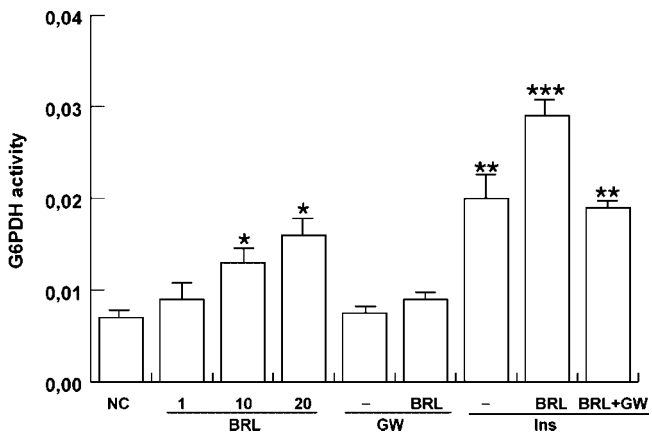

Fig. 7. BRL effect on G6PDH activity. Sperm were washed with the unsupplemented Earle's medium and were treated in the absence (NC) or in the presence of increasing BRL (1, 10, 20 μM). Some samples were incubated in the presence of 10 μM GW alone or combined with 10 μM BRL, in the presence of 3.3 nM insulin alone or plus 10 μM BRL or combined with 10 μM BRL plus 10 μM GW. Columns are mean ± SD of eight independent experiments performed in duplicate. Data are expressed as nanomoles per minute per 10^6 sperms. *$P < 0.05$ versus control; **$P < 0.01$ versus control, ***$P < 0.001$ versus control.

metabolically active sites, including the liver, adipocytes, muscle, and macrophage (Desvergne and Wahli, 1999 and references therein). Here we show that PPARγ is also expressed in human-ejaculated spermatozoa. The effects of both natural and synthetic PPARγ ligands on different sperm functions were investigated.

First, we have demonstrated the presence of PPARγ in human-ejaculated spermatozoa at different levels: mRNA expression, protein expression, and immunolocalization. As it concerns the presence of mRNA in mammalian ejaculated spermatozoa, originally it was hypothesized that these transcripts were carried over from earlier stages of spermatogenesis, however new reports revaluate significance of mRNA in these cells (Miller, 2000; Ostermeier et al., 2002) and the issue is currently under investigation. In good agreement with RT-PCR data, our immunohistochemical assays demonstrated that PPARγ protein is detectable in sperm, with specific signals being located in the subacrosomial region and in the middlepiece, to a lesser extent in the tail. PPARγ is highly expressed in adipose tissues but is expressed at much lower levels in other tissues, including major insulin target tissues, skeletal muscle, and liver (Desvergne and Wahli, 1999 and references therein). Expression of PPARγ in the male gamete, further confirmed by Western Blot, is a novel intriguing finding since it may have an important role in the regulation of sperm metabolism.

To investigate the functional role of PPARγ in sperm, we evaluated its action on different events that characterize the sperm cell as capacitation, acrosome reaction, and motility. PPARγ is activated by endogenous arachidonic acid metabolites such as PGJ2 (Desvergne and Wahli, 1999 and references therein) and it is the target for binding to a class of synthetic compounds, termed the TZD. In our experiments, we used both natural and synthetic ligands obtaining similar results on the abovementioned processes (in the figures are showed only the results referred to PGJ2 treatment). Particularly, we observed a significant increase in both cholesterol efflux and tyrosine phosphorylation of sperm proteins, this latter event tightly related to the capacitation (Visconti et al., 1995) and resulting downstream the cholesterol efflux. These effects were reduced by GW indicating a PPARγ involvement. PPARγ has been shown to be implicated in cholesterol export from macrophages and the ability of TZDs to promote cholesterol efflux is completely dependent on PPARγ, as assessed by the inability of these compounds to augment the efflux of cholesterol from *Pparg*$^{-/-}$ macrophages (Chawla et al., 2001). The molecular route by which TZDs promote cholesterol efflux involves a transcriptional cascade that is controlled by PPARγ (Zhang and Chawla, 2004 and references therein). Here we have to take into account that sperm are considered transcriptionally inactive, therefore very likely PPARγ in sperm acts through a non-genomic action. As it concerns acrosome reaction and motility, our results are in concordance with recent studies on human spermatozoa where prostaglandins are reported to enhance both processes (Aitken et al., 1986; Aitken and Kelly, 1985), although in addition, we showed that the effects of these compounds are PPARγ-mediated.

Several investigators have identified a pivotal role for PPARγ in fat cell differentiation, lipid storage, vascular function, and energy metabolism. Overall, the favorable metabolic effects of TZDs are supposedly related to the PPARγ-driven changes in lipid metabolism. It has long been recognized that capacitated sperm display an increase metabolic rate presumably to affect the changes in sperm signaling and function during capacitation process. The relationship between the signaling events associated with capacitation and changes in sperm energy metabolism is poorly understood. Under PPARγ-agonists treatment, our results evidenced a reduction in triglycerides content in sperm while at the same time, we observed an increased Fatty Acids (FA) β-oxidation. Particularly, the behavior of the two PPARγ-agonists diverges when we tested their effects on triglycerides levels: it appears that the action of PGJ2 is PPARγ-mediated while BRL effect is PPARγ-independent. It is well known that BRL treatment reduces hypertriglyceridemia however, it is not clear how TZDs lower free FA levels. Since they seem to have little or no effect on basal rates of lipolysis, it was supposed that the decrease in plasma-free FA levels is probably due to an increase in free FA clearance (oxidation and/or esterification) (Ciaraldi et al., 2002). Supporting this notion, we may hypothesize that during capacitation when energy expenditure increases, lipid reserve is mobilized and also used as energy substrate available.

The PPARγ controls many different target genes involved in both lipid metabolism and glucose homeostasis (Desvergne and Wahli, 1999). Given the beneficial effects of PPARγ ligands in therapies aimed at lowering glucose levels in type 2 diabetes, a role of PPARγ in glucose metabolism has been explored. Sperm energy metabolism is very complex because there are many metabolic pathways where hexoses can be diverted. In this sense, these cells not only have the glycolysis and Krebs cycle catabolic pathways but also the glycogen synthesis and pentose phosphate cycle, a very complex system that allows for a fine regulation of energy levels depending on their functional status. It emerged from our recent studies that insulin, one of the main regulators of energy homeostasis in somatic cells, may be also crucial in the management of sperm glucose metabolism since in autocrine fashion, it regulates G6PDH and glycogen synthase activities (Aquila et al., 2005a, b). It is generally accepted that TZDs exert their insulin sensitizing action through PPARγ, however, how exactly this occurs, it remains to be clarified. We previously showed that insulin activated G6PDH in sperm and in this study that the activation is additive or synergistic to that of BRL. In these circumstances, G6PDH activity would theoretically increase glucose utilization as a consequence of improved insulin signaling in sperm as well as a cause of insulin sensitization.

The enhanced activity of this enzyme produces an increase of NADPH that is essential for fatty acid synthesis from acetyl CoA. These fatty acids have two possible fates: β-oxidation to produce ATP or reesterification back into triacylglycerol. Inter-relationships of the classes of substrates of free FA and glucose utilized for energy as first proposed by Randle (1964), has been long established and also hypothesized in the spermatozoa (Andò and Aquila, 2005). In this study, we observed in ejaculated sperm that FA β-oxidation tested utilizing the octanoil-CoA as substrate, appears to be stimulated by PPARγ agonists. It may be assumed that PPARγ works to stimulate such enzymatic activity providing additional metabolic fuel to sustain capacitation process. Therefore, the autonomous capability of sperm to release insulin suggests that they through an autocrine short loop may provide the recruitment of energy substrate according to sperm metabolic needs

and that PPARγ may serve as a molecular means for maintaining energy balance, regulating sperm energy dissipation during capacitation.

The regulation of lipid and carbohydrate metabolism might have important implications in male reproduction for developing models of PPARγ function as a therapeutic target. In particular, TZDs are widely used in patients with diabetes, who also have high risk of infertility (Baccetti et al., 2002). The mechanisms controlling the interaction between energy balance and reproduction are the subject of intensive investigations. For example, negative energy balance caused by inadequate nutrient supply or excessive consumption is able to affect the fertility of female mammals. Interestingly, insulin-sensitizing agents such as BRL were also shown to ameliorate the ovulatory function of polycystic ovarian syndrome patients (Froment et al., 2005).

The physiological significance of the present observations are still incomplete. Prostaglandins are involved in the male reproductive tract, and high concentrations of prostaglandins are reported to exist in seminal fluid (Templeton et al., 1978) and cervical mucus (Charbonnel et al., 1982). In addition, human spermatozoa have been shown to synthesize prostaglandins (Roy and Ratnam, 1992). Prostaglandins treatment is reported to enhance sperm fertilizing ability (Aitken et al., 1986; Aitken and Kelly, 1985; Shimizu et al., 1998). On the basis of our data, PPARγ activation may induce both capacitation and acrosome reaction; however, it is also possible that prostaglandin, together with administration of BRL, could increase PPARγ activation in different pathological conditions thus leading to sperm function alterations.

Taken together, these results indicate that the role of PPARγ is more complex than was originally believed. Our findings also showed that sperm is a new target tissue for the lipid- and glucose-lowering effects of the TZDs in humans. Thus, the modulation of levels of PPARγ and/or its ligands may afford novel therapeutic opportunities for the treatment of the male fertility disorders imputable to metabolic diseases. Further work will be required to more fully elucidate the role that PPARγ plays in this area. Whatever the outcome, however, it is clear that future studies of reproductive regulation must take into account of this receptor.

ACKNOWLEDGMENTS

Our special thank to D. Sturino (Faculty of Pharmacy, University of Calabria—Italy) for the English review of the manuscript and to Dr. Vincenzo Cunsulo (Biogemina SAS, Catania—Italy).

LITERATURE CITED

Aitken RJ, Kelly RW. 1985. Analysis of the direct effects of prostaglandins on human sperm function. J Reprod Fertil 73:139–146.

Aitken RJ, Irvine S, Kelly RW. 1986. Significance of intracellular calcium and cyclic adenosine 3′,5′-monophosphate in the mechanisms by which prostaglandins influence human sperm function. J Reprod Fertil 77:451–462.

Andò S, Aquila S, 2005. Arguments raised by the recent discovery that insulin and leptin are expressed in and secreted by human ejaculated spermatozoa. Mol Cell Endocrinol 245:1–6.

Aquila S, Sisci D, Gentile ME, Middea E, Siciliano L, Andò S. 2002. Human ejaculated spermatozoa contain active P450 aromatase. J Clin Endocrinol Metab 87:3385–3390.

Aquila S, Sisci D, Gentile M, Carpino A, Middea E, Catalano S, Rago V, Ando S. 2003. Towards a physiological role for cytochrome P450 aromatase in ejaculated human sperm. Hum Reprod 18:1650–1659.

Aquila S, Sisci D, Gentile ME, Middea E, Catalano S, Carpino A, Rago V, Andò S. 2004. Estrogen Receptor (ER) α and ER β are both expressed in human ejaculated spermatozoa: Evidence of their direct interaction with phosphatidylinositol-3-OH kinase/Akt pathway. J Clin Endocrinol Metab 89:1443–1451.

Aquila S, Gentile M, Middea E, Catalano S, Ando S. 2005a. Autocrine regulation of insulin secretion in human ejaculated spermatozoa. Endocrinology 146:552–557.

Aquila S, Gentile M, Middea E, Catalano S, Morelli C, Pezzi V, Ando S. 2005b. Leptin secretion by human ejaculated spermatozoa. J Clin Endocrinol Metab 90:4753–4761.

Baccetti B, La Marca A, Piomboni P, Capitani S, Bruni E, Petraglia F, De Leo V. 2002. Insulin-dependent diabetes in men is associated with hypothalamo-pituitary derangement and with impairment in semen quality. Hum Reprod 17:2673–2677.

Bonofiglio D, Gabriele S, Aquila S, Catalano S, Gentile M, Middea E, Giordano F, Ando S. 2005. Estrogen receptor alpha binds to peroxisome proliferator-activated receptor response element and negatively interferes with peroxisome proliferator-activated receptor gamma signaling in breast cancer cells. Clin Cancer Res 11:6139–6147.

Cato ACB, Nestl A, Mink S. 2002. Rapid actions of steroid receptors in cellular signaling pathways. Sci STKE 138:RE9.

Chang TH, Szabo E. 2000. Induction of differentiation and apoptosis by ligands of peroxisome proliferator-activated receptor gamma in non-small cell lung cancer. Cancer Res 60:1129–1138.

Charbonnel B, Kremer M, Gerozissis K, Dray F. 1982. Human cervical mucus contains large amounts of prostaglandins. Fertil Steril 38:109–111.

Chawla A, Boisvert WA, Lee CH, Laffitte BA, Barak Y, Joseph SB, Liao D, Nagy L, Edwards PA, Curtiss LK, Evans RM, Tontonoz P. 2001. A PPAR gamma-LXR-ABCA1 pathway in macrophages is involved in cholesterol efflux and atherogenesis. Mol Cell 7:161–171.

Ciaraldi TP, Cha BS, Park KS, Carter L, Mudaliar SR, Henry RR. 2002. Free fatty acid metabolism in human skeletal muscle is regulated by PPARgamma and RXR agonists. Ann NY Acad Sci 967:66–70.

Cui Y, Miyoshi K, Claudio E, Siebenlist UK, Gonzalez FJ, Flaws J, Wagner K-U, Hennighausen L. 2002. Loss of the peroxisome proliferation-activated receptor gamma (PPARgamma) does not affect mammary development and propensity for tumor formation but leads to reduced fertility. J Biol Chem 277:17830–17835.

Datta SR, Brunet A, Greenberg ME. 1999. Cellular survival: A play in three Akts. Genes Dev 13:2905–2927.

Desvergne B, Wahli W. 1999. Peroxisome proliferator-activated receptors: Nuclear control of metabolism. Endocr Rev 20:649–688.

Elstner E, Muller C, Koshizuka K, Williamson EA, Park D, Asou H, Shintaku P, Said JW, Heber D, Koeffler HP., 1998. Ligands for peroxisome proliferator-activated receptor γ and retinoic acid receptor inhibit growth and induce apoptosis of human breast cancer cells in vitro and in BNX mice. Proc Natl Acad Sci USA 95:8806–8811.

Froment P, Gizard F, Staels B, Dupont J, Monget P. 2005. A role of PPARgamma in reproduction? Med Sci 2:507–511.

Genolet R, Wahli W, Michalik L. 2004. PPARs as drug targets to modulate inflammatory responses? Curr Drug Targets Inflamm Allergy 3:361–375.

Gurnell M. 2005. Peroxisome proliferator-activated receptor gamma and the regulation of adipocyte function: Lessons from human genetic studies. Best Pract Res Clin Endocrinol Metab 19:501–523.

Kennedy WP, Kaminsky JM, Van Der Ven HH, Jeyendran RS, Reid DS, Blackwell J, Biefeld P, Zaneveld LJD. 1989. A simple, clinical assay to evaluate the acrosin activity of human spermatozoa. J Androl 10:221–231.

Kintscher U, Law RE. 2005. PPARgamma-mediated insulin sensitization: The importance of fat versus muscle. Am J Physiol Endocrinol Metab 288:E287–291.

Knouff C, Auwerx J. 2004. Peroxisome proliferator-activated receptor-gamma calls for activation in moderation: Lessons from genetics and pharmacology. Endocr Rev 25:899–918.

Kobayashi Y, Ueki S, Mahemuti G, Chiba T, Oyamada H, Saito N, Kanda A, Kayaba H, Chihara J. 2005. Physiological levels of 15-deoxy-Delta12,14-prostaglandin J2 prime eotaxin-induced chemotaxis on human eosinophils through peroxisome proliferator-activated receptor-gamma ligation. J Immunol 175:5744–5750.

Kostadinova R, Wahli W, Michalik L. 2005. PPARs in diseases: Control mechanisms of inflammation. Curr Med Chem 12:2995–3009.

Kota BP, Huang TH, Roufogalis BD. 2005. An overview on biological mechanisms of PPARs. Pharmacol Res 51:85–94.

Lehman TC, Hale DE, Bhala A, Thorpe C. 1990. An acyl-coenzyme A dehydrogenase assay utilizing the ferricenium ion. Anal Biochem 186:280–284.

Lenhard JM, Kliewer SA, Paulik MA, Plunket KD, Lehmann JM, Weiel JE. 1997. Effects of troglitazone and metformin on glucose and lipid metabolism: Alterations of two distinct molecular pathways. Biochem Pharmacol 54:801–808.

Miller D. 2000. Analysis and significance of messenger RNA in human ejaculated spermatozoa. Mol Reprod Dev 56:259–226.

Moschos S, Chan JL, Mantzoros CS. 2002. Leptin and reproduction: A review. . Fertil Steril 77:433–444.

Nicol CJ, Adachi M, Akiyama TE, Gonzalez FJ. 2005. PPARgamma in endothelial cells influences high fat diet-induced hypertension. Am J Hypertens 18:549–556.

Ostermeier GC, Dix DJ, Miller D, Khatri P, Krawetz SA. 2002. Spermatozoal RNA profiles of normal fertile men. Lancet 360:772–777.

Pan GD, Wu H, Liu JW, Cheng NS, Xiong XZ, Li SF, Zhang GF, Yan LN., 2005. Effect of peroxisome proliferator-activated receptor-gamma ligand on inflammation of human gall bladder epithelial cells. World J Gastroenterol 11:6061–6065.

Petersen KF, Krssak M, Inzucchi S, Cline GW, Dufour S, Shulman GI. 2000. Mechanism of troglitazone action in type 2 diabetes. Diabetes 49:827–831.

Quandt SA. 1984. Nutritional thriftiness and human reproduction: Beyond the critical body composition hypothesis. Soc Sci Med 19:177–182.

Randle P. 1964. The interrelationships of hormones, fatty acid and glucose in the provision of energy. Postgrad Med J 40:457–463.

Rangwala SM, Lazar MA. 2004. Peroxisome proliferator-activated receptor gamma in diabetes and metabolism. Trends Pharmacol Sci 25:331–336.

Roy AC, Ratnam SS. 1992. Biosynthesis of prostaglandins by human spermatozoa in vitro and their role in acrosome reaction and fertilization. Mol Reprod Dev 33:303–306.

Seli E, Duleba AJ. 2002. Optimizing ovulation induction in women with polycystic ovary syndrome. Curr Opin Obstet Gynecol 14:245–254.

Shah C, Modi D, Sachdeva G, Gadkar S, D'Souza S, Puri C. 2005. N-terminal region of progesterone receptor B isoform in human spermatozoa. Int J Androl 28:360–371.

Shimizu Y, Yorimitsu A, Maruyama Y, Kubota T, Aso T, Bronson RA. 1998. Prostaglandins induce calcium influx in human spermatozoa. Mol Hum Reprod 4:555–561.

Skolnik PR, Rabbi MF, Mathys JM, Greenberg AS. 2002. Stimulation of peroxisome proliferator-activated receptors alpha and gamma blocks HIV-1 replication and TNFalpha production in acutely infected primary blood cells, chronically infected U1 cells, and alveolar macrophages from HIV-infected subjects. J Acquir Immune Defic Syndr 31:1–10. Erratum in: J Acquir Immune Defic Syndr 2003.33:657.

Standiford TJ, Keshamouni VG, Reddy RC. 2005. Peroxisome proliferator-activated receptor-{gamma} as a regulator of lung inflammation and repair. Proc Am Thorac Soc 2:226–231.

Stumpo DJ, Kletzien RF. 1984. Regulation of glucose-6-phosphate dehydrogenase mRNA by insulin and the glucocorticoids in primary cultures of rat hepatocytes. Eur J Biochem 144:497–502.

Templeton AA, Cooper I, Kelly RW. 1978. Prostaglandin concentrations in the semen of fertile men. J Reprod Fertil 52:147–150.

Travis AJ, Kopf GS. 2002. The role of cholesterol efflux in regulating the fertilization potential of mammalian spermatozoa. J Clin Invest 110:731–736.

Visconti PE, Baley JL, Moore GD, Pan D, Olds-Clarke P, Kopf GS. 1995. Capacitation in mouse spermatozoa I. Correlation between the capacitation state and protein phosphorylation. Development 121:1129–1137.

Wang K, Zhou Z, Zhang M, Fan L, Forudi F, Zhou X, Qu W, Lincoff AM, Schmidt AM, Topol EJ, Penn MS. 2006. Peroxisome proliferator-activated receptor gamma down-regulates receptor for advanced glycation end products and inhibits smooth muscle cell proliferation in a diabetic and non-diabetic rat carotid artery injury model. J Pharmacol Exp Ther 317:37–43.

World Health Organization. 1999. WHO laboratory manual for the examination of human semen and sperm-cervical mucus interactions. 4th ed. Cambridge, UK: Cambridge University Press.

Xu Y, Iyengar S, Roberts RL, Shappell SB, Peehl DMJ. 2003. Primary culture model of peroxisome proliferator-activated receptor gamma activity in prostate cancer cells. Cell Physiol 196:131–143.

Yee LD, Guo Y, Bradbury J, Suster S, Clinton SK, Seewaldt VL. 2003. The antiproliferative effects of PPARgamma ligands in normal human mammary epithelial cells. Breast Cancer Res Treat 78:179–192.

Zhang L, Chawla A. 2004. Role of PPARgamma in macrophage biology and atherosclerosis. Trends Endocrinol Metab 15:500–505.

Expression of Nuclear Insulin Receptor Substrate 1 (IRS-1) in Breast Cancer

Diego Sisci[1§] , Catia Morelli[1§], Cecilia Garofalo[1], Francesco Romeo[2], Lucio Morabito[2], Filomena Casaburi[2], Emilia Middea[1] , Sandra Cascio[3], Elvira Brunelli[4], Sebastiano Andò[5] and Eva Surmacz[3*]

[1] Department of Pharmaco-Biology, Faculty of Pharmacy, University of Calabria, Arcavacata di Rende, Italy; [2] Division of Anatomo-Pathology, Annunziata Hospital, Cosenza, Italy; [3]Sbarro Institute for Cancer Research and Molecular Medicine, Temple University, Philadelphia, PA, USA, [4]Department of Natural Science and [5]Department of Cellular Biology, Faculty of Pharmacy, University of Calabria, Arcavacata di Rende, Italy.

[§] D.S. and C.M. contributed equally to this work

***Corresponding author:** Eva Surmacz, Ph.D.
Sbarro Institute for cancer Research and Molecular Medicine
College of Science and Technology, Temple University
1900 N 12th St. Rm. 446, Philadelphia, PA 19122
Tel. 001/215-204-0306, Fax 001/215-204-0303
e-mail surmacz@temple.edu

Word count (Abstract included): 3475
Structured abstract: 251 words.

Abstract

Aims: Insulin receptor substrate 1 (IRS-1), a cytoplasmic protein transmitting signals from the insulin and insulin-like growth factor 1 receptors, has been implicated in breast cancer. Previously, we reported that IRS-1 can be translocated to the nucleus and modulate estrogen receptor α (ERα) activity in vitro. However, the expression of nuclear IRS-1 in breast cancer biopsies has never been examined. Consequently, we assessed whether nuclear IRS-1 is present in breast cancer and non-cancer mammary epithelium and if it correlates with other markers, especially ERα. Parallel studies were done for cytoplasmatic IRS-1.

Methods: IRS-1 and ERα expression was assessed by immunohistochemistry. Data were evaluated using Pearson correlation, linear regression, and ROC analysis.

Results: Median nuclear IRS-1 expression was low in normal mammary epithelial cells (1.6%) and higher in benign tumors (20.5%), ductal grade 2 carcinoma (11.0%), and lobular carcinoma (~30%). Median ERα expression in normal epithelium, benign tumors, ductal cancer grade 2 and 3 and lobular cancer grade 2 and 3 was 10.5, 20.5, 65.0, 0.0, 80, and 15%, respectively. Nuclear IRS-1 and ERα positively correlated in ductal cancer ($p<0.001$) and benign tumors ($p< 0.01$), but were not associated in lobular cancer and normal mammary epithelium. In ductal carcinoma, both nuclear IRS-1 and ERα negatively correlated with tumor grade, size, mitotic index, and lymph node involvement. Cytoplasmic IRS-1 was expressed in all specimens and positively correlated with ERα in ductal cancer.

Conclusions: A positive association between nuclear IRS-1 and ERα is a characteristic for ductal breast cancer and marks a more differentiated, non-metastatic phenotype.

Take-home messages

1. This is the first report examining the expression of nuclear IRS-1 in normal mammary tissue, benign breast tumors and breast cancer in relation to ERα and clinicopathological features.

2. Nuclear IRS-1 is more prevalent in cancer specimens than in normal mammary tissues.
3. Nuclear IRS-1 and ERα negatively correlated with tumor grade, size, mitotic index, and lymph node involvement.
4. A positive association between nuclear IRS-1 and ERα is a characteristic for ductal breast cancer and marks a more differentiated, non-metastatic phenotype.

Introduction

Recent experimental and clinical evidence suggests the involvement of the insulin-like growth factor I (IGF-I) receptor (IGF-IR) in breast cancer development and progression [1-6]. The tumorigenic action of IGF-IR is executed through multiple antiapoptotic, growth promoting, and/or pro-metastatic pathways [5-9]. Many of these pathways stem from IRS-1, a major IGF-I signaling molecule that becomes phosphorylated on multiple tyrosine residues upon IGF-IR activation. Tyrosine phosphorylated IRS-1 acts as a scaffolding protein sequestering downstream signaling molecules and propagating IGF-I signal through the PI-3K/Akt, Ras/Raf/ERK1/2, Jak2/Stat3 and other pathways [10-13].

Overexpression or downregulation of IRS-1 in breast cancer cell models suggested that the molecule controls several aspects of the neoplastic phenotype, especially anchorage-dependent and -independent cell growth and survival [14 15]. In breast cancer cell lines, IRS-1 appears to be expressed at higher levels in ERα-positive than in ERα-negative cells and there is evidence supporting the existence of a crosstalk between IRS-1 and ERα systems [1 4 6 16-18]. Overexpression of IRS-1 in MCF-7 ERα-positive cells has been shown to induce estrogen-independence and mediate antiestrogen-resistance [14 19 20]. High expression of IRS-1 can be in part attributed to ERα activity, as 17β-estradiol (E2) can upregulate IRS-1 expression and function [16 21 22], while antiestrogens reduce IRS-1 mRNA and protein levels and inhibit IRS-1 signaling [19 20 23]. In addition, ERα can directly interact with IRS-1, increasing its stability and potentiating its downstream signaling to Akt [24]. Notably, increased activity of IRS-1 is likely to modulate ERα, via ERK1/2- and Akt-mediated phosphorylation of ERα on Ser-118 and Ser-167, respectively [25-27].

Recent reports suggested that in addition to its cytoplasmic signaling function, IRS-1 is able to regulate nuclear processes in different cell models [28-33]. For instance, in mouse fibroblasts treated with IGF-I, a fraction of IRS-1 is translocated from the cytoplasm to the nuclear and nucleolar

compartments where it modulates the expression of genes controlling cell proliferation (i.e., Cyclin D1) and cell growth in size (i.e., rDNA) by physically interacting with transcriptional complexes of β-catenin and upstream binding factor 1 (UBF1), respectively [31 32]. Our recent work demonstrated that nuclear IRS-1 is also found in breast cancer cell lines. For instance, in MCF-7 cells treated with E2 nuclear IRS-1 physically interacted with ERα modulating its transcriptional activity at estrogen response element (ERE) DNA motifs [33]. The exact mechanism of nuclear IRS-1 transport is not clear, but most likely it involves other proteins containing nuclear localization signals (ERα, T antigen, importins).

Despite the evidence that IRS-1 signaling may play a critical role in tumorigenesis, only limited studies examined the clinical significance of IRS-1 expression in human breast cancer specimens [18 34-36]. In one study, cytoplasmatic IRS-1 has been reported to correlate with poorly differentiated breast tumor phenotype (G3) and lymph node involvement [35]. Another study correlated IRS-1 with shorter disease-free survival in patients with smaller tumors [18]. In contrast, Schnarr et al. found that IRS-1 marks a more differentiated phenotype and better prognosis [34]. Furthermore, one study examining cancer and normal specimens reported similar IRS-1 tyrosine phosphorylation in all tissues [36], while other analysis found decreased IRS-1 levels in poorly differentiated cancers relative to normal tissue and benign tumors [34].

Regarding nuclear IRS-1, its presence in breast cancer specimens has been noted by Schnarr et al. [34] and Koda et al. [35], but any association with the disease has never been formally addressed. Consequently, we examined the expression of nuclear IRS-1 in normal mammary tissue, benign breast tumors and breast cancer in relation to ERα and clinicopathological features. Parallel studies were done for cytoplasmatic IRS-1.

Materials and Methods

Patients and tissue specimens

Table 1 summarizes information on patient and specimen characteristics. The histopathological examination of sections was based on the WHO and pTN classification of breast tumors. Tumor size (pT) was scored as follows: 0, primary tumor not detectable; 1, tumor largest diameter <2cm; 2, diameter <5cm; 3, diameter >5cm; 4, inflammatory carcinoma of any size. Lymph node status (pN) was scored from 0, no node involvement; 1, proximal node involved; 2, distal node involved. The protocol of the present study was reviewed and approved by the local ethical committee.

Table 1. Patient characteristics and clinical parameters of breast tissues and cancers

Sample characteristics

	Cancers	**Controls**
Total specimens	60	34
Ductal carcinoma	38	
Lobular carcinoma	22	
Benign tumors		19
Macromasty		14

Patient Age

	Normal	**Benign**	**Ductal**	**Lobular**
Mean±SE	53.6±3.3	45.4±3.1	62.9±2.4	64.5±2.7
Median (Range)	56.5 (33-68)	43 (20-68)	61.5 (43-94)	66 (48-78)
Menopause (%)	64	39	87	82

Clinical parameters of breast cancer tissues

	Ductal (38)		**Lobular (22)**	
	G2 (19)	**G3 (19)**	**G2 (10)**	**G3 (12)**
pT	1-4	0-4	2-4	0-4
pN	0-2	0-2	0-1	0-2
Ki67	7.7 ± 0.9 (4-14)	14.2±1.3 (6-21)	7.2±1.5 (4-12)	9.0±1.9 (3-15)

The age of patients in each group is given as mean value ± SE with median age (range) for each population. The percentage of postmenopausal patients is indicated in each group. The range is

reported for tumor size (pT), and lymph node involvement (pN); median frequency of expression ±SE (range) is shown for Ki67.

Immunohistochemistry and confocal microscopy

Samples preparation

Immediately after excision, tissue samples were fixed in 10% buffered formaldehyde solution and embedded in paraffin blocks at 56°C. ERα and IRS-1 were analyzed by immunohistochemical (IHC) staining using 3µm-thick consecutive paraffin sections. The sections were dewaxed in xylene and rehydrated in graded alcohols. After antigen retrieval by boiling in 0.01M citrate buffer pH 6.

Immunohistochemistry

Endogenous peroxidase was removed with 3% H_2O_2; nonspecific binding was blocked by incubating the slides for 30 min with 1.5% BSA in PBS. Next, the sections were incubated with the primary antibodies (Abs) for 1h at room temperature. ERα was detected using ERα mouse monoclonal Ab (mAb) (DakoCytomation, Denmark) at dilution 1:35. IRS-1 was detected using the C-terminus IRS-1 rabbit polyclonal Ab (pAb) (Upstate, USA) at a concentration 4µg/ml. Ab-antigen reactions were revealed using Streptavidin-biotin-peroxidase complex (LSAB kit, DakoCytomation, Denmark). All slides were counterstained with hematoxylin. Breast specimens previously classified as positive for the expression of the studied markers were used for control and protocol standardization. In negative controls, primary Abs were omitted. The expression of ERα and IRS-1 was independently scored by two investigators (CM and CG) by light microscopy in 10 different section fields. For all nuclear markers, mean and median percentage, and the range of epithelial cells displaying positive staining was scored. In some analyses, specimens were grouped into ERα-negative (less than 5% of epithelial cells exhibiting ERα expression) and ERα-positive (5% or more of cells with ERα). The expression of cytoplasmic IRS-1 was classified using a four-point scale: 0, <10% positive cells with any staining

intensity; 1+, 10-50% positive cells with weak or moderate staining; 2+, >50% positive cells with weak or moderate staining; 3+, >50% positive cells with strong staining. No samples with less than 50% of positive cells with strong staining were recorded.

Confocal microscopy

Tissues sections were incubated for 30 min with 3% BSA in PBS to avoid nonspecific bindin, then for 1 h with a mixture of primary Abs (pAbs) recognizing IRS-1 and ERα.

The anti-IRS-1 pAb (UBI) at 4 μg/ml was used for IRS-1 staining; anti-ERa F-10 monoclonal Ab (mAb) (Santa Cruz) at 2 μg/ml was used to detect ERα. Following the incubation with primary Abs, the slides were washed three times with PBS, and incubated with a mixture of secondary Abs. A rhodamine-conjugated donkey anti-mouse IgG (Calbiochem) was used as a secondary Ab for ERα and a fluorescein-conjugated donkey anti-rabbit IgG (Calbiochem) was used for IRS-1. The cellular localization of IRS-1 and ERα was studied using the Bio-Rad MRC 1024 confocal microscope connected to a Zeiss Axiovert 135M inverted microscope with x1000 magnification. The optical sections were taken at the central plane. The fluorophores were imaged separately to ensure no excitation/emission wavelength overlap. In control samples, the staining was performed with the omission of the primary Abs.

Statistical analysis

Descriptive statistic for nuclear IRS-1 and ERα in normal, benign and tumor samples was reported as mean, standard error (±SE), median value and range. The relationship between nuclear IRS-1 and ERα was analyzed by linear regression and the statistical significance was evaluated by the Pearson correlation test. The distribution of ERα and nuclear IRS-1 in respect to tumor size, grade, and lymph node involvement are reported in scatterplots. The correlations between nuclear IRS-1, ERα,

cytoplasmatic IRS-1 and selected clinicopathologic features were examined with the Pearson correlation test.

The value of nuclear ERα or IRS-1 expression as diagnostic marker of tumor grade, pT, pN and Ki67 was evaluated calculating the areas under the receiver operating characteristic (ROC) curves [37], which assess the performance of a diagnostic test [38-40]. In the graphical representation of the ROC curve, the X-axis is the false-positive rate (1-specificity) and the Y-axis is the true positive rate (sensitivity). The diagonal line (from 0,0 to 1,1) reflects the characteristics of a test with no discriminating power. ROC curve was analyzed using MedCalc (MedCalc Software, Mariakerke, B).

Results

Nuclear IRS-1and ERα expression in normal mammary epithelium and benign breast tumors.

In general, the expression of nuclear IRS-1 in normal tissues was very low (~2% of positive cells) (Tab. 2). ERα was expressed in 11 of 14 samples; the median frequency of ERα in all samples was 10.5% (Fig. 1A, B and Tab. 2). Nuclear IRS-1 was found in 9 of 11 ERα-positive specimens at the median frequency 1.8%. Low expression (3.5%) of nuclear IRS-1 was also recorded in 2 specimens that did not express ERα (data not shown).

Compared with normal epithelium, benign tumors expressed higher median levels of nuclear IRS-1 (20.5%) and ERα (20.5.0%) (Tab. 2). Nuclear IRS-1 was found in 16 of 19 ERα-positive specimens, but was not present in any of ERα-negative cases. (Fig. 1C, D and data not shown).

Cytoplasmic IRS-1 was expressed in all epithelial cells of normal epithelium and benign tumors at the levels 1+ to 3+ (Fig. 1B, D and Tab. 3), while no evidence of cytoplasmic ERα staining was revealed in any of the specimens (Fig. 1A). The co-localization of nuclear IRS-1 and ERα was determined by confocal microscopy (Fig. 2).

Table 2. Descriptive statistics of nuclear IRS-1 and ERα in all samples.

	Normal Epithelium		Benign Tumors	
	ERα	**IRS-1**	**ERα**	**IRS-1**
Mean±SE	21.7±6.1	2.3±0.6	23.4±4.2	23±4.5
Median (Range)	10.5 (0-60)	1.6 (0-7)	20.5 (0-70)	20.5 (0-60)

Ductal Carcinoma	G2		G3	
	ERα	**IRS-1**	**ERα**	**IRS-1**
Mean±SE	51.8±10.1	23.4±7.1	6.2±3.4	4.1±1.8
Median (Range)	65 (0-92)	11 (0-72)	0 (0-40)	0 (0-20)

Lobular Carcinoma	G2		G3	
	ERα	**IRS-1**	**ERα**	**IRS-1**
Mean±SE	64.8±11.3	32±9.7	26.7±8.9	30.7±4.7
Median (Range)	80 (0-90)	35 (0-80)	15 (0-80)	33.5 (0-52)

The mean (±SE) expression with median (range) values for nuclear IRS-1 and ERα in all specimens (ERα-positive and ERα-negative) is given. Cancer samples of ductal and lobular origin were grouped into separate G2 and G3 populations.

Table 3. Descriptive statistics of cytoplasmatic IRS-1 in all samples

Cytoplasmic IRS-1 Expression (% of Cases in Class)				
Class	**Normal**	**Benign**	**Ductal**	**Lobular**
0	0	0	0	0
1+	29	21	16	0
2+	29	21	52	63
3+	42	58	32	37

Samples are grouped in 4 classes as described in Materials and Methods. The percentage of specimens with cytoplasmic IRS-1 in each staining category is given.

IRS-1 expression in ERα-positive and ERα-negative breast carcinoma.

In invasive ductal carcinoma, nuclear IRS-1 was found in 22 of 38 of specimens. The median level of expression in these samples was 13.7%. ERα was detected in 20 of 38 of specimens with a median expression of 29.2% (Fig. 1E, F). Twenty two specimens (15 of 19 in G2, and 7 of 19 in G3) expressed nuclear IRS-1 (Fig. 1F, Tab. 2). Among nuclear IRS-1-positive samples, 18 also expressed ERα, while 4 were ERα-negative. Thirteen of G2 ductal carcinomas and 5 of G3 cancers were positive for both IRS-1 and ERα. In 2 of 38 specimens, ERα was expressed in the absence of nuclear IRS-1.

In lobular cancer, nuclear IRS-1 staining was observed in 16 of 22 samples with the median frequency 31.2% (Fig. 1H). Eleven of these 16 samples were also ERα-positive. Within G2 lobular carcinomas, 6 of 10 specimens displayed nuclear IRS-1 at the median level 35.0%; all these samples expressed ERα at the median frequency 80.0% (Tab. 2). In the G3 subgroup, 10 of 12 tumors expressed nuclear IRS-1 (median 33.5%) and 5 of 10 expressed ERα (median 15.0%). In 5 of 16 lobular cancers, nuclear IRS-1 was found in the absence of ERα (Tab. 2).

Cytoplasmatic IRS-1 was identified in all ductal and lobular cancer samples displaying a weak to strong staining intensity (Tab. 3). In all specimens, the neoplasm surrounding tissue appeared normal and the pattern of ERα and IRS-staining comparable to that of the normal samples.

Correlation between nuclear IRS-1and ERα in breast cancer, benign tumors, and normal mammary epithelium.

A very strong positive correlation ($p<0.001$) between nuclear IRS-1 and ERα was found in invasive ductal breast cancer. The markers were also positively associated ($p<0.01$) in benign tumors cancer samples (Fig. 4). However, no correlations were found between nuclear IRS-1 and ERα in normal tissues ($p=0.28$) and lobular breast cancer ($p=0.24$) (Fig. 4).

Nuclear IRS-1 and ERα are correlated with some clinicopathological features in invasive ductal carcinomas.

The distribution of nuclear ERα and nuclear IRS-1 was analyzed with respect to tumor grade, tumor size, lymph node involvement, and proliferation index (Fig. 3). The frequency of both ERα and nuclear IRS-1 expression was the highest in node-negative G2 invasive ductal carcinomas of smaller size (Fig. 3). In the same group, a significant negative correlation between nuclear IRS-1 or ERα and differentiation grade, the tumor size, lymph node involvement and proliferation rate was found (Tab. 4).

In contrast, in lobular breast carcinomas, the distribution of nuclear IRS-1 or ERα appeared to be independent of and not correlated with tumor grade, size, or Ki67 expression (Fig. 3 and Tab. 4). Interestingly, both nuclear IRS-1 and ERα were more abundant in lymph node-negative samples (Fig. 3), but no significant associations were determined between these markers and lymph node status (Tab. 4).

The specificity and sensitivity of nuclear IRS-1 or ERα as a marker of tumor differentiation grade, tumor size and lymph node involvement was evaluated by the ROC curve analysis. The comparison of the areas under the ROC curves obtained for nuclear IRS-1 and ERα indicated that both nuclear IRS-1 and ERα are good markers for tumor grading in invasive ductal carcinomas, while in lobular carcinomas only ERα could be considered a marker for grading (Tab. 5 and Fig. 5).

Neither ERα nor nuclear IRS-1 was a useful marker of tumor size, node involvement, or tumor proliferation (data not shown). The distribution of nuclear IRS-1 or ERα was not related to patient's age and menopausal status in cancer, benign and normal samples (data not shown).

Table 4. Correlation between nuclear IRS-1, ERα and selected clinicopathological tumor features.

		Ductal Carcinoma		Lobular Carcinoma	
		ERα	IRS-1	ERα	IRS-1
G	r	**-0.573**	**-0.511**	-0.563	0.029
	p	**0.0015**	**0.0057**	0.065	0.94
pT	r	**-0.393**	**-0.382**	-0.326	0.153
	p	**0.039**	**0.044**	0.310	0.633
pN	r	**-0.381**	**-0.454**	-0.082	-0.122
	p	**0.044**	**0.015**	0.797	0.714
Ki67	r	**-0.591**	**-0.538**	-0.329	-0.016
	p	**0.0001**	**0.003**	0.31	0.94

The association between nuclear IRS-1 or ERa and tumor grade (G), size (pT), lymph node involvement (pN), and the expression of the proliferation marker Ki67 was statistically analyzed with Pearson correlation test; r, correlation coefficient; p, statistical significance. The statistically significant correlations are bolded.

Table 5. Association between nuclear IRS-1, ERα and tumor grade.

Diagnostic Marker	**ROC analysis for tumor grade**		
	AUC estimate (95% CI)	**Area under the ROC curve**	**Mann-Whitney test (p value)**
Ductal Carcinoma			
ERα	71.4 (41.9-91.4)	0.809	**0.001**
IRS-1	78.6 (49.2-95.1)	0.778	**0.001**
Lobular Carcinoma			
ERα	80.0 (28.8-96.7)	0.817	**0.02**
IRS-1	60.0 (15.4-93.5)	0.533	0.85

The analysis was performed with ROC curves, as described in Materials and Methods. The area under the ROC (receiver operating characteristic) curve (AUC) describes the value of nuclear IRS-1 or ERα to discriminate between G2 and G3 tumors. AUC estimate reports the confidence intervals considering an error of 5%. The statistical significance was evaluated by Mann-Whitney test for an area =0.5. Statistical significances are bolded.

Relationship between cytoplasmatic IRS-1 and clinicopathological features.

In ductal carcinomas, cytoplasmic IRS-1 (each staining intensity group) positively correlated with ERα. Moreover, in ductal cancer low and moderate IRS-1 expression was positively associated with tumor size, while high IRS-1 levels negatively correlated with tumor grade (Tab. 6).

In lobular carcinomas, high expression of cytoplasmic IRS-1 directly correlated with Ki67 (Tab. 6). In benign tumors, low expression of cytoplasmatic IRS-1 was negatively associated with ERα, while higher IRS-1 levels were not linked to ERα. No correlations between the two markers were found in normal samples (data not shown). Similarly, cytoplasmic IRS-1 expression was not related to age or menopausal status in all analyzed material (data not shown).

Table 6. Correlations between cytoplasmatic IRS-1 and selected clinicopathological features in ERα-positive tumors.

		Ductal				Lobular			
		0	**1+**	**2+**	**3+**	**0+**	**1+**	**2+**	**3+**
ERα	**r**	-	**0.978**	**0.637**	**0.987**	-	-	0.198	-0.029
	p		**0.025**	**0.019**	**0.013**			0.671	0.970
G	**r**	-	0.375	-0.082	**-0.962**	-	-	0.204	-0.376
	p		0.625	0.790	**0.037**			0.661	0.624
pT	**r**	-	**0.973**	**0.553**	-0.577	-	-	0.009	-0.225
	p		**0.026**	**0.050**	0.423			0.984	0.775
pN	**r**	-	0.00	0.301	-	-	-	-0.069	-
	p		1.00	0.318				0.883	
Ki67	**r**	-	0.724	-0.241	-0.905	-	-	-0.223	**0.978**
	p		0.276	0.428	0.095			0.631	**0.022**

The associations between cytoplasmatic IRS-1 and ERα positivity (ERα), tumor grade (G), tumor size (pT), lymph node involvement (pN), and the expression of the proliferation marker Ki67 were statistically analyzed with the Pearson correlation test; r, correlation coefficient; p, statistical significance. The statistically significant correlations are bolded. The absence of value is due to either the absence of samples in the group or to the homogeneity of samples (variance =0).

Discussion

Studies in cellular and animal models established that breast cancer cell growth is controlled by complex crosstalk between ERα and IGF-I systems [4-6 14 19 41-44]. However, while ERα is an established marker for breast cancer diagnosis and prognosis and a target for breast cancer therapy and prevention, the value of critical IGF-I system components like IGF-IR and IRS-1 as breast cancer markers needs

further examination. Until now, analysis of breast cancer samples did not establish a clear association between IGF-IR and breast cancer progression. Several studies demonstrated higher expression of IGF-IR compared with non-cancer mammary epithelium, however this feature has been associated with either favorable or unfavorable breast cancer prognosis [4 45-53]. The value of cytoplasmatic IRS-1 as a breast cancer marker is even less clear. Some studies provided evidence that IRS-1 expression is higher in cancer than in non-cancer breast epithelium, while others (including this study) reported that IRS-1 levels do not increase (but can decrease) during cancer development and progression [18 34 36]. Moreover, cytoplasmatic IRS-1 has been found either to correlate with ERα and associate with a more differentiated phenotype or be independent from ERα and associated with a more aggressive phenotype [16 34 41 52]. The significance of nuclear IRS-1 in breast cancer has never been addressed.

In view of the importance of cytoplasmatic and nuclear IRS-1 in breast cancer growth evidenced in vitro and conflicting or lacking data in vivo, we set out to investigate IRS-1 expression in normal mammary epithelium, benign tumors and breast cancer. Using IHC, we assessed cytoplasmic and nuclear IRS-1 abundance and examined its relations with some prognostic markers, especially ERα, and clinicopathological features.

Our data on cytoplasmic IRS-1 are consistent with those reported by Schnarr *et al.* who noted moderate to strong IRS-1 expression in normal and benign tissues, and in well differentiated carcinomas of both ductal and lobular origin [34]. Similarly, Finlayson *et al.* found no difference of IRS-1 phosphorylation in homogenates of normal and breast cancer tissues [36]. On the other hand, other groups reported low IRS-1 expression in normal tissue and overexpression in poorly differentiated tumors [18 35 48]. In agreement with Schnarr et al. we found a positive association between cytoplasmatic IRS-1 and ERα and a negative correlation between high expression of IRS-1 and tumor grade in ductal carcinomas. This observation is also consistent with coexpression of IRS-1 and ERα noted in less

invasive breast cancer cell lines [6]. In other studies ERα and IRS-1 were not positively correlated in primary tumors [18 35]. The causes for these different results are unclear, but could be related to different IHC protocols, including different Abs used.

We did not find any correlation between cytoplasmic IRS1 and lymph node involvement in ductal and lobular cancers. This partially confirms data of Koda *et al.*, who did not observe such a correlation in the whole group of primary tumours, but only in the subgroup of better differentiated (G2) cancers [35]. Our results also suggested a positive correlation between cytoplasmatic IRS-1 (weak to moderate) and tumor size in ERα-positive ductal cancers. This association has not been noted by others. Regarding cell proliferation, we found a positive correlation of IRS-1 and Ki-67 only in ERα-positive lobular cancers expressing high levels of IRS-1 and no associations in all other samples. Similarly, no link between cell proliferation and cytoplasmatic IRS-1 levels was reported by Rocha *et al*. In contrast, a negative correlation was reported by Schnarr *et al*., while Koda *et al*., noted a positive IRS-1/Ki-67 correlation in ERα-positive primary tumors [34 35]. Taken together, these data are still too few and inconsistent to suggest cytoplasmic IRS-1 as a marker for breast cancer prognosis and diagnosis.

Instead, our results suggest that nuclear IRS-1 is tightly linked to ERα expression and might serve as an additional clinical breast cancer marker. As expected, ERα levels were low in normal mammary epithelium, higher in benign tumors, and strongly increased in moderately differentiated (G2) cancers. ERα expression was downregulated in poorly differentiated (G3) ductal cancers but not in G3 lobular cancers, confirming the value of ERα as a marker of differentiation in ductal carcinoma [54-56]. Notably, the levels of nuclear IRS-1 were very low in normal tissue, increased in benign tumors and G2 ductal cancer, and decreased in G3 ductal cancer, displaying an expression trend similar to that of ERα.

In lobular cancer, the levels of nuclear IRS-1 were relatively high in both G2 and G3 tumors (~30%) and were not related to the abundance of ERα. Indeed, statistical analysis of data confirmed a very strong correlation between nuclear IRS-1 and ERα in ductal, but not lobular, cancers. Importantly, in ductal, but again not in lobular cancers, both nuclear IRS-1 and ERα negatively correlated with tumor grade, tumor size, lymph node involvement and proliferation rate, suggesting their association with a less aggressive phenotype. The ROC analysis confirmed that nuclear IRS-1 as for ERα, is highly reliable as diagnostic marker of differentiation grade. The observation that nuclear IRS-1 expression increases in benign as well as in highly and moderately differentiated tumors, compared to normal tissues, strongly supports this assumption.

Taken together, our data indicate that nuclear IRS-1 could serve as a novel predictive marker of good prognosis in ductal cancer. The lack of association between nuclear IRS-1 and ERα in lobular cancer and benign tumors, might suggest that, in this settings, IGF-I and ERα systems are not tightly linked.

List of Abbreviations

ERα (Estrogen Receptor alpha), IRS-1 (Insulin Receptor Substrate 1).

Authors'contributions

DS and CM participated in the design of the study, performed the statistical analysis and drafted the manuscript, CG carried out the immunostaining and participated to the statistical analysis, FR participated in the design of the study, LM participated to the statistical analysis, FC prepared the histological samples, EM carried out the immunostaining, SC participated to the statistical analysis, SA

participated in the design of the study and drafted the manuscript, ES designed the study and drafted the manuscript.

Acknowledgments: This work was supported by AIRC – 2004, MURST Ex 60% - 2005 and Sbarro Health Research Organization

References

1. Bartucci M, Morelli C, Mauro L, Ando S, Surmacz E. Differential insulin-like growth factor I receptor signaling and function in estrogen receptor (ER)-positive MCF-7 and ER-negative MDA-MB-231 breast cancer cells. *Cancer Res.* Sep 15 2001;61(18):6747-6754.
2. Pollak M. IGF-I physiology and breast cancer. *Recent Results Cancer Res.* 1998;152:63-70.
3. Sachdev D, Yee D. The IGF system and breast cancer. *Endocr Relat Cancer.* Sep 2001;8(3):197-209.
4. Surmacz E. Function of the IGF-I receptor in breast cancer. *J Mammary Gland Biol Neoplasia.* Jan 2000;5(1):95-105.
5. Surmacz E. Growth factor receptors as therapeutic targets: strategies to inhibit the insulin-like growth factor I receptor. *Oncogene.* Sep 29 2003;22(42):6589-6597.
6. Surmacz E, Bartucci M. Role of estrogen receptor alpha in modulating IGF-I receptor signaling and function in breast cancer. *J Exp Clin Cancer Res.* Sep 2004;23(3):385-394.
7. Baserga R. The contradictions of the insulin-like growth factor 1 receptor. *Oncogene.* Nov 20 2000;19(49):5574-5581.
8. Baserga R, Peruzzi F, Reiss K. The IGF-1 receptor in cancer biology. *Int J Cancer.* Dec 20 2003;107(6):873-877.
9. Mauro L, Salerno M, Morelli C, Boterberg T, Bracke ME, Surmacz E. Role of the IGF-I receptor in the regulation of cell-cell adhesion: implications in cancer development and progression. *J Cell Physiol.* Feb 2003;194(2):108-116.
10. Myers MG, Jr., Sun XJ, White MF. The IRS-1 signaling system. *Trends Biochem Sci.* Jul 1994;19(7):289-293.

11. Myers MG, Jr., White MF. Insulin signal transduction and the IRS proteins. *Annu Rev Pharmacol Toxicol.* 1996;36:615-658.
12. White MF. The insulin signalling system and the IRS proteins. *Diabetologia.* Jul 1997;40 Suppl 2:S2-17.
13. White MF. The IRS-signaling system: a network of docking proteins that mediate insulin and cytokine action. *Recent Prog Horm Res.* 1998;53:119-138.
14. Surmacz E, Burgaud JL. Overexpression of insulin receptor substrate 1 (IRS-1) in the human breast cancer cell line MCF-7 induces loss of estrogen requirements for growth and transformation. *Clin Cancer Res.* Nov 1995;1(11):1429-1436.
15. Nolan MK, Jankowska L, Prisco M, Xu S, Guvakova MA, Surmacz E. Differential roles of IRS-1 and SHC signaling pathways in breast cancer cells. *Int J Cancer.* Sep 4 1997;72(5):828-834.
16. Lee AV, Jackson JG, Gooch JL, et al. Enhancement of insulin-like growth factor signaling in human breast cancer: estrogen regulation of insulin receptor substrate-1 expression in vitro and in vivo. *Mol Endocrinol.* May 1999;13(5):787-796.
17. Lee AV, Guler BL, Sun X, et al. Oestrogen receptor is a critical component required for insulin-like growth factor (IGF)-mediated signalling and growth in MCF-7 cells. *Eur J Cancer.* Sep 2000;36 Suppl 4:109-110.
18. Rocha RL, Hilsenbeck SG, Jackson JG, et al. Insulin-like growth factor binding protein-3 and insulin receptor substrate-1 in breast cancer: correlation with clinical parameters and disease-free survival. *Clin Cancer Res.* Jan 1997;3(1):103-109.
19. Guvakova MA, Surmacz E. Tamoxifen interferes with the insulin-like growth factor I receptor (IGF-IR) signaling pathway in breast cancer cells. *Cancer Res.* Jul 1 1997;57(13):2606-2610.
20. Salerno M, Sisci D, Mauro L, Guvakova MA, Ando S, Surmacz E. Insulin receptor substrate 1 is a target for the pure antiestrogen ICI 182,780 in breast cancer cells. *Int J Cancer.* Apr 12 1999;81(2):299-304.
21. Mauro L, Salerno M, Panno ML, et al. Estradiol increases IRS-1 gene expression and insulin signaling in breast cancer cells. *Biochem Biophys Res Commun.* Nov 2 2001;288(3):685-689.
22. Molloy CA, May FE, Westley BR. Insulin receptor substrate-1 expression is regulated by estrogen in the MCF-7 human breast cancer cell line. *J Biol Chem.* Apr 28 2000;275(17):12565-12571.
23. Chan TW, Pollak M, Huynh H. Inhibition of insulin-like growth factor signaling pathways in mammary gland by pure antiestrogen ICI 182,780. *Clin Cancer Res.* Aug 2001;7(8):2545-2554.
24. Morelli C, Garofalo C, Bartucci M, Surmacz E. Estrogen receptor-alpha regulates the degradation of insulin receptor substrates 1 and 2 in breast cancer cells. *Oncogene.* Jun 26 2003;22(26):4007-4016.
25. Kato S, Endoh H, Masuhiro Y, et al. Activation of the estrogen receptor through phosphorylation by mitogen-activated protein kinase. *Science.* Dec 1 1995;270(5241):1491-1494.
26. Campbell RA, Bhat-Nakshatri P, Patel NM, Constantinidou D, Ali S, Nakshatri H. Phosphatidylinositol 3-kinase/AKT-mediated activation of estrogen receptor alpha: a new model for anti-estrogen resistance. *J Biol Chem.* Mar 30 2001;276(13):9817-9824.
27. Stoica A, Saceda M, Fakhro A, Joyner M, Martin MB. Role of insulin-like growth factor-I in regulating estrogen receptor-alpha gene expression. *J Cell Biochem.* Jan 2000;76(4):605-614.
28. Lassak A, Del Valle L, Peruzzi F, et al. Insulin receptor substrate 1 translocation to the nucleus by the human JC virus T-antigen. *J Biol Chem.* May 10 2002;277(19):17231-17238.

29. Prisco M, Santini F, Baffa R, et al. Nuclear translocation of insulin receptor substrate-1 by the simian virus 40 T antigen and the activated type 1 insulin-like growth factor receptor. *J Biol Chem.* Aug 30 2002;277(35):32078-32085.
30. Trojanek J, Croul S, Ho T, et al. T-antigen of the human polyomavirus JC attenuates faithful DNA repair by forcing nuclear interaction between IRS-1 and Rad51. *J Cell Physiol.* Jan 2006;206(1):35-46.
31. Chen J, Wu A, Sun H, et al. Functional significance of type 1 insulin-like growth factor-mediated nuclear translocation of the insulin receptor substrate-1 and beta-catenin. *J Biol Chem.* Aug 19 2005;280(33):29912-29920.
32. Drakas R, Tu X, Baserga R. Control of cell size through phosphorylation of upstream binding factor 1 by nuclear phosphatidylinositol 3-kinase. *Proc Natl Acad Sci U S A.* Jun 22 2004;101(25):9272-9276.
33. Morelli C, Garofalo C, Sisci D, et al. Nuclear insulin receptor substrate 1 interacts with estrogen receptor alpha at ERE promoters. *Oncogene.* Sep 30 2004;23(45):7517-7526.
34. Schnarr B, Strunz K, Ohsam J, Benner A, Wacker J, Mayer D. Down-regulation of insulin-like growth factor-I receptor and insulin receptor substrate-1 expression in advanced human breast cancer. *Int J Cancer.* Nov 20 2000;89(6):506-513.
35. Koda M, Sulkowska M, Kanczuga-Koda L, Sulkowski S. Expression of insulin receptor substrate 1 in primary breast cancer and lymph node metastases. *J Clin Pathol.* Jun 2005;58(6):645-649.
36. Finlayson CA, Chappell J, Leitner JW, et al. Enhanced insulin signaling via Shc in human breast cancer. *Metabolism.* Dec 2003;52(12):1606-1611.
37. Vanagas G. Receiver operating characteristic curves and comparison of cardiac surgery risk stratification systems. *Interact CardioVasc Thorac Surg.* 2004;3:319-322.
38. Greiner M, Pfeiffer D, Smith RD. Principles and practical application of the receiver-operating characteristic analysis for diagnostic tests. *Prev Vet Med.* May 30 2000;45(1-2):23-41.
39. Wynne-Jones K, Jackson M, Grotte G, Bridgewater B. Limitations of the Parsonnet score for measuring risk stratified mortality in the north west of England. The North West Regional Cardiac Surgery Audit Steering Group. *Heart.* Jul 2000;84(1):71-78.
40. Zweig MH. ROC plots display test accuracy, but are still limited by the study design. *Clin Chem.* Jun 1993;39(6):1345-1346.
41. Ando S, Panno ML, Salerno M, et al. Role of IRS-1 signaling in insulin-induced modulation of estrogen receptors in breast cancer cells. *Biochem Biophys Res Commun.* Dec 18 1998;253(2):315-319.
42. Huynh H, Nickerson T, Pollak M, Yang X. Regulation of insulin-like growth factor I receptor expression by the pure antiestrogen ICI 182780. *Clin Cancer Res.* Dec 1996;2(12):2037-2042.
43. Ignar-Trowbridge DM, Pimentel M, Parker MG, McLachlan JA, Korach KS. Peptide growth factor cross-talk with the estrogen receptor requires the A/B domain and occurs independently of protein kinase C or estradiol. *Endocrinology.* May 1996;137(5):1735-1744.
44. Migliaccio M, Di Domenico M, Castoria G, et al. Tyrosine kinase/p21ras/MAP-kinase pathway activation by estradiol-receptor complex in MCF-7 cells. *EMBO J.* 1996;15:1292-1300.
45. Pezzino V, Papa V, Milazzo G, Gliozzo B, Russo P, Scalia PL. Insulin-like growth factor-I (IGF-I) receptors in breast cancer. *Ann N Y Acad Sci.* Apr 30 1996;784:189-201.
46. Railo MJ, von Smitten K, Pekonen F. The prognostic value of insulin-like growth factor-I in breast cancer patients. Results of a follow-up study on 126 patients. *Eur J Cancer.* 1994;30A(3):307-311.

47. Papa V, Gliozzo B, Clark GM, et al. Insulin-like growth factor-I receptors are overexpressed and predict a low risk in human breast cancer. *Cancer Res.* Aug 15 1993;53(16):3736-3740.
48. Lee AV, Hilsenbeck SG, Yee D. IGF system components as prognostic markers in breast cancer. *Breast Cancer Res Treat.* Feb 1998;47(3):295-302.
49. Yee D. The insulin-like growth factor system as a target in breast cancer. *Breast Cancer Res Treat.* 1994;32(1):85-95.
50. Turner BC, Haffty BG, Narayanan L, et al. Insulin-like growth factor-I receptor overexpression mediates cellular radioresistance and local breast cancer recurrence after lumpectomy and radiation. *Cancer Res.* Aug 1 1997;57(15):3079-3083.
51. Happerfield LC, Miles DW, Barnes DM, Thomsen LL, Smith P, Hanby A. The localization of the insulin-like growth factor receptor 1 (IGFR-1) in benign and malignant breast tissue. *J Pathol.* Dec 1997;183(4):412-417.
52. Koda M, Sulkowski S, Garofalo C, Kanczuga-Koda L, Sulkowska M, Surmacz E. Expression of the insulin-like growth factor-I receptor in primary breast cancer and lymph node metastases: correlations with estrogen receptors alpha and beta. *Horm Metab Res.* Nov-Dec 2003;35(11-12):794-801.
53. Peyrat JP, Bonneterre J, Dusanter-Fourt I, Leroy-Martin B, Djiane J, Demaille A. Characterization of insulin-like growth factor 1 receptors (IGF1-R) in human breast cancer cell lines. *Bull Cancer.* 1989;76(3):311-319.
54. Mansour EG, Ravdin PM, Dressler L. Prognostic factors in early breast carcinoma. *Cancer.* Jul 1 1994;74(1 Suppl):381-400.
55. McGuire WL. Estrogen receptors in human breast cancer. *J Clin Invest.* Jan 1973;52(1):73-77.
56. Desombre ER. Steroid receptors in breast cancer. *Monogr Pathol.* 1984(25):149-174.

Figure Legends

Fig. 1. ERα and IRS-1 expression in normal mammary epithelium, benign breast tumors and breast cancers.

The expression of ERα (ER) and IRS-1 (IRS) were examined by IHC, as described in Materials and Methods. Normal breast tissue (A, B); benign breast tumor (C, D); invasive ductal ERα-positive carcinoma (E, F); ERα-positive lobular breast cancer (G, H). Negative control; IHC of lobular carcinomas with primary Abs substituted with PBS. Higher magnification of specific areas is reported as inset in the original images.

Fig. 2. Subcellular localization of IRS-1 and ERα in breast tumors.

The localization of IRS-1 and ERα in ductal cancers was analyzed by immunostaining and confocal microscopy as detailed in Materials and methods. The captured images of IRS-1 (green fluorescence), ERα (red fluorescence) and merged IRS-1 and ERα (yellow fluorescence) are shown in a representative ductal cancer tissue section.

Fig. 3. Correlations between nuclear IRS-1 and ERα in normal breast tissues, benign breast tumors and breast cancers.

Associations between nuclear IRS-1 and ERα in different tissues were analyzed with Pearson correlation test. For each linear regression graph, the linear equation, the correlation coefficient (R), and the statistical significance (p) is reported.

Fig. 4. Distribution of nuclear IRS-1 and ERα in ductal and lobular breast cancers.

Distributions of nuclear IRS-1 (%) and ERα (%) relative to tumor grade (Grade), size (pT), and the lymph node involvement (pN) in ductal and lobular breast cancers are shown in scatterplots.

Fig. 5. Value of nuclear IRS-1 and ERα as diagnostic markers of tumor grading.

Graphic evaluation of ERα and nuclear IRS-1 in respect to tumor differentiation grade in invasive ductal and lobular carcinomas, showing the true-positive rate (sensitivity) and the false-positive rate (specificity) of the analysis as a function of all possible cut-points for the two markers. ERα, solid line; nuclear IRS-1, dotted line.

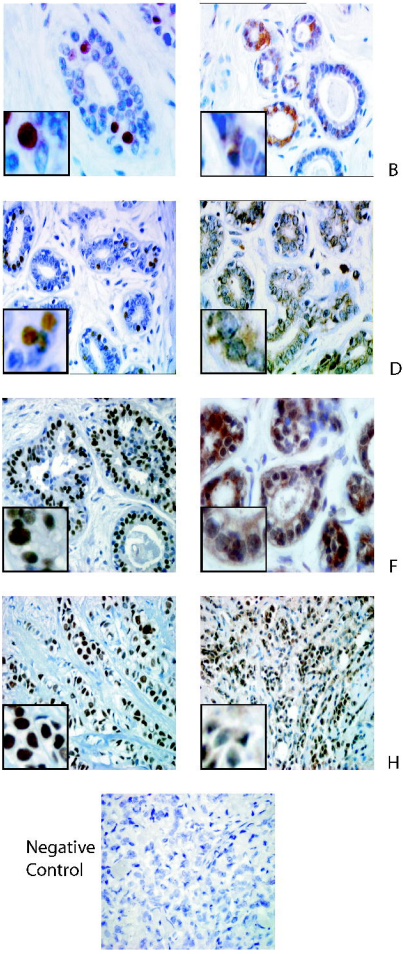

Figure 1

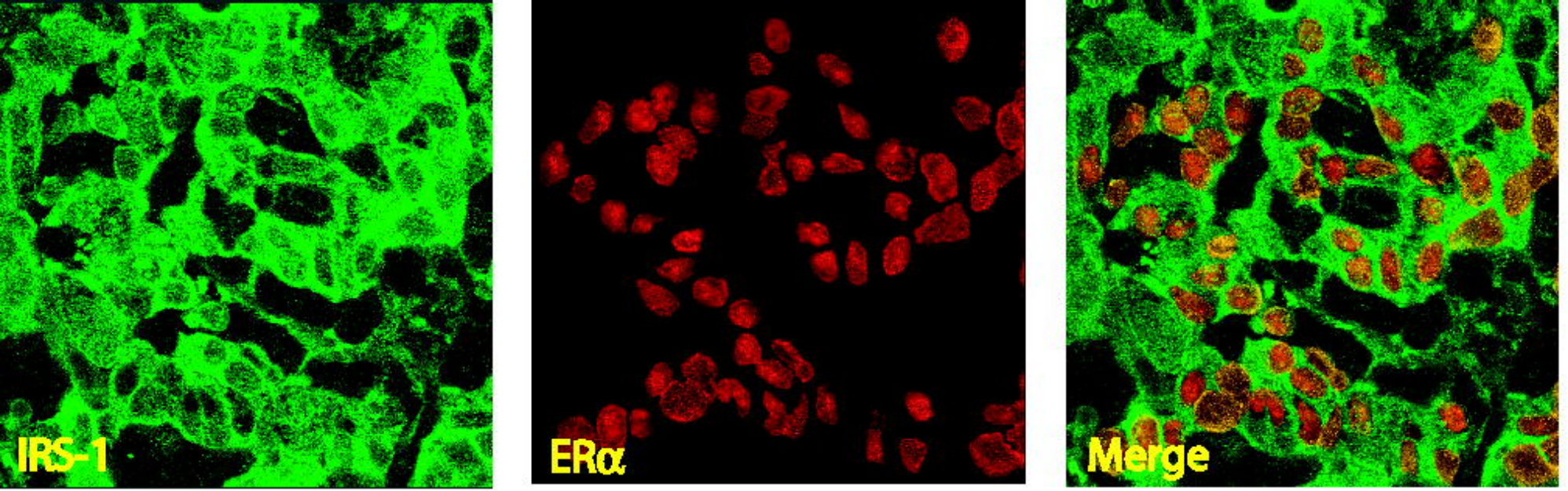

Figure 2

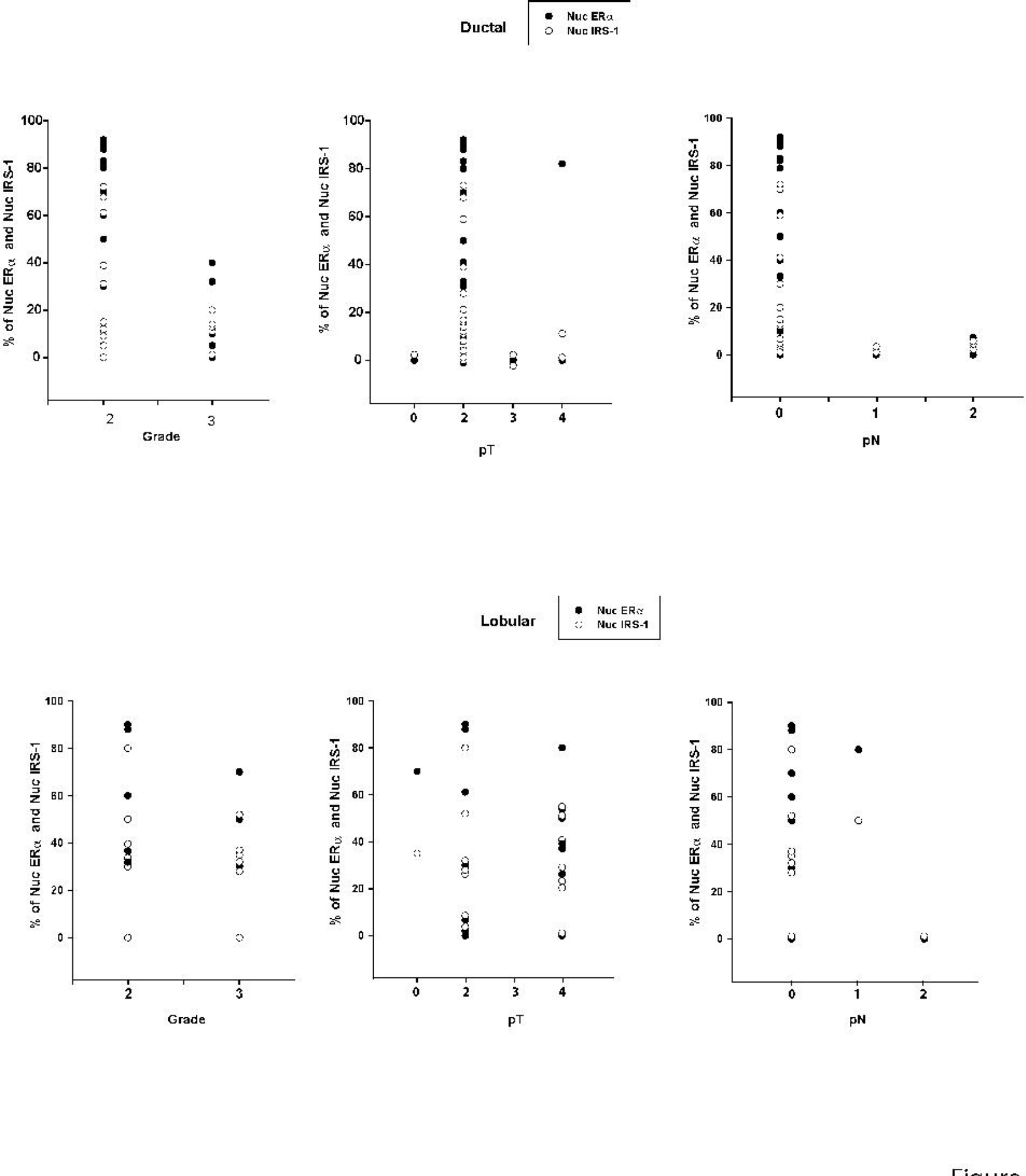
Ductal
Nuc ERα
Nuc IRS-1
% of Nuc ERα and Nuc IRS-1
Grade
pT
pN
Lobular
Nuc ERα
Nuc IRS-1
% of Nuc ERα and Nuc IRS-1
Grade
pT
pN

Figure 3

Normal

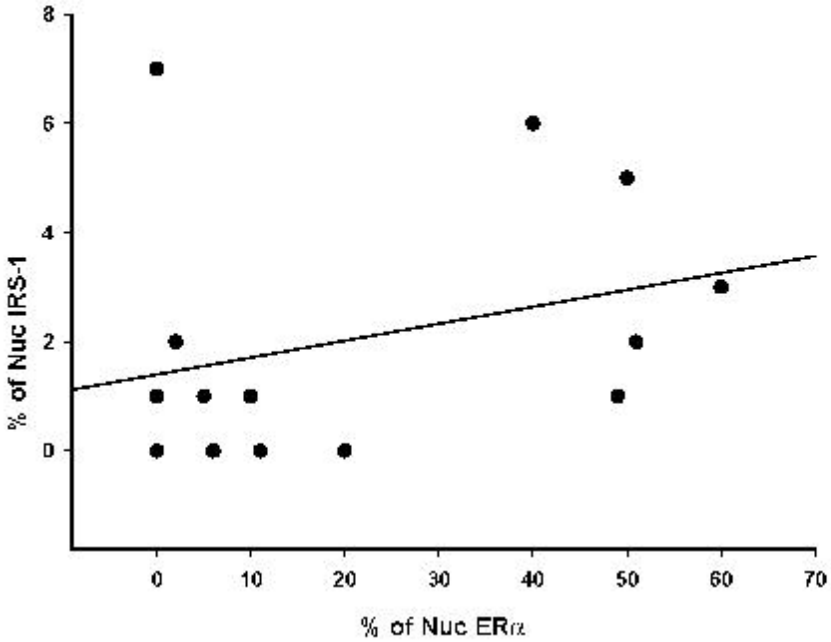

IRS Nuc=1.756+(0.03*ER) R=0.309 P=0.28

Benign

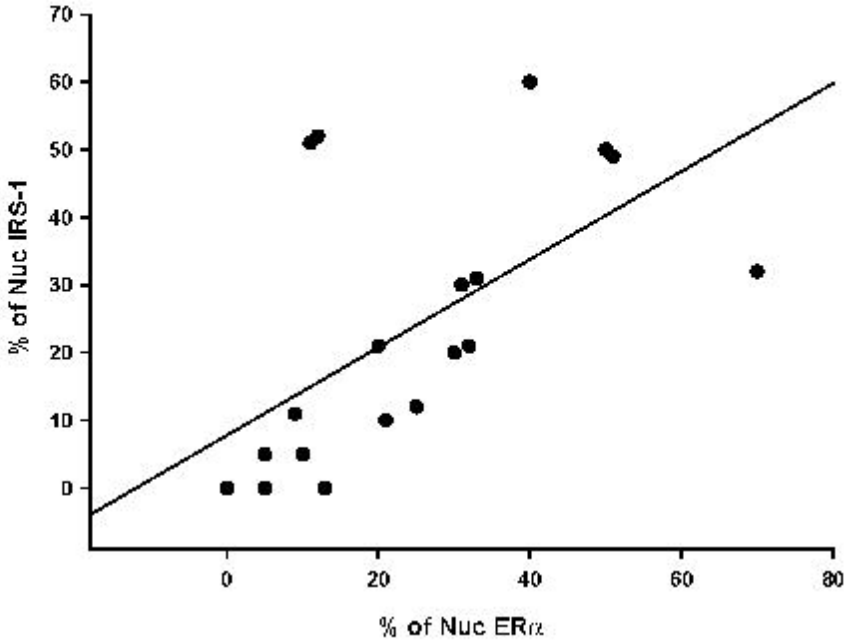

IRS Nuc=7.796+(0.650*ER) R=0.604 P<0.01

Ductal

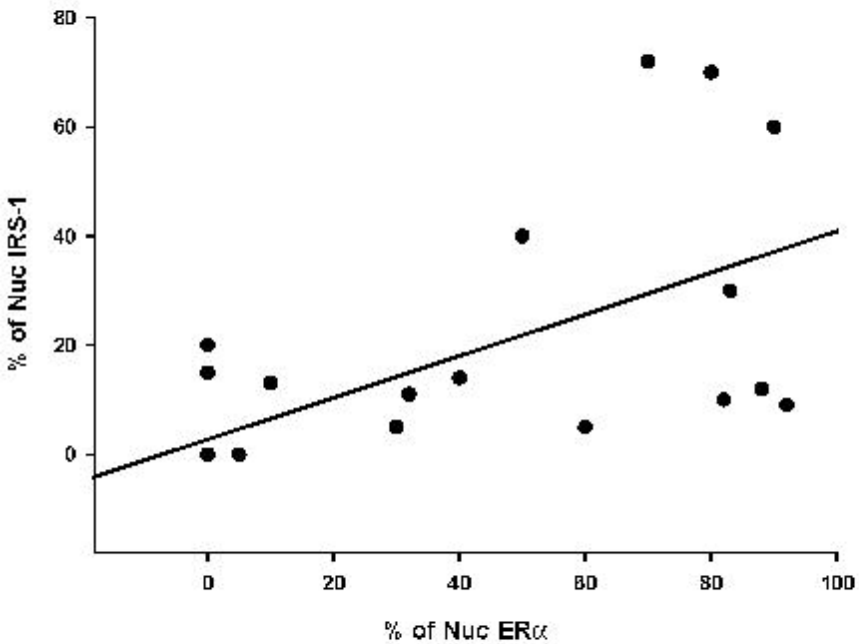

IRS Nuc=2.707+(0.382*ER) R=0.647 P<0.001

Lobular

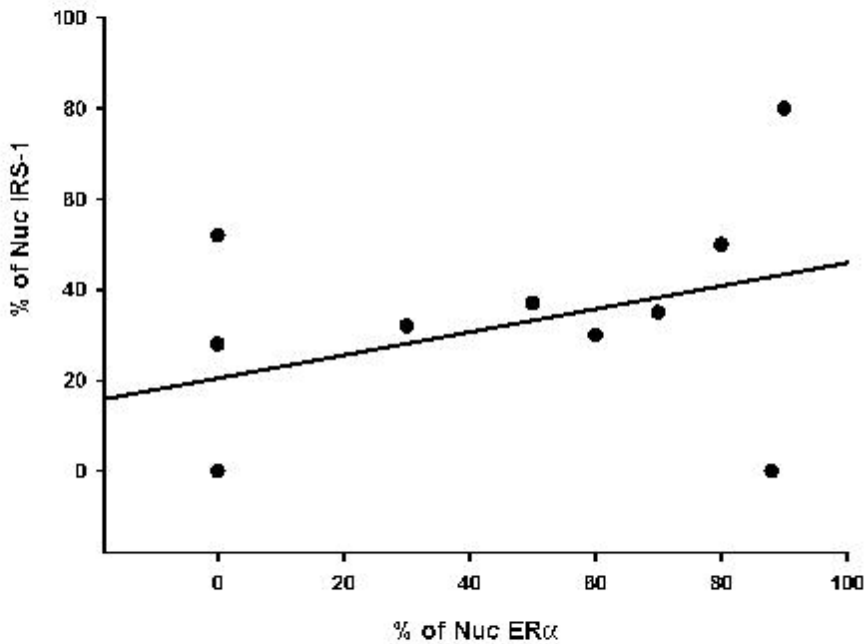

IRS Nuc=20.439+(0.255*ER) R=0.387 P=0.239

Figure 4

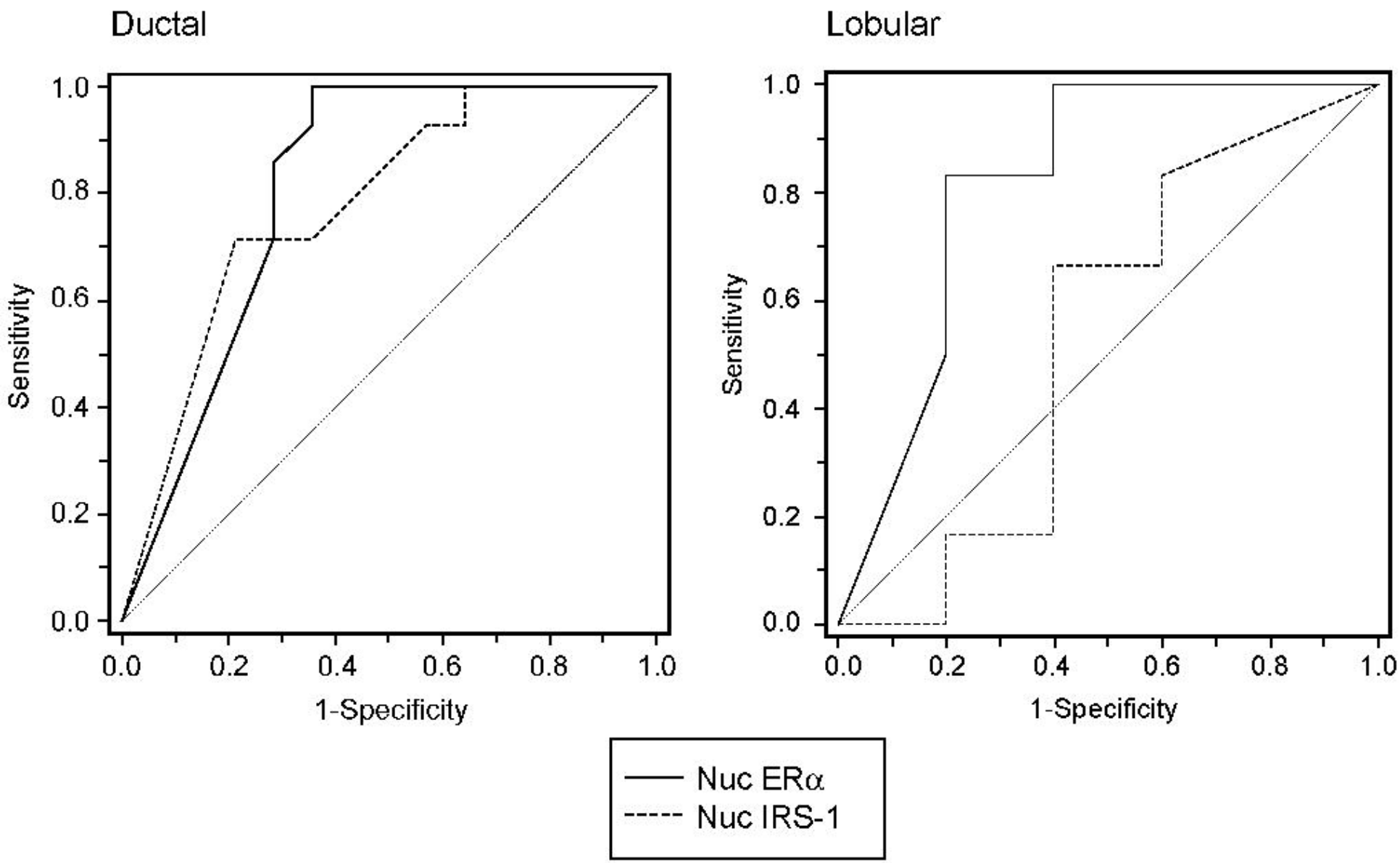
Ductal
Lobular
Sensitivity
1-Specificity
0.0
0.2
0.4
0.6
0.8
1.0
Nuc ERα
Nuc IRS-1

Figure 5

Title page

Peroxisome Proliferator-Activated Receptor (PPAR) gamma activates p53 gene promoter binding to the NF*k*B sequence in human MCF7 breast cancer cells

Bonofiglio Daniela[1*], Aquila Saveria[1*], Catalano Stefania[1], Gabriele Sabrina[1], Belmonte Maria[1], Middea Emilia[1], Qi Hongyan[1], Morelli Catia[1], Gentile Mariaelena[2], Maggiolini Marcello[1] and Andò Sebastiano[2, 3]

[1]Dept. Pharmaco-Biology, [2] Dept. Cellular Biology, [3]Faculty of Pharmacy University of Calabria 87030 Arcavacata di Rende (CS) Italy

Key words: PPAR γ, p53, p21$^{WAF1/Cip1}$, breast cancer cells, rosiglitazone

Running title: PPAR γ activates p53 in MCF7 cells

Corresponding Author: Prof. Sebastiano Andò

Faculty of Pharmacy-University of Calabria

Arcavacata - Rende (Cosenza) 87036

ITALY

TEL: +39 0984 496201

E-mail: sebastiano.ando@unical.it

E-mail: daniela.bonofiglio@tin.it

Footnotes: * The two authors equally contributed to this work.

This work was supported by Associazione Italiana Ricerca sul Cancro (AIRC), Ministero dell'Istruzione Università e Ricerca and Ministero della Salute

ABSTRACT

The aim of the present study was to provide new mechanistic insight into the growth arrest and apoptosis elicited by Peroxisome proliferator-activated receptor (PPAR) γ in breast cancer cells. We ascertained that PPARγ mediates the inhibition of cycle progression in MCF7 cells exerted by the specific PPARγ agonist rosiglitazone (BRL), since this response was no longer notable in presence of the receptor antagonist GW9662 (GW). We also evidenced that BRL is able to up-regulate in a time- and dose-dependent manner mRNA and protein levels of the tumor suppressor gene p53 and its effector $p21^{WAF1/Cip1}$. Moreover, in transfection experiments with deletion mutants of the p53 gene promoter, we documented that the Nuclear Factor *k*B (NF*k*B) sequence is required for the transcriptional response to BRL. Interestingly, electrophoretic mobility shift assay showed that PPARγ binds directly to the NF*k*B site located in the promoter region of p53 and chromatin immunoprecipitation experiments demonstrated that BRL increases the recruitment of PPARγ on the p53 promoter sequence. Next, both PPARγ and p53 were involved in the cleavage of caspases-9 and DNA fragmentation induced by BRL, given that GW and an expression vector for p53 antisense blunted these effects. Our findings evidenced that the PPARγ agonist BRL promotes the growth arrest and apoptosis in MCF7 cells, at least in part, through a crosstalk between p53 and PPARγ which may be considered an additional target for novel therapeutic interventions in breast cancer patients.

INTRODUCTION

Peroxisome proliferator-activated receptor γ (PPARγ) is a prototypical member of the nuclear receptor superfamily and integrates the control of energy, lipid, and glucose homeostasis (1-4). PPARγ regulates differentiation and induces cell growth arrest and apoptosis in a large variety of cells (5 and references therein), including both primary and metastatic breast malignancy (6-7). However, the molecular mechanisms involved in the inhibitory effects mediated by PPARγ remain to be elucidated.

It is well known that the p53 tumor suppressor gene regulates the transcription of effectors that are also responsible for growth arrest and apoptosis (reviewed in reference 8). Among the p53 target genes, the $p21^{WAF1/Cip1}$ has been recognized to exert an essential role in mediating cell cycle arrest at both G1 and G2/M checkpoints (9-11). $p21^{WAF1/Cip1}$ inhibits cyclin D1 or E/CDK in G1 and cyclin B/cdc2 in G2/M arrest, eliciting regulatory effects on DNA replication and repair (12). Moreover, it has been reported that p53 is able to promote apoptosis in certain cell types in a transcription independent manner (13).

The function of p53 as a tumor suppressor is finely tuned through an interaction with other transduction pathways regulating the cell network (14-18). For instance, a striking evidence has recently emerged for a crosstalk between p53 and relevant transcription factors, such as the glucocorticoid, androgen and estrogen receptors (19). It was therefore proved that these nuclear receptors are able to induce a cytosolic accumulation of p53, altering its stability and, consequently, its function (19).

In the present study, we provide new insight into the molecular mechanisms by which the specific PPARγ ligand rosiglitazone (BRL) induces the growth arrest and apoptosis in MCF7 human breast cancer cells. Performing a panel of different assays, we have demonstrated that the biological effects of BRL are triggered, at least in part, by PPARγ binding to the Nuclear Factor *k*B

1 sequence located within the p53 promoter region. Our findings have evidenced a crosstalk between
2 p53 and PPARγ which assumes a biological relevance in order to suggest new pharmacological
3 strategies in breast cancer.

RESULTS

BRL induces G_0/G_1 cycle arrest in MCF7 cells

On the basis of our (20) and other (21-22) studies demonstrating the inhibitory effects of the PPARγ-agonists on proliferation of breast cancer cells, we first investigated the activity of BRL on MCF7 cell cycle progression. A 48-h exposure to BRL caused in a dose-dependent manner the inhibition of G0-G1→S phase progression with concomitant decrease in the proportion of cells entering in S phase (TAB. 1). Of note, this effect was mediated by PPARγ, since it was no longer notable in presence of the specific antagonist GW9662 (GW).

BRL up-regulates p53 and $p21^{WAF1/Cip1}$ expression in MCF7 cells

Considering that the tumor suppressor gene p53 is mainly involved in the growth arrest promoted by different factors, we aimed to examine the potential ability of PPARγ to modulate the expression of p53 along with its natural target gene $p21^{WAF1/CIP1}$. The mRNA (Fig. 1) and protein (Fig. 2) levels of both p53 and $p21^{WAF1/CIP1}$ were up-regulated in a time- and dose-dependent manner in MCF7 cells treated with BRL. These stimulations were abrogated by GW (figures 1 and 2) suggesting a direct involvement of PPARγ.

BRL transactivates p53 gene promoter

The aforementioned observations prompted us to investigate whether PPARγ is able to transactivate an expression vector encoding p53 promoter gene. Thus, MCF7 cells were transiently transfected with a luciferase reporter construct (named p53-1) containing the upstream region of the p53 gene spanning from –1800 to +12 (Fig. 3A) and treated with increasing concentrations of BRL for 24-h. Interestingly, the dose-dependent activation of p53-1 by BRL was reversed in presence of GW indicating that a PPARγ-mediated mechanism was involved in the transcriptional response to BRL (Fig. 3B).

To identify the region within the p53 promoter responsible for transactivation, we used deletion constructs expressing different binding sites such as CTF-1/YY1, nuclear factor-Y (NF-Y) and NF*k*B (Fig. 3A). In transfection experiments performed using the mutants p53-6 and p-53-13 encoding the regions from -106 to +12 and from -106 to -40, respectively, the responsiveness to BRL was still observed, while using the mutant p53-14 encoding the sequence from -106 to -49 we did not detect increase in luciferase activity (Fig. 3C). Consequently, the region from -49 to -40, which corresponds to the NF*k*B site (Fig. 3A), was required for the transactivation of p53 by BRL.

PPARγ binds to NFkB sequence in EMSA

In order to further evaluate whether the NF*k*B site is responsible for the action triggered by BRL, we performed EMSA experiments. Using synthetic oligodeoxyribonucleotides corresponding to the NF*k*B sequence, we observed in nuclear extracts from MCF7 cells the formation of a single band (Fig. 4A, lane 1) which was abrogated by 100-fold molar excess of unlabeled probe (Fig. 4A, lane 2), demonstrating the specificity of the DNA binding complex. Of note, BRL treatment induced a strong increase in the specific band (Fig. 4A, lane 3), which was immunodepleted and supershifted using anti-PPARγ (Fig. 4A, lane 4) and anti-NF*k*B (Fig. 4A, lane 5) antibodies. Interestingly, the PPARγ transcribed and translated protein was able to bind to [^{32}P]-NF*k*B oligonucleotide (Fig. 4A, lane 6). The specificity of the band was proved by a 100-fold excess of cold probe (Fig. 4A, lane 7) and confirmed by a consensus PPRE used as a cold competitor (Fig. 4A, lane 8). Besides, the immunodepleted band obtained using the anti-PPARγ antibody (Fig. 4A, lane 9), but not evidenced with the anti-NF*k*B antibody (Fig. 4A, lane 10), confirmed that PPARγ binds in a specific manner to the NF*k*B site present in the promoter of p53. As next controls, we used NF*k*B protein alone (Fig. 4B, lane 1) and in combination with either cold competitor (Fig. 4B, lane 2) or the anti-NF*k*B antibody (Fig. 4B, lane 3).

Functional interaction of PPARγ with p53 in ChIP assay

The interaction of PPARγ with p53 was further elucidated by ChIP experiments. MCF7 cells were treated with formaldehyde to form DNA-protein cross-links and then sonicated. Thereafter, using anti-PPARγ, anti-NF*k*B and anti-RNA Pol II antibodies we immunoprecipitated the complexes and the binding of PPARγ, NF*k*B and, respectively RNA Pol II, respectively, to the NF*k*B site within the p53 promoter was revealed by PCR. As shown in panel A of figure 5, BRL increased the recruitment of PPARγ to the promoter of p53. The BRL-induced effect was slightly reduced by TGFβ, but not altered in presence of the specific inhibitor of NF*k*B parthenolide (P) (23) (Fig. 5A). As it concerns the recruitment of NF*k*B to p53, evaluated using the anti-NF*k*B antibody, TGFβ enhanced such interaction which was abolished by P (Fig.5A). Moreover, P was able to prevent the binding of RNA Pol II to p53 induced by TGFβ, but not that determined by BRL (Fig. 5A). These findings confirmed the ability of PPARγ to stimulate the transcription of p53 in a NF*k*B independent manner (Fig. 5A). Next, the anti-PPARγ antibody did not immunoprecipitate a region upstream the NF*k*B site located within the p53 promoter gene (Fig. 5B).

BRL induces caspase-9 cleavage and DNA fragmentation in MCF7 cells

Having demonstrated that PPARγ mediates p53 expression induced by BRL, we investigated the cleavage of caspase 9, which is an important component of the intrinsic apoptotic process (24). Notably, the treatment of MCF7 cells with BRL for 48-h promoted the caspase-9 activation which was prevented by GW and in presence of an expression vector encoding p53 antisense (AS/p53) (Fig. 6A), which abolished p53 expression (Fig. 6B). On the contrary, the effect of BRL on the cleavage of caspase 9 was still notable using the NF*k*B inhibitor P (Fig. 6A), which abrogating the NF*k*B protein levels (Fig. 6C) excluded the contribution of such factor in the action elicited by BRL.

As evidenced in DNA fragmentation assay, PPARγ was also involved in the apoptotic process triggered by BRL since this effect was completely and partially reversed by GW and the AS/p53, respectively (Fig. 6D). Again, P did not modify the activity of BRL (Fig. 6D). Taken together, these results indicate that, at least in part, a crosstalk between PPARγ and p53 may be responsible for the growth arrest and apoptosis induced by BRL in MCF7 cells.

DISCUSSION

In recent years, a great deal of attention focused on the antiproliferative effects of PPARγ in a variety of cancer cell types. Treatments with PPARγ ligands have been demonstrated to induce cell cycle arrest and apoptosis in different cancer models (6-7, 25). Besides, an interaction between PPARγ and p53 was hypothesized but not clarified at molecular level in cholangiocarcinoma (26), in human gastric cancer cells (27) and even in rat vascular smooth muscle cells (28). In addition, from our and other studies emerged the ability of PPARγ to up-regulate the expression of the tumor suppressor gene PTEN which is required for both a negative modulation of PI3K/Akt-dependent cell proliferation (20, 29-30) and a p53-mediated regulation of cell survival and apoptosis (31). Consequently, PPARγ and p53 may converge in a tumor suppressor activity which remains to be further elucidated.

In order to provide new insight into the inhibitory action exerted by the cognate PPARγ-ligand BRL, we first demonstrated that PPARγ mediates the growth arrest in G0-G1 phase induced by BRL in MCF7 cells. Besides, considering the key role elicited by p53 in the growth inhibition and apoptosis (14, 17), we have evaluated whether PPARγ signalling converges on p53 transduction pathway in MCF7 cells. Of interest, we found that BRL exposure up-regulates both p53 mRNA and protein levels with a concomitant increase of $p21^{WAF1/Cip1}$ expression. These effects were abrogated in presence of the specific antagonist GW, addressing a PPARγ-mediated mechanism. Therefore, investigating the potential ability of BRL to modulate p53 promoter gene, we performed transient transfections in MCF7 cells using diverse deletion mutants of p53 promoter gene (32). The dose-dependent transactivation of p53 by BRL involved directly PPARγ since the transcriptional activity was prevented by GW treatment. Moreover, we documented that the region spanning from -49 to -40, which corresponds to the NF*k*B site, is required for the responsiveness to BRL.

It deserves to be mentioned that the transcription factor NF*k*B can regulate both pro- and antiapoptotic signalling pathways depending on cell type, the extent of NF*k*B activation and the nature of the apoptotic stimuli (33). NF*k*B was reported to physically interact with PPARγ (34), which in some circumstances binds to DNA cooperatively with NF*k*B (35-36), further enhancing the NF*k*B-DNA binding (37). Besides, PPARγ agonists were able to enhance the binding of NF*k*B to the upstream *k*B regulatory element site of c-*myc* (38). Our EMSA experiments extended the aforementioned observations since nuclear extracts of MCF7 cells treated with BRL showed an increased binding to the NF*k*B sequence located in the p53 promoter region. Given that the anti-PPARγ and anti-NF*k*B antibodies were both able to induce shifted bands, we performed an EMSA study using a cell free system to ascertain the potential direct interaction of PPARγ with NF*k*B site. Interestingly, we observed the formation of a single DNA-binding complex which was again shifted by the anti-PPARγ antibody. These findings were supported by ChIP assay in MCF7 cells demonstrating the ability of BRL to enhance the recruitment of PPARγ and RNA Pol II to the promoter of p53 even in presence of the NF*k*B inhibitor P. Overall, these data indicate that the PPARγ-mediated growth arrest upon addition of BRL in MCF7 cells involves, at least in part, the direct stimulation of p53 transcription.

p53 acts as a tumor suppressor depending on its physical and functional interaction with diverse cellular proteins (39), like some nuclear receptors that in turn exert an inhibitory activity on p53 biological outcomes (19). In *Supplemental Data* we show an evident co-immunoprecipitation and co-localization of PPARγ and p53 after BRL treatment. However, additional experiments are required to better characterize such interaction and its functional consequences.

A large body of evidence has suggested the straightforward role of p53 signalling in the apoptotic cascades which include the activation of caspases, a family of cytoplasmic cysteine proteases (40). The intrinsic apoptotic pathway involves a mitochondria-dependent process, which

results in cytochrome *c* release and, thereafter, activation of caspase-9 (24). Besides, apoptosis is characterized by distinct morphological changes including the internucleosomal cleavage of DNA, which is recognized as a 'DNA ladder' (24 and references therein). Notably, we evidenced that in a consecutive series of events BRL i) up-regulates the expression of p53 and ii) its effector $p21^{WAF1/Cip1}$, iii) triggers the cleavage of caspases-9, and iv) induces DNA fragmentation in a PPARγ-mediated manner. Given the ability of AS/p53 to reduce the last two biological effects of BRL, it may be argued an involvement of p53 in such PPARγ-dependent activity. On the contrary, the cleavage of caspase-9 and DNA fragmentation observed upon BRL treatment did not show changes suppressing the NF*k*B at protein level with P, suggesting that this factor is not required for the apoptotic events elicited by BRL.

In the present study we have provided new insight into the molecular mechanism through which PPARγ mediates the growth arrest and apoptosis induced by BRL in MCF7 cells. Our findings suggest that a crosstalk between p53 and PPARγ may assume biological relevance in setting novel therapeutic interventions in breast cancer.

MATERIALS AND METHODS

Reagents

Rosiglitazone, BRL49653, was a gift from GlaxoSmithKline (West Sussex, UK), the irreversible PPARγ-antagonist GW9662 was purchased by Sigma (Milan, Italy), human recombinant TGFβ was obtained from ICN Biomedicals (DBA, Milan, Italy), and the Parthenolide was purchased by Alexis (San Diego, CA USA).

Plasmids

The p53 promoter-luciferase reporters, constructed using pGL2 for cloning of p53–1 and -6, and TpGL2 for p53–13 and -14 were kindly provided by Dr. Stephen H. Safe (Texas A&M University, Texas, USA). The constructs used were generated by Safe (32) from the human p53 gene promoter: p53-1 (containing the -1800 to +12 region), p53-6 (containing the – 106 to +12 region), p53-13 (containing the – 106 to -40 region) and p53-14 (containing the – 106 to -49 region).

As an internal transfection control, we co-transfected the plasmid pRL-CMV (Promega Corp., Milan, Italy) that expresses Renilla luciferase enzymatically distinguishable from firefly luciferase by the strong cytomegalovirus enhancer/promoter. The p53 antisense plasmid (AS/p53) and PPARγ expression plasmid were gifts from Dr. Moshe Oren (Weizmann Institute of Science, Rehovot, Israel) and Dr. R. Evans (The Salk Institute, San Diego, CA, USA), respectively.

Cell cultures

Wild-type human breast cancer MCF7 cells (a gift from Dr. Ewa Surmacz, Sbarro Institute for Cancer Research and Molecular Medicine, Philadelphia, USA) were grown in DMEM plus glutamax containing 10 % fetal calf serum (FCS) (Invitrogen, Milan, Italy) and 1 mg/ml penicillin-streptomycin.

DNA Flow cytometry

MCF7 cells at 50-60 % confluence were shifted to serum free medium (SFM) for 24 hours and then treatments were added in SFM for 48 hours. Thereafter, cells were trypsinized, centrifuged at 1500 rpm for 3 minutes, washed with PBS, and then treated with 20 μg/ml RNase A (Calbiochem, La Jolla, CA). DNA was stained with 100 μg/ml propidium iodide for 30 minutes at 4°C protected from light, and cells were analyzed with the FACScan (Becton, Dickinson, NJ).

RT-PCR assay

MCF7 cells were grown in 10-cm dishes to 70-80 % confluence and exposed to treatments for 24 and 48 hours in SFM. Total cellular RNA was extracted using TRIZOL reagent (Invitrogen) as suggested by the manufacturer. The purity and integrity were checked spectroscopically and by gel electrophoresis before carrying out the analytical procedures. The evaluation of gene expression was performed by semiquantitative RT-PCR method as previously described (41). For p53, $p21^{WAF1/Cip1}$, and the internal control gene 36B4, the primers were: 5'-GTGGAAGGAAATTTGCGTGT-3' (p53 forward) and 5'-CCAGTGTGATGATGGTGAGG-3' (p53 reverse), 5'-GCTTCATGCCAGCTACTTCC-3' (p21 forward) and 5'-CTGTGCTCACTTCAGGGTCA-3' (p21 reverse), 5'-CTCAACATCTCCCCCTTCTC-3' (36B4 forward) and 5'-CAAATCCCATATCCTCGTCC-3' (36B4 reverse) to yield respectively products of 190 bp with 18 cycles, 270 bp with 18 cycles and 408 bp with 12 cycles. The results obtained as optical density arbitrary values were transformed to percentage of the control (percent control) taking the samples from untreated cells as 100 %.

Transfection assay

MCF7 cells were transferred into 24-well plates with 500 μl of regular growth medium/well the day before transfection. The medium was replaced with SFM on the day of transfection, which was performed using Fugene 6 reagent as recommended by the manufacturer (Roche Diagnostics,

Mannheim, Germany) with a mixture containing 0.5 μg of promoter-luc reporter plasmid, 5 ng of pRL-CMV. After 24 hours transfection, treatments were added in SFM as indicated and cells were incubated for further 24 hours. Firefly and Renilla luciferase activities were measured using the Dual Luciferase Kit (Promega, Madison, WI). The firefly luciferase values of each sample were normalized by Renilla luciferase activity and data were reported as Relative Light Units (RLU) values.

MCF7 cells plated into 10-cm dishes were transfected with 5 μg of AS/p53 using Fugene 6 reagent as recommended by the manufacturer (Roche Diagnostics, Mannheim, Germany). The activity of AS/p53 was verified utilizing western blot to detect changes in p53 protein levels. Time course analysis revealed that p53 levels were effectively suppressed at 18 hours after transfection (data not shown). Empty vector was used to ensure that DNA concentrations were constant in each transfection.

Electrophoretic Mobility Shift Assay (EMSA)

Nuclear extracts from MCF7 cells were prepared as previously described for EMSA (42). Briefly, MCF7 cells plated into 10-cm dishes were grown to 70-80 % confluence shifted to SFM for 24 hours and then treated with 10 μM BRL for 6 hours. Thereafter, cells were scraped into 1.5 ml of cold phosphate-buffered saline (PBS). Cells were pelleted for 10 seconds and resuspended in 400 μl cold buffer A (10 mM HEPES-KOH pH 7.9 at 4 °C, 1.5mM $MgCl_2$, 10 mM KCl, 0.5 mM dithiothreitol, 0.2 mM PMSF, 1 mM leupeptin) by flicking the tube. The cells were allowed to swell on ice for 10 minutes and then vortexed for 10 seconds. Samples were then centrifuged for 10 seconds and the supernatant fraction discarded. The pellet was resuspended in 50 μl of cold Buffer B (20 mM HEPES-KOH pH 7.9, 25 % glycerol, 1.5 mM $MgCl_2$, 420 mM NaCl, 0.2 mM EDTA, 0.5 mM dithiothreitol, 0.2 mM PMSF, 1 mM leupeptin) and incubated in ice for 20 minutes for high-salt extraction. Cellular debris were removed by centrifugation for 2 minutes at 4 °C and the

supernatant fraction (containing DNA binding proteins) was stored at –70 °C. *In vitro* transcribed and translated PPARγ was synthesized using the T7 polymerase in the rabbit reticulocyte lysate system from PPARγ plasmid as directed by the manufacturer (Promega). The probe was generated by annealing single stranded oligonucleotides and labeled with [γ^{32}P] ATP (Amersham Pharmacia, Buckinghamshire, UK) and T4 polynucleotide kinase (Promega) and then purified using Sephadex G50 spin columns (Amersham Pharmacia). The DNA sequence of the nuclear factor *k*B (NF*k*B) used as probe or as cold competitor is the following: NF*k*B, 5'-AGT TGA GGG GAC TTT CCC AGG C-3' (Sigma Genosys, Cambridge, UK). As cold competitor we also used PPRE oligonucleotide: 5'-GGGACCAGGACAAAGGTCACGTT-3' (Sigma Genosys). The protein binding reactions were carried out in 20 μl of buffer [20 mM Hepes pH 8, 1 mM EDTA, 50 mM KCl, 10 mM DTT, 10% glicerol, 1mg/ml BSA, 50 μg/ml poly dI/dC] with 50000 cpm of labeled probe, 5 μg of MCF7 nuclear protein, or 2 μl of transcribed and translated *in vitro* PPARγ protein, or 1 μl of NF*k*B protein (Promega), and 5 μg of poly (dI-dC). The mixtures were incubated at room temperature for 20 minutes in the presence or absence of unlabeled competitor oligonucleotides. For the experiments involving anti-PPARγ and anti-NF*k*B antibodies (Santa Cruz Biotechnology, Santa Cruz, CA), the reaction mixture was incubated with these antibodies at 4 °C for 30 minutes before addition of labeled probe. The entire reaction mixture was electrophoresed through a 6 % polyacrylamide gel in 0.25 X Tris borate-EDTA for 3 hours at 150 V. Gel was dried and subjected to autoradiography at –70 °C.

Chromatin immunoprecipitation (ChIP)

MCF7 cells were grown in 10-cm dishes to 50-60 % confluence, shifted to SFM for 24 hours and then treated with 10 μM BRL for 1 hour. Thereafter, cells were washed twice with PBS and crosslinked with 1 % formaldehyde at 37 °C for 10 minutes. Next, cells were washed twice with PBS at 4 °C, collected and resuspended in 200 μl of lysis buffer (1% SDS, 10 mM EDTA, 50

mM Tris-HCl pH 8.1) and left on ice for 10 minutes. Then, cells were sonicated four times for 10 seconds at 30 % of maximal power (Sonics, Vibra Cell 500 W) and collected by centrifugation at 4 °C for 10 minutes at 14,000 rpm. The supernatants were diluted in 1.3 ml of IP buffer (0.01 % SDS, 1.1 % Triton X-100, 1.2 mM EDTA, 16.7 mM Tris-HCl pH 8.1, 16.7 mM NaCl) followed by immunoclearing with 80 µl of sonicated salmon sperm DNA/protein A agarose (UBI, DBA Srl, Milan - Italy) for 1 hour at 4 °C. The precleared chromatin was immunoprecipitated with anti-PPARγ, anti-NF*k*B and anti-RNA Pol II antibodies (Santa Cruz Biotechnology). At this point, 60 µl salmon sperm DNA/protein A agarose were added and precipitation was further continued for 2 hours at 4 °C. After pelleting, precipitates were washed sequentially for 5 minutes with the following buffers: Wash A (0.1 % SDS, 1 % Triton X-100, 2 mM EDTA, 20 mM Tris-HCl pH 8.1, 150 mM NaCl), Wash B (0.1 % SDS, 1 % Triton X-100, 2 mM EDTA, 20 mM Tris-HCl pH 8.1, 500 mM NaCl), and Wash C (0.25 M LiCl, 1 % NP-40, 1 % sodium deoxycholate, 1 mM EDTA, 10 mM Tris-HCl pH 8.1), and then twice with TE buffer (10 mM Tris, 1 mM EDTA). The immunocomplexes were eluted with elution buffer (1 % SDS, 0.1 M $NaHCO_3$). The eluates were reverse crosslinked by heating at 65 °C and digested with proteinase K (0.5 mg/ml) at 45 °C for 1 hour. DNA was obtained by phenol/chloroform/isoamyl alcohol extraction. 2 µl of 10 mg/ml yeast tRNA (Sigma) were added to each sample and DNA was precipitated with 70 % ethanol for 24 hours at –20 °C, and then washed with 95 % ethanol and resuspended in 20 µl of TE buffer. A 5 µl volume of each sample was used for PCR with primers flanking a sequence present in the p53 promoter: 5'-CTGAGAGCAAACGCAAAAG-3' (forward) and 5'-CAGCCCGAACGCAAAGTGTC-3' (reverse) containing the *k*B site from -254 to -42 region and 5'-GAAAACGTTAGGGTGTGG-3' (forward) and 5'-GGTGCAGAGTCAGGATTC-3' (reverse) upstream of the *k*B site from -528 to -452 region (Gene Bank AC: J0423). The PCR conditions for the two p53 promoter fragments were respectively 45 seconds at 94 °C, 40 seconds at 57 °C, 90

seconds at 72 °C and 45 seconds at 94 °C, 40 seconds at 55 °C, 90 seconds at 72 °C. The amplification products obtained in 30 cycles were analysed in a 2 % agarose gel and visualized by ethidium bromide staining. The negative control was provided by PCR amplification without DNA sample. The specificity of reactions was ensured using normal mouse and rabbit IgG (Santa Cruz Biotechnology).

Immunoblotting

MCF7 cells were grown in 10-cm dishes to 70-80% confluence and exposed to treatments for 24 and 48 hours in SFM as indicated. Cells were then harvested in cold PBS and resuspended in lysis buffer containing 20 mM HEPES pH 8, 0.1mM EDTA, 5mM $MgCl_2$, 0.5M NaCl, 20 % glycerol, 1 % NP-40, inhibitors (0.1mM Na_3VO_4, 1 % PMSF, 20 mg/ml aprotinin). Protein concentration was determined by Bio-Rad Protein Assay (Bio-Rad Laboratories, Hercules, CA).

A 50 μg portion of protein lysates was used for Western Blotting (WB), resolved on a 10 % SDS-polyacrylamide gel, transferred to a nitrocellulose membrane and probed with an antibody directed against the p53, $p21^{WAF1/Cip1}$, caspases-9 and NF*k*B (Santa Cruz Biotechnology). As internal control, all membranes were subsequently stripped (glycine 0.2 M, pH 2.6 for 30 minutes at room temperature) of the first antibody and reprobed with anti-β-actin antibody.

The antigen-antibody complex was detected by incubation of the membranes for 1 hour at room temperature with peroxidase-coupled goat anti-mouse or anti-rabbit IgG and revealed using the enhanced chemiluminescence system (ECL system, Amersham Pharmacia). Blots were then exposed to film (Kodak film, Sigma).The intensity of bands representing relevant proteins was measured by Scion Image laser densitometry scanning program.

DNA Fragmentation

DNA fragmentation was determined by gel electrophoresis. MCF7 cells were grown in 10-cm dishes to 70 % confluence and treated with 10 μM BRL and/or 10 μM GW and /or 15 μM P. After 72 hours cells were collected and washed with PBS and pelletted at 1800 rpm for 5 minutes. The samples were resuspended in 0.5 ml of extraction buffer (50 mM Trios-HCl pH 8, 10mM EDTA, O.5% SDS) for 20 minutes in rotation at 4 °C. DNA was extracted with phenol/chloroform for 3 times and once with chloroform. The aqueous phase was used to precipitate acids nucleic with 0.1 volumes or of 3 M sodium acetate and 2.5 volumes cold EtOH overnight at -20 °C. The DNA pellet was resuspended in 15 μl of H_2O treated with RNAse A for 30 minutes at 37 °C. The absorbance of the DNA solution at 260 and 280 nm was determined by spectrophotometry. The extracted DNA (40 μg/lane) was subjected to electrophoresis on 1.5 % agarose gels. The gels were stained with ethidium bromide and then photographed.

STATISTICAL ANALYSIS

Statistical analysis was performed using ANOVA followed by Newman-Keuls testing to determine differences in means. $p<0.05$ was considered as statistically significant.

REFERENCES

1. Shearer BG, Hoekstra WJ 2003Recent advances in peroxisome proliferator-activated receptor science. Curr Med Chem 10:267–280
2. Francis GA, Fayard E, Picard F, Auwerx J 2003Nuclear receptors and the control of metabolism. Ann Rev Physiol 65:261–311
3. Chawla A, Repa JJ, Evans RM, Mangelsdorf DJ 2001Nuclear receptors and lipid physiology: opening the X-files. Science 294:1866–1870
4. Yamauchi T, Kamon J, Waki H, Murakami K, Motojima K, Komeda K, Ide T, Kubota N, Terauchi Y, Tobe K, Miki H, Tsuchida A, Akanuma Y, Nagai R, Kimura S, Kadowaki T 2001 The mechanisms by which both heterozygous peroxisome proliferator-activated receptor gamma (PPARgamma) deficiency and PPAR gamma agonist improve insulin resistance. J Biol Chem 276:41245-41254
5. Fajas L, Egler V, Reiter R, Miard S, Lefebvre AM, Auwerx J 2003 PPAR gamma controls cell proliferation and apoptosis in an RB-dependent manner. Oncogene 22: 4186–4193
6. Mueller E, Sarraf P, Tontonoz P, Evans RM, Martin KJ, Zhang M, Fletcher C, Singer S, Spiegelman BM 1998 Terminal differentiation of human breast cancer through PPAR gamma. Mol Cell 1:465-470
7. Elstner E, Muller C, Koshizuka K, Williamson EA, Park D, Asou H, Shintaku P, Said JW, Heber D, Koeffler HP 1998 Ligands for peroxisome proliferator-activated receptor gamma and retinoic acid receptor inhibit growth and induce apoptosis of human breast cancer cells in vitro and in BNX mice. Proc Natl Acad Sci USA 95:8806-8811
8. Vousden KH, Lu X 2002 Live or let die: the cell's response to p53. Nat Rev Cancer 2:594-604
9. Liu G, Lozano G 2005 p21 stability: linking chaperones to a cell cycle checkpoint. Cancer Cell 7:113-114

10. el-Deiry WS, Tokino T, Velculescu VE, Levy DB, Parsons R, Trent JM, Lin D, Mercer WE, Kinzler KW, Vogelstein B 1993 WAF1, a potential mediator of p53 tumor suppression. Cell 75:817-825
11. Harper JW, Adami GR, Wei N, Keyomarsi K, Elledge SJ 1993 The p21 Cdk-interacting protein Cip1 is a potent inhibitor of G1 cyclin-dependent kinases. Cell 75:805-816
12. Tom S, Ranalli TA, Podust VN, Bambara RA 2001 Regulatory roles of p21 and apurinic/apyrimidinic endonuclease 1 in base excision repair. J Biol Chem 276:48781-48789
13. Caelles C, Helmberg A, Karin M 1994 p53-dependent apoptosis in the absence of transcriptional activation of p53-target genes. Nature 370:220-223
14. Yu J, Zhang L 2005 The transcriptional targets of p53 in apoptosis control. Biochem Biophys Res Commun 331:851-858
15. O'Brate A, Giannakakou P 2003 The importance of p53 location: nuclear or cytoplasmic zip code? Drug Resistance Updates 6:313-322
16. Appella E 2001 Modulation of p53 function in cellular regulation. Eur J Biochem 268:2763
17. Haupt S, Berger M, Goldberg Z, Haupt Y 2003 Apoptosis - the p53 network. J Cell Sci 116:4077-4085
18. Woods DB, Vousden KH 2001 Regulation of p53 function. Exp Cell Res 264:56-66
19. Sengupta S, Wasylyk B 2004 Physiological and pathological consequences of the interactions of the p53 tumor suppressor with the glucocorticoid, androgen, and estrogen receptors. Ann N Y Acad Sci 1024:54–71
20. Bonofiglio D, Gabriele S, Aquila S, Catalano S, Gentile M, Middea E, Giordano F, Andò S 2005 Estrogen Receptor alpha binds to Peroxisome Proliferator-Activated Receptor (PPAR) Response Element and negatively interferes with PPAR gamma signalling in breast cancer cells. Clin Cancer Res 11:6139-6147

21. Patel L, Pass I, Coxon P, Downes CP, Smith SA, Macphee CH 2001 Tumor suppressor and anti-inflammatory actions of PPARγ agonist are mediated via upregulation of PTEN. Curr Biol 11:764-768
22. Clay CE, Namen AM, Atsumi G, Willingham MC, High KP, Kute TE, Trimboli AJ, Fonteh AN, Dawson PA, Chilton FH 1999 Influence of J series prostaglandins on apoptosis and tumorigenesis of breast cancer cells. Carcinogenesis 20:1905-1911
23. Hehner SP, Heinrich M, Bork PM, Vogt M, Ratter F, Lehmann V, Schulze-Osthoff K, Droge W, Schmitz ML 1998 Sesquiterpene lactones specifically inhibit activation of NF-kappa B by preventing the degradation of I kappa B-alpha and I kappa B-beta. J Biol Chem 273:1288-1297
24. Cohen GM 1997 Caspases: the executioners of apoptosis. Biochem J 326:1-16
25. Brockman JA, Gupta RA, Dubois RN 1998 Activation of PPAR gamma leads to inhibition of anchorage-independent growth of human colorectal cancer cells. Gastroenterology 115:1049-1055
26. Han C, Demetris AJ, Michalopoulos GK, Zhan Q, Shelhamer JH, Wu T 2003 PPARgamma ligands inhibit cholangiocarcinoma cell growth through p53-dependent GADD45 and p21 pathway. Hepatology 38:167-177
27. Nagamine M, Okumura T, Tanno S, Sawamukai M, Motomura W, Takahashi N, Kohgo Y 2003 PPAR gamma ligand-induced apoptosis through a p53-dependent mechanism in human gastric cancer cells. Cancer Sci 94:338-343
28. Okura T, Nakamura M, Takata Y, Watanabe S, Kitami Y, Hiwada K 2000 Troglitazone induces apoptosis via the p53 and Gadd45 pathway in vascular smooth muscle cells. Eur J Pharmacol 407:227-235
29. Di Cristofano A, Pandolfi PP 2000 The multiple roles of PTEN in tumor suppression. Cell 100:387-390

30. Yamada KM, Araki M 2001 Tumor suppressor PTEN: modulator of cell signaling, growth, migration and apoptosis. J Cell Sci 114:2375-2382
31. Stambolic V, MacPherson D, Sas D, Lin Y, Snow B, Jang Y, Benchimol S, Mak TW 2001 Regulation of PTEN transcription by p53. Mol Cell 8:317-325
32. Qin C, Nguyen T, Stewart J, Samudio I, Burghardt R, Safe S 2002 Estrogen up-regulation of p53 gene expression in MCF-7 breast cancer cells is mediated by calmodulin kinase IV-dependent activation of a nuclear factor kappaB/CCAAT-binding transcription factor-1 complex. Mol Endocrinol 16:1793-1809
33. Fujioka S, Schmidt C, Sclabas GM, Li Z, Pelicano H, Peng B, Yao A, Niu J, Zhang W, Evans DB, Abbruzzese JL, Huang P, Chiao PJ 2004 Stabilization of p53 is a novel mechanism for proapoptotic function of NF-kappaB. J Biol Chem 279:27549-27559
34. Chung SW, Kang BY, Kim SH, Pak YK, Cho D, Trinchieri G, Kim TS 2000 Oxidized low density lipoprotein inhibits interleukin-12 production in lipopolysaccharide-activated mouse macrophages via direct interactions between peroxisome proliferator-activated receptor-gamma and nuclear factor-kappa B. J Biol Chem 275:32681-32687
35. Coutureir C, Brouillet A, Couriaud C, Koumanov K, Bereziat G, Andreani M 1999 Interleukin 1β induces type II-secreted phospholipase A_2 gene in vascular smooth muscle cells by a nuclear factor kB and peroxisome proliferator-activated receptor-mediated process. J Biol Chem 274:23085-23093
36. Sun YX, Wright HT, Janciasukiene S 2002 α1-Antichymotrypsin/Alzheimer's peptide Aβ (1–42) complex perturbs lipid metabolism and activates transcription factors PPARγ and NF*k*B in human neuroblastoma (Kelly) cells. J Neurosci Res 67:511-522

37. Ikawa H, Kameda H, Kamitani H, Baek SJ, Nixon JB, Hsi LC, Eling TE 2001 Effect of PPAR activators on cytokine-stimulated cyclooxygenase-2 expression in human colorectal carcinoma cells. Exp Cell Res 267:73-80
38. Schlezinger JJ, Jensen BA, Mann KK, Ryu HY, Sherr DH 2002 Peroxisome proliferator-activated receptor gamma-mediated NF-kappa B activation and apoptosis in pre-B cells. J Immunol 169:6831-6841
39. Oren M, Damalas A, Gottlieb T, Michael D, Taplick J, Leal JF, Maya R, Moas M, Seger R, Taya Y, Ben-Ze'Ev A 2002 Regulation of p53: intricate loops and delicate balances. Ann N Y Acad Sci 973:374-383
40. Schuler M, Green DR 2001 Mechanisms of p53-dependent apoptosis Biochem Soc Trans 29:684–688
41. Maggiolini M, Donzé O, Picard D 1999 A non-radioactive method for inexpensive quantitative RT-PCR. Biol Chem 380:695-697
42. Andrews NC, Faller DV 1991 A rapid micropreparation technique for extraction of DNA-binding proteins from limiting numbers of mammalian cells. Nucleic Acids Res 19:2499

ACKNOWLEDGMENTS

Our thanks to Dr. Stephen H. Safe to provide us the human p53 gene promoter and the deletion mutants, to Moshe Oren and R.M. Evans for the gifts of the p53 antisense and PPARγ expression plasmid, respectively. We also thank D. Sturino (Faculty of Pharmacy, University of Calabria – Italy) for the English review. This work was supported by Associazione Italiana Ricerca sul Cancro (AIRC), Ministero dell'Istruzione Università e Ricerca and Ministero della Salute.

FIGURE LEGENDS

Table 1 BRL induces G_0/G_1 arrest of cell cycle progression in MCF7 cells. MCF7 cells were treated as indicated. DNA was stained with 100 μg/ml propidium iodide for 30 minutes at 4 °C protected from light and then the cells were analyzed with the FACScan (Becton, Dickinson, NJ). Each data point represents the percentage of three independent experiments performed in triplicate. The data are presented as mean ± S.D. *p<0.05 and **p<0.01 BRL-treated *vs* untreated cells.

Figure 1 BRL up-regulates p53 and $p21^{WAF1/Cip1}$ mRNA expression in MCF7 cells. Semiquantitative RT-PCR evaluation of p53 and $p21^{WAF1/Cip1}$ mRNAs expression. MCF7 cells were treated for 24 **(A)** and 48 **(B)** hours with increasing concentrations of BRL as indicated, 10 μM GW alone or in combination with 1 μM BRL. 36B4 mRNA levels were determined as control. The *side panels* show the quantitative representation of data (mean ± S.D.) of three independent experiments after densitometry and correction for 36B4 expression. *p<0.05 and **p<0.01 BRL-treated *vs* untreated cells

Figure 2 BRL up-regulates p53 and $p21^{WAF1/Cip1}$ protein expression in MCF7 cells. Immunoblots of p53 and $p21^{WAF1/Cip1}$ from MCF7 cells extracts treated for 24 h (**A**) and 48 (**B**) with increasing BRL concentrations, 10 μM GW alone or in combination with 1 μM BRL. β-actin was used as loading control. The *side panels* show the quantitative representations of data (mean ± S.D.) of three independent experiments performed for each condition. * p<0.05 and **p<0.01 BRL-treated *vs* untreated cells

Figure 3 Effects of BRL on p53-gene promoter-luciferase reporter constructs in MCF7 cells. **A**: Schematic map of the p53 promoter fragments used in this study. **B:** MCF7 cells were transiently transfected with p53 gene promoter-luciferase reporter construct (p53-1) and treated for 24 hours with increasing BRL concentrations, 10 μM GW alone or in combination with 1 μM BRL. **C**: MCF7 cells were transiently transfected with p53 gene promoter-luc reporter constructs (p53-1,

p53-6, p53-13, p53-14) and treated for 24 hours with 1 μM BRL and/or 10 μM GW. The luciferase activities were normalized to the Renilla luciferase as internal transfection control and data were reported as RLU values. Columns are mean ± S.D. of three independent experiments performed in triplicate. *p<0.05 BRL-treated *vs* untreated cells. pGL_2: basal activity measured in cells transfected with pGL_2 basal vector; RLU, Relative Light Units. CTF-1, CCAAT-binding transcription factor-1; NF-Y, nuclear factor-Y; NF*k*B, nuclear factor *k*B.

Figure 4 PPARγ binds to NF*k*B site in the p53 promoter region in EMSA.

A: Nuclear extracts from MCF7 cells (lane 1) or 2 μl of PPARγ translated protein (lane 6) were incubated with a double-stranded NF*k*B sequence probe labeled with [γ^{32}P] and subjected to electrophoresis in a 6% polyacrylamide gel. Competition experiments were performed adding as competitor a 100-fold molar excess of unlabeled NF*k*B probe (lanes 2 and 7) or as cold competitor PPRE (lane 8). In lane 3, nuclear extracts from MCF7 were treated with 10 μM BRL. Anti-PPARγ and anti-NF*k*B Abs were incubated with nuclear extracts from MCF7 cells treated with 10 μM BRL (lanes 4 and 5, respectively) or added to PPARγ protein (lanes 9 and 10, respectively). Lane 11 contains probe alone, lane 12 contains 2 μl of unprogrammed rabbit reticulocyte lysate incubated with NF*k*B (URRL). **B:** 1 μl of NF*k*B protein (lane 1) was incubated with a double-stranded NF*k*B sequence probe labeled with [γ^{32}P] and subjected to electrophoresis in a 6% polyacrylamide gel. A 100-fold molar excess of unlabeled NF*k*B probe (lanes 2) or anti-NF*k*B antibody (lane 3) was added to NF*k*B protein.

Figure 5 Functional interaction of PPARγ and p53 in ChIP assay. MCF7 cells were treated for 1 hour with 10 μM BRL, 10 ng/ml TGFβ, 15 μM Parthenolide (P), as indicated. The soluble chromatin was immunoprecipitated with anti-PPARγ, anti-NFkB and anti-RNA Pol II antibodies. The p53 promoter sequence including the NF*k*B site (panel A) and that located upstream the NF*k*B

site (panel B) were detected by PCR with specific primers, as described in *Materials and Methods*. To control input DNA, p53 promoter was amplified from 30 μl of initial preparations of soluble chromatin (before immunoprecipitations). Normal rabbit antiserum was used as negative control (N).

Figure 6 BRL induces cleavage of caspase-9 and DNA laddering. **A:** MCF7 cells were treated with BRL alone or in combination with GW or parthenolide (P) for 48-h as indicated, or transfected with an expression plasmid encoding for p53 antisense (AS/p53). Positions of procaspase-9 and its cleavage products are indicated by *arrowheads* to the *right*. One of three similar experiments is presented. β-actin was used as loading control on the same stripped blot. **B:** p53 protein expression (evaluated by WB) in MCF7 cells transfected with an empty vector (v) or a AS/p53 and treated as indicated. β-actin was used as loading control. **C**: NF*k*B expression in MCF7 cells untreated or treated with P as indicated. β-actin was used as loading control. **D**: DNA laddering was performed in MCF7 cells treated for 72-h as indicated, or transfected with AS/p53.

Table 1

Treatment	μM	Cell cycle phase (%)		
		G_0 - G_1	S	G_2 - M
C		53 ± 7.2	30 ± 4.4	17 ± 2.1
BRL	1	67* ± 7.4	20* ± 3.3	13 ± 2.2
BRL	10	76* ± 8.1	14* ± 3.1	10* ± 2.6
BRL	50	82** ± 8.3	10** ± 2.4	8** ± 1.2
GW	10	54 ± 6.5	29 ± 3.5	17 ± 2.1
BRL + GW	1+10	53 ±6.1	29 ± 3.2	18 ± 2.3

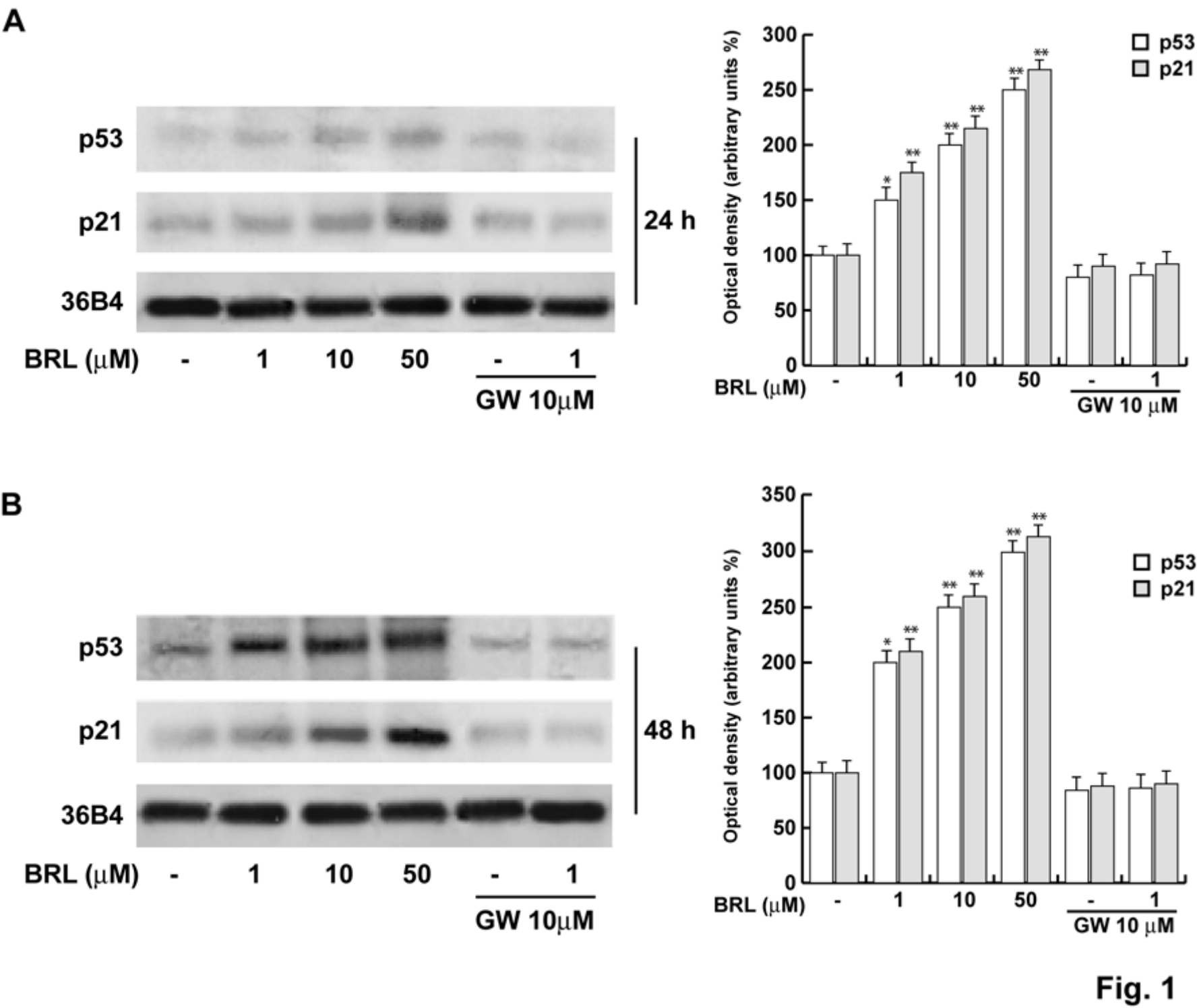
A
p53
p21
36B4
24 h
BRL (μM) - 1 10 50 - 1
GW 10μM
Optical density (arbitrary units %)
300
250
200
150
100
50
0
p53
p21
*
**
BRL (μM) - 1 10 50 - 1
GW 10 μM
B
p53
p21
36B4
48 h
BRL (μM) - 1 10 50 - 1
GW 10μM
Optical density (arbitrary units %)
350
300
250
200
150
100
50
0
p53
p21
*
**
BRL (μM) - 1 10 50 - 1
GW 10 μM

Fig. 1

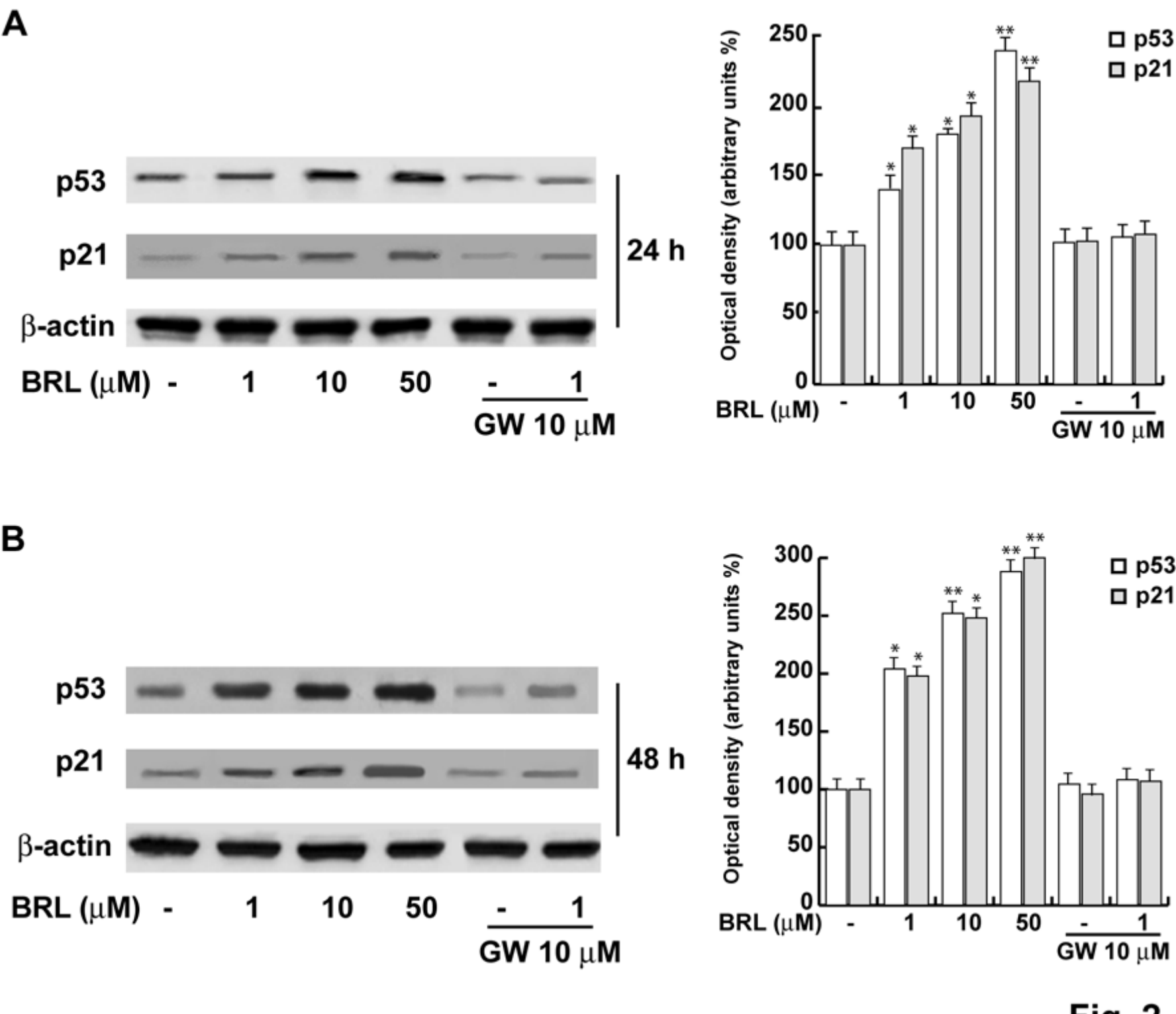
A
p53
p21
β-actin
24 h
BRL (μM) - 1 10 50 - 1
GW 10 μM
Optical density (arbitrary units %)
250
200
150
100
50
0
p53
p21
BRL (μM) - 1 10 50 - 1
GW 10 μM
B
p53
p21
β-actin
48 h
BRL (μM) - 1 10 50 - 1
GW 10 μM
Optical density (arbitrary units %)
300
250
200
150
100
50
0
p53
p21
BRL (μM) - 1 10 50 - 1
GW 10 μM

Fig. 2

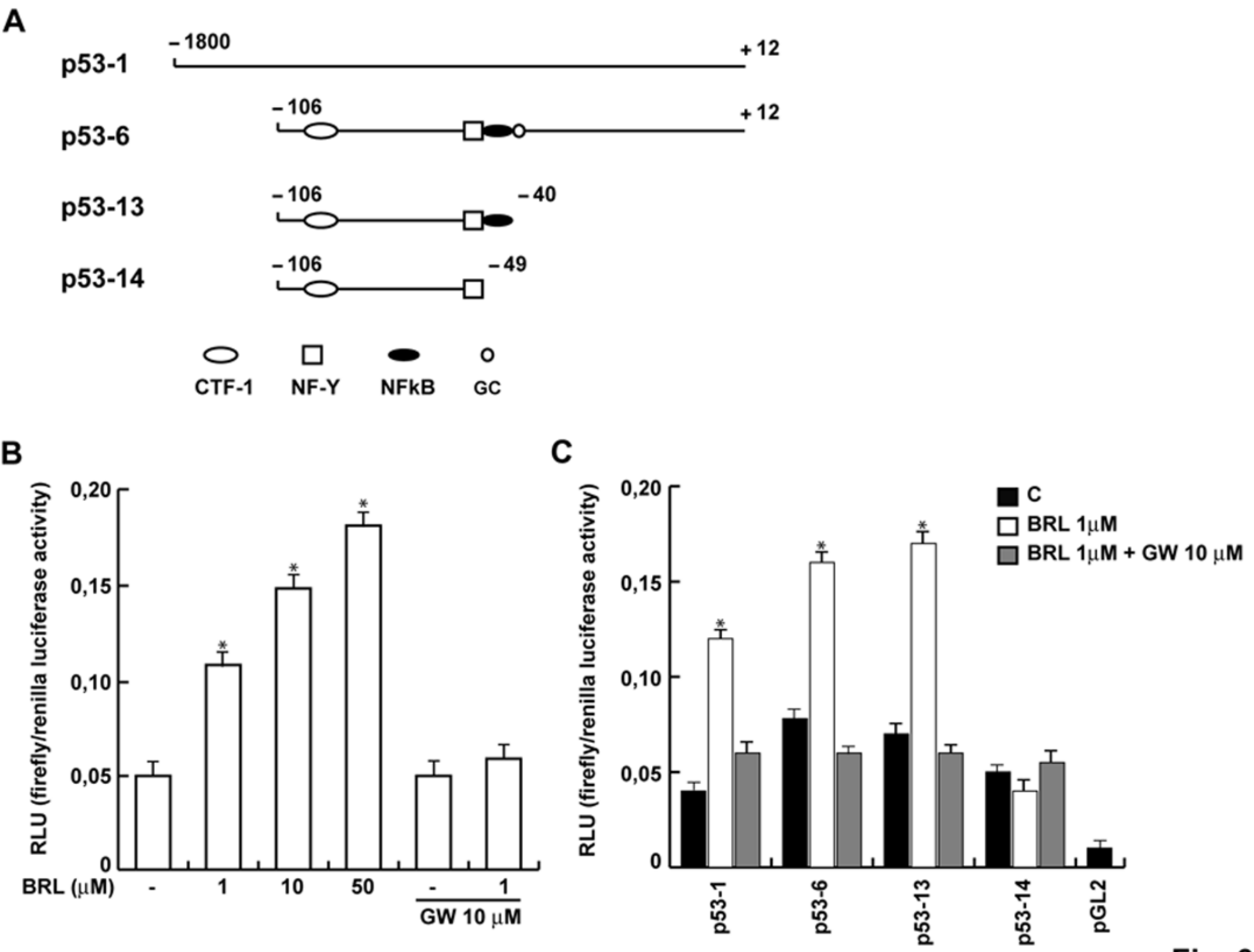
A
p53-1
−1800
+12
p53-6
−106
+12
p53-13
−106
−40
p53-14
−106
−49
CTF-1
NF-Y
NFkB
GC
B
RLU (firefly/renilla luciferase activity)
0,20
0,15
0,10
0,05
0
BRL (μM)
-
1
10
50
-
1
GW 10 μM
C
RLU (firefly/renilla luciferase activity)
0,20
0,15
0,10
0,05
0
C
BRL 1μM
BRL 1μM + GW 10 μM
p53-1
p53-6
p53-13
p53-14
pGL2

Fig. 3

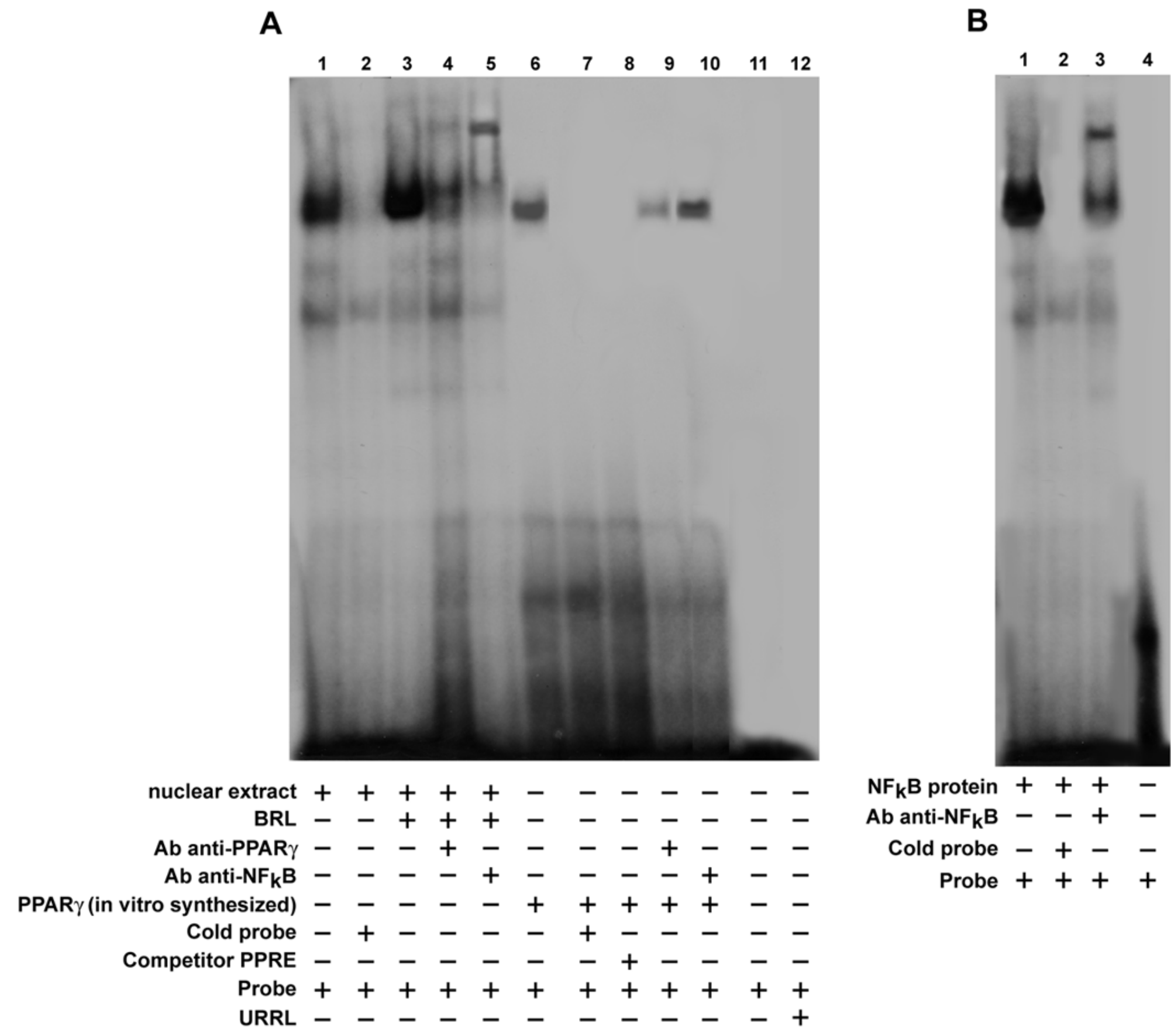
A
1 2 3 4 5 6 7 8 9 10 11 12
nuclear extract + + + + + − − − − − − −
BRL − − + + + − − − − − − −
Ab anti-PPARγ − − − + − − − − + − − −
Ab anti-NFkB − − − − + − − − − + − −
PPARγ (in vitro synthesized) − − − − − + + + + + − −
Cold probe − + − − − − + − − − − −
Competitor PPRE − − − − − − − + − − − −
Probe + + + + + + + + + + + +
URRL − − − − − − − − − − − +
B
1 2 3 4
NFkB protein + + + −
Ab anti-NFkB − − + −
Cold probe − + − −
Probe + + + +

Fig. 4

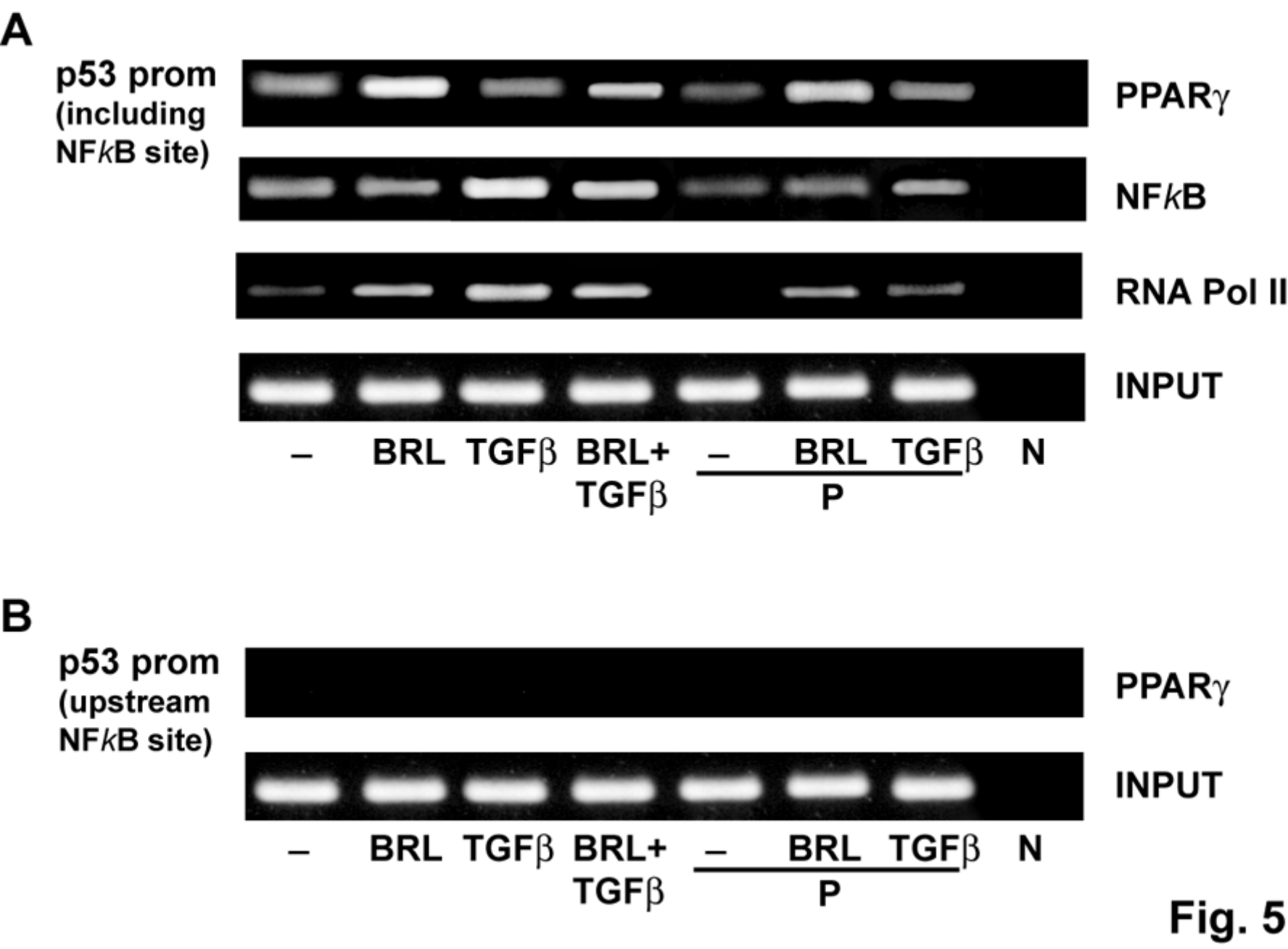
A
p53 prom
(including
NFkB site)
PPARγ
NFkB
RNA Pol II
INPUT
–
BRL
TGFβ
BRL+
TGFβ
–
BRL
TGFβ
N
P
B
p53 prom
(upstream
NFkB site)
PPARγ
INPUT
–
BRL
TGFβ
BRL+
TGFβ
–
BRL
TGFβ
N
P

Fig. 5

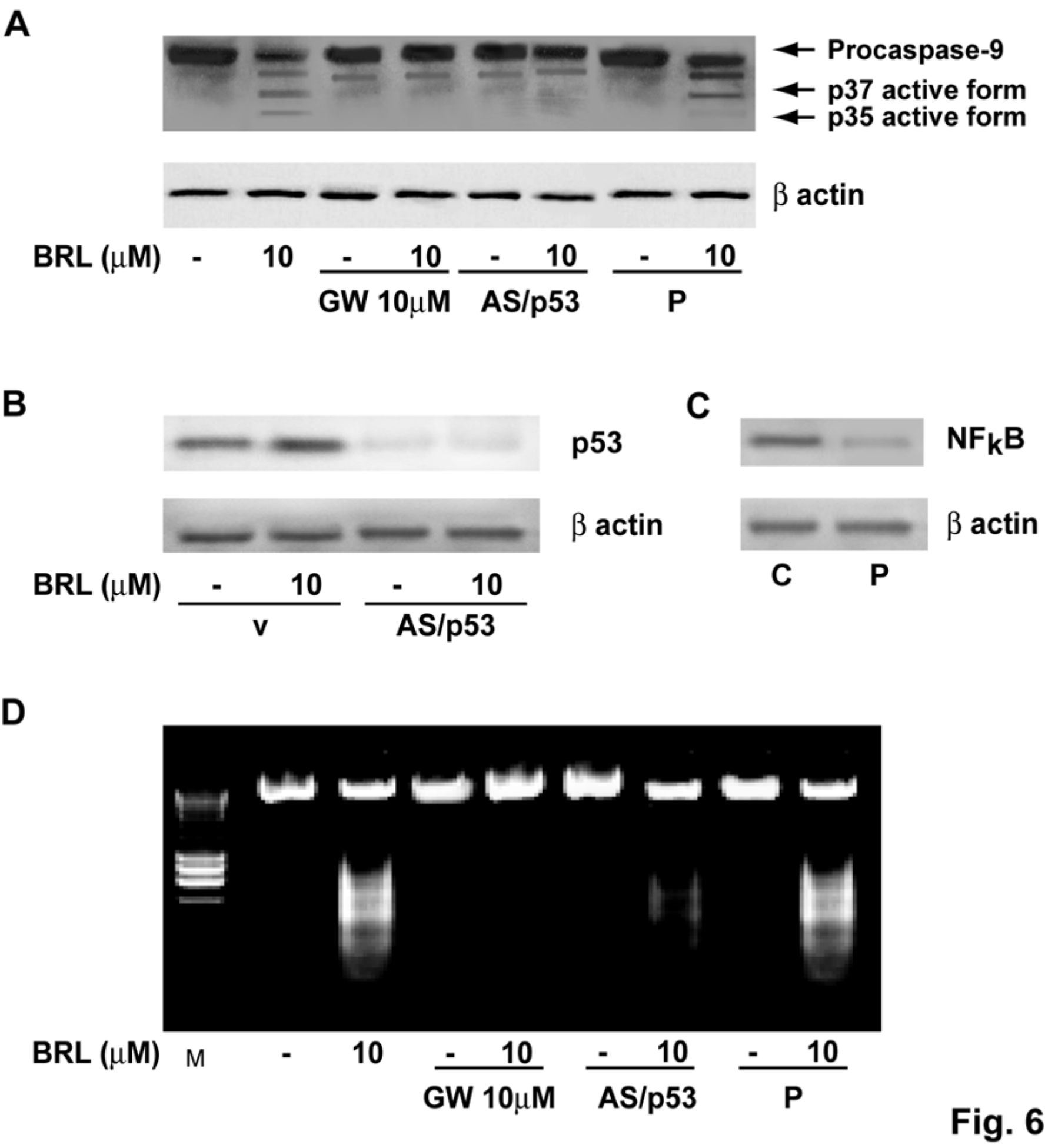
A
Procaspase-9
p37 active form
p35 active form
β actin
BRL (μM) - 10 - 10 - 10 - 10
GW 10μM
AS/p53
P
B
p53
β actin
BRL (μM) - 10 - 10
v
AS/p53
C
NFkB
β actin
C
P
D
BRL (μM) M - 10 - 10 - 10 - 10
GW 10μM
AS/p53
P

Fig. 6

Estrogen Receptor α Binds to Peroxisome Proliferator–Activated Receptor Response Element and Negatively Interferes with Peroxisome Proliferator–Activated Receptor γ Signaling in Breast Cancer Cells

Daniela Bonofiglio,[1] Sabrina Gabriele,[1] Saveria Aquila,[1] Stefania Catalano,[1] Mariaelena Gentile,[2] Emilia Middea,[1] Francesca Giordano,[2] and Sebastiano Andò[2,3]

Abstract

Purpose: The molecular mechanisms involved in the repressive effects exerted by estrogen receptors (ER) on peroxisome proliferator–activated receptor (PPAR) γ–mediated transcriptional activity remain to be elucidated. The aim of the present study was to provide new insight into the crosstalk between ERα and PPARγ pathways in breast cancer cells.

Experimental Design: Using MCF7 and HeLa cells as model systems, we did transient transfections and electrophoretic mobility shift assay and chromatin immunoprecipitation studies to evaluate the ability of ERα to influence PPAR response element–mediated transcription. A possible direct interaction between ERα and PPARγ was ascertained by coimmunoprecipitation assay, whereas their modulatory role in the phosphatidylinositol 3-kinase (PI3K)/AKT pathway was evaluated by determining PI3K activity and AKT phosphorylation. As a biological counterpart, we investigated the growth response to the cognate ligands of both receptors in hormone-dependent MCF7 breast cancer cells.

Results: Our data show for the first time that ERα binds to PPAR response element and represses its transactivation. Moreover, we have documented the physical and functional interactions of ERα and PPARγ, which also involve the p85 regulatory subunit of PI3K. Interestingly, ERα and PPARγ pathways have an opposite effect on the regulation of the PI3K/AKT transduction cascade, explaining, at least in part, the divergent response exerted by the cognate ligands 17β-estradiol and BRL49653 on MCF7 cell proliferation.

Conclusion: ERα physically associates with PPARγ and functionally interferes with PPARγ signaling. This crosstalk could be taken into account in setting new pharmacologic strategies for breast cancer disease.

Peroxisome proliferator–activated receptors (PPAR) are ligand-activated transcription factors belonging to the nuclear receptor superfamily (1). Activation of PPARs is a multistep process that involves ligand binding, heterodimerization with retinoic X receptor (RXR), interaction with cognate DNA sequences, and recruitment of coregulatory proteins (1). Three PPAR isoforms, α, β/δ, and γ, are expressed in multiple species in a tissue-specific manner (2–4). As for PPARγ, its involvement has been reported in several metabolic pathways, in adipocyte differentiation, and even in the growth inhibition of different cancer cell lines (5–14). In addition, PPARγ promoted terminal differentiation of malignant breast epithelial cells *in vitro* and induced morphologic changes associated with apoptosis and fibrosis in breast tumor cells injected in mice (15, 16).

A large body of evidence has shown that estrogen receptor (ER) α is involved in the development of breast cancer (17–20). On ligand binding, ERα undergoes a conformational change allowing chromatin interaction and the transcriptional regulation of target genes (21). It has also been reported that ERα binds to the p85 regulatory subunit of phosphatidylinositol 3-kinase (PI3K), leading to the activation of the protein kinase B/AKT pathway, which in turn regulates diverse processes like cell survival and proliferation (22, 23).

Recently, an increasing physiologic significance has been attributed to the crosstalk among nuclear receptors, which was observed at several levels of the signal transduction cascades (24–28). As it concerns the interaction between PPAR and ER pathways, the PPAR/RXR heterodimer has been shown to bind to estrogen response element (ERE)–related palindromic sequences; however, it cannot transactivate due to a nonpermissive natural promoter structure (26). On the other hand, ERs negatively interfere with PPAR response element (PPRE)–mediated transcriptional activity (29); however, the molecular mechanisms involved still remain to be elucidated.

Authors' Affiliations: Departments of [1]Pharmaco-Biology and [2]Cell Biology, and [3]Centro Sanitario, University of Calabria, Cosenza, Italy

Received 11/30/04; revised 6/7/05; accepted 6/15/05.

Grant support: Associazione Italiana per la Ricerca sul Cancro 2003.

The costs of publication of this article were defrayed in part by the payment of page charges. This article must therefore be hereby marked *advertisement* in accordance with 18 U.S.C. Section 1734 solely to indicate this fact.

Requests for reprints: Sebastiano Andò, Department of Cell Biology, University of Calabria, Cosenza 87036, Italy. Phone: 39-0984-496201; Fax: 39-0984-496203; E-mail: sebastiano.ando@unical.it.

doi:10.1158/1078-0432.CCR-04-2453

Herein, we have shown for the first time, to our knowledge, that ERα binds to PPRE even in the context of the endogenous phosphatase and tensin homologue deleted on chromosome 10 (PTEN) promoter sequence, physically interacts with PPARγ, and generates a ternary complex involving the p85 regulatory subunit of PI3K. Moreover, ERα and PPARγ induce opposite effects on the regulation on the PI3K/AKT pathway eliciting consequently divergent growth responses on treatment with the respective cognate ligands 17β-estradiol and rosiglitazone (BRL49653) in hormone-dependent MCF7 breast cancer cells.

Materials and Methods

Reagents. BRL49653 was a kind gift from GlaxoSmithKline (West Sussex, United Kingdom). The irreversible PPARγ antagonist GW9662, 17β-estradiol, and hydroxytamoxifen were purchased by Sigma (Milan, Italy). ICI182780 was generously provided by Zeneca Pharmaceuticals (Cheshire, United Kingdom). All compounds were solubilized in DMSO or in ethanol (Sigma).

Plasmids. The pGL_3 vector containing three copies of a PPRE sequence upstream of the minimal thymidine kinase promoter ligated to a luciferase reporter gene (3XPPRE-TK-pGL_3) and the PPARγ expression plasmid were a gift from Dr. R. Evans (The Salk Institute, San Diego, CA). The expression vector of ERα and androgen receptor were previously described (30, 31). The ERβ expression vector was provided by Dr. J.A. Gustafsson (Karoliska Institute, Stockholm, Sweden). The constitutively active myristilated AKT mutant (myr-AKT) was kindly provided by Dr. T. Simoncini (University of Pisa, Pisa, Italy).

Cell cultures. Wild-type human breast cancer ERα-positive MCF7 cells (a gift from E. Surmacz, Sbarro Institute for Cancer Research and Molecular Medicine, Philadelphia, PA) were grown in DMEM-F12 containing 10% FCS, 1% L-glutamine, 1% Eagle's nonessential amino acids, and 1 mg/mL penicillin-streptomycin. The ER-negative HeLa cells were maintained with DMEM supplemented with 10% FCS, 1% L-glutamine, and 1 mg/mL penicillin-streptomycin.

Transfection assay. Transient transfection experiments were done using 3XPPRE-TK ligated to a luciferase reporter gene into the pGL_3 vector. Cells were transferred into 24-well plates with 500 μL of regular growth medium/well the day before transfection. The medium was replaced with DMEM or DMEM-F12 lacking phenol red and serum on the day of transfection, which was done using Fugene 6 reagent as recommended by the manufacturer (Roche Diagnostics, Mannheim, Germany) with a mixture containing 0.5 μg of reporter plasmid, 5 ng of pRL-CMV, and 0.1 μg of effector plasmid where applicable. Empty vectors were used to ensure that DNA concentrations were constant in each transfection. After 6 hours of transfection, the medium was changed and the cells were treated in serum-free DMEM or DMEM-F12 in the presence of 10 μmol/L BRL49653, 1 μmol/L ICI182780, 1 μmol/L hydroxytamoxifen, and 10 μmol/L GW9662 for 18 hours.

Firefly and *Renilla* luciferase activities were measured using the Dual Luciferase Kit (Promega, Madison, WI). The firefly luciferase values of each sample were normalized by *Renilla* luciferase activity and data were reported as relative light units.

HeLa cells were plated in 10 cm dishes and then transfected with 5 μg ERα expression plasmid using Fugene 6 reagent to perform the electrophoretic mobility shift assay (EMSA). To determine PI3K activity, MCF7 cells were plated in 10 cm dishes and then transfected with 5 μg PPARγ and 5 μg ERα expression plasmids using FuGENE 6 reagent. To evaluate the role of PI3K/AKT pathway in MCF7 cell growth, 0.5 μg constitutively active myr-AKT was transfected using Fugene 6 reagent in six-well plates every 2 days where applicable.

Electrophoretic mobility shift assay. Nuclear extracts from MCF7 and HeLa cells were prepared as previously described (32). Briefly, MCF7 and HeLa cells plated into 10 cm dishes were scraped into 1.5 mL of cold PBS. Cells were pelleted for 10 seconds and resuspended in 400 μL cold buffer A [10 mmol/L HEPES-KOH (pH 7.9) at 4°C, 1.5 mmol/L $MgCl_2$, 10 mmol/L KCl, 0.5 mmol/L DTT, 0.2 mmol/L phenylmethylsulfonyl fluoride, 1 mmol/L leupeptin] by flicking the tube. The cells were allowed to swell on ice for 10 minutes and then vortexed for 10 seconds. Samples were then centrifuged for 10 seconds and the supernatant fraction discarded. The pellet was resuspended in 50 μL of cold buffer B [20 mmol/L HEPES-KOH (pH 7.9), 25% glycerol, 1.5 mmol/L $MgCl_2$, 420 mmol/L NaCl, 0.2 mmol/L EDTA, 0.5 mmol/L DTT, 0.2 mmol/L phenylmethylsulfonyl fluoride, 1 mmol/L leupeptin] and incubated on ice for 20 minutes for high-salt extraction. Cellular debris were removed by centrifugation for 2 minutes at 4°C and the supernatant fraction (containing DNA binding proteins) was stored at −70°C. *In vitro* transcribed and translated PPARγ and ERα were synthesized using the T7 polymerase in the rabbit reticulocyte lysate system as directed by the manufacturer (Promega). The probe was generated by annealing single-stranded oligonucleotides and labeled with [γ-^{32}P]ATP (Amersham Pharmacia, Buckinghamshire, United Kingdom) and T4 polynucleotide kinase (Promega), and then purified using Sephadex G50 spin columns (Amersham Pharmacia).

A double-stranded PPRE was prepared by annealing the following sense and antisense-oligonucleotides: 5′-GGGACCAGGACAAAGGTCACGTT-3′ and 5′-GGGAACGTGACCTTTGTCCTGGTC-3′ (Sigma Genosys, Cambridge, United Kingdom). As control for nonspecific binding, a cold PPRE competitor was included. The protein binding reactions were carried out in 20 μL of buffer [20 mmol/L HEPES (pH 8), 1 mmol/L EDTA, 50 mmol/L KCl, 10 mmol/L DTT, 10% glycerol, 1 mg/mL bovine serum albumin, 50 μg/mL poly(deoxyinosinic-deoxycytidylic acid)] with 50,000 cpm of labeled probe, 5 μg of MCF7 and HeLa nuclear protein, or 2 μL of *in vitro* transcribed and translated PPARγ and ERα proteins, and 5 μg of poly(deoxyinosinic-deoxycytidylic acid). The mixtures were incubated at room temperature for 20 minutes in the presence or absence of unlabeled competitor oligonucleotides or *in vitro* transcribed and translated PPARγ and ERα proteins. For the experiments involving PPARγ and ERα (F-10 and D-12) antibodies (Santa Cruz Biotechnology, Santa Cruz, CA), the reaction mixture was incubated with these antibodies at 4°C for 30 minutes before addition of labeled probe. Under the conditions employed, cross-reactivity of the PPARγ and ERα antibodies was not observed in EMSA supershift assays (data not shown). The entire reaction mixture was electrophoresed through a 6% polyacrylamide gel in 0.25× Tris-borate-EDTA for 3 hours at 150 V. Gel was dried and subjected to autoradiography at −70°C.

Chromatin immunoprecipitation. According to the chromatin immunoprecipitation (ChIP) assay procedure previously described (33), MCF7 cells were grown in 10 cm dishes to 50% to 60% confluence, shifted to serum-free medium for 24 hours, and then treated with 10 μmol/L BRL49653, 10 μmol/L GW9662, 100 nmol/L 17β-estradiol, and 1 μmol/L ICI182780 for 1 hour. Thereafter, cells were washed twice with PBS and cross-linked with 1% formaldehyde at 37°C for 10 minutes. Next, cells were washed twice with PBS at 4°C, collected and resuspended in 200 μL of lysis buffer [1% SDS, 10 mmol/L EDTA, 50 mmol/L Tris-HCl (pH 8.1)], and left on ice for 10 minutes. Then, cells were sonicated four times for 10 seconds at 30% of maximal power (Sonics, Vibra Cell 500 W) and collected by centrifugation at 4°C for 10 minutes at 14,000 rpm. The supernatants were diluted in 1.3 mL of immunoprecipitation buffer [0.01% SDS, 1.1% Triton X-100, 1.2 mmol/L EDTA, 16.7 mmol/L Tris-HCl (pH 8.1), 16.7 mmol/L NaCl] followed by immunoclearing with 80 μL of sonicated salmon sperm DNA/protein A agarose (UBI, Lake Placid, NY) for 1 hour at 4°C. The precleared chromatin was immunoprecipitated with specific antibodies anti-PPARγ (H-100, Santa Cruz Biotechnology) and anti-ERα (F-10, Santa Cruz Biotechnology). At this point, 60 μL of salmon sperm DNA/protein A agarose were added and precipitation was further continued for 2 hours at 4°C. After pelleting, precipitates were sequentially washed for 5 minutes with the following buffers: wash A [0.1% SDS, 1% Triton X-100, 2 mmol/L EDTA, 20 mmol/L Tris-HCl (pH 8.1), 150 mmol/L NaCl], wash B [0.1% SDS, 1% Triton X-100, 2 mmol/L EDTA, 20 mmol/L Tris-HCl (pH 8.1), 500 mmol/L NaCl], and

wash C [0.25 mol/L LiCl, 1% NP40, 1% sodium deoxycholate, 1 mmol/L EDTA, 10 mmol/L Tris-HCl (pH 8.1)], and then twice with Tris-EDTA buffer (10 mmol/L Tris, 1 mmol/L EDTA). The immunocomplexes were eluted with elution buffer (1% SDS, 0.1 mol/L $NaHCO_3$). The eluates were reverse cross-linked by heating at 65°C and digested with proteinase K (0.5 mg/mL) at 45°C for 1 hour. DNA was obtained by phenol/chloroform/isoamyl alcohol extraction. Two microliters of 10 mg/mL yeast tRNA (Sigma) were added to each sample and DNA was precipitated with 70% ethanol for 24 hours at −20°C, and then washed with 95% ethanol and resuspended in 20 μL of Tris-EDTA buffer. Five microliters of each sample were used for PCR amplification with the following primers flanking a PPRE sequence present in the *PTEN* promoter region: 5′-AGAGACTTATAACTGGGCAGG-3′ (forward) and 5′-CAAGTGATATCATATGTGATGCTG-3′ (reverse). The PCR conditions for PPRE in *PTEN* promoter fragment were 45 seconds at 94°C, 40 seconds at 57°C, and 90 seconds at 72°C. The amplification products obtained in 30 cycles were analyzed in 2% agarose gel and visualized by ethidium bromide staining. The negative control was provided by PCR amplification without DNA sample. The specificity of reactions was ensured using normal mouse and rabbit immunoglobulin G (Santa Cruz Biotechnology).

Reverse chromatin immunoprecipitation. According to the reverse ChIP procedure previously described (34), pellets obtained by immunoprecipitation of soluble chromatin with PPARγ antibody were eluted with 500 μL of reverse-ChIP buffer [0.5 mmol/L DTT, 1% Triton X-100, 2 mmol/L EDTA, 150 mmol/L NaCl, 20 mmol/L Tris-HCl (pH 8.1)]. Next, the eluate from PPARγ immunoprecipitation was precipitated with anti-p85 (B-9, Santa Cruz Biotechnology) and anti-ERα (F-10) antibodies. The presence of PPRE in the *PTEN* promoter sequences in the resulting reverse-ChIP pellets was examined as described above for one-step ChIP.

Reverse transcription-PCR assay. MCF7 cells were grown in 10 cm dishes to 70% to 80% confluence and exposed to treatments for 24 hours in 1% charcoal-stripped FCS. Total cellular RNA was extracted using TRIZOL reagent (Invitrogen, Carlsbad, CA) as suggested by the manufacturer. The purity and integrity were checked spectroscopically and by gel electrophoresis before carrying out the analytic procedures. The evaluation of gene expression was done by semiquantitative reverse transcription-PCR method as previously described (35). For *PTEN* and the internal control gene *36B4*, the primers were 5′-CCACCACAGCTA-GAACTTATC-3′ (*PTEN* forward) and 5′-ATCTGCACGCTCTATACTGC-3′ (*PTEN* reverse), and 5′-CTCAACATCTCCCCCTTCTC-3′ (*36B4* forward) and 5′-CAAATCCCATATCCTCGTCC-3′ (*36B4* reverse) to yield products of 647 bp with 25 cycles and 408 bp with 12 cycles, respectively. The results obtained as absorbance arbitrary values were transformed to percentage of the control (percent control) taking the samples from untreated cells as 100%.

Immunoprecipitation and immunoblotting. MCF7 cells were grown in 10 cm dishes to 70% to 80% confluence and exposed to treatments for 1 hour or 24 hours in 1% charcoal-stripped FCS before lysis in 500 μL of lysis buffer >[50 mmol/L HEPES (pH 7.5), 150 mmol/L NaCl, 1.5 mmol/L $MgCl_2$, 1 mmol/L EGTA, 10% glycerol, 1% Triton X-100, a mixture of protease inhibitors (aprotinin, phenylmethylsulfonyl fluoride, and Na-orthovanadate)]. Cell lysates were centrifuged at 12,000 × *g* for 5 minutes and 500 μg of total protein were incubated overnight with the anti-PPARγ antibody (1 μg; Santa Cruz Biotechnology) and 500 μL of HNTG (immunoprecipitation) buffer [50 mmol/L HEPES (pH 7.4), 50 mmol/L NaCl, 0.1% Triton X-100, 10% glycerol, 1 mmol/L phenylmethylsulfonyl fluoride, 10 μg/mL leupeptin, 10 μg/mL aprotinin, 2 μg/mL pepstatin]. Immunocomplexes were recovered by incubation with protein A/G-agarose. The beads containing bound proteins were washed thrice by centrifugation in immunoprecipitation buffer, then denatured by boiling in Laemmli sample buffer and analyzed by Western blot to identify the coprecipitating effector proteins. Membranes were stripped of bound antibodies by incubation in 0.2 mol/L glycine (pH 7.6) for 30 minutes at room temperature. Before reprobing with different primary antibodies (anti-ERα and anti-p85; Santa Cruz Biotechnology), stripped membranes were extensively washed in Tween 20 in TBS (TTBS) and placed in blocking buffer (TTBS containing 5% milk) overnight.

Equal amounts of total protein were resolved on an 11% SDS-polyacrylamide gel. Proteins were transferred to a nitrocellulose membrane, probed with rabbit polyclonal antiserum directed against PTEN, AKT, and phospho-AKT (Ser473) and with goat polyclonal antiserum directed against β-actin (all purchased from Santa Cruz Biotechnology). The antigen-antibody complex was detected by incubation of the membranes for 1 hour at room temperature with peroxidase-coupled goat anti-rabbit immunoglobulin G and revealed using the enhanced chemiluminescence system (Amersham Pharmacia). Blots were then exposed to film (Kodak film, Sigma).

p85-associated phosphatidylinositol 3-kinase activity. p85 was precipitated from 500 μg of MCF7 cell lysates. The negative control was done using a cell lysate where the p85 regulatory subunit of PI3K was previously removed by preincubation with the respective antibody (1 hour at room temperature) and subsequently immunoprecipitated with protein A/G-agarose. As a positive control, MCF7 cells were treated with 100 nmol/L insulin for 30 minutes before lysis and IRS-1 was precipitated from 500 μg of cell lysates. The immunoprecipitates were washed once with cold PBS, twice with 0.5 mol/L LiCl, 0.1 mol/L Tris (pH 7.4), and finally with 10 mmol/L Tris, 100 mmol/L NaCl, 1 mmol/L EDTA. The presence of PI3K activity in immunoprecipitates was determined by incubating the beads with reaction buffer containing

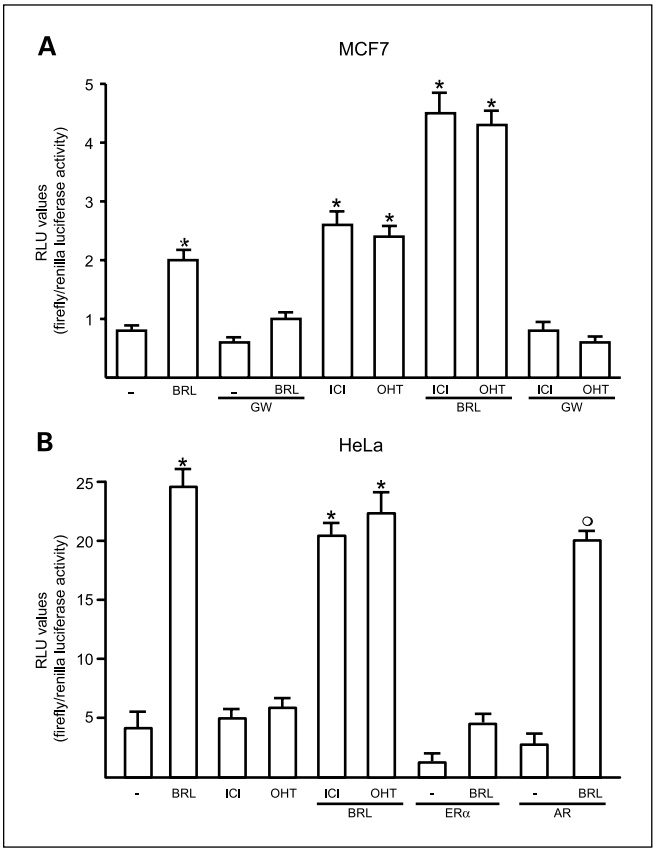

Fig. 1. ERα negatively regulates the PPRE-mediated transcriptional activity. *A*, MCF7 cells were transfected with a PPRE reporter gene and treated with 10 μmol/L BRL49653 (*BRL*), 10 μmol/L PPARγ antagonist GW9662 (*GW*), 1 μmol/L ICI182780 (*ICI*), and 1 μmol/L hydroxytamoxifen (*OHT*), as indicated. *B*, HeLa cells were cotransfected with a PPRE reporter gene and expression vectors of ERα and androgen receptor (*AR*), treated with 10 μmol/L BRL49653, 1 μmol/L ICI182780, and 1 μmol/L hydroxytamoxifen, as indicated. *Columns,* mean of three independent experiments done in triplicate; bars, SD. *, $P < 0.05$, treated versus untreated cells; ○, $P < 0.05$, BRL49653-treated versus untreated cells transfected with androgen receptor. RLU, relative light units.

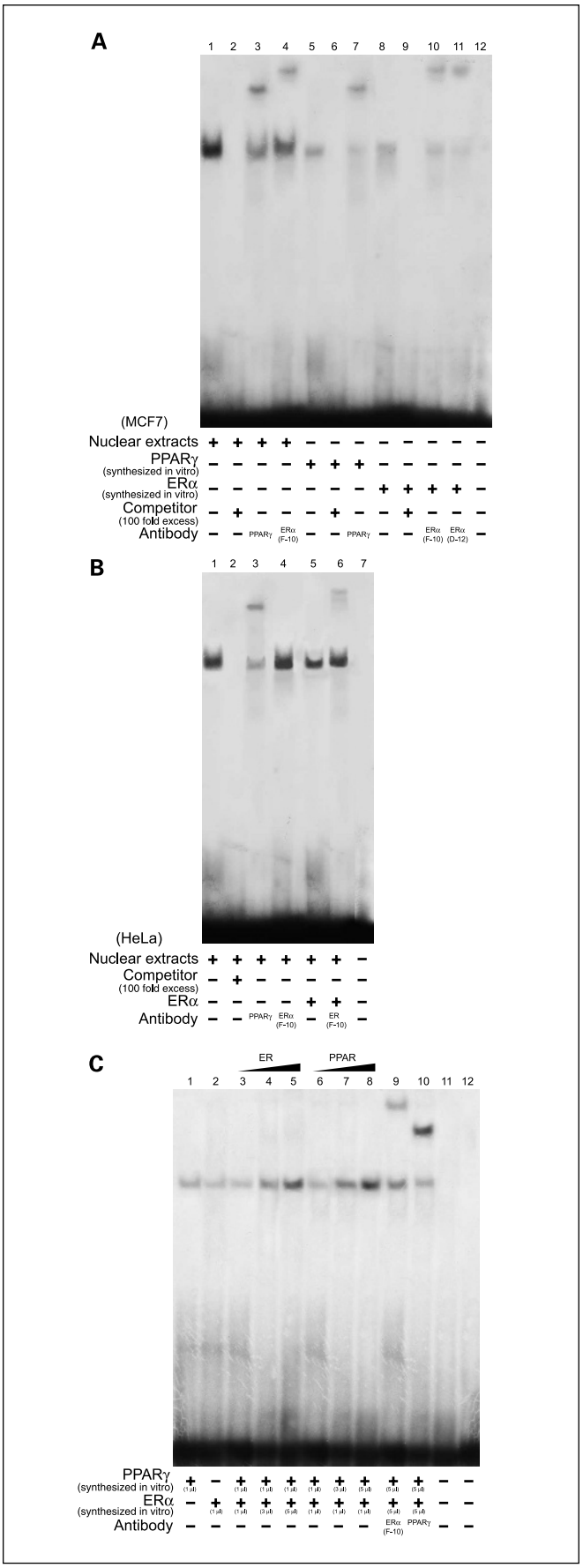

10 mmol/L HEPES (pH 7.4), 10 mmol/L $MgCl_2$, 50 μmol/L ATP, 20 μCi [γ-^{32}P]ATP, and 10 μg of phosphatidylinositol for 20 minutes at 37°C. The reactions were stopped by adding 100 μL of 1 mol/L HCl. Phospholipids were extracted with 200 μL of $CHCl_3$/methanol. Phase separation was facilitated by centrifugation at 5,000 rpm for 2 minutes in a tabletop centrifuge. The upper phase was removed, and the lower chloroform phase was washed once more with clear upper phase. The washed chloroform phase was dried under a stream of nitrogen gas and redissolved in 30 μL of chloroform. The labeled products of the kinase reaction, the phosphatidylinositol phosphates, were then spotted onto *trans*-1,2-diaminocyclohexane-*N*,*N*,*N*′,*N*′-tetraacetic acid – treated silica gel 60 TLC plates. Radioactive spots were visualized by autoradiography.

[^{3}H]Thymidine incorporation. MCF7 and HeLa cells were seeded in six-well plates in regular growth medium. On the second day, cells were incubated in DMEM-F12 or DMEM supplemented with 1% charcoal-stripped FCS for the indicated times in the presence of increasing BRL49653 concentrations or GW9662, 17β-estradiol, and ICI182780.

The medium was renewed every 2 days together with the appropriate treatments. [^{3}H]Thymidine (1 μCi/mL; New England Nuclear, Newton, MA) was added to the medium for the last 6 hours. After rinsing with PBS, the cells were washed once with 10% and thrice with 5% trichloroacetic acid. Cells were lysed by adding 0.1 N NaOH and then incubated 30 minutes at 37°C. Thymidine incorporation was determined by scintillation counting.

Statistical analysis. Statistical analysis was done using ANOVA followed by Newman-Keuls testing to determine differences in means. $P < 0.05$ was considered as statistically significant.

Results

Estrogen receptor α negatively regulates the peroxisome proliferator–activated receptor response element–mediated transcriptional activity. We first aimed to evaluate in MCF7 cells the response of a PPRE reporter gene to BRL49653, a synthetic ligand of PPARγ. As reported in Fig. 1A, BRL49653 activated PPARγ directly because the transcriptional activity was abrogated by the specific PPARγ antagonist GW9662. Interestingly, the ER antagonists ICI182780 and hydroxytamoxifen were able to stimulate the PPRE transactivation, which was reversed by GW9662 treatment (Fig. 1A). Furthermore, the response to BRL49653 treatment was potentiated by both antiestrogens (Fig. 1A).

To ascertain whether ERα is involved in the PPRE-mediated transcriptional activity induced by ICI182780 and hydroxytamoxifen in MCF7 cells, we turned to the ER-negative HeLa cells. Basal and BRL49653-stimulated reporter activity was higher

Fig. 2. ERα binds to PPRE in EMSA. *A*, nuclear extracts from MCF7 cells (*lane 1*) or 2 μL of PPARγ and ERα (*lanes 5* and *8*, respectively) translated proteins were incubated with a double-stranded PPRE consensus sequence probe labeled with [γ-^{32}P] and subjected to electrophoresis in a 6% polyacrylamide gel. Competition experiments were done, adding as competitor a 100-fold molar excess of unlabeled PPRE probe (*lanes 2, 6*, and *9*). Anti-PPARγ or anti-ERα antibodies were incubated with nuclear extracts from MCF7 cells (*lanes 3* and *4*, respectively) or added to PPARγ (*lane 7*) and ERα translated proteins (*lanes 10* and *11*). Lane 12 contains probe alone. *B*, nuclear extracts from HeLa cells were subjected to similar experimental conditions of MCF7 cells (*lane 1*). Competition experiment was done, adding as competitor a 100-fold molar excess of unlabeled PPRE probe (*lane 2*). Anti-PPARγ or anti-ERα antibodies were incubated with nuclear extracts from HeLa cells (*lanes 3* and *4*, respectively). HeLa cells were transfected with 5 μg of an ERα expression vector (*lane 5*) and incubated with an anti-ERα antibody (*lane 6*). Lane 7 contains probe alone. *C*, PPARγ translated proteins were incubated in the absence (*lane 1*) or in the presence of increasing amounts of ERα translated proteins (*lanes 3-5*). ERα translated proteins were incubated alone (*lane 2*) or together with increasing amounts of PPARγ translated proteins (*lanes 6-8*). Anti-ERα or anti-PPARγ antibodies were added to the reaction (*lanes 9* and *10*, respectively). Lane 11 contains probe alone; lane 12 contains 2 μL of unprogrammed rabbit reticulocyte lysate incubated with PPRE.

in HeLa than in MCF7 cells, whereas both antiestrogens had no effects alone or in combination with BRL49653 treatment (Fig. 1B). According to a previous study (29), the PPARγ transactivation by BRL49653 was no longer noticeable transfecting ERα (Fig. 1B) and ERβ (data not shown) in HeLa cells, whereas an expression vector encoding the androgen receptor did not alter the PPRE-mediated transcriptional activity on BRL49653 (Fig. 1B).

Estrogen receptor α binds to peroxisome proliferator–activated receptor response element in electrophoretic mobility shift assay. To provide further insight into the mechanisms by which ERα negatively interferes with PPRE-mediated transcriptional activity, we did EMSA using a [γ-^{32}P]-labeled consensus sequence of PPRE as probe. Nuclear extracts from MCF7 cells showed strong DNA binding activity for PPRE (Fig. 2A, *lane 1*) in a specific manner because a 100-fold molar excess of unlabeled probe abrogated the formation of this complex (Fig. 2A, *lane 2*). The inclusion in the reaction mix of an anti-PPARγ antibody attenuated the specific band and induced the formation of a supershifted complex (Fig. 2A, *lane 3*). Surprisingly, an anti-ERα antibody also caused a supershift of the band together with a reduced intensity of the specific signal (Fig. 2A, *lane 4*). On the basis of these observations, we aimed to determine whether ERα is capable of binding directly to the PPRE sequence. Thus, we did EMSA using the same radiolabeled PPRE probe with PPARγ and ERα proteins transcribed and translated *in vitro* in a cell-free system. As expected, the synthesized PPARγ protein bound specifically to PPRE because the complex was absent in the presence of a 100-fold molar excess of unlabeled probe (Fig. 2A, *lanes 5* and *6*). Adding an anti-PPARγ antibody to the reaction, the signal was drastically reduced due to the formation of a supershifted complex (Fig. 2A, *lane 7*). Of note, using the synthesized ERα protein, we obtained a single band migrating at the same level as that of PPARγ (Fig. 2A, *lane 8*). The incubation of a 100-fold excess of unlabeled probe abrogated this signal, indicating its specificity (Fig. 2A, *lane 9*). In addition, two distinct monoclonal antibodies against ERα (see Materials and Methods) were both able to form supershifts and showed a reduced intensity of the ERα-PPRE band (Fig. 2A, *lanes 10* and *11*). To confirm the above-mentioned results, we turned to HeLa cells which were transfected with an ERα expression vector. Results obtained were similar to those observed in MCF7 cells (Fig. 2B). Next, using equal amounts of PPARγ and increasing concentrations of ERα and *viceversa*, a progressive enhancement of bands was observed in both cases (Fig. 2C, *lanes 3-8*). Incubating the highest amount of both ERα and PPARγ in the presence of anti-ERα or anti-PPARγ antibodies, supershifted complexes were formed together with an attenuation of the specific signals (Fig. 2C, *lanes 9* and *10*).

Physical and functional interactions of peroxisome proliferator–activated receptor γ and estrogen receptor α. To determine whether crosstalk between ERα and PPARγ transduction pathways may also occur at the protein-protein level, we did coimmunoprecipitation assays in MCF7 cells. It is worth noting that PPARγ was constitutively associated with ERα (Fig. 3A). Treatment with BRL49653 or 17β-estradiol slightly decreased this association, whereas ICI182780 strongly inhibited the interaction (Fig. 3A). Given that ERα binds to the p85 regulatory subunit of PI3K (22), we investigated a possible association of ERα, PPARγ, and p85. We observed the formation of this ternary complex in an ERα-dependent manner because ICI182780 was able to abrogate the coprecipitation (Fig. 3A).

Considering the above-mentioned observations, we investigated whether ERα, alone or together with PPARγ, binds to an endogenous PPRE sequence like that contained in the promoter region of the *PTEN* gene (36). Thus, we did a ChIP

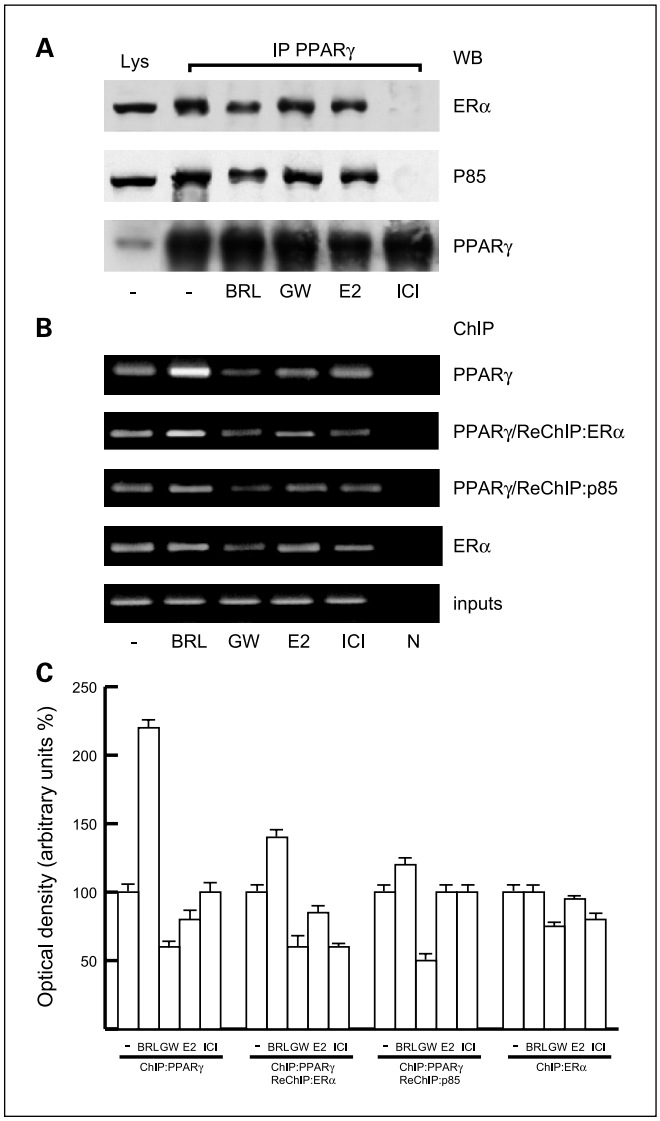

Fig. 3. Physical and functional interactions of PPARγ and ERα. *A*, MCF7 cells were treated for 24 hours with 10 μmol/L BRL49653, 10 μmol/L GW9662, 100 nmol/L 17β-estradiol (*E2*), and 1 μmol/L ICI182780. Cell lysates were immunoprecipitated with an antiserum against PPARγ (IP: anti-PPARγ) and then the immunocomplexes were resolved in SDS-PAGE. The membrane was probed with ERα and p85 antibodies. To verify equal loading, the membrane was probed with an antibody against PPARγ. *B*, MCF7 cells were treated for 1 hour with 10 μmol/L BRL49653, 10 μmol/L GW9662, 100 nmol/L 17β-estradiol, and 1 μmol/L ICI182780, then cross-linked with formaldehyde and lysed. The soluble chromatin was immunoprecipitated with either anti-PPARγ (reverse ChIP with anti-ERα or anti-p85) or anti-ERα. The immunocomplexes were reverse cross-linked, and DNA was recovered by phenol/chloroform extraction and ethanol precipitation. The PTEN promoter sequences containing PPRE were detected by PCR with specific primers, as described in Materials and Methods. To control input DNA, PTEN promoter was amplified from 30 μL of initial preparations of soluble chromatin (before immunoprecipitations). N, negative control provided by PCR amplification without DNA sample. *C*, quantitative representation of data of three independent experiments including that of *B*.

assay in MCF7 cells using agonists and antagonists of both receptors. The results indicated that PPARγ as well as ERα bound to the *PTEN* promoter along with p85 in untreated cells (Fig. 3B). Interestingly, on treatment with BRL49653 and GW9662, we observed an enhanced and a decreased recruitment of PPARγ to the *PTEN* promoter sequence, respectively. 17β-Estradiol did not induce substantial changes whereas ICI182780 reduced the recruitment of ERα (Fig. 3B). To evaluate the specificity of the reactions, we also used normal mouse and rabbit immunoglobulin G that did not reveal DNA amplifications (data not shown).

BRL49653 down-regulates the phosphatidylinositol 3-kinase/AKT pathway in MCF7 cells. To assess the influence of the complex formed by PPARγ/ERα/p85 on the PI3K/AKT transduction cascade, we evaluated the short (30 minutes) and late (24 hours) effects of BRL49653 on PI3K activity and AKT phosphorylation. Interestingly, BRL49653 showed a dose-dependent negative interference with this pathway at both times (Fig. 4A-D). In agreement with previous reports (22, 37), an opposite regulation was induced by 17β-estradiol (data not shown). Besides, the overexpression of ERα in MCF7 cells enhanced the PI3K activity, which was further potentiated in the presence of 17β-estradiol (Fig. 4E, *lanes 3* and *4*). On the contrary, the overexpression of PPARγ in MCF7 cells reduced the PI3K activity, which resulted to further repression with BRL49653 (Fig. 4E, *lanes 5* and *6*). Of note, the latter inhibitory effects were no longer noticeable with a combination of ERα overexpression and 17β-estradiol treatment (Fig. 4E, *lane 7*).

17β-Estradiol reverses the up-regulation of PTEN by BRL49653 in MCF7 cells. It has been reported that PPARγ up-regulates PTEN expression through two cognate response elements located upstream to the promoter region (36). It is worth noting that PTEN controls several cell functions, including survival and proliferation, by antagonizing the PI3K signaling cascade (38). These observations and our findings prompted us to evaluate the potential effects of both BRL49653 and 17β-estradiol on PTEN expression. Both compounds had no rapid effects (up to 3 hours; data not shown), whereas a 24-hour exposure to 10 μmol/L BRL49653 induced a significant enhancement of PTEN mRNA and protein levels, which was

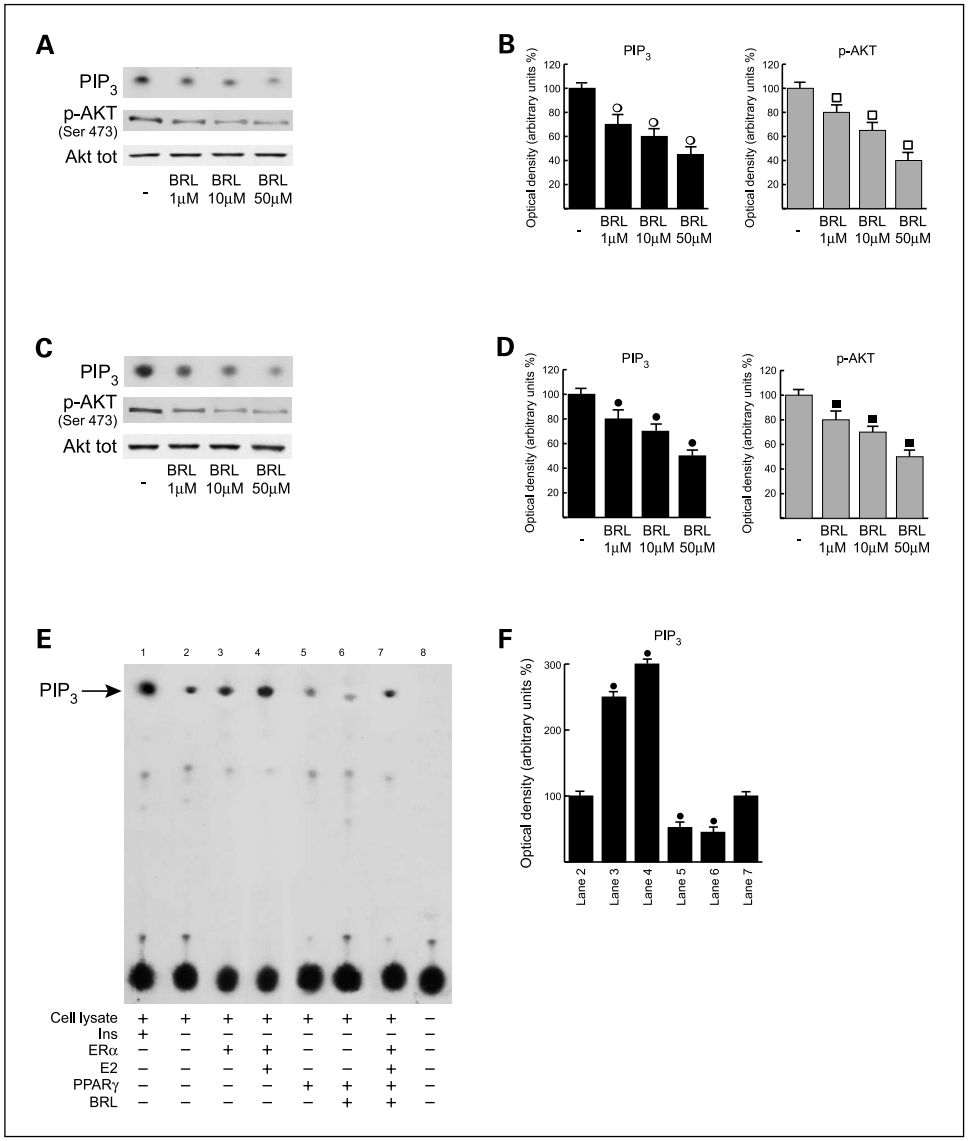

Fig. 4. BRL49653 negatively interferes with PI3K/AKT pathway in MCF7 cells. MCF7 cells were treated for 30 minutes (*A*) and 24 hours (*C*) with increasing concentrations of BRL49653. p85-associated PI3K activity was measured in MCF7 lysates immunoprecipitated with the anti-p85 antibody and incubated in the presence of 200 μmol/L phosphatidylinositol and 10 μCi of [γ-^{32}P]ATP for 20 minutes as described in Materials and Methods. Protein lysates were immunoblotted for phospho-AKT (Ser473) and total AKT. Autoradiographs are representative of six independent experiments, which are cumulatively represented in *B* and *D*, respectively (*columns,* mean; *bars,* SD). *E*, MCF7 cells were transfected with an empty vector (*lane 2*), with 5 μg of an ERα expression vector (*lane 3*) and in the presence of 100 nmol/L 17β-estradiol (*lane 4*), with 5 μg of PPARγ expression vector (*lane 5*) and in the presence of 10 μmol/L BRL49653 (*lane 6*), with 5 μg of both ERα and PPARγ plasmids in the presence of 100 nmol/L 17β-estradiol and 10 μmol/L BRL49653 (*lane 7*). Cell lysates were immunoprecipitated using the anti-p85 antibody, incubated in the presence of 200 μmol/L phosphatidylinositol and 10 μCi of [γ-^{32}P]ATP for 20 minutes. As a positive control, we used MCF-7 cells treated with 100 nmol/L insulin for 30 minutes before lysis and immunoprecipitated with anti – IRS-1 from 500 μg of cell lysates (*lane 1*). As a negative control, we used MCF7 cell lysates in which p85 was previously removed by preincubation with specific antibody (1 hour at room temperature) and subsequent immunoprecipitation with protein A/G-agarose (*lane 8*). *F*, quantitative representations of data of three independent experiments including that of *E*. ○, ●, □, ■: $P < 0.05$, treated versus untreated cells. PIP_3, phosphatidylinositol 3,4,5-triphosphate.

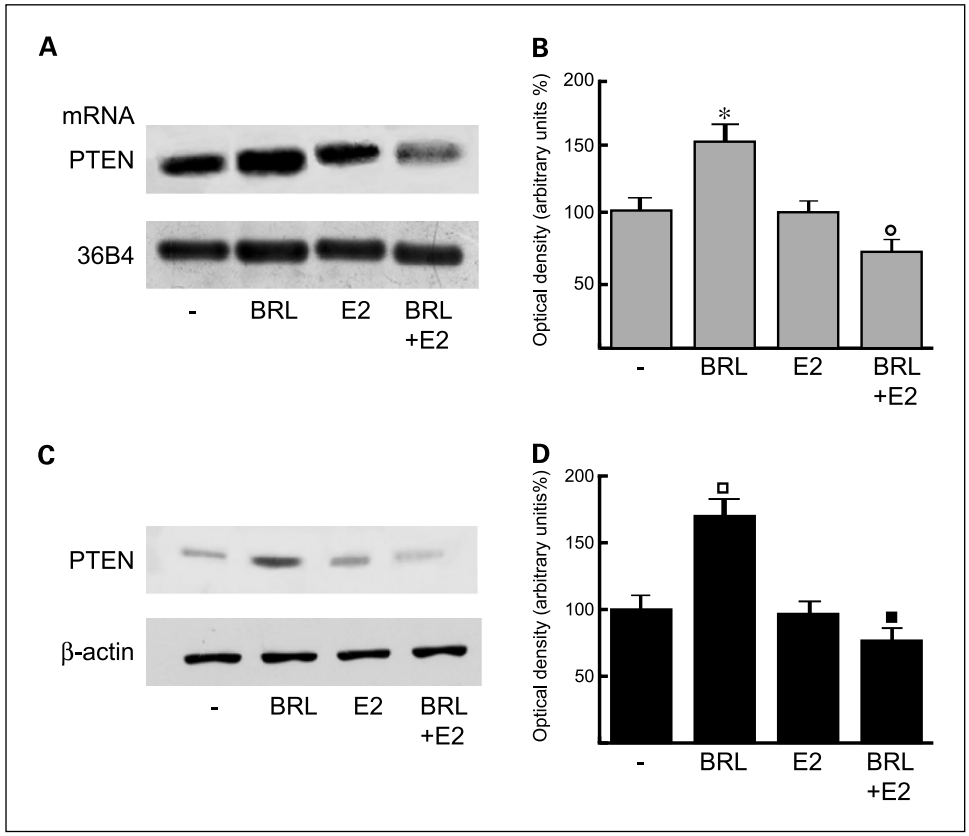

Fig. 5. 17β-Estradiol reverses the up-regulation of PTEN induced by BRL49653 in MCF7 cells. *A*, semiquantitative reverse transcription-PCR evaluation of PTEN mRNA. MCF7 cells were treated for 24 hours with 10 μmol/L BRL49653 and/or 100 nmol/L 17β-estradiol as indicated. 36B4 mRNA levels were determined as a control. *B*, quantitative representation of data of three independent experiments including that of *A* after densitometry and correction for 36B4. *C*, immunoblots of PTEN from MCF7 cells treated as in *A*. β-Actin was used as loading control. *D*, quantitative representations of data of three independent experiments including that of *C*. *, □: $P < 0.05$, BRL49653-treated versus untreated cells; ○, ■: $P < 0.05$, cells treated with BRL49653 and 17β-estradiol versus cells treated with BRL49653 alone.

no longer noticeable in the presence of 17β-estradiol (Fig. 5A-C). Collectively, our results argue that the rapid inhibition of the PI3K/AKT pathway induced by BRL49653 does not directly involve PTEN, which may only contribute to long-term repression.

Growth inhibitory effects of BRL49653 in MCF7 cells. Having shown a functional interaction between ERα and PPARγ and their ability to modulate the PI3K transduction pathway, we evaluated the effects on cell proliferation as a biological counterpart. BRL49653 treatments elicited a time- and dose-dependent growth inhibition in MCF7 cells and, to a higher extent, in HeLa cells (Fig. 6A). The PPARγ antagonist GW9662 reversed the growth inhibitory effects induced by BRL49653, indicating that the repressive action was directly PPARγ-mediated (Fig. 6B). Considering the ability of PPARγ to down-regulate the PI3K/AKT pathway, we did a growth assay using as a model system MCF7 cells transfected with a constitutively active myr-AKT. Notably, under these conditions, the growth inhibition observed on BRL49653 was no longer noticeable (Fig. 6B), suggesting the involvement of the PI3K/AKT pathway in the biological effects triggered by PPARγ activation. Next, the antiproliferative activity exerted by ICI182780 in MCF7 cells was potentiated in the presence of BRL49653 irrespective of 17β-estradiol treatment (Fig. 6B).

Discussion

The present study shows for the first time, to our knowledge, that ERα binds to PPRE sequences and forms a ternary complex with PPARγ and the p85 regulatory subunit of PI3K. As a biological counterpart, the crosstalk between ERα and PPARγ signaling pathways modulates the growth response to cognate ligands in hormone-dependent breast cancer cells.

A large body of evidence has been accumulated about the mechanisms by which nuclear receptors interact at different levels of the transduction cascades, including (*a*) utilization of common response elements such as androgen receptors, glucocorticoid receptors, progesterone receptors, and mineralocorticoid receptors (39); (*b*) heterodimerization of RXR with other receptors (40); and (*c*) receptor associations with several transcription factors and/or other components of the signaling systems located at the level of the cell membrane (41–44).

For PPARs, the heterodimers formed with RXR are able to bind to diverse hormone responsive elements such as ERE (26, 28, 45–47), which can occur independently of the ERs (47). However, natural ERE-containing promoters including those for PS2, the very-low-density apolipoprotein II, and the vitellogenin A2 genes exhibited considerable differences in the binding to PPAR/RXR heterodimers because the ERE flanking sequences influence the binding affinity (26). On the other hand, functional analysis of the vitellogenin A2 promoter showed that the PPAR/RXR complex binds to ERE but cannot transactivate due to a nonpermissive promoter structure (26). Hence, cross-talk between the PPAR/RXR complex and ERE-mediated signals requires further studies to be completely understood.

In the current study, we have provided new evidence on the molecular mechanisms by which ERα negatively interferes with PPRE-mediated transcriptional activity. Of note, in MCF7 cells the ER antagonists ICI182780 and hydroxytamoxifen were both able to stimulate PPRE transcription, which was potentiated by the cognate ligand BRL49653 and reversed by the PPARγ-antagonist GW9662. To better define the inhibitory

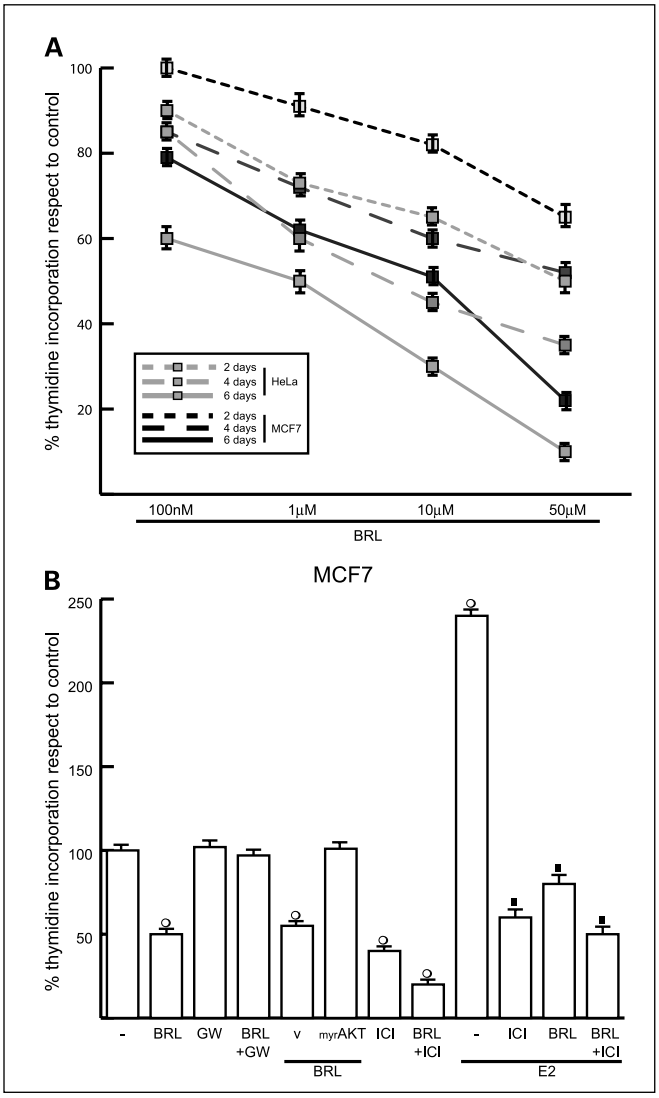

Fig. 6. Antiproliferative effects exerted by BRL49653 in MCF7 and HeLa cells. *A*, MCF7 and HeLa cells were cultured in the presence of increasing concentrations of BRL49653. Six hours before lysis, [^{3}H]thymidine was added and cells were counted. *Columns,* mean of three independent experiments; *bars,* SD. *B*, MCF7 cells were treated with 10 μmol/L BRL49653, 10 μmol/L GW9662, 1 μmol/L ICI182780, and 100 nmol/L 17β-estradiol as indicated, or transfected with an empty vector (*v*) or with 0.5 μg of myr-AKT where applicable (see Materials and Methods for other details). On day 6, 6 hours before lysis, [^{3}H]thymidine was added and cells were counted. Columns, mean of three independent experiments done in triplicate; bars, SD. ○, $P < 0.05$, treated versus untreated cells; ○, $P < 0.05$, BRL49653-treated cells transfected with an empty vector versus cells transfected with a constitutive active myr-AKT; ■, $P < 0.05$, cells treated with 17β-estradiol + ICI182780, 17β-estradiol + BRL49653, or 17β-estradiol + BRL49653 + ICI182780 versus cells treated with 17β-estradiol alone.

action of ERα on the PPARγ transduction pathway, we did EMSA experiments using a [γ-^{32}P]-labeled consensus sequence of PPRE. Nuclear extracts of MCF7 and HeLa cells transfected with an ERα expression vector showed a single band that, in the presence of an anti-ERα antibody, supershifted and reduced the signal intensity. These intriguing observations prompted us to evaluate the binding of PPARγ and ERα translated proteins to the [γ-^{32}P]-labeled PPRE sequence. The band generated by ERα was similar in size to that of PPARγ and, using two distinct ERα antibodies, seemed immunodepleted and supershifted. Taken together, our data show that ERα binds to the PPRE sequence mimicking the ability of the PPAR/RXR complex to interact with ERE (26, 29). Hence, ERα and PPARγ share the ability to bind to the AGGTCA half-sites contained as a palindrome and as a direct repeat in the ERE and PPRE sequences, respectively (26). Consequently, both receptors can potentially influence ERE- and PPRE-mediated responses, likely depending on the cell and promoter context. In this respect, our findings documented a functional interaction between ERα and PPRE contained in an endogenous *PTEN* promoter sequence. Besides, the crosstalk of ERα and PPARγ involves their physical association at the protein level, which is even extended to p85, as we have shown. Such phenomenon may provide an explanation for the opposite functional interplay on PI3K/AKT signaling exerted by ERα and PPARγ transduction pathways. Previous studies have reported the ability of PPARγ to up-regulate the expression of the *PTEN* tumor suppressor gene, which in turn antagonizes the PI3K/AKT cascade (48, 49). Of note, the binding of PPARγ to a pair of PPRE sequences located upstream to the transcription starting site of *PTEN* is responsible for the modulation of its expression (37). Our data confirmed that PPARγ mediates the up-regulation of PTEN because it was enhanced by a 24-hour exposure to BRL49653. Interestingly, this effect was no longer noticeable in the presence of 17β-estradiol, demonstrating the opposite action of ERα in respect to PPARγ on the PI3K pathway. On the basis of our findings, the rapid inhibition of PI3K/AKT signaling with BRL49653 is not mediated by PTEN; however, it may act to prolong the PI3K/AKT repression.

The possible cellular localization of the complex formed by ERα with PPARγ and p85 remains an interesting open question. In resting cells, inactive PI3K and AKT are located in the cytoplasm and activator signals recruit p85 to cell membrane through phosphatidylinositide phosphorylation (50). This process induces the activation of AKT, which in turn moves to the nucleus and other subcellular compartments. As for ERα, its localization mainly at the nuclear level has been clearly established; however, numerous studies have shown the involvement of membrane-associated ER in several cellular responses (ref. 22 and references therein). Our findings provide further evidence on the intriguing interplay between the rapid effects triggered at the membrane level and genomic events requiring different mechanisms which control cell survival and proliferation.

Indeed, the opposite functional role elicited by ERα and PPARγ was recapitulated in the biological responses provided by the growth assay. BRL49653 repressed the PI3K/AKT pathway and induced antiproliferative effects in MCF7 cells. The constitutively active myr-AKT reversed the inhibitory action of BRL49653, indicating that the PI3K/AKT pathway is involved in the negative growth regulation mediated by PPARγ. The ER antagonist ICI182780 potentiated the antiproliferative activity exerted by BRL49653 in MCF7 cells, suggesting that the combination of such compounds could be considered as an adjuvant pharmacologic tool in ERα-positive breast tumors.

Acknowledgments

Our special thanks to R.M. Evans for the gifts of tk-PPREx3-luc and pCMX-mPPARg, and to T. Simoncini for the gift of myr-AKT. We also thank D. Sturino and P. Cicirelli (Faculty of Pharmacy, University of Calabria, Italy) for the English review and the graphical support of the manuscript, respectively.

References

1. Mangelsdorf DJ, Thummel C, Beato M, et al. The nuclear receptor superfamily: the second decade. Cell 1995;83:835–9.
2. Kliewer SA, Forman BM, Blumberg B, et al. Differential expression and activation of a family of murine peroxisome proliferator-activated receptors. Proc Natl Acad Sci U S A 1994;91:7355–9.
3. Mukherjee R, Jow L, Noonan D, McDonnell DP. Human and rat peroxisome proliferator activated receptors (PPARs) show similar tissue distribution but different responsiveness to PPAR activators. J Steroid Biochem Mol Biol 1994;51:157–66.
4. Braissant O, Foufelle F, Scotto C, Dauca M, Wahli W. Differential expression of peroxisome proliferator activated receptor (PPARs): tissue distribution of PPAR-α, -β, and -γ in the adult rat. Endocrinology 1996;137: 354–66.
5. Tontonoz P, Hu E, Graves RA, Budavari AI, Spiegelman BM. mPPARγ 2: tissue-specific regulator of an adipocyte enhancer. Genes Dev 1994;8:1224–34.
6. Tontonoz P, Hu E, Spiegelman BM. Stimulation of adipogenesis in fibroblasts by PPARγ 2, a lipid-activated transcription factor. Cell 1994;79:1147–56.
7. Lowell BB. PPARγ: An essential regulator of adipogenesis and modulator of fat cell function. Cell 1999; 99:239–42.
8. Kubota T, Koshizuka K, Williamson EA, et al. Ligand for peroxisome proliferator-activated receptor γ (troglitazone) has potent antitumor effect against human prostate cancer both *in vitro* and *in vivo*. Cancer Res 1998;58:3344–52.
9. Sarraf P, Mueller E, Jones D, et al. Differentation and reversal of malignant changes in colon cancer through PPARγ. Nat Med 1998;4:1046–52.
10. Takahashi N, Okumura T, Motomura W, Fujimoto Y, Kawabata I, Kohgo Y. Activation of PPARγ inhibits cell growth and induces apoptosis in human gastric cancer cells. FEBS Lett 1999;455:135–9.
11. Chang TH, Szabo E. Induction of differentiation and apoptosis by ligands of peroxisome proliferator-activated receptor γ in non-small cell lung cancer. Cancer Res 2000;60:1129–38.
12. Motomura W, Okumura T, Takahashi N, Obara T, Kohgo Y. Activation of peroxisome proliferator-activated receptor γ by troglitazone inhibits cell growth through the increase of $p27^{KiP1}$ in human pancreatic carcinoma cells. Cancer Res 2000;60: 5558–64.
13. Sato H, Ishihara S, Kawashima K, et al. Expression of peroxisome proliferator-activated receptor (PPAR) γ in gastric cancer and inhibitory effects of PPARγ agonists. Br J Cancer 2000;83:1394–400.
14. Tontonoz P, Singer S, Forman BM, et al. Terminal differentiation of human liposarcoma cells induced by ligands for peroxisome proliferator-activated receptor γ and the retinoid X receptor. Proc Natl Acad Sci U S A 1997;94:237–41.
15. Elstner E, Muller C, Koshizuka K, et al. Ligands for peroxisome proliferator-activated receptor γ and retinoic acid receptor inhibit growth and induce apoptosis of human breast cancer cells *in vitro* and in BNX mice. Proc Natl Acad Sci U S A 1998;95:8806–11.
16. Mueller E, Sarraf P, Tontonoz P, et al. Terminal differentiation of human breast cancer through PPAR γ. Mol Cell 1998;1:465–70.
17. Aronica SM, Kraus WL, Katzenellenbogen BS. Estrogen action via the cAMP signaling pathway:stimulation of adenylate cyclase and cAMP-regulated gene trascription. Proc Natl Acad Sci U S A 1994; 91:8517–21.
18. Migliaccio A, Di Domenico M, Castoria G, et al. Tyrosine kinase/p21ras/MAP-kinase pathway activation by estradiol-receptor complex in MCF-7 cells. EMBO J 1996;15:1292–300.
19. Eisen A, Weber BL. Recent advances in breast cancer biology. Curr Opin Oncol 1998;10:486–91.
20. Nicholson RI, McClelland RA, Robertson JF, Gee JM. Involvement of steroid hormone and growth factor cross-talk in endocrine response in breast cancer. Endocr Relat Cancer 1999;6:373–87.
21. Jensen EV. Steroid hormones, receptors and antagonists. Ann N Y Acad Sci 1995;761:1–4.
22. Simoncini T, Hafezi-Moghadam A, Brazil DP, Ley K, Chin WW, Liao JK. Interaction of oestrogen receptor with the regulatory subunit of phosphatidylinositol-3-OH kinase. Nature 2000;407:38–541.
23. Datta SR, Brunet A, Greenberg ME. Cellular survival: a play in three Akts. Genes Dev 1999;13: 2905–27.
24. Glass CK, Holloway JM, Devary OV, Rosenfeld MG. The thyroid hormone receptor binds with opposite transcriptional effects to a common sequence motif in thyroid hormone and estrogen response elements. Cell 1988;54:313–23.
25. Segars JH, Marks MS, Hirschfeld S, et al. Inibitionof estrogen-responsive gene activation by the retinoid x receptor β: evidence for multiple inhibitory pathways. Mol Cell Biol 1993;13:2258–68.
26. Keller H, Givel F, Perroud M, Wahli W. Signaling cross-talk between peroxisome proliferator-activated receptor/retinoid X receptor and estrogen receptor through estrogen response element. Mol Endocrinol 1995;2:1265–75.
27. Chawla A, Lazar MA. Peroxisome proliferators and retinoid signaling pathways co-regulate preadipocyte phenotype and survival. Proc Natl Acad Sci U S A 1994;91:1786–90.
28. Kliewer SA, Umesono K, Noonan DJ, Heyman RA, Evans RM. Convergence of 9-*cis* retinoic acid and peroxisome proliferator signaling pathways through heterodimer formation of their receptors. Nature 1992; 358:771–4.
29. Wang X, Kilgore MW. Signal crosstalk between estrogen receptor α and β and the peroxisome proliferator-activated receptor γ1 in MDA-MB-231 and MCF7 breast cancer cells. Mol Cell Endocrinol 2002; 194:123–33.
30. Tora L, Mullick A, Metzger D, Ponglikitmongkol M, Park I, Chambon P. The cloned human estrogen receptor contains a mutation which alters its hormone binding properties. EMBO J 1989;8:1981–6.
31. Lubahn DB, Joseph DR, Sar M, et al. The human androgen receptor: complementary deoxyribonucleic acid cloning, sequence analysis and gene expression in prostate. Mol Endocrinol 1988; 2:1265–75.
32. Andrews NC, Faller DV. A rapid micropreparation technique for extraction of DNA-binding proteins from limiting numbers of mammalian cells. Nucleic Acids Res 1991;19:2499.
33. Shang Y, Hu X, DiRenzo J, Lazar MA, Brown H. Cofactor dynamics and sufficiency in estrogen receptor-regulated transcription. Cell 2000;103: 843–52.
34. Reid G, Hubner MR, Metiver R, et al. Cyclic, proteasome-mediated turnover of unliganded and liganded ERα on responsive promoters is an integral feature of estrogen signaling. Mol Cell 2003;11: 695–707.
35. Maggiolini M, Donzé O, Picard D. A non-radioactive method for inexpensive quantitative RT-PCR. Biol Chem 1999;380:695–7.
36. Patel L, Pass I, Coxon P, Downes CP, Smith SA, Macphee CH. Tumor suppressor and anti-inflammatory actions of PPARγ agonist are mediated via up-regulation of PTEN. Curr Biol 2001;11:764–8.
37. Sun M, Paciga JE, Feldman RI, et al. Phosphatidylinositol 3-OH Kinase (PI3K)/AKT2, activated in breast cancer, regulates and is induced by estrogen receptor α.(ERα) via interaction between ERα and PI3K. Cancer Res 2001;61:5985–91.
38. Cantley LC, Neel BG. New insights into tumor suppression: PTEN suppresses tumor formation by restraining the phosphoinositide 3-kinase/AKT pathway. Proc Natl Acad Sci U S A 1999;96: 4240–5.
39. Parker MG. Steroid and related receptors. Curr Opin Cell Biol 1993;5:499–504.
40. Stunnenberg HG. Mechanisms of transactivation by retinoic acid receptors. Bioessays 1993;15:309–15.
41. Miner JN, Yamamoto KR. Regulatory crosstalk at composite response elements. Trends Biochem Sci 1991;16:423–6.
42. Schüle R, Evans RM. Cross-coupling of signal transduction pathways-Zinc finger meets leucine zipper. Trends Genet 1991;7:377–81.
43. Schüle R, Muller M, Kaltschmidt C, Renkawitz R. Many transcription factors interact synergistically with steroid receptors. Science 1988;242:1418–20.
44. Martinez E, Dusserre Y, Wahli W, Mermod N. Synergistic transcriptional activation by CTF/NF-1 and the estrogen receptor involves stabilized interactions with a limiting target factor. Mol Cell Biol 1991;11: 2937–45.
45. Issemann I, Prince RA, Tugwood JD, Green S. The retinoid X receptor enhances the function of the peroxisome proliferator-activated receptor. Biochimie 1993; 75:251–6.
46. Nunez SB, Medin JA, Keller H, et al. Retinoid X receptor β and peroxisome proliferator-activated receptor activate an estrogen response element. Recent Prog Horm Res 1995;50:409–16.
47. Nunez SB, Medin JA, Braissant O, et al. Retinoid X receptor and peroxisome proliferator-activated receptor activate an estrogen responsive gene independent of the estrogen receptor. Mol Cell Endocrinol 1995; 127:27–40.
48. Di Cristofano A, Pandolfi PP. The multiple roles of PTEN in tumor suppression. Cell 2000;100:387–90.
49. Yamada KM, Araki M. Tumor suppressor PTEN: modulator of cell signaling, growth, migration and apoptosis. J Cell Sci 2001;114:2375–82.
50. Coffer PJ, Woodgett JR. Protein kinase B (c-Akt): a multifunctional mediator of phosphatidylinositol 3-kinase activation. Biochem J 1998;335:1–13.

0021-972X/05/$15.00/0
Printed in U.S.A.

The Journal of Clinical Endocrinology & Metabolism 90(8):4753–4761

doi: 10.1210/jc.2004-2233

Leptin Secretion by Human Ejaculated Spermatozoa

Saveria Aquila, Mariaelena Gentile, Emilia Middea, Stefania Catalano, Catia Morelli, Vincenzo Pezzi, and Sebastiano Andò

Department of Pharmaco-Biology (S.Aq., E.M., S.C., C.M., V.P., S.An.), Faculty of Pharmacy; Department of Cell Biology (M.G.); and Centro Sanitario (S.Aq., M.G., E.M., S.C., C.M., V.P., S.An.), University of Calabria, 87030 Arcavacata di Rende (Cosenza), Italy

Introduction: Leptin action is a dynamic area of investigation that continues to broaden beyond the basic lipostatic model originally envisaged. Here, we show that leptin is expressed in and secreted from human ejaculated spermatozoa.

Methods: By RT-PCR, Western blot, and immunofluorescence techniques, we have demonstrated that human sperm express leptin. RIA method evidenced leptin secretion. Phosphatidyl-inositol-kinase-3 (PI3K)/Akt pathway was examined by PI3K activity assay and Western blot. Leptin and insulin regulation of glycogen synthesis was evaluated by glycogen synthase activity (GSA).

Results: The large differences of leptin secretion between uncapacitated and capacitated sperm suggest a functional role for leptin in capacitation. Indeed, in uncapacitated sperm, leptin enhances both cholesterol efflux and protein tyrosine phosphorylation. In uncapacitated sperm, both insulin and leptin increased PI3K activity, Akt S473, and glycogen synthase kinase-3 S9 phosphorylation. Interestingly, during capacitation, concomitantly to the massive release of both hormones, we observed a strong reduction in the phosphorylation of glycogen synthase kinase-3 S9, kinase downstream of Akt that regulates the glycogen synthase. Our results from GSA showed that the enzymatic activity was significantly higher in uncapacitated than in capacitated sperm. Particularly, in uncapacitated sperm, GSA appeared to depend on the hormones concentration, because the enzymatic activity was stimulated at low doses, whereas it was inhibited at high doses. Moreover, both leptin and insulin regulate in autocrine fashion sperm glycogen synthesis.

Conclusion: Leptin secretion by sperm suggests that the male gamete may be able to modulate its metabolism independently by systemic leptin. These data open new considerations about leptin significance in male fertility. **(*J Clin Endocrinol Metab* 90: 4753–4761, 2005)**

RECENT OBSERVATIONS SUGGEST that leptin plays an important role in relaying energetic status to reproduction; to date, the molecular mechanisms underlying the effects of leptin in this context remain elusive (1). Various evidence has pointed to a direct role of leptin in the control of testicular function (2). However, in contrast to its well-proven effects in female fertility, the actual role of the hormone in the regulatory network controlling male reproductive function has been a matter of debate.

The ob/ob mice (lacking of functional leptin) or OB-R/OB-R mice (lacking of functional leptin receptor) are infertile and fail to undergo normal sexual maturation. Importantly, fertility of ob/ob mice is restored by leptin and not by simply reducing body weight, indicating an effect of the hormone *per se* on reproductive function (3, 4). Particularly, male mice (*ob/ob*) had small testes, azoospermia, and multinucleated spermatids. As in the female, hypogonadotropic hypogonadism and infertility are common features in male *ob/ob* mice (5). In line with results from experimental studies, in humans the absence of endogenous leptin is associated with hypogonadism and absence of pubertal development (6–8).

Leptin is expressed in the seminiferous tubules and in seminal plasma (9), but its cellular origin in these contexts is not exactly defined. Several studies support the role of serum leptin in the regulation of gonadal functions in men (10) indirectly via the central neuroendocrine system and directly via peripheral tissue membrane receptors (11, 12). Besides, compelling evidence indicates that leptin functional regulation of the male gonadal axis appears to be a tightly regulated action, carried out at different levels of the hypothalamic-pituitary-testicular system, involving not only stimulatory, but also inhibitory, effects. Recently (13), it was hypothesized that the net effect of leptin upon male reproductive function may depend on the circulating level of the molecule. Thus, predominant stimulatory effects, primarily at the hypothalamus, are observed at physiological leptin levels above a minimal threshold. In contrast, direct inhibitory actions at the testicular level may take place in the presence of a significantly elevated leptin concentration, as detected in obesity (2).

Leptin in various cell types has a range of roles, but the principal role is as a lipostat, signaling to other systems the energy reserves available to the body, mediating fuel use, and consequently energy expenditure. Recently, a new target for leptin in the male genital tract was evidenced because leptin receptor was found to be present in human spermatozoa (9). It has long been recognized that capacitated sperm display an increased metabolic rate and overall energy expenditure, presumably to affect the changes in sperm signaling and function during capacitation (14). However, the relationship between the signaling events associated with capacitation and the changes in sperm energy metabolism is

First Published Online June 8, 2005

Abbreviations: CHOD, Cholesterol-oxidase; GSA, glycogen synthase activity; GSK, glycogen synthase kinase; M-MLV, Moloney murine leukemia virus; PI3K, phosphatidyl-inositol-kinase-3; POD, peroxidase; UDP, uridine diphosphate.

JCEM is published monthly by The Endocrine Society (http://www.endo-society.org), the foremost professional society serving the endocrine community.

poorly understood. Overall, there is a lack of information regarding how mammalian spermatozoa manage their energy status. In somatic cells, both leptin and insulin play a central role in regulation of energy homeostasis (15). Particularly, i*n vitro* and *in vivo* evidence supports the hypothesis that leptin may mimic insulin action on glycogen synthesis (16). Sperm glycogen metabolism seems to be regulated by modulation of glycogen synthase in a manner similar to that observed in other tissues (17).

In the present study, we showed that leptin is expressed in, and secreted from, human ejaculated spermatozoa, providing evidence for a role of the hormone in sperm physiology.

Subjects and Methods

Chemicals

PMN cell isolation medium was from BIOSPA (Milan, Italy). Total RNA Isolation System kit, enzymes, buffers, and nucleotides 100-bp ladder used for RT-PCR were purchased from Promega Corp. (Milan, Italy). Moloney murine leukemia virus (M-MLV) was from Life Technologies Italia (Milan, Italy). Oligonucleotide primers were made by Invitrogen (Milan, Italy). DMEM-F12 medium, BSA protein standard, Laemmli sample buffer, prestained molecular weight markers, Percoll (colloidal polyvinylpyrrolidone-coated silica for cell separation), sodium bicarbonate, sodium lactate, sodium pyruvate, dimethylsulfoxide, Earle's balanced salt solution, and all other chemicals were purchased from Sigma Chemical (Milan, Italy). Acryl amide bisacrylamide was from Labtek Eurobio (Milan, Italy). Triton X-100, Eosin Y was from Farmitalia Carlo Erba (Milan, Italy). ECL Plus Western blotting detection system, Hybond ECL, [γ-^{32}P]ATP, and HEPES sodium salt were purchased from Amersham Pharmacia Biotech (Buckinghamshire, UK). Human leptin RIA kit was from Linco Research, Inc. (St. Charles, MO-Biogemini Sas, Catania, Italy). Cholesterol-oxidase (CHOD)-peroxidase (POD) enzymatic colorimetric kit was from Inter-Medical (Biogemini Sas, Catania, Italy). Monoclonal mouse p85-regulatory subunit of phosphatidyl-inositol-kinase-3 (PI3K) antibody, goat polyclonal actin antibody, polyclonal rabbit antileptin (A-20) antibody, rabbit antiinsulin antibody, rabbit antiphosphotyrosine antibody (PY99), rabbit anti-p-Akt1/Akt2/Akt3 S473 antibody, POD-coupled antirabbit and antigoat, antirabbit IgG fluorescein isothiocyanate-conjugated were from Santa Cruz Biotechnology (Heidelberg, Germany). Rabbit anti-p-glycogen synthase kinase 3 (-GSK-3) S9 antibody was from Cell Signaling (Milan, Italy). Nylon membranes were provided by Roche Diagnostics Corp. (Indianapolis, IN). Uridine diphosphate (UDP) [U-^{14}C]glucose (25 μCi/ml) was from Amersham.

Semen samples and spermatozoa preparations

Ejaculates were collected from healthy volunteers undergoing semen analysis, by masturbation (18), after 3 d of sexual abstinence. The study was approved by the local medical-ethical committees, and all participants gave their informed consent. Sperm samples with normal parameters of semen as volume, sperm count, motility, vitality, and morphology, according to the World Health Organization Laboratory Manual (18), were included in this study. In each experiment, three normal samples were pooled. Spermatozoa preparations were performed as previously described (19).

Evaluation of sperm viability

Viability was assessed using Eosin Y to evaluate potential toxic effects of different treatments. A blinded observer scored 100 cells for stain uptake (dead cells) or exclusion (live cells). Viability was evaluated before and after pooling the samples. There were no adverse effects among the different treatments on human sperm viability (data not shown).

RNA isolation, RT-PCR, and Southern blotting

Total RNA was isolated from human ejaculated spermatozoa purified as previously described (19). PCR amplification of cDNA was performed with 2 U *Taq* DNA polymerase, 50 pmol primer pair (forward, 5′-CAT TGG GGA ACC CTG TGC GGA TTC-3′; reverse, 5′-TGG CAG CTC TTA GAG AAG GCC AGC-3′) in 10 mM Tris-HCl (pH 9.0) containing 0.1% Triton X-100, 50 mM KCl, 1.5 mM $MgCl_2$, and 0.25 mM of each deoxynucleotide triphosphate. The conditions for PCR were: denaturation at 95 C for 1 min, annealing at 55 C for 1 min, and extension at 72 C for 2 min (40 cycles). A DNA marker (100-bp DNA ladder) was used to determine the size of amplified product, that is 348 bp. To check out the presence of DNA contamination, a RT-PCR was performed without M-MLV reverse transcriptase (negative control). The identity of the PCR-amplified cDNA fragment of leptin transcript from human spermatozoa was verified using Southern hybridization. A total of 1–2 ng cDNA probe (5′-CACGCAGTCAGTGTCCTCCA-3′, which corresponds to nucleotide cDNA sequence for human leptin) was labeled with [γ-^{32}P]ATP using polynucleotide kinase. Hybridization was performed overnight at room temperature. Then, membranes were washed with decreasing salt concentrations containing 0.1% sodium dodecyl sulfate, and then exposed to autoradiography with intensifying screens.

Western blot analysis of sperm proteins

Sperm samples, washed twice with Earle's balanced salt solution (uncapacitating medium), were incubated without or with the indicated treatments and then centrifuged for 5 min at 5000 $\times$ *g*. The pellet was resuspended in lysis buffer as previously described (19). Equal amounts of proteins (60 μg) were boiled for 5 min, separated by 10% PAGE, transferred to nitrocellulose sheets, and probed with an appropriate dilution of the indicated antibody. The bound of the secondary antibody was revealed with the ECL Plus Western blotting detection system according to the manufacturer's instructions. The negative control was performed using a sperm lysate that was immunodepleted of leptin (*i.e.* preincubate lysate with antileptin antibody for 1 h at room temperature and immunoprecipitate with protein A/G-agarose).

As internal control, all membranes were subsequently stripped (glycine, 0.2 M, pH 2.6, for 30 min at room temperature) of the first antibody and reprobed with antiactin antibody.

Immunofluorescence assay

Sperm cells, recovered from Percoll gradient, were rinsed three times with 0.5 mM Tris-HCl buffer (pH 7.5) and fixed with absolute methanol for 7 min at −20 C. Leptin staining was carried out, after blocking with normal horse serum (10%), using a rabbit polyclonal antihuman leptin as primary antibody and an antirabbit IgG fluorescein isothiocyanate conjugated (1:100) as secondary antibody. Sperm cells incubated without the primary antibodies were used as the negative controls. The slides were examined under a fluorescence microscope (Olympus BX41; Olympus Corp., Milan Italy), and a minimum of 200 spermatozoa per slide were scored.

Measurement of leptin secreted by human ejaculated spermatozoa

A competitive RIA was applied to measure leptin in sperm culture media. Increasing numbers of spermatozoa were washed twice with unsupplemented Earle's medium (uncapacitating medium) and were incubated in the same medium for 1 h at 37 C and 5% CO_2. Besides, some samples were incubated in Earle's balanced salt solution medium supplemented with 600 mg BSA/100 ml and 200 mg sodium bicarbonate/100 ml (capacitating medium). At the end of the sperm incubation, the culture media were recovered by centrifugation, lyophilized, and subsequently dissolved in 120 μl kit buffer. Human leptin concentrations were determined in duplicate by a human leptin RIA Kit according to manufacturer's instructions. Leptin standards ranged between 0.2–100 ng/ml. The limit of sensitivity for the assay was 0.05 ng/ml. Inter- and intraassay variations were 5.4% and 5.1%, respectively. Leptin results are presented as the original concentrations of the supernatants and are given as nanograms per milliliter.

Measurement of cholesterol in the sperm culture media

Cholesterol was measured in duplicate by a CHOD-POD enzymatic colorimetric method according to manufacturer's instructions in the incubation medium of human spermatozoa. Sperm samples, washed twice with uncapacitating medium, were incubated in the same medium or in capacitating medium for 1 h at 37 C and 5% CO_2. Other samples were incubated without (control) or in the presence of increasing leptin concentrations (10, 50, and 100 ng/ml). At the end of the sperm incubation, the culture media were recovered by centrifugation, lyophilized, and subsequently dissolved in 1 ml buffer reaction. The samples were incubated for 10 min at room temperature; then the cholesterol content was measured with the spectrophotometer at 505 nm. The cholesterol standard used was 200 mg/dl. The limit of sensitivity for the assay was 0.05 mg/dl. Inter- and intraassay variations were 0.71% and 0.57%, respectively. Cholesterol results are presented as the original concentrations and are given per 10×10^6 number of spermatozoa.

PI3K assay

Spermatozoa were washed twice in uncapacitating medium and centrifuged at $800 \times g$ for 20 min. Sperm samples were then incubated for 1 h at 37 C and 5% CO_2 without or with the indicated treatments, and the PI3K assay was performed as previously described (20). A p85 regulatory subunit of PI3K was precipitated from 500 μg sperm lysates. The negative control was performed using a sperm lysate, where p110 catalyzing subunit of PI3K was previously removed by preincubation with the respective antibody (1 h at room temperature) and subsequently immunoprecipitated with protein A/G-agarose.

Glycogen synthase activity (GSA)

The GSA was determined by the principle: glycogen + UDP[U-^{14}C]glucose→glycogen(^{14}C) + UDP.

Washed spermatozoa were incubated for 1 h at 37 C under uncapacitating or capacitating conditions as described above. Both uncapacitated and capacitating sperm were treated with leptin (10 and 50 ng/ml), insulin (3.3 or 10 nM), antileptin (or normal) rabbit serum (1:100) alone or combined with 10 ng/ml leptin, antiinsulin (or normal) rabbit serum (1:100) alone or combined with 3.3 nM insulin, wortmannin (10 μM) alone or combined with 10 ng/ml leptin or 3.3 nM insulin, monensin (25 μM), antileptin (1:100) plus antiinsulin (1:100) antibodies, LiCl (2 mM). After treatment, sperm extracts were performed in KCl (100 mM); EDTA (2 mM); HEPES (20 mM), pH 7.1; phenylmethylsulfonyl fluoride (1 mM). Aliquots of 100 μl were then assayed immediately in a reaction mixture containing glycogen (20 mg/ml), EDTA (5 mM), NaF (50 mM),

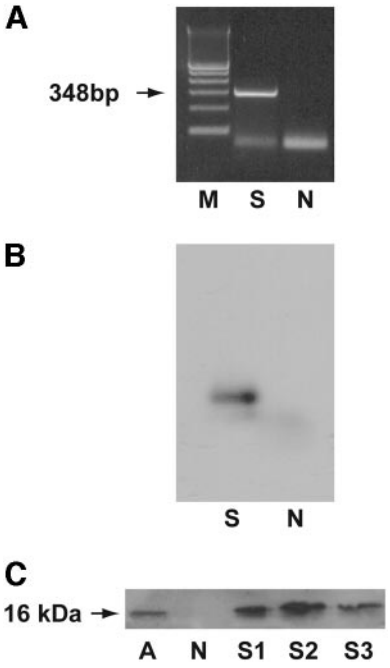

FIG. 1. Leptin expression in human ejaculated spermatozoa. A, RT-PCR analysis of human leptin gene in percolled human ejaculated spermatozoa (S), negative control (no M-MLV reverse transcriptase added) (N), and marker (lane M). *Arrow*, Expected size of the PCR product. B, Southern blot analysis of human leptin gene in percolled human ejaculated spermatozoa (S) and negative control (N). C, Western blot of leptin protein: extracts of pooled purified ejaculated spermatozoa were subjected to electrophoresis on 10% SDS-PAGEs, blotted onto nitrocellulose membranes, and probed with rabbit polyclonal antibody to human leptin. Expression in three samples of ejaculated spermatozoa from normal men (S1, S2, S3). Adipocytes extract was used as control (A). The negative control performed using sperm lysates, where leptin was previously removed by preincubation with the antibody to human leptin (1 h at room temperature) and immunoprecipitated with protein A/G-agarose, is represented in lane 2. The experiments were repeated at least three times for RT-PCR and at least six times for the Western blot, and the autoradiographs of the figure show the results of one representative experiment.

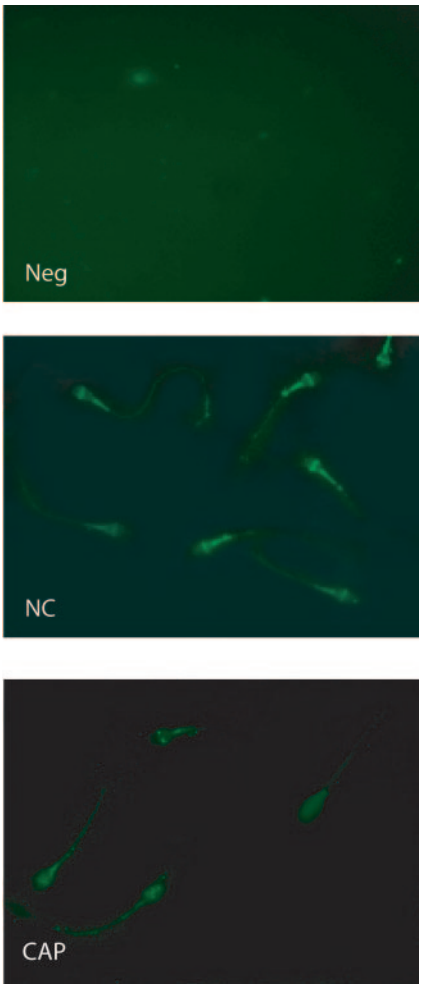

FIG. 2. Immunolocalization of leptin in human ejaculated spermatozoa. Washed spermatozoa were extensively washed and incubated in the unsupplemented Earle's medium (NC) for 1 h at 37 C and 5% CO_2, or in the presence of capacitating medium for 2 h (CAP) under the same experimental conditions. Spermatozoa were then fixed and analyzed by staining with the polyclonal antibody to human leptin. Sperm cells incubated without the primary antibody were used as negative control (Neg). The pictures shown are representative examples of experiments that were performed at least three times with repetitive results.

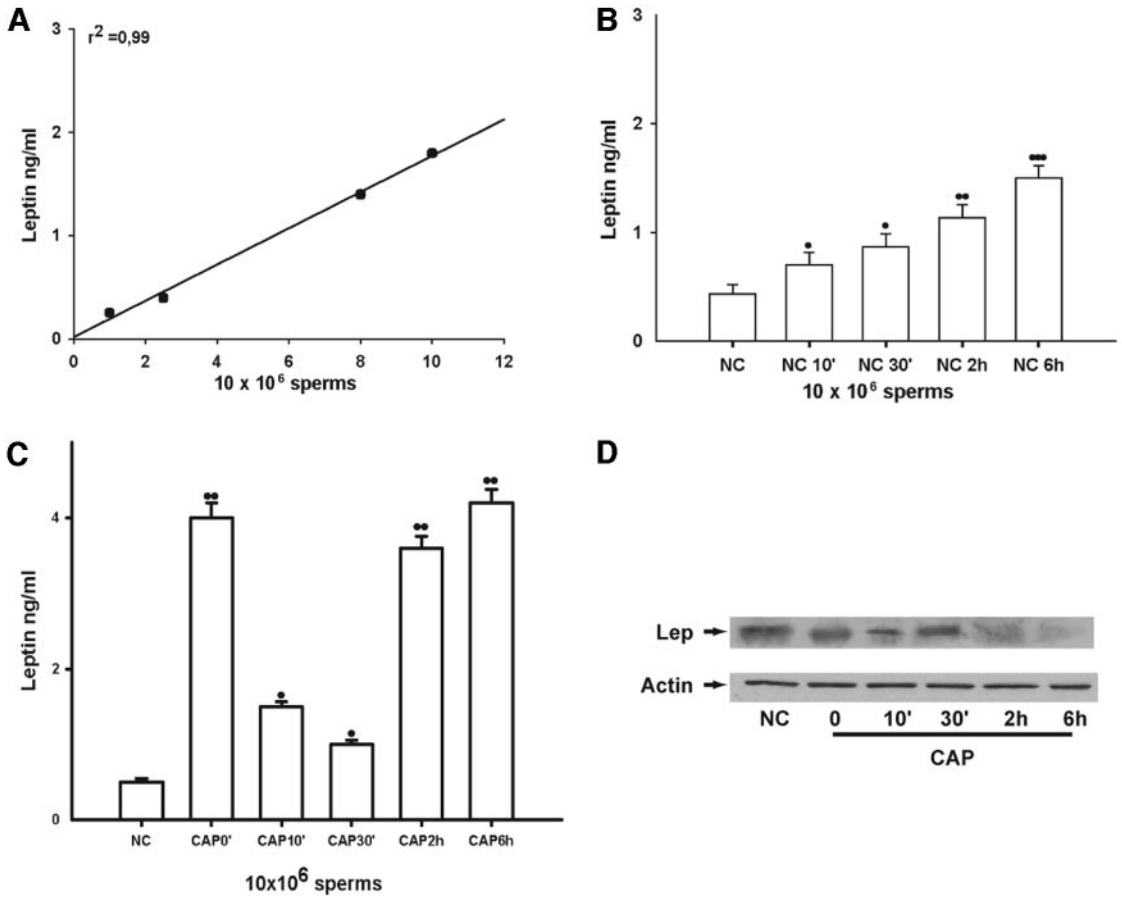

FIG. 3. Leptin secretion from human ejaculated spermatozoa. Washed human spermatozoa were incubated in unsupplemented Earle's balanced salt solution for 1 h at 37 C, 5% CO_2. Leptin secretion in culture medium from human ejaculated spermatozoa was measured by RIA. A, Increasing number of sperm were incubated in unsupplemented Earle's balanced salt solution for 1 h at 37 C, 5% CO_2. Linear regression analysis was performed, and the r was calculated ($r^2 = 0.99$). B, Time course of leptin secretion, at the indicated times, from human spermatozoa incubated in uncapacitating medium (NC). C, Time course of leptin secretion, at the indicated times, from human spermatozoa incubated in capacitating medium (CAP). D, Western blot analysis of protein lysates from sperm incubated under capacitating conditions at the indicated times. Values are means ± SEM of six determinations in a typical experiment. ●, $P < 0.05$; ●●, $P < 0.005$; ●●●, $P < 0.01$ *vs.* control.

UDP glucose (2.5 mM), Tris/HCl (25 mM), UDP [U-^{14}C]glucose (0.0005 mCi/ml), and glucose 6-phosphate (8 mM). The assay was buffered at pH 8.0. The reaction was performed at 37 C; after 15 min, 50 μl of the homogenate/assay buffer was spotted on a Whatman filter paper (1 cm × 2.5 cm). The filters were dropped into cold (4 C) 66% ethanol for 30 min to precipitate glycogen; in addition, they were washed twice at room temperature for 20 min each in 66% ethanol to remove [^{14}C]glucose 1-phosphate. After being dried, the filters were transferred to scintillation vials; 3 ml scintillation solution was added to each, and mixtures were counted for radioactivity. Data are expressed as milliunits UDP-glucose incorporated per milligram protein.

Statistical analysis

The experiments for RT-PCR were repeated on at least three independent occasions, whereas Western blot analysis was performed in at least six independent experiments. The data obtained from RIA (six replicate experiments using duplicate determinations), CHOD-POD enzymatic colorimetric method (six replicate experiments using duplicate determinations), GSA (eight replicate experiments using duplicate determinations) were presented as the mean ± SEM. The differences in mean values were calculated using a paired *t* test, with a significance level of $P < 0.05$. Regression analysis was performed using the SPSS program (SPSS, Inc., Richmond, CA).

Results

RT-PCR, Southern blot, and Western blot showed leptin expression in human sperm

To determine whether mRNA for leptin is present in human ejaculated spermatozoa, RNA, isolated from Percoll-separated samples of normal men, was subjected to reverse PCR and then to Southern blot analysis. The RT-PCR products for leptin in sperm were not a result of any DNA contamination, because the RNA samples were subjected to deoxyribonuclease treatment before RT-PCR. The primer sequences were based on the human leptin gene sequence, and the RT-PCR amplification revealed the expected PCR product size of 348 bp (Fig. 1A). To verify the identity of the amplified products, we performed Southern blot analysis (Fig. 1B). The presence of leptin protein in human ejaculated spermatozoa was investigated by Western blot using an antibody raised against the carboxyl terminus of the mature human leptin protein (Fig. 1C). One immunoreactive band was observed at the same mobility of the adipocytes extract (lane A), used as positive control.

Immunolocalization of leptin in human ejaculated sperm

Using immunofluorescence technique, we identified a positive signal for leptin in human spermatozoa (Fig. 2). Leptin immunoreactivity is specifically compartmentalized in uncapacitated sample at the equatorial segment and at the midpiece (NC), whereas capacitated sperm showed an overall decrease and a more uniform distribution in the signal intensity (CAP).

Measurement of leptin secretion by sperm

The RIA method was used to evaluate whether sperm are able to secrete leptin. After the assay was validated for sperm, we demonstrated that the increase in leptin secretion was dependent on sperm concentration (Fig. 3A). The time course of leptin secretion from spermatozoa into the uncapacitating medium is shown in Fig. 3B. Leptin secretion from 10×10^6 sperm incubated in uncapacitating medium (range, 0.2–2 ng/ml) was significantly lower than that obtained from sperm incubated in capacitating conditions (range, 0.8–4.0 ng/ml) (Fig. 3C). We have attempted to measure the amount of leptin remaining in the sperm after secretion; however, the lysis buffer somehow interferes with the kit-system, altering the binding between antigen and antibody. Then we performed the Western blot analysis of sperm lysates. The time course of capacitating sperm showed a decrease of the hormone inside the sperm (Fig. 3D), according to the increased secretion during capacitation.

Leptin affects both cholesterol efflux and protein tyrosine phosphorylation in sperm

The increased leptin secretion during capacitation suggests a possible role of the hormone in the process. Therefore, we investigated leptin effect on two different and representative aspects of capacitation: cholesterol efflux and protein tyrosine phosphorylation. The importance of the cholesterol efflux in inducing capacitation is historical known, and it has also been demonstrated that it initiates signaling events leading to tyrosine phosphorylation of sperm proteins (21, 22). Washed pooled sperm from normal samples were treated with increasing concentrations of leptin (0, 10, 50, and 100 ng/ml) and incubated under uncapacitating conditions. Then, samples were centrifuged, the upper phase was used to determinate the cholesterol levels, whereas the sperm were lysed to evaluate protein tyrosine phosphorylation. Our results showed a significant increase both in cholesterol efflux (Fig. 4A) and in protein tyrosine phosphorylation (Fig. 4B) upon leptin treatment, suggesting its involvement in the induction of capacitation. However, leptin induction of both processes was not dose-dependent; indeed, concentration as low as 10 ng/ml was able to sustain the greatest increase.

Leptin and insulin effects on PI3K/Akt pathway

The signaling events associated with capacitation and the changes in sperm energy metabolism are issues that remain to be resolved. In somatic cells, leptin and insulin play a central role in regulation of energy homeostasis. In several cell types, including muscle cells (23), adipocytes (24), and hypothalamic neurons (25), both insulin and leptin activate

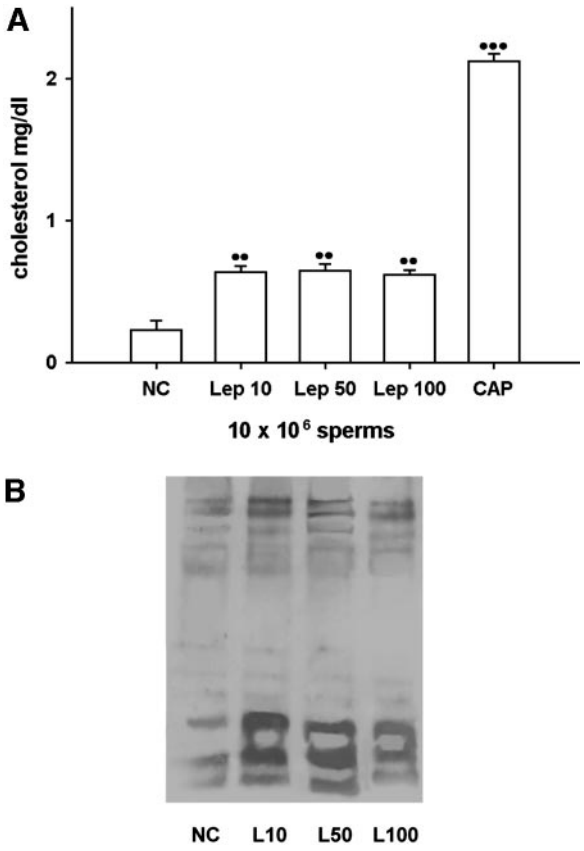

FIG. 4. Leptin affects both cholesterol efflux and protein tyrosine phosphorylation of sperm. Washed spermatozoa were incubated in the unsupplemented Earle's medium for 1 h at 37 C and 5% CO_2, in the absence (NC) or in the presence of increasing concentrations of leptin (Lep) (10, 50, and 100 ng/ml). A, Cholesterol in culture medium from human ejaculated spermatozoa was measured by enzymatic colorimetric assay. Values are means ± SEM of six determinations in a typical experiment. B, Fifty micrograms of sperm lysates were used for Western blot analysis of protein tyrosine phosphorylation. The autoradiograph presented is a representative example of experiments that were performed at least six times with repetitive results. ••, $P < 0.05$; •••, $P < 0.001$ *vs.* control.

PI3K, which may account, at least in part, for similarities in the metabolic effects of these hormones. Our results showed that, in uncapacitated sperm, both leptin and insulin stimulation increased PI3K activity (Fig. 5A) as well as the phosphorylation of Akt and GSK3, two of the major metabolic intermediates downstream of PI3K (Fig. 5B). Intriguingly, GSK3 phosphorylation was abolished in capacitating sperm, suggesting that, during capacitation, there is a block in glycogen synthesis. Concomitantly, in capacitating sperm, we observed a reduction of both hormones inside the sperm (Fig. 5C).

Leptin and insulin effects on GSA

The above reported data led us to further investigate the mechanism underlying the regulation of glycogen synthesis in sperm. Therefore, we evaluated the action of the two hormones on GSA. In somatic cells, i*n vitro* and *in vivo* evidence supports the hypothesis that leptin may mimic insulin action on glycogen synthesis (16). Our results showed that

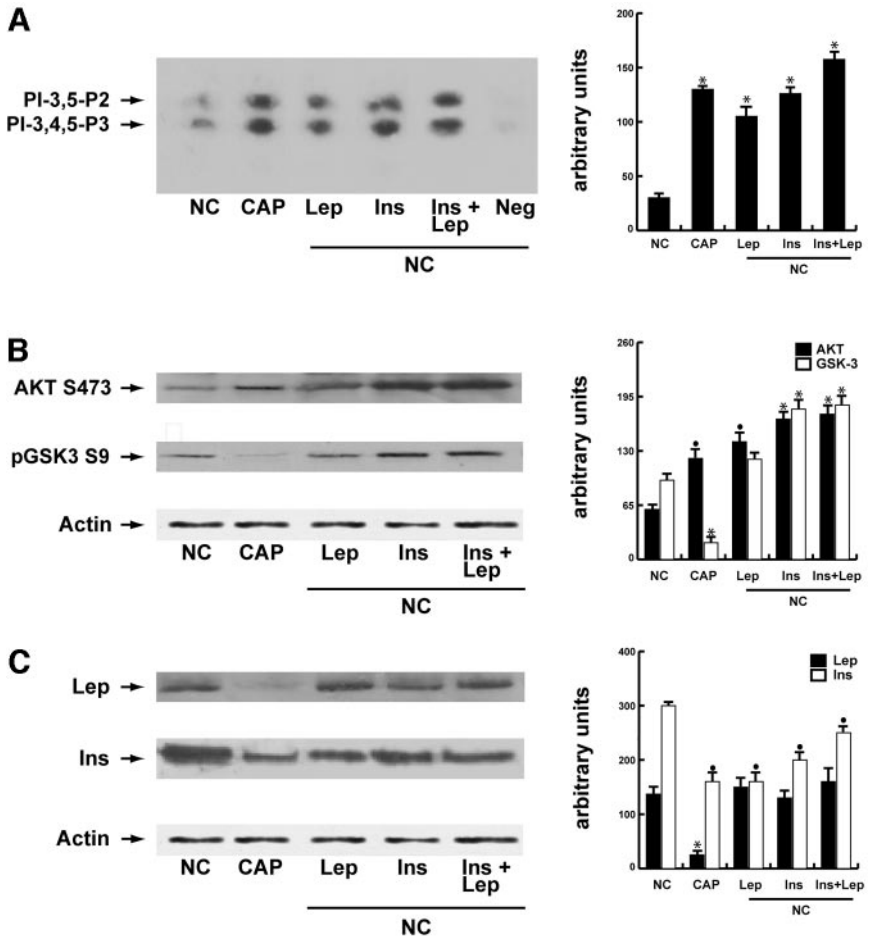

FIG. 5. Leptin and insulin action on PI3K/Akt pathway in human ejaculated spermatozoa. Washed spermatozoa were incubated in the unsupplemented Earle's medium for 1 h at 37 C and 5% CO_2, in the absence (NC) or in the presence of 10 nM leptin (Lep) or in the presence of 3.3 nM insulin (Ins) alone or combined with 10 nM leptin (Ins + Lep). Some samples were washed with the unsupplemented Earle's medium and incubated in capacitating medium for 1 h (CAP). A, A total of 500 μg sperm lysates was immunoprecipitated using anti-p85 regulatory subunit of PI3K incubated in the presence of 200 μM phosphatidylinositol and 10 μCi [γ-^{32}P]ATP for 30 min. The negative control (Neg) was performed using a sperm lysate, where p110 catalyzing subunit of PI3K was previously removed by preincubation with the respective antibody (1 h at room temperature) and subsequently immunoprecipitated with protein A/G-agarose (lane 6). PI-3,4,5-P3, phosphatidylinositol 3,4,5-triphosphate; PI-3,5-P2, phosphatidylinositol 3,5-diphosphate. B and C, A total of 50 μg sperm lysates was used for Western blot analysis of p-AKT S473 or p-GSK3 S9 (B), leptin or insulin (C). The autoradiographs presented are representative examples of experiments that were performed at least six times with repetitive results. •, $P < 0.05$; *, $P < 0.001$ *vs.* control.

GSA was significantly higher in uncapacitated than in capacitated sperm (Figs. 6 and 7). Particularly, in uncapacitated sperm, GSA appears to depend on the hormones concentration: low concentrations (leptin, 10 ng/ml; insulin, 3.3 nM) stimulated the GSA, whereas high concentrations (leptin, 50 ng/ml; insulin, 10 nM) inhibited enzymatic activity. In capacitated sperm, the GSA was unable to discriminate between low and high hormone doses.

Besides, to ascertain whether, in sperm, insulin and leptin regulation of GSA may occur through a short autocrine loop, we used a variety of experimental approaches: immune neutralization of the released hormones, blockage of the hormones release, and blockage of the intracellular messengers activity. To prove that insulin and leptin secreted by sperm are acting on GSA, we absorbed the secreted hormones with the respective antibody. In uncapacitated sperm, antileptin rabbit serum (1:100) plus leptin (Fig. 6) and antiinsulin rabbit serum (1:100) plus insulin (Fig. 7) significantly decreased GSA, compared with sperm incubated in the same conditions with normal rabbit serum (1:100) plus leptin or insulin. As further evidence of autocrine regulation of the hormones on glycogen metabolism, monensin (which blocks cell secretion) (26, 27) significantly decreased GSA. Besides, wortmannin plus leptin or wortmannin plus insulin disrupted the hormones signaling through PI3K (24–26). LiCl, an inhibitor of GSK3β (28), was used as positive control of GSA enzymatic activity. In capacitating sperm, the decrease of GSA was not observed during the same experimental conditions.

Finally, to evaluate whether, in sperm, the GSA was exclusively regulated by insulin and leptin, we used both antibodies simultaneously. Although we observed a significant decrease, the enzymatic activity still persists, suggesting that redundant actions of alternative pathways may exist in the sperm.

Discussion

Animal (4) and human (7, 8) models of leptin resistance and deficiency showed a severe impairment of the reproductive function. However, the contribution of leptin to the proper functioning of the male reproductive system is still pending (2, 29). Leptin is found in the seminiferous tubules and in seminal plasma (9, 30), but the origin of seminal plasma leptin is not exactly defined. In this study, we investigated whether leptin is expressed in and secreted from human ejaculated spermatozoa and whether the hormone may affect their fertilizing ability.

Expression of leptin in the male gamete is a novel finding. In our study, we have demonstrated the presence of leptin in human sperm at different levels: mRNA expression, protein expression and immunolocalization. New reports firmly establish the presence of messenger RNAs in mammalian

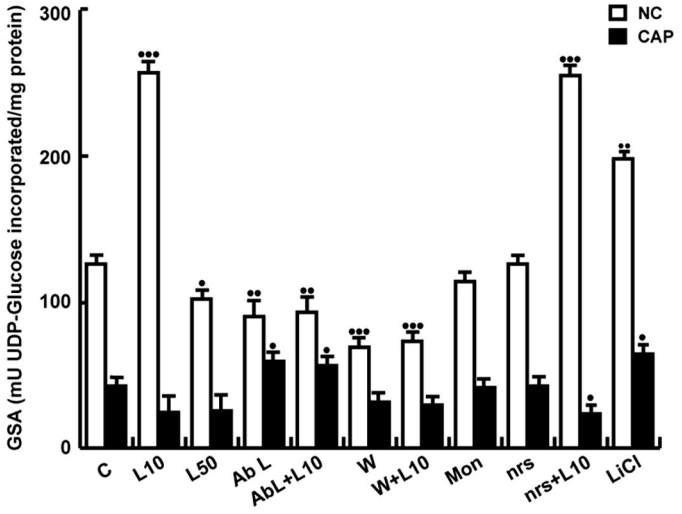

FIG. 6. Effect of leptin, antileptin antibody, wortmannin, and monensin on GSA. Washed spermatozoa were incubated for 1 h at 37 C under uncapacitating or capacitating conditions as described above. Sperm were treated with leptin (10 or 50 ng/ml) (L10 or L50), antileptin antibody (1:100) (Ab L) with or without L10, normal rabbit serum (1:100) (nrs) with or without L10, 10 μM wortmannin (W) with or without L10, 25 μM monensin (Mon), 2 mM LiCl. Data are expressed in nanomoles/min $\times$ 10^6 sperm. Values are means $\pm$ SEM of eight determinations in a typical experiment. ●, $P < 0.05$ *vs.* control (C); ●●, $P < 0.01$ *vs.* control; ●●●, $P < 0.005$ *vs.* control; □, uncapacitated sperm (NC); ■, capacitated sperm (CAP).

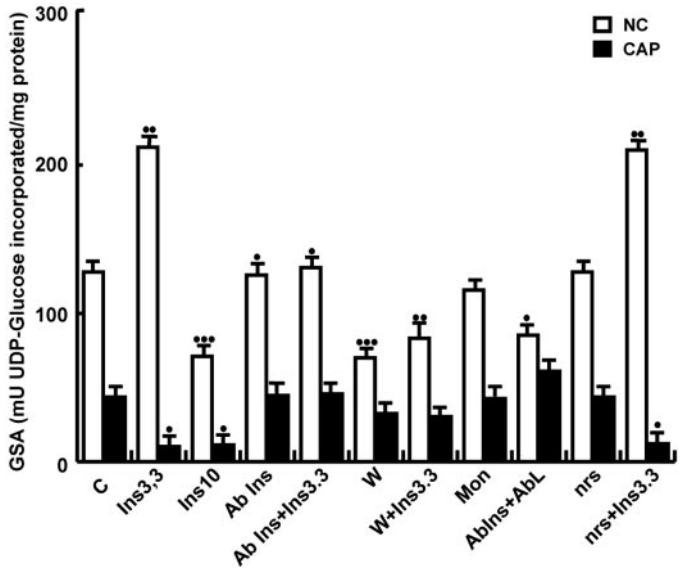

FIG. 7. Effect of insulin, antiinsulin antibody, wortmannin, and monensin on GSA. Washed spermatozoa were incubated for 1 h at 37 C under uncapacitating or capacitating conditions as described above. Sperm were treated with insulin (3.3 nM) or 10 nM (Ins3,3 or Ins10), antiinsulin (or normal, nrs) rabbit serum (1:100) (Ab Ins) alone or combined with 3.3 nM Ins (Ab Ins+Ins3.3) (nrs+Ins3.3), wortmannin 10 μM (W) alone or combined with 3.3 nM Ins, 25 μM monensin (Mon), antiinsulin plus antileptin rabbit serum (AbIns+AbL). Data are expressed in nanomoles per min per 10^6 sperm. Values are means $\pm$ SEM of eight determinations in a typical experiment. ●, $P < 0.05$ *vs.* control (C); ●, $P < 0.05$ *vs.* control; ●●, $P < 0.01$ *vs.* control; ●●●, $P < 0.005$ *vs.* control; □, uncapacitated sperm (NC); ■, capacitated sperm (CAP).

ejaculated spermatozoa. Originally, it was hypothesized that these transcripts were carried over from earlier stages of spermatogenesis, but the analysis and significance of mRNA in these cells are currently under investigation (31). Worthy new findings suggest that some of these transcripts code for proteins essential in early embryo development (32). In our study, leptin expression has also been evidenced by Western blot and by immunofluorescence. Particularly, immunocytochemical analysis showed that the hormone is specifically compartmentalized in uncapacitated sample at the equatorial segment and the midpiece, whereas capacitated sperm showed an overall decrease and a uniform distribution in the signal intensity. These data fit well with the RIA values that showed a significant increase of leptin secretion from capacitating sperm, suggesting an involvement of the hormone in capacitation.

Ejaculated spermatozoa require an extratesticular maturation termed 'capacitation' (14) that *in vivo* occurs within the female reproductive tract. It consists of several molecular events that involve different aspects of sperm physiology whose final aim is making the ejaculated sperm competent to fertilize an egg. Intriguingly, capacitation *in vitro* occurs spontaneously, after the removal of seminal plasma, without a requirement for exogenous mediator, suggesting an autocrine induction of the process (14) by endogenous sperm-derived factors. Despite the importance of capacitation, the biochemical and molecular events of the phenomenon are still poorly understood, and the identities of factors that trigger gamete activation are still unknown.

The efflux of cholesterol is historically known to be one of the first steps of capacitation, and most work has been concentrated on it (Ref. 21 and references therein). Our results showed a significant increase in cholesterol efflux upon leptin treatment in uncapacitated sperm. Moreover, leptin increases the sperm proteins tyrosine phosphorylation, which is an event tightly related to the capacitation and resulting downstream cholesterol efflux (21). However, leptin action on these two events was not dose dependent. These findings may be in context with the hypothesis of a possibly double role of leptin in the male gonads. So far, most studies indicated both positive and negative effects of leptin in gonadal functions (13, 33). Besides, seminal plasma leptin levels were significantly lower in patients with normal spermiogram parameters, compared with pathological semen samples, and showed a negative correlation with the motility of human spermatozoa (9).

It has long been recognized that capacitated sperm display an increased metabolic rate, presumably to affect the changes in sperm signaling and function during capacitation (34). The relationship between the signaling events associated with capacitation and changes in sperm energy metabolism is poorly understood. Recently, we have demonstrated that insulin is expressed in and secreted from human ejaculated spermatozoa (26). In somatic cells, both leptin and insulin play a central role in regulation of energy homeostasis, acting on PI3K/Akt pathway, which principally mediates their metabolic effects (16). Similarly, in uncapacitated sperm, both insulin and leptin increased PI3K activity, Akt S473 and GSK-3 S9 phosphorylations, leading us to hypothesize a similar action of the two hormones in modulating sperm energetic substrates availability during capacitation. Interest-

ingly, during capacitation, when the insulin and leptin secretions are maximal, we observed a strong decrease of GSK-3 S9 phosphorylation, suggesting a potential role of these hormones in modulating sperm glycogen synthesis. In somatic cells, the regulation of glycogen metabolism involves GSK-3 activity, which, in turn, is regulated by tyrosine and serine/threonine phosphorylations, the latter mediated by PI3K and Akt (35). Akt phosphorylates GSK3 on serine residue 9 and then deactivates this enzyme, which, in turn, reduces the phosphorylation and thus enhances the activity of glycogen synthase (36, 37). The conversion of UDP-glucose to glycogen by glycogen synthase is the rate-limiting step in glycogen synthesis (38); and in somatic cells, both leptin and insulin are central in the regulation of GSA.

Worthy, in our study, was the observation that GSA was significantly higher in uncapacitated than in capacitated sperm. Particularly, in uncapacitated sperm, the GSA was stimulated at low levels of both leptin and insulin, whereas it was inhibited at high concentrations. The outcome of signaling activation can depend on differences in ligand concentration (40, 41). Besides, recently it was hypothesized that the net effect of leptin upon male reproductive function may depend on the circulating level of the molecule. Thus, predominant stimulatory effects are observed at leptin levels above a minimal threshold; in contrast, direct inhibitory actions may take place in the presence of a significantly elevated leptin concentration (2, 13).

Furthermore, we have showed an autocrine regulation of GSA by both insulin and leptin in sperm. Particularly, the autocrine blockage significantly decreased GSA in uncapacitated sperm; whereas in capacitating sperm, it was not observed in the same experimental conditions. Besides, because, during capacitation, hormones efflux and multiple changes of the membrane structure rapidly occur, the autocrine blockage may be not appreciable. Our study suggests that, in uncapacitated sperm, the GSK3 is tightly blocked; whereas during capacitation, there is an activation of the enzyme, which, in turn, blocks the GSA. This effect may have physiological relevance in sperm because, during capacitation, energy demand increases, and then sperm mobilizes the glycogen reserves rather than produce it. Our results, together with the presence of leptin receptor in human ejaculated spermatozoa, create the condition for an autocrine leptin loop at this level. Upon achieving threshold concentrations, leptin may act on sperm receptors to induce signal transduction and molecular changes of capacitation.

It also has to be mentioned that mammalian spermatozoa have a fully functional glycogen metabolism, resulting in the presence of glycogen deposits and of GSK3 in the head and in the midpiece (17). Our results regarding the immunolocalization of leptin in uncapacitated sperm fit well with these findings, given that leptin works in the same sites. Glucose is needed for spermatozoa during zona pellucida penetration and sperm-oocyte fusion and to ensure that tyrosine phosphorylation occurs during capacitation (42, 43). Glucose is provided to sperm by the female reproductive tract fluid *in vivo* or by the culture medium *in vitro*; besides, several studies have indicated that stores of glycogen are endogenous sources of glucose in sperm allowing sperm to accommodate glucose-free conditions (39). It may be hypothesized that leptin in uncapacitated sperm is involved in the accumulation of energy substrates, which would be spent during capacitation.

This study shows a new possible endogenous mediator of capacitation, because we found that human ejaculated spermatozoa secrete leptin able to affect some events tightly related to this process. Leptin secretion suggests that the sperm has the ability to modulate its metabolism, according to its energy needs, independently by systemic leptin. In other words, sperm is an alternative site of leptin expression that may represent a protective mechanism in male reproduction to guarantee the accumulation of energy substrates to maintain the gamete fertilizing capability.

Acknowledgments

Our special thanks to D. Sturino (Faculty of Pharmacy, University of Calabria, Italy) for the English review of the manuscript and to Dr. V. Cunsulo (Biogemini Sas, Catania, Italy).

Received November 16, 2004. Accepted May 26, 2005.

Address all correspondence and requests for reprints to: Dr. Sebastiano Andò, Faculty of Pharmacy, University of Calabria, Arcavacata-Rende (Cosenza) 87036, Italy. E-mail: aquisav@libero.it or sebastiano.ando@unical.it.

This work was supported by PRIN 2004 Prot. N. 0067227, AIRC-2003 and MURST and Ex 60%–2004.

References

1. **Barash IA, Cheung CC, Weigle DS** 1996 Leptin is a metabolic signal to the reproductive system. Endocrinology 137:3144–3147
2. **Tena-Sempere M, Barreiro ML** 2002 Leptin in male reproduction: the testis paradigm. Mol Cell Endocrinol 188:9–13
3. **Hileman SM, Pierroz DD, Masuzaki H, Bjorbaek C, El-Haschimi K, Banks WA, Flier JS** 2002 Characterization of short isoforms of the leptin receptor in rat cerebral microvessels and of brain uptake of leptin in mouse models of obesity. Endocrinology 143:775–783
4. **Mounzih K, Lu R, Chehab FF** 1997 Leptin treatment rescues the sterility of genetically obese ob/ob males. Endocrinology 138:1190–1193
5. **Strobel A, Issad T, Camoin L, Ozata M, Strosberg AD** 1998 A leptin missense mutation associated with hypogonadism and morbid obesity. Nat Med 18: 213–215
6. **Wauters M, Considine RV, Van Gaal LF** 2000 Human leptin: from an adipocyte hormone to an endocrine mediator. Eur J Endocrinol 143:293–311
7. **Montague CT, Farooqi IS, Whitehead JP** 1997 Congenital leptin deficiency is associated with severe early-onset obesity in humans. Nature 387:903–908
8. **Farooqi IS, Jebb SA, Langmack G** 1999 Effect of recombinant leptin therapy in a child with congenital leptin deficiency. N Engl J Med 341:879–884
9. **Glander HJ, Lammert A, Paasch U, Glasow A, Kratzsch J** 2002 Leptin exists in tubuli seminiferi and in seminal plasma. Andrologia 34:227–233
10. **Steinman N, Gamzu R, Yogev L, Botchan A, Schreiber L, Yavetz H** 2001 Serum leptin concentrations are higher in azoospermic than in normozoospermic men. Fertil Steril 75:821–822
11. **Caprio M, Isidori AM, Carta AR, Moretti C, Dufau ML, Fabbri A** 1999 Expression of functional leptin receptors in rodent Leydig cells. Endocrinology 140:4939–4947
12. **Tena-Sempere M, Pinilla L, Gonzalez LC, Dieguez C, Casanueva FF, Aguilar E** 1999 Leptin inhibits testosterone secretion from adult rat testis *in vitro*. J Endocrinol 161:211–218
13. **Caprio M, Fabbrini E, Isidori AM, Aversa A, Fabbri A** 2001 Leptin in reproduction. Trends Endocrinol Metab 12:65–72
14. **Visconti PE, Galantino-Homer H, Moore GD, Baley JL, Ning X, Fornes M, Kopf GS** 1998 The molecular basis of sperm capacitation. J Androl 19:242–248
15. **Szanto I, Kahn CR** 2000 Selective interaction between leptin and insulin signaling pathways in a hepatic cell line. Proc Natl Acad Sci USA 97:2355–2360
16. **Aiston S, Agius L** 1999 Leptin enhances glycogen storage in hepatocytes by inhibition of phosphorylase and exerts an additive effect with insulin. Diabetes 48:15–11
17. **Ballester J, Fernandez-Novell JM, Rutllant J, Garcia-Rocha M, Jesus Palomo M, Mogas T, Pena A, Rigau T, Guinovart JJ, Rodriguez-Gil JE** 2000 Evidence for a functional glycogen metabolism in mature mammalian spermatozoa. Mol Reprod Dev 56:207–219
18. **World Health Organization** 1999 Laboratory manual for the examination of

human semen and sperm-cervical mucus interactions. 4th ed. Cambridge, UK: Cambridge University Press
19. **Aquila S, Sisci D, Gentile ME, Middea E, Siciliano L, Andò S** 2002 Human ejaculated spermatozoa contain active P450 aromatase. J Clin Endocrinol Metab 87:3385–3390
20. **Aquila S, Sisci D, Gentile M, Middea E, Catalano S, Carpino A, Rago V, Andò S** 2004 Estrogen receptor (ER)α and ERβ are both expressed in human ejaculated spermatozoa: evidence of their direct interaction with phosphatidylinositol-3-OH kinase/Akt pathway. J Clin Endocrinol Metab 89:1443–1451
21. **Travis AJ, Kopf GS** 2002 The role of cholesterol efflux in regulating the fertilization potential of mammalian spermatozoa. J Clin Invest 110:731–736
22. **Visconti PE, Baley JL, Moore GD, Pan D, Olds-Clarke P, Kopf GS** 1995 Capacitation in mouse spermatozoa I. Correlation between the capacitation state and protein phosphorylation. Development 121:1129–1137
23. **Berti L, Kellerer M, Capp E, Haring HU** 1997 Leptin stimulates glucose transport and glycogen synthesis in C2C12 myotubes: evidence for a PI3-kinase mediated effect. Diabetologia 40:606–609
24. **Venable CL, Frevert EU, Kim YB, Fischer BM, Kamatkon S, Neel BG, Kahn BB** 2000 Overexpression of protein-tyrosine phosphatase-1B in adipocytes inhibits insulin-stimulated phosphoinositide 3-kinase activity without altering glucose transport or Akt/Protein kinase B activation. J Biol Chem 275:18318–18326
25. **Niswender KD, Morrison CD, Clegg DT, Olson R, Baskin DG, Myers Jr MG, Seeley RJ, Schwartz MW** 2003 Insulin activation of phosphatidylinositol 3-kinase in the hypothalamic arcuate nucleus: a key mediator of insulin-induced anorexia. Diabetes 52:227–231
26. **Aquila S, Gentile M, Middea E, Catalano S, Andò S** 2005 Autocrine regulation of insulin secretion in human ejaculated spermatozoa. Endocrinology 146: 552–557
27. **Nabarra B, Andrianarison I** 1987 Pattern of secretion in thymic epithelial cells: ultrastructural studies of the effect of blockage at various levels. Cell Tissue Res 249:171–178
28. **Gould TD, Gray NA, Manji HK** 2003 Effects of a glycogen synthase kinase-3 inhibitor, lithium, in adenomatous polyposis coli mutant mice. Pharmacol Res 48:49–53
29. **Magni P, Martini L, Motta M** 2001 Leptin actions on the reproductive axis. J Clin Endocrinol Metab 86:946–947
30. **Jope T, Lammert A, Kratzsch J, Paasch U, Glander HJ** 2003 Leptin and leptin receptor in human seminal plasma and in human spermatozoa. Int J Androl 26:335–341
31. **Miller D** 2000 Analysis and significance of messenger RNA in human ejaculated spermatozoa. Mol Reprod Dev 56:259–264
32. **Ostermeier GC, Dix DJ, Miller D, Khatri P, Krawetz SA** 2002 Spermatozoal RNA profiles of normal fertile men. Lancet 360:772–777
33. **Clarke IJ, Henry BA** 1999 Leptin and reproduction. Rev Reprod 4:48–55
34. **Travis AJ, Jorgez CJ, Merdiushev T, Jones BH, Dess DM, Diaz-Cueto L, Storey BT, Kopf GS, Moss SB** 2003 Functional relationships between capacitation-dependent cell signaling and compartmentalized metabolic pathways in murine spermatozoa. J Biol Chem 276:7630–7636
35. **Van Weeren PC, De Bruyn KM, De Vries-Smits AM, Van Lint J, Burgering BM** 1998 Essential role for protein kinase B (PKB) in insulin-induced glycogen synthase kinase 3 inactivation. Characterization of dominant-negative mutant of PKB. J Biol Chem 273:13150–13156
36. **Cross DA, Alessi DR, Cohen P, Andjelkovich M, Hemmings BA** 1995 Inhibition of glycogen synthase kinase-3 by insulin mediated by protein kinase B. Nature 378:785–789
37. **Markuns JF, Wojtaszewski JF, Goodyear LJ** 1999 Insulin and exercise decrease glycogen synthase kinase-3 activity by different mechanisms in rat skeletal muscle. J Biol Chem 274:24896–24900
38. **Gomis RR, Ferrer JC, Guinovart JJ** 2000 Shared control of hepatic glycogen synthesis by glycogen synthase and glucokinase. Biochem J 3:811–816
39. **Albarracin JL, Fernandez-Novell JM, Ballester J, Rauch MC, Quintero-Moreno A, Pena A, Mogas T, Rigau T, Yanez A, Guinovart JJ, Slebe JC, Concha II, Rodriguez-Gil JE** 2004 Gluconeogenesis-linked glycogen metabolism is important in the achievement of in vitro capacitation of dog spermatozoa in a medium without glucose. Biol Reprod 71:1437–1445
40. **Marshall CJ** 1995 Specificity of receptor tyrosine kinase signaling: transient versus sustained extracellular signal-regulated kinase activation. Cell 80:179–185
41. **Castoria G, Lombardi M, Barone MV, Bilancio A, Di Domenico M, Bottero D, Vitale F, Migliaccio A, Auricchio F** 2003 Androgen-stimulated DNA synthesis and cytoskeletal changes in fibroblasts by a nontranscriptional receptor action. J Cell Biol 161:547–556
42. **Urner F, Leppens-Luisier G, Sakkas D** 2001 Protein tyrosine phosphorylation in sperm during gamete interaction in the mouse: the influence of glucose. Biol Reprod 64:1350–1357
43. **Williams AC, Ford WC** 2001 The role of glucose in supporting motility and capacitation in human spermatozoa. J Androl 22:680–695

JCEM is published monthly by The Endocrine Society (http://www.endo-society.org), the foremost professional society serving the endocrine community.

0013-7227/05/$15.00/0
Printed in U.S.A.

Endocrinology 146(2):552–557

doi: 10.1210/en.2004-1252

Autocrine Regulation of Insulin Secretion in Human Ejaculated Spermatozoa

Saveria Aquila, Mariaelena Gentile, Emilia Middea, Stefania Catalano, and Sebastiano Andò

Department of Pharmaco-Biology (Faculty of Pharmacy) (S.A., E.M.), Department of Cell Biology (M.G., S.A.), and Centro Sanitario (S.C.), University of Calabria, 87030 Arcavacata di Rende, Italy

A striking feature of insulin expression is its almost complete restriction to β-cells of the pancreatic islet in normal mammals. Here we show that insulin is expressed in and secreted from human ejaculated spermatozoa. Both insulin transcript and protein were detected. In addition, the large differences in insulin secretion, assessed by RIA, between noncapacitated and capacitated sperm suggest a role for insulin in capacitation. Insulin had an oscillatory secretory pattern involving glucose dose-dependent increases and significant decreases during the blockage of an insulin autocrine effect. It appears that the effect of glucose on the fertilizing ability of sperm is mediated by glucose metabolism through the pentose phosphate pathway. Then we evaluated the autocrine effect of sperm insulin on glucose metabolism by studying the activity of glucose-6-phosphate dehydrogenase, the key rate-limiting enzyme in the pentose phosphate pathway. The simultaneous decrease in both insulin release and glucose-6-phosphate dehydrogenase activity induced by blocking the autocrine insulin effect with three different procedures (blockage of insulin release by nifedipine, immune neutralization of the released insulin by antiinsulin serum, and blockage of an insulin intracellular effector such as phosphotidylinositol 3-kinase by wortmannin) strongly suggests a physiological role of sperm insulin on these two events. Insulin secretion by spermatozoa may provide an autocrine regulation of glucose metabolism based on their energetic needs independent of systemic insulin. In conclusion, these data open a new area of study in male reproduction. (*Endocrinology* 146: 552–557, 2005)

INSULIN IS IMPORTANT for promoting and regulating growth, differentiation, and metabolism. During embryonic development, extrapancreatic insulin gene expression is detectable in the yolk sac (1) and brain (2) of rodents. In adult mammals, apart from the thymus, insulin is thought to be produced only in β-cells in the pancreas (3). In addition, insulin has been shown to play a central role in the regulation of gonadal function. However, the significance of insulin in male fertility is not complete. It was reported that IGF-II and insulin as well as IGF-I promote spermatogonial differentiation into primary spermatocytes by binding to the IGF-I receptor (4). It was also shown that both the sperm plasma membrane and the acrosome represent cytological targets for insulin (5). In men affected by insulin-dependent diabetes, sperm have severe structural defects, significantly lower motility (6), and lower ability to penetrate hamster eggs (7). In this study we show that insulin is expressed in and secreted from human ejaculated spermatozoa.

Materials and Methods

Chemicals

The Total RNA Isolation System kit, enzymes, buffers, nucleotides, and 100-bp ladder used for RT-PCR were purchased from Promega Corp. (Milan, Italy). Moloney murine leukemia virus (M-MLV) was obtained from Invitrogen Life Technologies, Inc., Italia (Milan, Italy). Oligonucleotide primers were made by Invitrogen Life Technologies, Inc., Italia. BSA protein standard, Laemmli sample buffer, prestained molecular weight marker, Percoll (colloidal polyvinylpyrrolidone-coated silica for cell separation), sodium bicarbonate, dimethylsulfoxide, Earle's balanced salt solution, triethanolamine buffer, $MgCl_2$, glucose-6-phosphate, $NADP^+$, and all other chemicals were purchased from Sigma-Aldrich Corp. (Milan, Italy). The ECL Plus Western blotting detection system, Hybond ECL, was purchased from Amersham Biosciences (Little Chalfont, UK). The human insulin RIA kit was purchased from Diagnostic Systems Laboratories ICN (Biogemina Sas, Catania, Italy). Antibodies (rabbit antiinsulin, peroxidase-coupled antirabbit, and fluorescein isothiocyanate-conjugated antirabbit immunoglobulin G) were obtained from Santa Cruz Biotechnology, Inc. (Heidelberg, Germany).

Semen samples and spermatozoa preparations

Sperm samples with normal parameters of semen volume as well as sperm count, motility, vitality, and morphology, as specified in the WHO Laboratory Manual (8), were pooled and included in this study. In each experiment, four normal samples were pooled. Spermatozoa preparations were performed as previously described (9).

Evaluation of sperm viability

Viability was assessed using Eosin Y to evaluate potential toxic effects of different treatments. A blinded observer scored 100 cells for stain uptake (dead cells) or exclusion (live cells). Viability was evaluated before and after pooling the samples. There were no adverse effects of the different treatments on human sperm viability (data not shown).

RNA isolation and RT-PCR

Total RNA was isolated from human ejaculated spermatozoa purified as previously described (10). PCR amplification of cDNA was performed using the following primer pair: forward, 5′-GCC TTT GTG AAC CAA CAC CTG-3′; and reverse, 5′-GTT GCA GTA GTT CTC CAG CTG-3′. The forward primer, located in exon II, and the reverse primer, located

First Published Online November 18, 2004

Abbreviations: G6PDH, Glucose-6-phosphate dehydrogenase; M-MLV, Moloney murine leukemia virus; PPP, pentose phosphate pathway.

***Endocrinology* is published monthly by The Endocrine Society (http://www.endo-society.org), the foremost professional society serving the endocrine community.**

in exon III, produce a 261-bp cDNA. Because the primers span an intron, the genomic product is about 1200 bp.

The conditions for PCR were: denaturation at 95 C for 1 min, annealing at 62 C for 1 min, and extension at 72 C for 2 min (40 cycles). A DNA marker (100-bp DNA ladder) was used to determine the size of the amplified product. As a negative control, an RT-PCR was performed without M-MLV reverse transcriptase.

Western blot analysis of sperm proteins

During Western blot analysis, sperm samples were processed as previously described (10). The negative control was performed using a sperm lysate that was immunodepleted of insulin [*i.e.* preincubate lysate with antiinsulin antibody (1 h at room temperature) and immunoprecipitate with protein A/G-agarose].

Immunofluorescence assay

Sperm cells were rinsed three times with 0.5 mM Tris-HCl buffer, pH 7.5, and fixed with absolute methanol for 7 min at −20 C. Insulin staining was carried out after blocking with normal horse serum (10%) using a rabbit polyclonal antihuman insulin antibody (1:100) and an antirabbit immunoglobulin G fluorescein isothiocyanate-conjugated antibody (1:200). Sperm cells incubated without the primary antibodies were used as negative controls. The slides were examined under a fluorescence microscope (BX41, Olympus, Milan, Italy), and a minimum of 200 spermatozoa/slide were scored.

Measurement of insulin secreted by human ejaculated spermatozoa

A competitive RIA was applied to measure insulin in the sperm culture medium. Increasing numbers of spermatozoa were washed twice with unsupplemented Earle's medium and incubated in the same medium for 1 h at 37 C in 5% CO_2. In other experiments, sperm cultures were split into two series, then incubated under noncapacitating (unsupplemented Earle's medium alone) or capacitating conditions (Earle's balanced salt solution medium supplemented with 600 mg BSA/100 ml and 200 mg sodium bicarbonate/100 ml) for 1 h in a 37 C water bath at a final concentration of 10×10^6 sperm/500 μl. Each group was treated with 0.6, 8.3, and 16.7 mM glucose or with 3.3 or 10 nM insulin, antiinsulin (or normal) rabbit serum (1:100) plus 16.7 mM glucose, 10 μM wortmannin plus 16.7 mM glucose, or 25 μM nifedipine. The antiinsulin (or normal) rabbit serum and wortmannin were added 30 min before glucose stimulation. The antiinsulin serum dilution of 1:100 was empirically determined to neutralize 97% of the insulin released into the incubation medium from 10×10^6 sperm (data not shown). Nifedipine (11) and wortmannin (9) were used at concentrations tested by other researchers or used in our previous experiments. At the end of the sperm incubations, the culture media were recovered by centrifugation. Human insulin concentrations were determined in duplicate using an insulin RIA kit according to manufacturer's instructions. Insulin standards ranged from 0–300 μIU/ml. The limit of sensitivity for the assay was 0.01 μIU/ml. Inter- and intraassay variations were 6.4% and 5.1%, respectively. Insulin results are presented as the original concentrations of the supernatants and are expressed as microinternational units per milliliter.

Glucose-6-phosphate dehydrogenase (G6PDH) activity

The conversion of $NADP^+$ to NADPH, catalyzed by G6PDH, was measured by the increase in absorbance at 340 nm. Washed spermatozoa were incubated for 1 h at 37 C under noncapacitating or capacitating conditions as described above. Both noncapacitated and capacitated sperm were treated with 0.6, 8.3, and 16.7 mM glucose or with insulin (3.3 or 10 nM), antiinsulin (or normal) rabbit serum (1:100) plus 16.7 mM glucose, 10 μM wortmannin plus 16.7 mM glucose, or 25 μM nifedipine. The antibody and wortmannin were added 30 min before glucose stimulation. After treatment, 50 μl sperm extracts were loaded into individual cuvettes containing buffer (100 mM triethanolamine, 100 mM $MgCl_2$, 10 mg/ml glucose-6-phosphate, and 10 mg/ml $NADP^+$, pH 7.6) for spectrophotometric determination. The absorbance of samples was read at 340 nm every 20 sec for 1.5 min. Data are expressed as nanomoles per minute per 10^6 sperm. The enzymatic activity was determined with three control media: one without glucose-6-phosphate as substrate, one without the coenzyme ($NADP^+$), and the third without either substrate or coenzyme (data not shown). Every experiment was performed six times, including three replicates within each experiment.

Statistical analysis

The experiments for RT-PCR were repeated on at least three independent occasions, whereas Western blot analysis was performed in at least 10 independent experiments. The data obtained from RIA were presented as the mean ± SEM, and differences in mean values were calculated using a paired t test, with a significance level of $P < 0.05$. Regression analysis was performed using the SPSS program (SPSS, Inc., Richmond, CA).

Results

RT-PCR and Western blot

To determine whether mRNA for insulin is present in human ejaculated spermatozoa, RNA isolated from pooled Percoll-separated samples from normal men was analyzed by RT-PCR. The primer sequences were based on the human insulin gene sequence, and RT-PCR amplification revealed the expected PCR product size of 261 bp (Fig. 1A).

The presence of insulin protein in human ejaculated spermatozoa was investigated by Western hybridization using an antibody raised against the carboxyl terminus of the mature human insulin protein. Our antibody principally revealed one immunoreactive band at 36 kDa in different lysates from noncapacitated sperm (Fig. 1B), whereas no bands were observed in the negative control. The 36-kDa protein corresponds to the hexameric insulin form, which is present within the storage granules.

Immunolocalization of insulin in human sperm

Using an immunofluorescence technique, we identified a positive signal for insulin in human spermatozoa (Fig. 2).

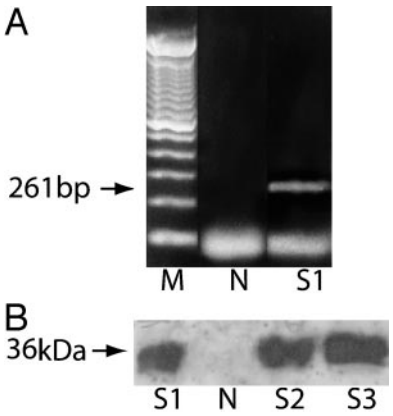

FIG. 1. Insulin expression in human ejaculated spermatozoa. A, RT-PCR analysis of human insulin gene in Percoll-separated human ejaculated spermatozoa (S1). N, Negative control (no M-MLV reverse transcriptase added); M, marker. The *arrow* indicates the expected size of the PCR product. B, Western blot of insulin protein: expression in three samples of ejaculated spermatozoa from normal men (S1, S2, and S3). The negative control (N), performed using sperm lysates, where insulin was previously removed by preincubation with the antibody to human insulin (1 h at room temperature) and immunoprecipitated with protein A/G-agarose, is represented in lane 2. The experiments were repeated more than four times, and this autoradiograph shows the results of one representative experiment.

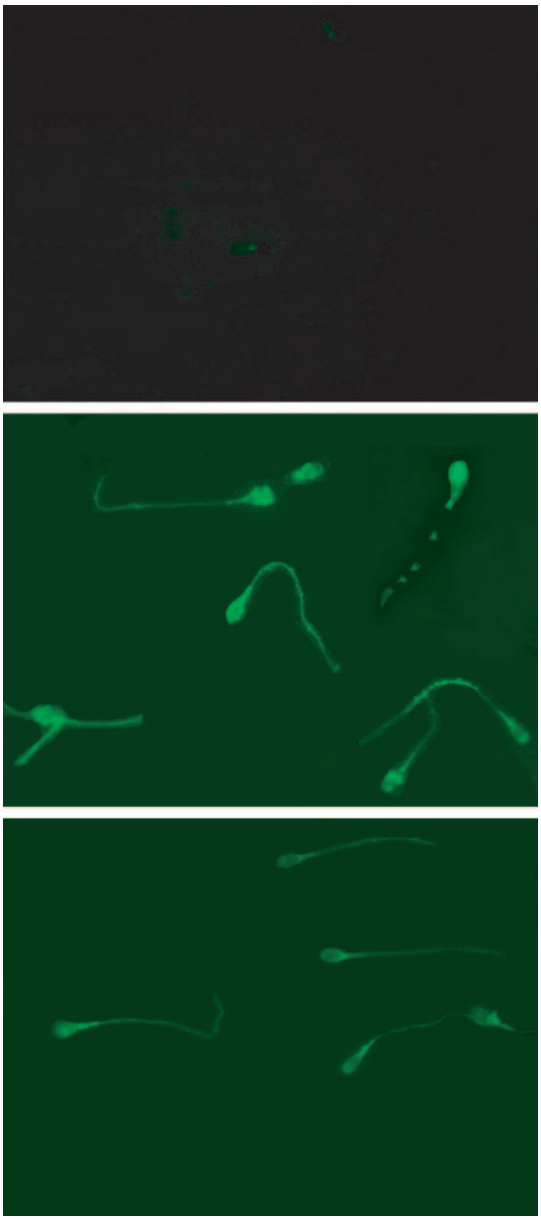

FIG. 2. Immunolocalization of insulin in human ejaculated spermatozoa. Washed spermatozoa were incubated in unsupplemented Earle's medium for 1 h at 37 C in 5% CO_2 (NC) or in capacitating medium (CAP) at the same conditions. Sperm cells incubated without the primary antibody were used as the negative control (NEG). The pictures shown are representative examples of experiments that were performed at least three times with consistent results.

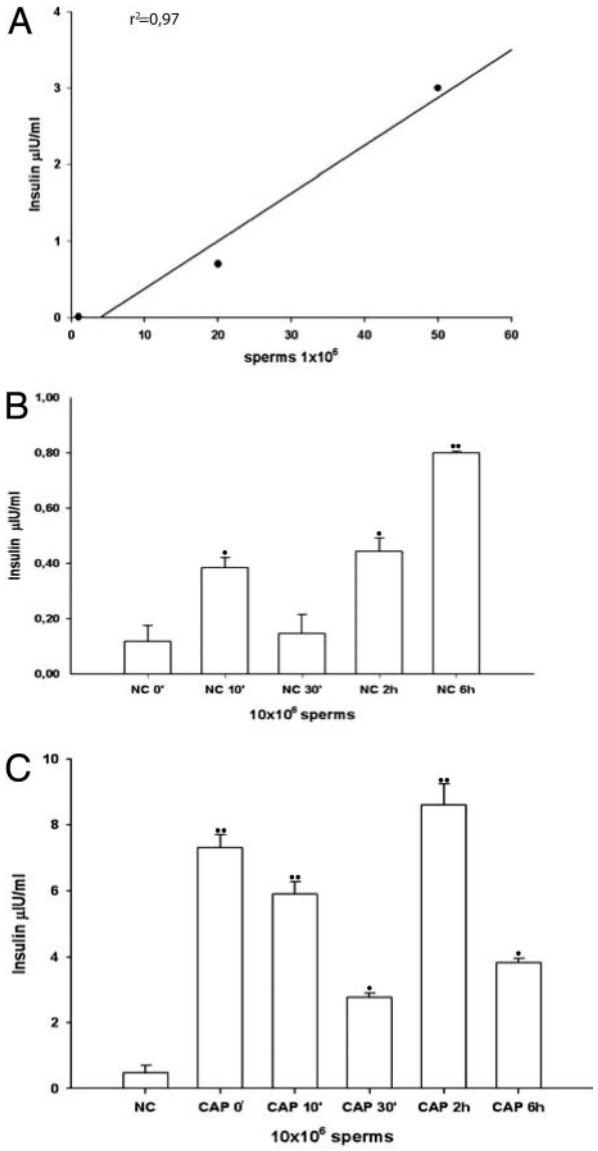

FIG. 3. Insulin secretion from human ejaculated spermatozoa. Insulin secretion in culture medium from human ejaculated spermatozoa was measured by RIA. A, An increasing number of washed sperm were incubated in unsupplemented Earle's balanced salt solution for 1 h at 37 C in 5% CO_2. Linear regression analysis was performed, and the correlation coefficient (r) was calculated ($r^2 = 0.97$). B, Time course of changes in insulin secretion from noncapacitated sperm (NC) at the indicated times. C, Time course of changes in insulin secretion from capacitated sperm (CAP) at the indicated times. Values are the mean ± SEM of 10 replicates. •, $P < 0.05$; ••, $P < 0.01$ (*vs.* control).

Insulin immunoreactivity showed a different distribution between noncapacitated and capacitated sperm. It is worth noting that the signal was less intense in capacitated sperm.

Measurement of insulin secretion

RIAs were used to evaluate whether sperm secrete insulin. After the assay was validated for spermatozoa, experiments showed that the increase in insulin secretion was dependent on the sperm concentration (Fig. 3A). Insulin production from 10×10^6 sperm incubated in noncapacitating medium (range, 0.1–0.73 μIU/ml) was significantly lower than that measured from sperm incubated under capacitating conditions (range, 4–12 μIU/ml). The time courses of insulin secretion from sperm incubated in noncapacitating and capacitating media are shown in Fig. 3, B and C, respectively.

Glucose is the main physiological secretagogue of insulin in pancreatic β-cells (12). To evaluate whether insulin secretion from sperm is also responsive to D-glucose, we generated a dose-response curve of exogenous glucose and evaluated insulin secretion from both noncapacitated and capacitated sperm. These experiments used 0.6, 8.3, or 16.7

mM glucose so that results could be compared with previously published reports. As shown in Fig. 4, glucose significantly stimulated insulin secretion in a dose-dependent fashion. Pretreatment with 10 μM wortmannin significantly decreased the amount of insulin released in response to 16.7 mM glucose. A similar decrease was observed in the presence of antiinsulin serum (1:100) or 25 μM nifedipine. These data suggest that insulin secretion is regulated in sperm.

Insulin effects on G6PDH activity

We evaluated possible autocrine regulation of G6PDH activity by sperm insulin, because the effect of glucose on the fertilizing ability of sperm appears to be mediated by the pentose phosphate pathway (PPP) (13–15). The production of NADPH from glucose-6-phosphate by sperm increased significantly when the concentration of exogenous insulin (3.3 and 10 nM) was increased and when the glucose concentration in the incubation medium was raised from 0.6 to 16.7 mM (Fig. 5). To prove that insulin secreted by sperm is acting on G6PDH activity, we stimulated insulin secretion with 16.7 mM glucose, but absorbed the secreted insulin with antiinsulin antibody. Antiinsulin rabbit serum (1:100) significantly decreased G6PDH activity in sperm lysates compared with sperm incubated under the same conditions, with normal rabbit serum (1:100). As additional evidence of autocrine regulation of insulin on glucose metabolism, nifedipine significantly decreased insulin secretion in sperm. This protocol has been shown to abolish the Ca^{2+} influx via L-type Ca^{2+} channels and to completely block insulin secretion (11). Finally, insulin signaling in sperm was disrupted using wortmannin, which inhibits the activity of phosphotidylinositol 3-kinase, the kinase principally involved in the insulin signaling cascade (11).

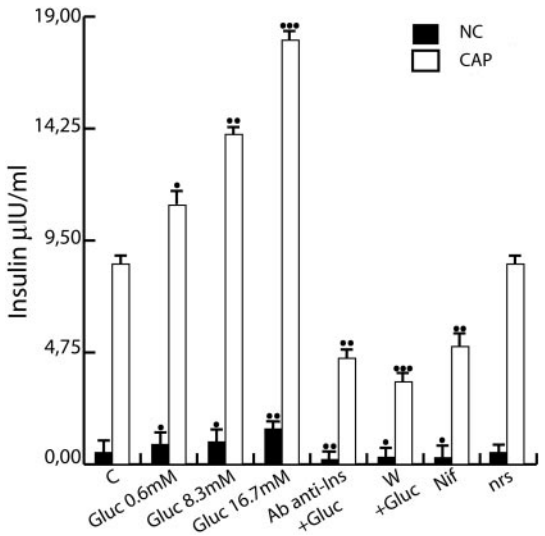

FIG. 4. Effects of glucose, antiinsulin serum, wortmannin, and nifedipine on insulin secretion from human ejaculated spermatozoa. Washed sperm pooled from normal seminal samples was split into two samples and incubated under noncapacitating (■) or capacitating (□) conditions. Each group was treated with 0.6, 8.3, and 16.7 mM glucose (Gluc) or with antiinsulin [or normal (nrs)] rabbit serum (1:100) plus 16.7 mM glucose (Ab anti-ins + gluc), 10 μM wortmannin plus 16.7 mM glucose (W + gluc), or 25 μM nifedipine (Nif). Values are the mean ± SEM of 10 replicates. •, $P < 0.05$; ••, $P < 0.01$; •••, $P < 0.005$ (*vs.* control).

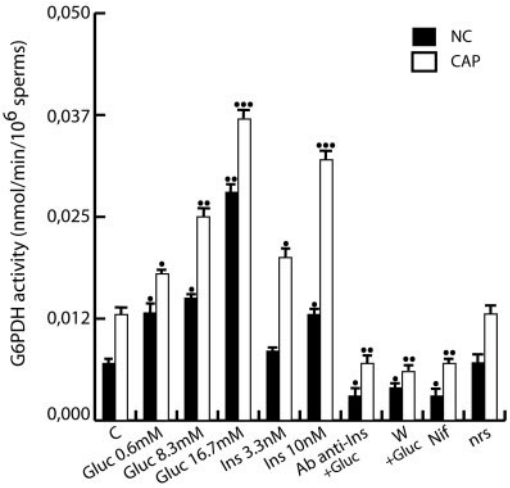

FIG. 5. Effects of insulin, glucose, antiinsulin serum, wortmannin, and nifedipine on G6PDH activity in human ejaculated spermatozoa. Washed spermatozoa were incubated for 1 h at 37 C under noncapacitating (■) or capacitating conditions (□) as described previously. Both groups were treated with 0.6, 8.3, and 16.7 mM glucose (Gluc) or with insulin (3.3 nM or 10 nM[SCAP]; Ins), antiinsulin [or normal (nrs)] rabbit serum (1:100) plus 16.7 mM glucose (Ab anti-ins + gluc), 10 μM wortmannin plus 16.7 mM glucose (W + gluc), or 25 μM nifedipine (Nif). Data are expressed as nanomoles per minute per 10^6 sperm. •, $P < 0.05$; ••, $P < 0.01$; •••, $P < 0.005$ (*vs.* control).

Discussion

In the present study we reported the novel finding that insulin is expressed in human sperm, as demonstrated by evaluation of mRNA expression, protein expression, and protein immunolocalization. In addition, we detected insulin secretion by sperm and the existence of an autocrine feedback of insulin on its own secretion and on G6PDH activity.

New reports firmly establish the presence of mRNA in mammalian ejaculated spermatozoa. To date about 14 transcripts have been identified. Originally, it was hypothesized that these transcripts were carried over from earlier stages of spermatogenesis, but the analysis and significance of mRNA in these cells are currently under investigation (16). Worthy new findings suggest that some of these transcripts code for proteins essential in early embryo development (17). In our study insulin expression has been evidenced by Western blot and immunofluorescence. In particular, immunocytochemical analysis of insulin showed a heterogeneous expression pattern, implying different degrees of energetic status among sperm. In a majority of the sperm in noncapacitated samples, insulin was located at the subacrosomial level, in the midpiece, and throughout the tail. Moreover, insulin is arranged within granules, similar to the insulin storage granules within pancreatic β-cells. An overall decrease and uniform distribution in the signal intensity for insulin were observed in capacitated sperm. This result can be attributed to a major release of hormone in accordance with the high levels (RIA values) of insulin in the medium of capacitating sperm. In pancreatic β-cells, changes in insulin release are accompanied by simultaneous changes in glucose metabolism.

Changes in insulin release are also related to different physiological conditions, such as when sperm switch from noncapacitated to capacitated status. It is worth noting that insulin secretion from spermatozoa into the capacitating medium takes place immediately (at time zero), suggesting a possible involvement of insulin in the induction of capacitation.

Our time-course studies showed that insulin from sperm is released in a pulsatile manner that results in oscillatory concentrations in the incubation medium in both noncapacitated and capacitated sperm. Similarly, under basal as well as stimulated conditions, pancreatic β-cells secrete insulin in a pulsatile manner, and the oscillatory pattern is believed to improve release control and to enhance hormonal action (18). Glucose is the main secretagogue of insulin in pancreatic β-cells (12), and we now have shown that insulin secretion from sperm is also responsive to glucose.

Moreover, our results indicate that insulin exerts a physiological autocrine stimulatory effect on glucose-induced insulin release. Specifically, the blockage of insulin release, immune neutralization of the released insulin, or blockage of the activity of intracellular insulin messenger significantly decreased insulin secretion (~50%) in both noncapacitated and capacitated sperm. These data address an autocrine regulation of insulin on its own secretion in sperm, which is in agreement with recent data in pancreatic β-cells showing that secreted insulin may have a positive effect on insulin exocytosis (19).

In pancreatic islets, the release of insulin requires hexose metabolism mediated by glucokinase (20), which has also been identified in sperm (21). Insulin secretion is triggered by ATP generated in the course of glucose metabolism that depolarizes the β-cell membrane and increases the cytosolic concentration of Ca^{2+} (22). Of note, these latter events are also important in the initiation of capacitation (23), such as when insulin efflux was detected. In addition, the IGF-I receptor has been found in human sperm (24), and spermatozoa have been reported to bind radioinsulin in a time- and concentration-dependent manner (5). These conditions create the potential for an autocrine insulin loop during the induction of capacitation.

The insulin secretion by spermatozoa suggests an autocrine regulation of glucose metabolism. Glucose is provided to sperm by seminal plasma, by female reproductive tract fluid *in vivo* (25), or by culture medium *in vitro* (26, 27), and several studies have indicated that stores of glycogen are endogenous sources of glucose in sperm, allowing sperm to accommodate glucose-free conditions (27). Hexokinase, in the initial step of glycolysis, generates glucose-6-phosphate from glucose, supplying this substrate to both glycolysis and the PPP. Although glycolysis is important for sperm functions such as hyperactivated motility, this metabolic pathway does not appear to be responsible for successful gamete fusion (28, 29). Instead, the beneficial effect of glucose on the acquisition of fertilizing ability as well as on gamete fusion is mediated by glucose metabolism through the PPP (13–15). We evaluated the possible autocrine insulin modulatory effect on G6PDH activity, because G6PDH is the key rate-limiting enzyme in the PPP, which has been shown to be functional in human spermatozoa (29). G6PDH regulates the production of NADPH by controlling the metabolism of glucose (14). Insulin induction of G6PDH activity has been studied both *in vivo* and *in vitro* (30). In our study the blockage of insulin release, immune neutralization of the released insulin, or blockage of intracellular insulin signaling significantly decreased G6PDH activity in sperm in both noncapacitated and capacitated sperm. A similar decrease in the effect of insulin on glucose metabolism was recently obtained in pancreatic islets (19).

Ejaculated spermatozoa require extratesticular maturation, termed capacitation, that allows them to become competent to fertilize an egg. Capacitation is a multifaceted process that has been shown to correlate with changes in spermatozoal metabolism, intracellular ion concentrations, plasma membrane fluidity, intracellular pH, intracellular cAMP concentration, and reactive oxygen species (23). Intriguingly, capacitation *in vitro* occurs spontaneously after the removal of seminal plasma and without a requirement for an exogenous mediator, suggesting autocrine induction (31) by endogenous sperm-derived factors. Despite the importance of capacitation, the biochemical and molecular events of the phenomenon are still poorly understood, and the identities of factors that trigger gamete activation are as yet unknown. On the basis of our results, sperm-derived insulin might be considered a factor involved in the induction of capacitation. Upon achieving threshold concentrations, insulin may act on sperm receptors to induce the signal transduction and molecular changes of capacitation.

This study showed a new possible endogenous mediator of capacitation, because we found that human ejaculated spermatozoa are able to secrete insulin during this process. Using a variety of experimental approaches, we found abundant pancreatic β-cell features, most notably insulin secretion. It is unexpected that insulin expression would be found in sperm, considering the limited cell types that produce insulin and considering the differences between sperm and pancreatic β-cells. However, given the essential role in the propagation of life, it would be conceivable that metabolic and signaling pathways expressed in terminally differentiated cells might be subsumed into a sperm cell. The spermatozoon leaves the testis and moves through the female genital tract in the host body of the opposite gender, so sperm needs to be autonomous.

The secretion of insulin by spermatozoa may provide an autocrine regulation of glucose metabolism according to their energetic needs independent of systemic insulin. Given the simultaneous decrease in both insulin release and hexose metabolism by blocking the autocrine effect of sperm insulin, we have shown a modulatory effect of the hormone on these two events. Insulin, in addition to other candidates, may be implicated in control of the energy status in the various sperm compartments as well as during the different stages of fertilization.

In conclusion, the findings of insulin expression and secretion from human sperm open a new area of study in male reproduction.

Acknowledgments

Our special thanks to Dr. Vincenzo Cunsulo (Biogemina SAS, Catania, Italy). We also thank D. Sturino (Faculty of Pharmacy, University

of Calabria, Calabria, Italy) and Dr. M. Young assistance with reviewing the manuscript text.

Received September 21, 2004. Accepted November 9, 2004.

Address all correspondence and requests for reprints to: Dr. Saveria Aquila , Centro Sanitario, University of Calabria, Arcavacata di Rende (CS) 87030, Italy. E-mail: sebastiano.ando@unical.it and aquisav@libero.it.

This work was supported by COFIN 2004 and MURST ex 60%.

References

1. **Philippe J** 1991 Structure and pancreatic expression of the insulin and glucagon genes. Endocr Rev 12:1–20
2. **Alpert S, Hanahan D, Teitelman G** 1988 Hybrid insulin genes reveal a developmental lineage for pancreatic endocrine cells and imply a relationship with neurons. Cell 53:295–308
3. **Throsby M, Homo-Delarche F, Chevenne D, Goya R, Dardenne M, Pleau JM** 1998 Pancreatic hormone expression in the murine thymus: localization in dendritic cells and macrophages. Endocrinology 139:2399–2406
4. **Nakayama Y, Yamamoto T, Abe SI** 1999 IGF-I, IGF-II and insulin promote differentiation of spermatogonia to primary spermatocytes in organ culture of newt testes. Int J Dev Biol 43:343–347
5. **Silvestroni L, Modesti A, Sartori C** 1992 Insulin-sperm interaction: effects on plasma membrane and binding to acrosome. Arch Androl 28:201–211
6. **Baccetti B, La Marca A, Piomboni P, Capitani S, Bruni E, Petraglia F, De Leo V** 2002 Insulin-dependent diabetes in men is associated with hypothalamo-pituitary derangement and with impairment in semen quality. Hum Reprod 17:2673–2677
7. **Shrivastav P, Swann J, Jeremy JY, Thompson C, Shaw RW, Dandona P** 1989 Sperm function and structure and seminal plasma prostanoid concentrations in men with IDDM. Diabetes Care 12:742–744
8. **World Health Organization** 1999 WHO laboratory manual for the examination of human semen and sperm-cervical mucus interactions. 4th ed. Cambridge: Cambridge University Press
9. **Aquila S, Sisci D, Gentile M, Middea E, Catalano S, Carpino A, Rago V, Andò S** 2004 Estrogen receptor (ER)α and ERβ are both expressed in human ejaculated spermatozoa: evidence of their direct interaction with phosphatidylinositol-3-OH kinase/Akt pathway. J Clin Endocrinol Metab 89:1443–1451
10. **Aquila S, Sisci D, Gentile M, Middea E, Siciliano L, Andò S** 2002 Human ejaculated spermatozoa contain active P450 aromatase. J Clin Endocrinol Metab 87:3385–3390
11. **Aspinwall CA, Qian WJ, Roper MG, Kulkarni RN, Kahn CR, Kennedy RT** 2000 Roles of insulin receptor substrate-1, phosphatidylinositol 3-kinase, and release of intracellular Ca^{2+} stores in insulin-stimulated insulin secretion in β-cells. J Biol Chem 275:22331–22338
12. **Aspinwall CA, Lakey JR, Kennedy RT** 1999 Insulin-stimulated insulin secretion in single pancreatic β cells. J Biol Chem 274:6360–6365
13. **Urner F, Sakkas D** 1999 A possible role for the pentose phosphate pathway of spermatozoa in gamete fusion in the mouse. Biol Reprod 60:733–739
14. **Urner F, Sakkas D** 1999 Characterization of glycolysis and pentose phosphate pathway activity during sperm entry into the mouse oocyte. Biol Reprod 60:973–978
15. **Urner F, Leppens-Luisier G, Sakkas D** 2001 Protein tyrosine phosphorylation in sperm during gamete interaction in the mouse: the influence of glucose. Biol Reprod 64:1350–1357
16. **Miller D** 2000 Analysis and significance of messenger RNA in human ejaculated spermatozoa. Mol Reprod Dev 56:259–264
17. **Ostermeier GC, Dix DJ, Miller D, Khatri P, Krawetz SA** 2002 Spermatozoal RNA profiles of normal fertile men. Lancet 360:772–777
18. **Schmitz O, Brock B, Hollingdal M, Juhl CB, Porksen N** 2002 High-frequency insulin pulsatility and type 2 diabetes: from physiology and pathophysiology to clinical pharmacology. Diabetes Metab Dec 28:4S14–4S20
19. **Borelli MI, Arancini F, Gagliardino JJ** 2004 Autocrine regulation of glucose metabolism in pancreatic islets. Am J Physiol 286:E111–E115
20. **Ashcroft SJ** 1980 Glucoreceptor mechanisms and the control of insulin release and biosynthesis. Diabetologia 18:5–15
21. **Travis AJ, Foster JA, Rosenbaum NA, Visconti PE, Gerton GL, Kopf GS, Moss SB** 1998 Targeting of a germ cell-specific type 1 hexokinase lacking a porin-binding domain to the mitochondria as well as to the head and fibrous sheath of murine spermatozoa. Mol Biol Cell 9:263–276
22. **De Fronzo RA** 1997 Pathogenesis of type 2 diabetes: metabolic and molecular implications for identifying diabetes genes. Diabetes Rev 5:177–269
23. **Visconti PE, Galantino-Homer H, Moore GD, Baley JL, Ning X, Fornes M, Kopf GS** 1998 The molecular basis of sperm capacitation. J Androl 19:242–248
24. **Naz RK, Padman P** 1999 Identification of insulin-like growth factor (IGF)-1 receptor in human sperm cell. Arch Androl 43:153–159
25. **Koch JU** 1980 Sperm migration in the human female genital tract with and without intrauterine devices. Acta Eur Fertil 11:33–60
26. **Mahadevan MM, Miller MM, Moutos DM** 1997 Absence of glucose decreases human fertilization and sperm movement characteristics in vitro. Hum Reprod 12:119–123
27. **Travis AJ, Tutuncu L, Jorgez CJ, Ord TS, Jones BH, Kopf GS, Williams CJ** 2004 Requirements for glucose beyond sperm capacitation during in vitro fertilization in the mouse. Biol Reprod 71:139–145
28. **Urner F, Sakkas D** 1996 Glucose is not essential for the occurrence of sperm binding and zona pellucida-induced acrosome reaction in the mouse. Int J Androl 19:91–96
29. **Travis AJ, Jorgez CJ, Merdiushev T, Jones BH, Dess DM, Diaz-Cueto L, Storey BT, Kopf GS, Moss SB** 2001 Functional relationships between capacitation-dependent cell signaling and compartmentalized metabolic pathways in murine spermatozoa. J Biol Chem 276:7630–7636
30. **Stumpo DJ, Kletzien RF** 1984 Regulation of glucose-6-phosphate dehydrogenase mRNA by insulin and the glucocorticoids in primary cultures of rat hepatocytes. Eur J Biochem 144:497–502
31. **Wu C, Stojanov T, Chami O, Ishii S, Shimizu T, Li A, O'Neill C, Shimuzu T** 2001 Evidence for the autocrine induction of capacitation of mammalian spermatozoa. J Biol Chem 276:26962–26968

***Endocrinology* is published monthly by The Endocrine Society (http://www.endo-society.org), the foremost professional society serving the endocrine community.**

0021-972X/04/$15.00/0
Printed in U.S.A.

The Journal of Clinical Endocrinology & Metabolism 89(3):1443–1451

doi: 10.1210/jc.2003-031681

Estrogen Receptor (ER)α and ERβ Are Both Expressed in Human Ejaculated Spermatozoa: Evidence of Their Direct Interaction with Phosphatidylinositol-3-OH Kinase/Akt Pathway

SAVERIA AQUILA, DIEGO SISCI, MARIAELENA GENTILE, EMILIA MIDDEA, STEFANIA CATALANO, AMALIA CARPINO, VITTORIA RAGO, AND SEBASTIANO ANDÒ

Centro Sanitario (S.Aq., M.G., E.M., S.C.), Department of Cell Biology (A.C., V.R.), Faculty of Pharmacy (D.S., S.An.), University of Calabria 87030 Arcavacata di Rende (Cosenza - Italy)

Human and animal models have evidenced how estrogen insufficiency is associated with abnormal spermatogenesis and male infertility. We previously demonstrated that estradiol is able to influence both capacitation and acrosome reaction in human ejaculated spermatozoa. It remains to be elucidated whether the biochemical changes induced by estradiol, in a rapid nongenomic way, are mediated by a single estrogen receptor (ER) or by the two ER subtypes, ERα and ERβ. In the present study, we have first demonstrated the concomitant expression of ERβ and ERα in human ejaculated spermatozoa. By RT-PCR and Southern blot, transcripts of both ERs were detected. Western blot analysis showed ERα and ERβ proteins at the same size as the "classical" ERs. The localization of ERα and ERβ with the immunocytochemistry shows a differential distribution of the two ER subtypes, the former being prevalently located in the midpiece, but the latter being in the tail. Estradiol has been associated with sperm longevity; however, the mechanism through which estradiol acts in sperm survival was never investigated. Upon estradiol exposure, we observed an enhanced phosphorylation of the proteins involved in the phosphatidylinositol-3-OH kinase (PI3K)/Akt pathway like PDK1, Akt, GSK-3, Bcl-2, together with ERK1/2, which was also involved in cell survival signals. Moreover, such phosphorylations were reduced in the presence of ICI 182, 780, addressing the role of estradiol and ERs in sperm survival. For instance we have provided, for the first time, a different interaction of the two ERs with the PI3K/Akt pathway, because ERα interacts with the p55 regulatory subunit of PI3K, whereas ERβ interacts with Akt1. However, it still remains to be elucidated whether the functional role of each of the ER subtypes in sperm survival signaling is redundant or distinct. (*J Clin Endocrinol Metab* 89: 1443–1451, 2004)

IN THE LAST YEARS, considerable emphasis has been focused on the role of estrogens in the regulation of male reproduction (1–3). The physiological responses to estrogen are known to be mediated by at least two distinct receptor subtypes, estrogen receptor (ER)α and ERβ, each encoded by a unique gene, differing in the C-terminal ligand-binding domain and in the N-terminal *trans*-activation domain (3). Both receptors seem to be expressed in germ cells in various stages of development from spermatogonia to elongated spermatids (Ref. 3 and references therein). ERβ expression appears to be the predominant ER in germ cells (Ref. 3 and references therein), whereas ERα was found in early meiotic spermatocytes and elongated spermatids only in one study (4) and in human ejaculated spermatozoa (5, 6).

The human and animal phenotypes related to aromatase deficiency and estrogen resistance have been previously detailed (7). For instance, ERα knockout (ERαKO) mouse was infertile from the onset of puberty (8, 9), whereas P450arom knockout (ArKO) mouse displayed a progressive long-term deterioration of spermatogenesis consisting of abnormalities in postmeiotic early cells associated with an increase in apoptosis that suggests a role for estrogen in germ cell survival (10, 11).

A stimulatory role for estrogen in germ cell differentiation was demonstrated; moreover, during development, germ cells are able to synthesize estrogen, directly modulating via paracrine and/or intracrine actions their own maturation (Ref. 3 and references therein). Recent data from our laboratory have demonstrated that a biologically active P450arom is present in ejaculated spermatozoa (12); in addition, its physiological role is associated either with capacitation or acrosome reaction (13). This raises the possibility that sperm not only would be exposed to estrogens in female genital tract but can provide itself a persisting local source of estrogen that may target on its own receptors modulating sperm extratesticular maturation. The biochemical changes during capacitation induced by estrogens occur rapidly, addressing the nongenomic action of ERs as demonstrated in other cell types (14). On the other hand, the fast ERs responses, instead to their classic genomic action, represent the exclusive modality of ERs action in spermatozoa because they are considered transcriptionally inactive. However, the mechanism by which ERs mediate the rapid effects of estrogen is still not well understood. The identification of ERβ has indicated that the cellular responses to estrogen are far more complex (15). It was suggested that the two receptors may play

Abbreviations: Dnase, Deoxyribonuclease; E_2, estradiol; ER, estrogen receptor; FITC, fluorescein isothiocyanate; ICI, ICI 182, 780; KO, knockout; LY, LY294002; M-MLV, Moloney murine leukemia virus; PI3K, phosphatidylinositol-3-OH kinase; SDS, sodium dodecyl sulfate; SSC, saline sodium citrate; TBS-T, Tween-20 in Tris-buffered saline.

JCEM is published monthly by The Endocrine Society (http://www.endo-society.org), the foremost professional society serving the endocrine community.

redundant roles in estrogen signaling. On the other hand, this appears questionable, on the basis of localization studies that have revealed distinct expression patterns for each receptor.

In the present study, we demonstrated that both ERα and ERβ are expressed in human ejaculated spermatozoa. Focusing on the phosphatidylinositol-3-OH kinase (PI3K)/Akt pathway involved in cell survival, we have evidenced, together with its up-regulation upon estradiol exposure, that ERα coprecipitates with the p55 regulatory subunit of PI3K, whereas ERβ coprecipitates with the downstream protein Akt1. This makes it extremely intriguing to investigate a potential distinct role of each ER in controlling sperm survival.

Materials and Methods

Chemicals

PMN cell isolation medium was from BIOSPA (Milan, Italy). Total RNA Isolation System kit, enzymes, buffers, nucleotides, and 100-bp ladder used for RT-PCR were purchased from Promega (Milan, Italy). Moloney murine leukemia virus (M-MLV) was from Life Technologies, Inc. - Life Technologies Italia (Milan, Italy). Oligonucleotide primers were made by Invitrogen (Milan, Italy). DMEM-F12 medium, BSA protein standard, activated charcoal, Laemmli sample buffer, prestained molecular weight markers, Percoll (colloidal PVP-coated silica for cell separation), sodium bicarbonate, sodium lactate, sodium pyruvate, estradiol (E_2), dimethylsulfoxide, IgG Texas-red conjugated, antirabbit IgG fluorescein isothiocyanate (FITC) conjugated, Earle's balanced salt solution, and all other chemicals were purchased from Sigma Chemical (Milan, Italy). Acrylamide bisacrylamide was from Labtek Eurobio (Milan, Italy). Triton X-100, Eosin Y was from Farmitalia Carlo Erba (Milan, Italy). Enhanced chemiluminescence (ECL) Plus Western blotting detection system, Hybond ECL, [γ-^{32}P]ATP, and HEPES sodium salt were purchased from Amersham Pharmacia Biotech (Buckinghamshire, UK). ICI 182, 780 (ICI) was purchased from Zeneca Pharmaceuticals (Cheshire, UK). Monoclonal mouse antibody to human ERα (F-10), rabbit polyclonal antibody to human ERβ (H-150), mouse anti-p85 regulatory subunit monoclonal antibody, goat policlonal actin (1–19), peroxidase-coupled antirabbit, antigoat, antimouse IgG, and protein A/G-agarose plus were from Santa Cruz Biotechnology (Heidelberg, Germany). Rabbit policlonal antibody to human ERβ was from Upstate (Lake Placid,). Rabbit anti-p-ERK (p-ERK1/2) policlonal antibody, rabbit anti-p-Bcl-2 antibody, rabbit anti-p-Akt1/Akt2/Akt3 S473 or anti-p-Akt1/Akt2/Akt3 T308 antibodies, rabbit anti-p-PDK1 antibody, rabbit anti-p-GSK-3 antibody, and mouse anti-ERK1/2 were from Cell Signaling (Milan, Italy). Nylon membranes were provided by Roche diagnostics Corporation (Indianapolis, IN). Thin-layer chromatography aluminum sheets were from MERK (Milan, Italy).

Semen samples and spermatozoa preparations

Semen specimens from normozoospermic men were obtained by masturbation (approved by the University of Virginia Human Investigation Committee) after 3 d of sexual abstinence. The samples were produced into sterile containers and left for at least 30 min to completely liquefy before being processed. Sperm samples with normal parameters of semen volume, sperm count, motility, vitality, and morphology, according to the WHO Laboratory Manual (16), were pooled and included in this study. Ejaculates with observed spermatozoa agglutination or abnormal viscosity were discarded. Spermatozoa preparations were performed as previously described (12).

RNA isolation

Total RNA was isolated from human ejaculated spermatozoa using a Total RNA Isolation System kit as described by the manufacturer. The purity and quantity of the RNA was assessed spectroscopically before carrying out the analytical procedures. All RNA preparations were evaluated by denaturating formaldehyde-agarose gel electrophoresis.

RT-PCR

RNA was amplified by the technique of RT-PCR. Before RT-PCR, RNA was incubated with ribonuclease-free deoxyribonuclease (Dnase) I in single-strength reaction buffer at 37 C for 15 min. This was followed by heat inactivation of Dnase I at 65 C for 10 min. Five micrograms of Dnase-treated RNA samples were reverse transcribed by 200 IU M-MLV reverse transcriptase in a reaction vol of 20 μl (0.4 μg oligo-dT, 0.5 mM deoxy-NTP and 24 IU Rnasin) for 30 min at 37 C, followed by heat denaturation for 5 min at 95 C. PCR amplification of cDNA was performed with 2 U of Taq DNA polymerase, 50 pmol primer pair for ERα (forward, 5′-GTG TAC AAC TAC CCC GAGG-3′; reverse, 5′-CAG ATT CAT CAT GCG GAA CCG AGATG-3′) or 50 pmol primer pair for ERβ (forward, 5′-CCA TGA TGA TGT CCC TGA CCA-3′; reverse, 5′-GCC CTC TTT GCT TTT ACT GTCC-3′) in 10 mM Tris-HCL (pH 9.0) containing 0.1% Triton X-100, 50 mM KCl, 1.5 mM $MgCl_2$, and 0.25 mM of each deoxy-NTP. The reactions were carried out for 35 cycles, with each consisting of denaturation for 1 min at 95 C, annealing for 1 min at 59 C, and extension for 2 min at 72 C. Standard DNA marker (100-bp DNA ladder) was also run to determine the size of amplified products. To check for the presence of DNA contamination, a RT-PCR was performed without M-MLV reverse transcriptase (negative control). In each reaction, HEG0 (containing human ERα gene) and pCMV5-hERβ (containing human ERβ gene) served as positive control for ERα and ERβ, respectively.

Southern blotting

The identity of the PCR-amplified cDNA fragment of ERα and ERβ transcripts from human spermatozoa was verified using Southern hybridization. The PCR-amplified products were subjected to electrophoresis in 2% agarose gels and transferred on nylon membranes with the use of a capillary method and lasted for 16 h. The DNA, covalently linked to the nylon membrane by exposure to UV light (254 nm) at 1.5 J/cm^2, were prehybridized for 4 h at room temperature in 6× saline sodium citrate (SSC). A total of 1–2 ng cDNA probes (5′-GTGCAATGACTATG-CTTCAGGCTACCAT-3′ for ERα and 5′-TCGAGAGTTAAAACTCCAACACAAAGAATA-3′ for ERβ) were labeled with [γ^{32}P] ATP using polynucleotide kinase and were added to a second solution identical to the prehybridization solution. The hybridization was carried out overnight at room temperature. The membranes were washed first for 45 min at 50 C with 2× SSC containing 0.1% sodium dodecyl sulfate (SDS), then with 1× SSC, and finally with 0.1× SSC for 30 min at the same temperature. Washed blots were exposed to Kodak XAR-2 film (Sigma, Milan, Italy) with intensifying screens.

Western blot analysis

Sperm samples were washed twice with Earle's balanced salt solution (uncapacitating medium), incubated with the various compounds as indicated in *Results*, and then centrifuged for 5 min at 5000 × *g*. The pellet was resuspended in lysis buffer as previously described (13). Briefly, the pellet was resuspended in lysis buffer (62.5 mmol/liter Tris-HCl, pH 6.8; 150 mM NaCl; 2% SDS; 1% Triton X100; 10% glycerol; 1 mM phenylmethylsulfonylfluoride; 10 μg/ml leupeptin; 10 μg/ml aprotinin; 2 μg/ml pepstatin). Lysates were quantified using Bradford protein assay reagent (17). Equal amounts of protein (20 μg) were boiled for 5 min, separated under denaturing conditions, by SDS-PAGE on 10% polyacrylamide Tris-glycine gels, and electroblotted to nitrocellulose membrane. Nonspecific sites were blocked with 5% nonfat dry milk in 0.2% Tween-20 in Tris-buffered saline (TBS-T) for 1 h at room temperature and then probed with an appropriate dilution of the various antibodies as indicated in the figure legends. After extensive washings (three times for 15 min each time in TBS-T), the secondary antirabbit or antimouse horseradish peroxidase-conjugated antibody was added for 1 h at 22 C. Blots were again washed three times for 15 min in TBS-T, and the bound of secondary antibody was located with the ECL Plus Western blotting detection system according to the manufacturer's instructions. Each membrane was exposed to the film for 2 min. As internal control, all membranes in which the phosphorylation levels were determined were subsequently stripped (glycine, 0.2 M, pH 2.6, for 30 min at room temperature) of the first antibody and reprobed with the antibody recognizing the nonphosphorylated form of the proteins or with actin.

Immunoprecipitation of spermatozoa proteins

Spermatozoa were washed twice with unsupplemented Earle's medium and were incubated in the unsupplemented Earle's medium for 1 h at 37 C and 5% CO_2, without (control) or in the presence of 10 nM E_2. Besides, some samples were washed and incubated in capacitating medium (Earle's balanced salt solution medium supplemented with 266 mg/100 ml $CaCl_2$, 600 mg/100 ml BSA, 3 mg/100 ml sodium pyruvate, 360 μl/100 ml sodium lactate, and 200 mg/100 ml sodium bicarbonate). To avoid aspecific binding, the sperm lysates were incubated for 2 h with protein A/G-agarose beads at 4 C and centrifuged at 12,000 × *g* for 5 min. The supernatants (each containing 500 μg total protein) were then incubated overnight with 10 μl anti-ERα or 10 μl anti-ERβ or 5 μl anti-p-Akt1/2/3 and 500 μl HNTG (IP) buffer (50 mM HEPES, pH 7.4; 50 mM NaCl; 0.1% Triton X-100; 10% glycerol; 1 mM phenylmethylsulfonylfluoride; 10 μg/ml leupeptin; 10 μg/ml aprotinin; 2 μg/ml pepstatin) for each. Immune complexes were recovered by incubation with protein A/G-agarose. The beads containing bound proteins were washed three times by centrifugation in IP buffer, then denaturated by boiling in Laemmli sample buffer and analyzed by Western blot to identify the coprecipitating effector proteins. Immunoprecipitation with protein A/G alone was used as negative control. Membranes were stripped of bound antibodies by incubation in glycine (0.2 M, pH 2.6) for 30 min at room temperature. Before reprobing with different primary antibodies, stripped membranes were washed extensively in TBS-T and placed in blocking buffer (TBS-T containing 5% milk) overnight.

Immunofluorescence assay

Sperm cells, recovered from Percoll gradient, were rinsed three times with 0.5 mM Tris-HCl buffer (pH 7.5) and were allowed to settle onto slides in a humid chamber. The overlying solution was carefully pipetted off and replaced by absolute methanol for 7 min at −20 C. After methanol removal, sperm cells were washed in TBS, containing 0.1% Triton X-100, and were treated for immunocytochemistry. ERα staining was carried out, after blocking with normal horse serum (10%), using a mouse antihuman ERα IgG as primary antibody and a Texas-red-conjugated antimouse IgG (1:50) as secondary antibody. ERβ immunocytochemical staining was performed, after blocking with normal goat serum (10%), using a rabbit antihuman ERβ (1:100) followed by an FITC-conjugated antirabbit IgG (1:50). Sperm cells incubated without the primary antibodies were used as the negative controls. The slides were examined under a fluorescence microscope (Olympus BX41, Milan, Italy) with a suitable filter for FITC and Texas-red, scoring a minimum of 200 spermatozoa per slide.

ERα-associated PI-3K activity

Purified spermatozoa were washed in Earle's balanced salt solution (uncapacitating medium) and centrifuged at 800 × *g* for 20 min. Sperm were resuspended in the same uncapacitating medium and in different tubes containing no E_2 (control) or 100 nM E_2. Some samples were resuspended in capacitating medium. Some samples were treated with ICI (100 nM) or LY294002 (LY) (10 μM alone or with 100 nM E_2) after a preincubation of 30 min. The negative control was performed using a sperm lysate, where p110 catalyzing subunit of PI3K was previously removed by preincubation with the respective antibody (1 h at room temperature) and subsequently immunoprecipitated with protein A/G-agarose. As a positive control, MCF-7 samples were treated with 100 nM insulin for 10 min before lysis and immunoprecipitated with anti-IRS-1 from 500 μg of cell lysates. ERα was precipitated from 500 μg of sperm lysates. The immunoprecipitates were washed once with cold PBS, twice with 0.5 M LiCl, 0.1 M Tris (pH 7.4), and finally with 10 mM Tris, 100 mM NaCl, 1 mM EDTA. The presence of PI3K activity in immunoprecipitates was determined by incubating the beads with reaction buffer containing 10 mM HEPES (pH 7.4), 10 mM $MgCl_2$, 50 μM ATP, 20 μCi [γ-^{32}P] ATP, and 10 μg L-α-phosphatidylinositol-4,5-bis phosphate (PI-4,5-P_2) for 20 min at 37 C. The reactions were stopped by adding 100 μl of 1 M HCl. Phospholipids were extracted with 200 μl $CHCl_3$/methanol. For extraction of lipids, 200 μl chloroform:methanol (1:1, vol/vol) were added to the samples and vortexed for 20 sec. Phase separation was facilitated by centrifugation at 5000 rpm for 2 min in a tabletop centrifuge. The upper phase was removed, and the lower chloroform phase was washed once more with clear upper phase. The washed chloroform phase was dried under a stream of nitrogen gas and redissolved in 30 μl chloroform. The labeled products of the kinase reaction, the PI phosphates, then were spotted onto *trans*-1,2-diaminocyclohexane-*N*,*N*,*N*′,*N*′-tetraacetic acid–treated silica gel 60 thin-layer chromatography plates. Radioactive spots were visualized by autoradiography.

Results

RT-PCR and Southern blot

To determine whether mRNAs for both ERs are present in human ejaculated spermatozoa, RNA isolated from pooled purified sample of normal men was subjected to reverse PCR and then to Southern blot analysis. The products were not a result of any contamination in semen samples because the RNA was extracted from a pooled sperm population selected by Percoll procedure. Moreover, sperm samples were checked under ×100 magnification under a bright-field light microscope to rule out the possibility of any contamination with other cells. Furthermore, the samples were also subjected to RT-PCR using primers specific for Myelo Pox to rule out the possibility of granulocyte contamination, and no product was detected for Myelo Pox in sperm RNA (12). The RT-PCR products for ERα and ERβ in sperm were also not a result of any DNA contamination because the RNA samples were subjected to Dnase treatment before RT-PCR. Therefore, sequences of the two ERs were deduced from the cDNA sequence of the human conventional ERα and ERβ. Further, we did not obtain any product when RT was omitted from the amplification reaction carried out in the presence of *Taq* polimerase alone. RT-PCR amplification of ERα and ERβ in human ejaculated spermatozoa revealed the expected PCR product size of 1170 bp for ERα and of 692 bp ERβ. To verify the identity of the amplified products, we performed Southern blot analysis. The results depicted in Fig. 1 show the hybridized bands (S) with similar mobility in the positive controls (+).

Western blot analysis of human spermatozoa proteins showed expression of both ERα and ERβ

To demonstrate the presence of the two ERs proteins, we performed Western blot analysis. We observed that human ejaculated spermatozoa showed the expression of both ERα and ERβ as a single band corresponding to the molecular mass values of 67 kDa for ERα (Fig. 2A) and of 55 kDa for ERβ (Fig. 2B) noted in other tissues. ERα was detected with a monoclonal ERα antibody (epitope mapping at the carboxy terminus of ERα of human origin), whereas ERβ was detected with two different polyclonal antibodies raised against the ammino terminus of ERβ, tested separately. The negative controls (lane 2) were performed using a sperm lysate, where ERα and ERβ were previously removed by preincubation with the respective antibodies (1 h at room temperature) and subsequently immunoprecipitated with protein A/G-agarose. As positive controls, MCF-7 (breast cancer cell line) was used for ERα (lane 1), whereas LnCap (prostate cancer cell line) was used for ERβ (lane 1).

Localization of ERα and ERβ in the human spermatozoa

To investigate the cellular localization of the two ERs, we did perform immunofluorescence assay. Positive stainings

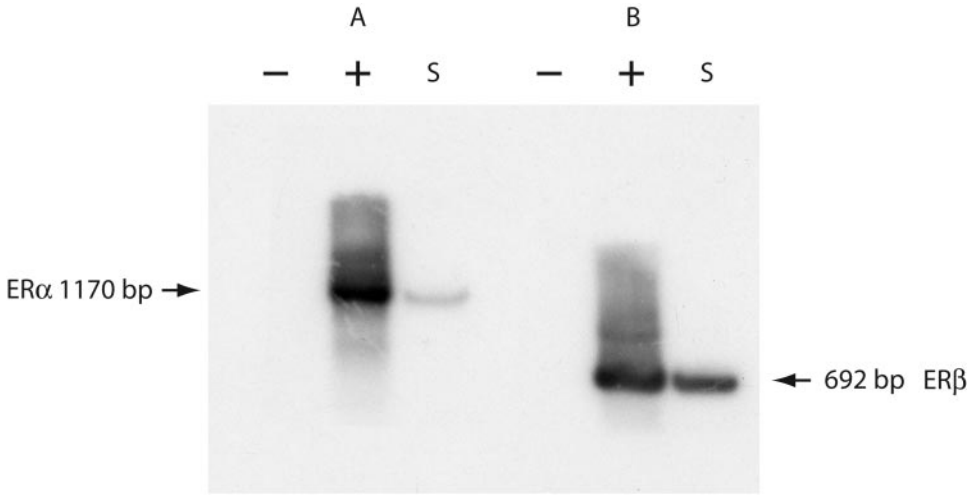

FIG. 1. Southern blot detection of ERα and ERβ in ejaculated spermatozoa of normal man. Total RNA was isolated from purified pooled spermatozoa of normal men, amplified by RT-PCR, and subjected to Southern blot analysis. ERα- and ERβ-specific fragments were detected by hybridization of the membrane with specific oligonucleotides as described in *Materials and Methods*. A, Negative control (no reverse transcriptase added) (−); vector containing the coding region of the human ERα cDNA used as the positive control (+); spermatozoa (S). B, negative control (no cDNA added) (−; vector containing the coding region of the human ERβ cDNA used as the positive control (+); spermatozoa (S). Molecular weight marker is shown *on the left* (in base pairs). The autoradiography presented in the figure is a representative example of experiments that were performed at least three times with repetitive results.

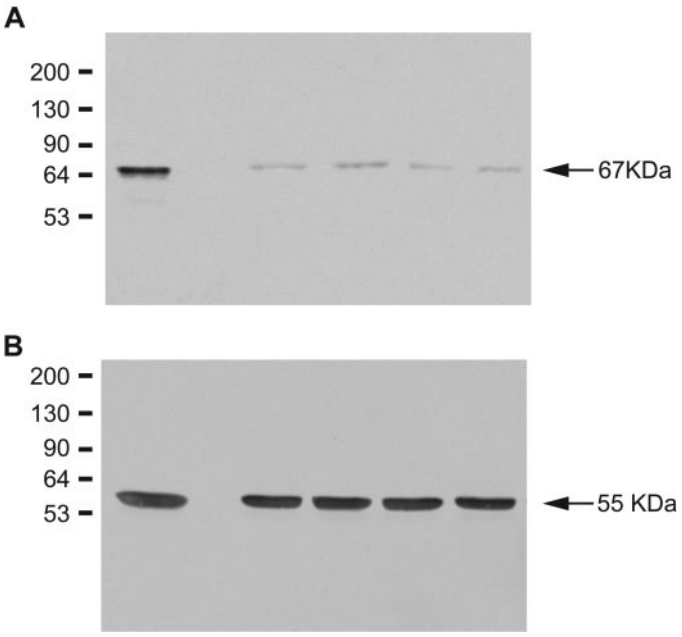

FIG. 2. Western blotting analysis of ERα and ERβ in human ejaculate spermatozoa. Extracts of pooled purified ejaculated spermatozoa were subjected to electrophoresis on 10% SDS-polyacrylamide gels, blotted onto nitrocellulose membranes, and probed with mouse monoclonal antibody to human ERα (A) or rabbit polyclonal antibody to human ERβ (B). A, ERα expression in four samples of ejaculated spermatozoa from normal men (lanes 3–5). MCF-7 extract was used as control (lane 1). B, ERβ expression in four samples of ejaculated spermatozoa from normal men (lanes 3–5). LNCaP extract was used as control (lane 1). The negative controls performed using sperm lysates, where ERα or ERβ were previously removed by preincubation with the respective antibodies (1 h at room temperature) and subsequently immunoprecipitated with protein A/G-agarose, are represented in lane 2 of each blot. The *number on the left* corresponds to molecular masses (kilodaltons) of the marker proteins. The experiments were repeated at least 10 times, and the autoradiographs of the figure show the results of one representative experiment.

for both ER proteins were observed (Fig. 3). Furthermore, a different localization of the two ERs was detected in sperm cells. In fact, ERα was prevalently localized in the midpiece region (A1), according to a previous report (5), whereas ERβ was detected in all the tail region (B1), with an overlapping distribution of ERα and ERβ in the proximal region of the tail. No immunoreaction was detected in the negative controls (A2, B2), thus demonstrating the immunostaining specificity.

Activation of the PI3K/AKT pathway, Bcl-2, and ERK 1/2 by estradiol

To determine the potential role of estrogen/ERs in sperm survival signaling, E_2 was added to spermatozoa at the increasing concentrations of 10 nM, 100 nM, and 1 μM for 30 min. To test whether the effects of E_2 were mediated by ERs, ICI was added at a final concentration of 100 nM alone or with E_2 (100 nM) after a preincubation of 30 min. An increase on the activation of PDK-1, Akt S473, Akt T308, GSK-3, and Bcl-2 was observed in sperm lysates in a dose-dependent manner, whereas ICI reduces E_2-induced activation (Fig. 4A). Because ERK1/2 (18) also play an important role in survival signaling, we evaluated whether they were activated by E_2 in human ejaculated spermatozoa. E_2 induced the activation of the kinases in a dose-dependent manner, whereas ICI is able to reduce this effect, suggesting an involvement of ERs (Fig. 4B). A total of 10 μM wortmannin or 10 μM LY reduced estrogen-induced Akt S473 and Akt T308 phosphorylations, suggesting how this occurs through a PI3K activation (Fig. 4C).

ERα coprecipitates with the p55 regulatory subunit of PI3K

Recent studies demonstrated that ERα binds to the p85 regulatory subunit of PI3K in endotelial cells (19, 20), so we asked whether the association would occur in human ejaculated spermatozoa. As shown in Fig. 5A, ERα constitutively associated with the p55 regulatory subunit of PI3K. Our

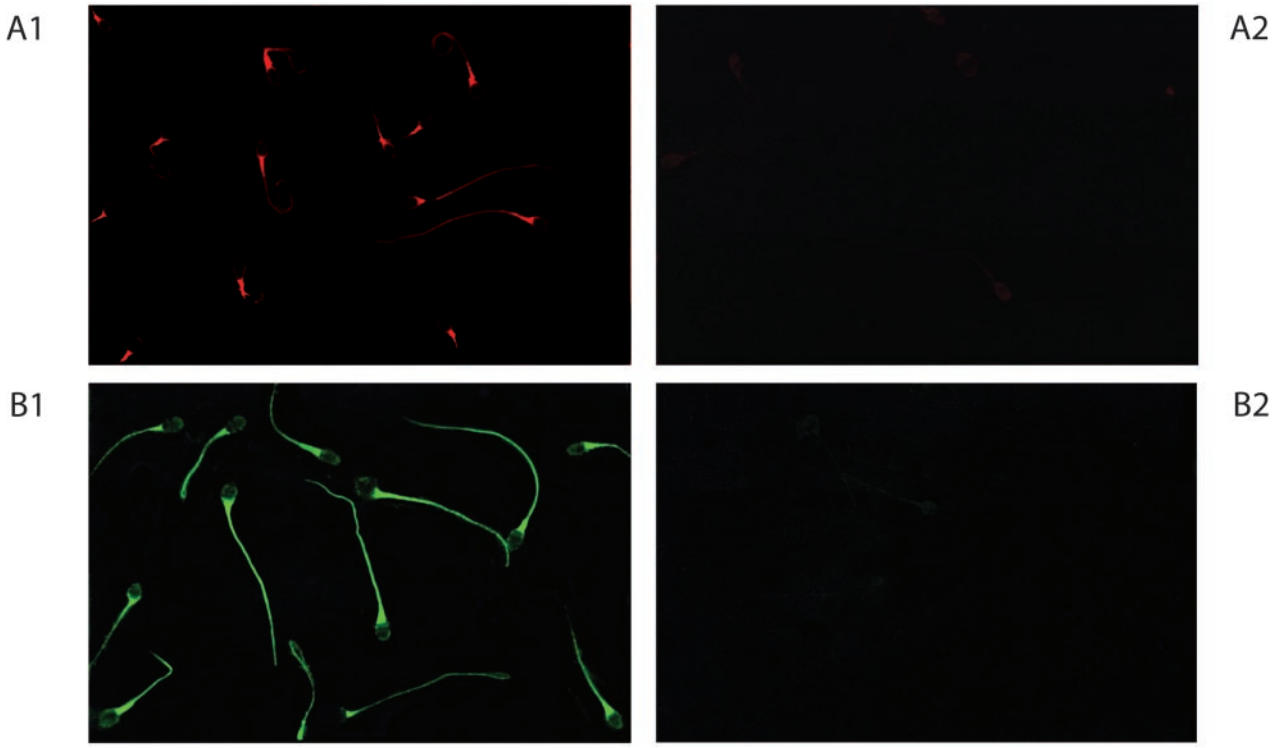

FIG. 3. Immunolocalization of ERα and ERβ in human ejaculated spermatozoa. Percolled spermatozoa were fixed and analyzed by staining with monoclonal ERα antibody (epitope mapping at the carboxy terminus of ERα of human origin) (A1) or with the polyclonal antibody to ERβ (epitope corresponding to amino acids 1–150 mapping at the amino terminus of ERβ of human origin) (B1). Sperm cells incubated without the primary antibodies were used as the negative controls (A2 and B2). The pictures shown are representative examples of experiments that were performed at least three times with repetitive results.

antibody anti-p85 regulatory subunit of PI3K recognized in spermatozoa a single band of 55 kDa; whereas in other cellular types (*i.e.* TM4 and MCF-7), it recognized both 85-kDa and 55-kDa bands (Fig. 5A). This result fits well with previous findings reporting the 55 kDa as the predominant regulatory subunit of PI3K in human testis (21). As can be noted, the interaction is specific for the subtype α of the ER, because we were unable to detect any association between ERβ and the p55 regulatory subunit of PI3K in any experimental condition. The ERα/p55 complex exhibits an intrinsic PI3K activity that is enhanced in the presence of E_2, and it is reduced by ICI as well as by LY (Fig. 5B).

ERβ coprecipitates with Akt

To further investigate the effects of the two ERs in the PI3K pathway, sperm lysates were immunoprecipitated with anti-ERα or two different antibodies raised against ERβ and detected with anti-Akt1 or anti-pAkt1/2/3Ser or anti-Akt1Threo or *vice versa* (Fig. 6A). As shown, the interaction is specific for the subtype β of the ER, because we were unable to detect association between ERα and Akt in our experimental conditions. Besides, ERβ constitutively associated with Akt1 or p-Akt1/Akt2/Akt3 S473 or p-Akt1/Akt2/Akt3 T308 or *vice versa*, and this interaction was unaffected by 10 nM E_2 as well as by 100 nM ICI or 10 μM LY (Fig. 6B). We were unable to assign Akt phosphorylation to different Akt isoforms, because the commercially available antibodies recognize sites analogous to S473 and T308 in Akt1, Akt2, and Akt3.

Discussion

Earlier, it was thought that a single ER was responsible for the biological actions of estrogen (22). However, the identification of ERβ and the discovery that ERα and ERβ can heterodimerize *in vitro* (23) have complicated the analysis of the molecular mechanisms of estrogen action. ERα expression has already been reported in human ejaculated spermatozoa (5), whereas the concomitant presence of ERs subtype has never been investigated. In the present study, we have first demonstrated the presence of both ERα and ERβ in human ejaculated spermatozoa at different levels: mRNA, protein content, and immunolocalization.

The presence and the significance of several mRNAs shown in mammalian spermatozoa are currently under investigation (24). New findings suggest that some of these transcripts code for proteins essential in early embryo development (25). Expression of ERβ protein in the male gamete is a novel finding. In Western blot analysis, ERα and ERβ were recognized at the same sizes as reported for the human native ERα and ERβ. It is now quite clear that ERs, in addition to their classic genomic action, also regulate cellular processes through their nongenomic mechanism (26). For instance, we demonstrated how the rapid effect of either estrogens or aromatizable steroids in ejaculated spermatozoa may trigger both capacitation and acrosome reaction (13). Because here we provide evidence that estrogens may also modulate an important pathway related to survival in dif-

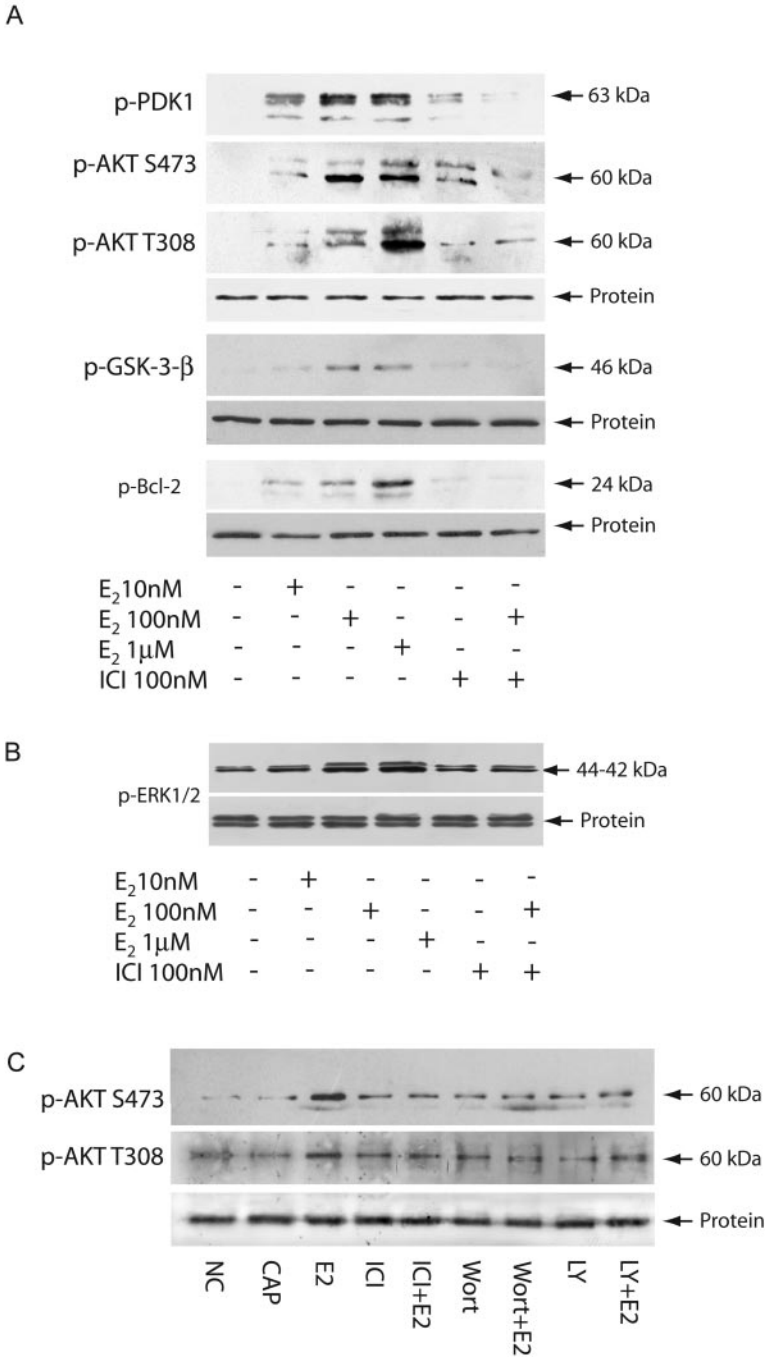

FIG. 4. Effect of increasing concentrations of estradiol on PI3K/Akt pathway, Bcl-2, and ERK1/2 activation. A and B, Washed human spermatozoa were incubated in unsupplemented Earle's balanced salt solution for 30 min at 37 C, 5% CO_2 in the presence of 10 nM, 100 nM, and 1 μM 17β-estradiol. To test whether the effects of estradiol were mediated by ERs, ICI was added at a final concentration of 100 nM alone or with E_2 (100 nM) after a preincubation of 30 min. Protein extracts were made from human sperms under reducing conditions, separated by electrophoresis, transferred to a membrane, and immunoblotted with the indicated antibodies (see *Materials and Methods*). C, Washed human spermatozoa were incubated in unsupplemented Earle's balanced salt solution for 30 min at 37 C, 5% CO_2 in the presence of 100 nM estradiol (E_2), 100 nM ICI, 10 μM wortmannin (Wort), 10 μM LY. The effects of estradiol were tested both on Akt S473 and Akt T308 phosphorylations. NC, Noncapacitated; Cap, capacitated. The autoradiographs presented are representative examples of experiments that were performed at least three times with repetitive results. Molecular weight markers are indicated *on the left* of the blot.

ferent cell types, it remains to be clarified the specific role of each receptor in mediating the sperm survival.

To date, most of the localization studies for both ERs have been performed in rodents (27, 28). In human testis, conflicting data are present with regard to the distribution of the different ER types; both receptors are expressed in germ cells at various stages of development from spermatogonia to elongated spermatids (29, 30). By using specific antibodies to the ER subtypes, we have immunolocalized ERα prevalently in the midpiece region as previously demonstrated (5), whereas ERβ is uniformly distributed along the tail. An overlap of the two ERs occurs in the proximal region of the tail. On the basis of these observations, it is reasonable to presume how each receptor subtype exerts different functions potentially linked to its specific cellular localization. Indeed, the highly polarized structure and function of spermatozoa do compartmentalize specific metabolic and signaling pathways to regions where they are needed.

Recent data show how estradiol acts as a germ cell survival factor in the human testis (4), even though its mechanism of action remains to be elucidated. We have explored the most important pathways involved in cell survival and previously investigated in other cell types, PI3K/Akt (31) and ERK1/2 (32, 33). In various cell types, estradiol stimulates the cascade

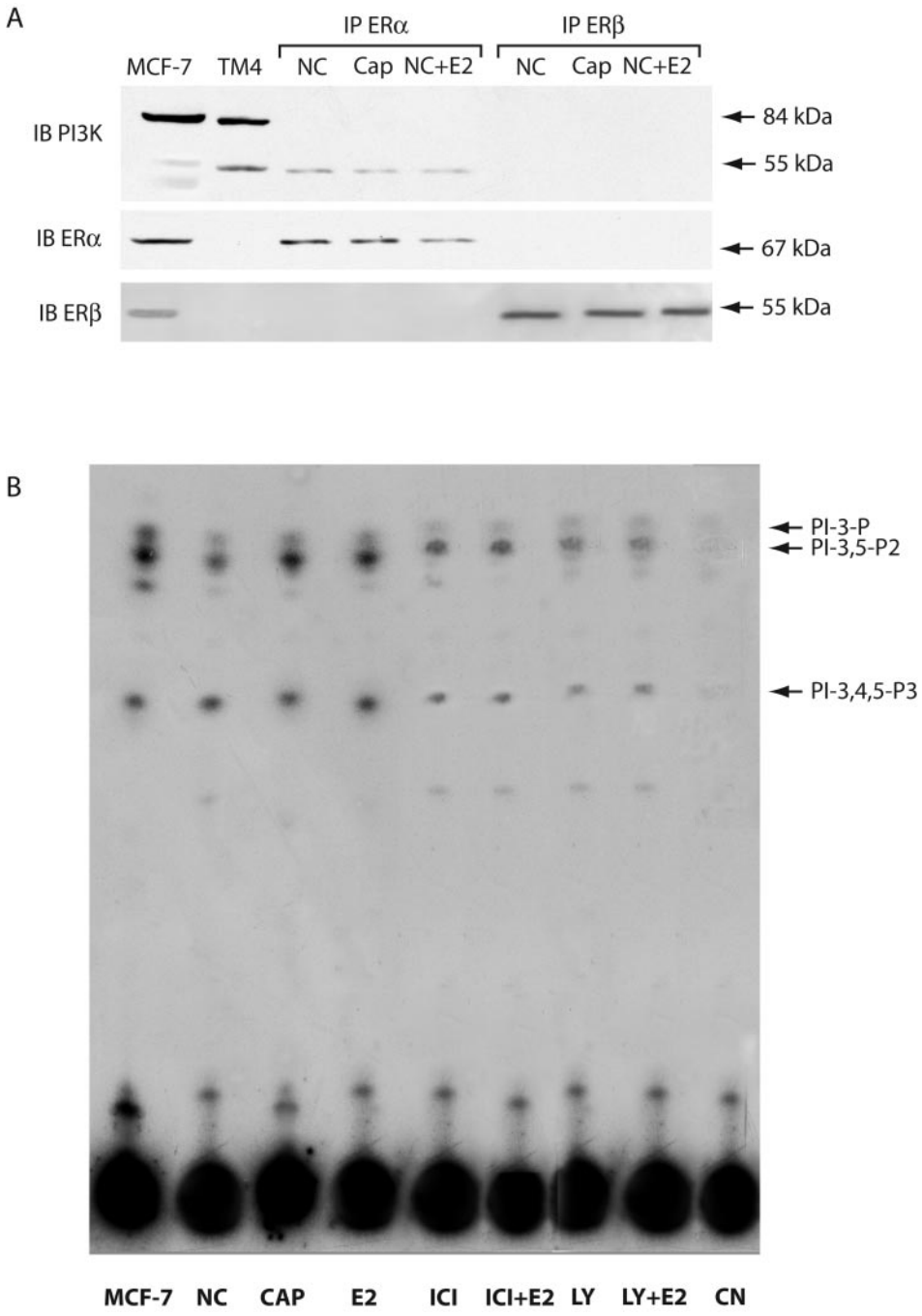

FIG. 5. Coprecipitation between ERα and the p55 regulatory subunit of PI3K induces PI3K activity in human spermatozoa. A, Spermatozoa were washed twice with unsupplemented Earle's medium and were incubated in the unsupplemented Earle's medium for 1 h at 37 C and 5% CO_2, without (NC) or in the presence of 100 nM estradiol (NC+E). Besides, some samples were washed and incubated in capacitating medium (Cap). Five hundred micrograms of sperm lysates were immunoprecipitated using anti-ERα or anti-ERβ antibodies. MCF-7 and TM4 lysates were used as controls (lanes 1 and 2). Molecular weight markers are indicated *on the left* of the blot. B, Spermatozoa were incubated in the unsupplemented Earle's medium for 1 h at 37 C and 5% CO_2, in the absence (NC) or in the presence of 100 nM estradiol (E_2). ICI and LY were added at a final concentration of 100 nM and 10 μM, respectively, alone or with 100 nM E2 after a preincubation of 30 min. Some samples were washed and incubated in Cap. Five hundred micrograms of sperm lysates were immunoprecipitated using anti-ERα antibody, incubated in the presence of 200 μM phosphatidilinositol and 10 μCi of [γ-^{32}P] ATP for 30 min. The negative control (CN) was performed using a sperm lysate, where p110 catalyzing subunit of PI3K was previously removed by preincubation with the respective antibody (1 h at room temperature) and subsequently immunoprecipitated with protein A/G-agarose (lane 9). MCF-7 treated with 100 nM insulin for 10 min before lysis and immunoprecipitated with anti-IRS-1 from 500 μg of cell lysates was used as positive control (lane 1). PI-3,4,5-P3, Phosphatidilinositol 3,4,5-triphosphate; PI-3,5-P2, phosphatidilinositol 3,5-diphosphate; PI-3-P, phosphatidilinositol 3-phosphate. The autoradiographs presented are representative examples of experiments that were performed at least three times with repetitive results.

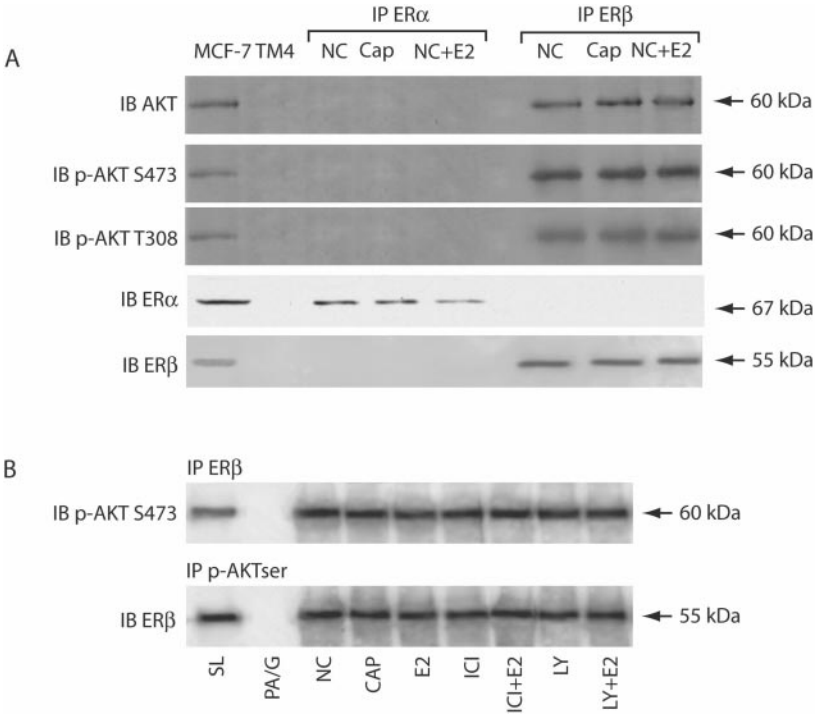

FIG. 6. Coprecipitation between ERβ and Akt1. A, Washed spermatozoa were incubated in the unsupplemented Earle's medium for 1 h at 37 C and 5% CO_2, without (NC) or in the presence of 100 nM E_2 (NC+E). Besides, some samples were washed and incubated in Cap as described in *Materials and Methods*. Five hundred micrograms of sperm lysates were immunoprecipitated using anti-ERα or anti-ERβ antibodies and then blotted with specific antibodies raised to Akt1, AktS473, AktT308, ERα, ERβ. MCF-7 and TM4 lysates were used as controls (lanes 1–2). B, Five hundred micrograms of sperm lysates at different experimental conditions, as indicated in the figure, were immunoprecipitated using anti-ERβ and then blotted with AktS473. Conversely, 500 μg of sperm lysates at different experimental conditions, as indicated in the figure, was immunoprecipitated using anti-AktS473 and then blotted with anti-ERβ. Sperm lysate was used as positive control (SL) (lane 1); negative control samples were precipitated with carrier beads only (PA/G), with the omission of the primary antibody (lane 2). The autoradiographs presented are representative examples of experiments that were performed at least three times with repetitive results. Molecular weight markers are indicated *on the left* of the blot.

that activates the ERK1/2 to inhibit apoptosis (18). This kinase is recognized to mediate cell survival in response to a variety of growth factors targeting a myriad of cell types and has also been proposed to act as a survival protein (18). In human ejaculated spermatozoa, both PI3K/Akt and ERK1/2 pathways appear activated by E_2, and ICI reduces E_2-induced activation of some protein, addressing the involvement of estradiol and ERs in these events. In the same vein, Bcl-2 (34), a key protein in survival signaling, phosphorylated at Serine 70, the physiologically relevant phosphorylation site, necessary for its full and potent antiapoptotic function, is enhanced upon E_2 exposure and inhibited in the presence of ICI. A recent described nongenomic estrogen-signaling pathway exhibits the direct interaction of ERα with the p85 regulatory subunit of PI3K (20, 21). So, we questioned whether the two ERs were able to interact with the PI3K/Akt pathway in human ejaculated spermatozoa. It is worth noting that ERα coprecipitates with the p55 kDa regulatory subunit of PI3K, reported to be the prevalent regulatory subunit expressed in the testis (21), whereas ERβ coprecipitates with Akt1. The complex ERα/p55 contains an intrinsic PI3K activity enhanced in the presence of E_2. The fact that the above described pathway, upon E_2 exposure, is inhibited in a similar extent in the presence of either ICI or the specific PI3K inhibitor led us to postulate that ERα *per se* enhances PI3K activity and consequently also the activity of the downstream effector proteins: PDK1, Akt, and GSK-3. Further, we observed that in the presence of ICI, the ERK1/2, PDK1, and Akt phosphorylations are somehow activated. This unexpected effect could be argued by the fact that the ICI-induced conformational changes of ERα able to abrogate ERα transcriptional activity do not necessary interfere in the ER nongenomic signaling in the absence of its natural ligand.

Even though Akt phosphorylation either in S473 or in T308 residues appears to be not influenced by E_2 in ERβ coprecipitates, it appears clearly up-regulated upon E_2 exposure in cell lysate. Such apparent discrepancy could be due to the fact that the Akt fraction, much more phosphorylated upon E_2 exposure, may not be necessarily involved in the coimmunoprecipitation with ERβ, or that the conformational changes induced by coprecipitation make the phosphorylated Akt not discriminated by our antibody. The selective coimmunoprecipitation of ERα and of ERβ with the p55 regulatory subunit of PI3K and Akt, respectively, discloses a potential separate action of the two ERs on the same pathway. At present, we are unable to distinguish whether the functional role of each ER subtype in sperm survival signaling is redundant or distinct.

Normal male fertility relies on normal spermatogenesis, and the importance of ERs and aromatase in the process was shown at all stages of testicular development, both in somatic cells (35) and in the germ cells (Ref. 3 and references therein). A specific role of estrogen in maintaining sperm fertilizing capability (36–

38) appears to be questioned by a recent study demonstrating that mice germ cells do not require ERα (39) for their terminal morphofunctional differentiation when implanted in normal seminiferous tubules of a wild-type recipient. However, in these circumstances, we should consider that the production and secretion of many proteins/factors by Sertoli cells, involved in germ cells development, may overcome the lack of ERα, adapting themselves to the changed needs of transplanted germ cells. Besides, the potential action of estrogens in germ cells via nonclassical receptors cannot be ruled out.

On the other hand, several findings have demonstrated how estradiol may influence sperm fertilizing capability (36–38) as well as sperm survival (Ref. 5 and references therein). However, the molecular mechanisms related to these events did remain to be disclosed. In the present study, we provided evidence that estrogens in ejaculated spermatozoa activate the PI3K/Akt pathway: ERα and ERβ seem to influence this pathway at different levels and may co-work in controlling sperm survival.

Acknowledgments

Our special thanks to D. Picard and J.-A. Gustafsson for the gifts of pSG5-HeG0 and pCMV5-hERβ, respectively. We also thank D. Sturino and P. Cicirelli (Faculty of Pharmacy, University of Calabria - Italy) for the English review and the graphical support of the manuscript, respectively.

Received September 24,2003. Accepted November 26, 2003.

Address all correspondence and requests for reprints to: Prof. Sebastiano Andò, Faculty of Pharmacy, University of Calabria, Arcavacata di Rende (CS) 87030, Italy. E-mail: sebastiano.ando@unical.it. Alternate E-mail: aquisav@libero.it.

This work was supported by Grant Prot. Number 2003067201 from the COFIN-MIUR-2003.

S.A. and D.S. contributed equally to this work.

References

1. **Hess RA, Bunick D, Lee KH, Bahr J, Taylor JA, Korach KS, Lubahn DB** 1997 A role of oestrogens in the male reproductive system. Nature 390:509–512
2. **Sharpe RM** 1998 The roles of oestrogen in the male. Trends Endocrinol Metab 9:371–376
3. **O'Donnel L, Robertson KM, Jones ME, Simpson ER** 2001 Estrogen and spermatogenesis. Endocr Rev 22:289–318
4. **Pentikainen V, Erkkila K, Suomalainen L, Parvinen M, Dunkel L** 2000 Estradiol acts as a germ cell survival factor in the human testis *in vitro*. J Clin Endocrinol Metab 85:2057–2067
5. **Durkee TJ, Mueller M, Zinaman M** 1998 Identification of estrogen receptor protein and messenger ribonucleic acid in human spermatozoa. Am J Obstet Gynecol 178:1288–1297
6. **Luconi M, Muratori M, Forti G, Baldi E** 1999 Identification and characterisation of a novel functional estrogen receptor on human sperm membrane that interferes with progesterone effects. J Clin Endocrinol Metab 84:1671–1678
7. **Carani C, Qin K, Simoni M, Faustini-Faustini M, Serpente S, Boyd J, Korach KS, Simpson ER** 1997 Effect of testosterone and estradiol in a man with aromatase deficiency. N Engl J Med 337:91–95
8. **Lee KH, Hess RA, Bahr JM, Lubahn DB, Taylor Bunich D** 2000 Estrogen receptor α has a functional role in the mouse rete testis and efferent ductules. Biol Reprod 63:1873–1880
9. **Eddy EM, Washburn TF, Bunch DO, Goulding EH, Gladen BC, Lubahn DB, Korach KS** 1996 Targeted disruption of the estrogen receptor gene in male mice causes alteration of spermatogenesis and infertility. Endocrinology 137:4796–4805
10. **Fisher CR, Graves KH, Parlow AF, Simpson ER** 1998 Characterisation of mice deficient in aromatase (ArKO) because of targeted disruption of the *cyp19* gene. Proc Natl Acad Sci USA 95:6965–6970
11. **Robertson KM, O'Donnell L, Jones ME, Meachem SJ, Boon WC, Fisher CR, Graves KH, McLachlan RI, Simpson ER** 1999 Impairment of spermatogenesis in mice lacking a functional aromatase (*cyp 19*) gene. Proc Natl Acad Sci USA 96:7986–7991
12. **Aquila S, Sisci D, Gentile ME, Middea E, Siciliano L, Andò S** 2002 Human ejaculated spermatozoa contain active P450 aromatase. J Clin Endocrinol Metab 87:3385–3390
13. **Aquila S, Sisci D, Gentile ME, Carpino A, Middea E, Catalano S, Rago V, Andò S** 2003 Towards a physiological role for cytochrome P450 aromatase in ejaculated human sperm. Hum Reprod 18:1650–1659
14. **Ho KJ, Liao JK** 2002 Nonnuclear action of estrogen. Arterioscler Thromb Vasc Biol 22:1952–1961
15. **Mosselman S, Polman J, Dijkema R** 1996 ERβ: identification and characterization of a novel human estrogen receptor. FEBS Lett 392:49–53
16. **World Health Organization** 1999 WHO laboratory manual for the examination of human semen and sperm-cervical mucus interactions. 4th ed. Cambridge, UK: Cambridge University Press
17. **Bradford MM** 1976 A rapid and sensitive method for the quantitation of microgram quantities of protein utilizing the principle of protein-dye binding. Anal Biochem 72:248–254
18. **Razandi M, Pedram A, Levin ER** 2000 Plasma membrane estrogen receptors signal to antiapoptosis in breast cancer. Mol Endocrinol 14:1434–1447
19. **Simoncini T, Hafezi-Moghadam A, Brazil DP, Ley K, Chin WW, Liao JK** 2000 Interaction of oestrogen receptor with the regulatory subunit of phosphatidylinositol-3-OH kinase. Nature 407:538–541
20. **Sun M, Paciga JE, Feldman RI, Yuan Z, Coppola D, Lu YY, Shelley SA, Nicosia SV, Cheng JQ** 2001 Phosphatidylinositol-3-OH kinase (PI3K)/AKT2, activated in breast cancer, regulates and is induced by estrogen receptor α(ERα) via interaction between ERα and PI3K. Cancer Res 61:5985–5991
21. **Pons S, Asano T, Glasheen E, Miralpeix M, Zhang Y, Fisher TL, Myers Jr MG, Sun XJ, White MF** 1995 The structure and function of p55PI3K reveal a new regulatory subunit for phosphatidylinositol 3-kinase. Mol Cell Biol 15:4453–4465
22. **Sounders PT** 1998 Oestrogen receptor β. Rev Reprod 3:164–171
23. **Ogawa S, Inoue S, Watanabe T, Hiroi H, Orimo A, Hosoi T, Ouchi Y, Muramatsu M** 1998 The complete primary structure of human estrogen receptor β (hERβ) and its heterodimerization with ERα *in vivo* and *in vitro*. Biochem Biophys Res Commun 243:122–126
24. **Miller D** 2000 Analysis and significance of messenger RNA in human ejaculated spermatozoa. Mol Reprod Dev 56:259–264
25. **Ostermeier GC, Dix DJ, Miller D, Khatri P, Krawetz SA** 2002 Spermatozoal RNA profiles of normal fertile men. Lancet 360:772–777
26. **Cato ACB, Nestl A, Mink S** 2002 Rapid actions of steroid receptors in cellular signaling pathways. Sci STKE 138:RE9
27. **Pelletier G, Labrie C, Labrie F** 2000 Localization of oestrogen receptor α, oestrogen receptor β and androgen receptors in the rat reproductive organs. J Endocrinol 165:359–370
28. **Shughrue PJ, Lane MV, Scrimo PJ, Merchenthaler I** 1998 Comparative distribution of estrogen receptor-α (ER-α) and β (ER-β) mRNA in the rat pituitary, gonad, and reproductive tract. Steroids 63:498–504
29. **Makinen S, Makela S, Weihua Z, Warner M, Rosenlund B, Salmi S, Hovatta O, Gustafsson JK** 2001 Localization of oestrogen receptors α and β in human testis. Mol Hum Reprod 7:497–503
30. **Pelletier G, El-Alfy M** 2000 Immunocytochemical localization of estrogen receptors α and β in the human reproductive organs. J Clin Endocrinol Metab 85:4835–4840
31. **Cantley LC** 2002 Phosphoinositide 3-kinase pathway. Science 296:1655–1657
32. **Aikawa R, Komuro I, Yamazaki T, Zou Y, Kudoh S, Tanaka M, Shiojima I, Hiroi Y, Yazaki Y** 1997 Oxidative stress activates extracellular signal-regulated kinases through Src and Ras in cultured cardiac myocytes of neonatal rats. J Clin Invest 100:1813–1821
33. **Berra E, Municio MM, Sanz L, Frutos S, Diaz-Meco MT, Moscat J** 1997 Positioning atypical protein kinase C isoforms in the UV-induced apoptotic signaling cascade. Mol Cell Biol 17:4346–4354
34. **Ito T, Deng X, Carr BK, May WS** 1997 Bcl-2 phosphorylation required for anti-apoptosis function. J Biol Chem 272:11671–11673
35. **Mahato D, Goulding EH, Korach KS, Eddy EM** 2001 Estrogen receptor-α is required by the supporting somatic cells for spermatogenesis. Mol Cell Endocrinol 178:57–63
36. **Adeoya-Osiguva SA, Markoulaki S, Pocock V, Milligan SR, Fraser LR** 2003 17β-Estradiol and environmental estrogens significantly affect mammalian sperm function. Hum Reprod 18:100–107
37. **Idaomar M, Guerin JF, Lorange J, Cziba JC** 1989 Stimulation of motility and energy metabolism of spermatozoa from astenozoospermic patients by 17β-estradiol. Arch Androl 22:197–202
38. **Saberwal GS, Sharma MK, Balasinor N, Choudhary J, Juneja HS** 2002 Estrogen receptor, calcium mobilization and rat sperm motility. Mol Cell Biochem 237:11–20
39. **Mahato D, Goulding EH, Korach KS, Eddy EM** 2000 Spermatogenic cells do not require estrogen receptor-α for development or function. Endocrinology 141:1273–1276

Oncogene (2004), 1–11

www.nature.com/onc

ORIGINAL PAPER

Fibronectin and type IV collagen activate ERα AF-1 by c-Src pathway: effect on breast cancer cell motility

Diego Sisci[1,3], Saveria Aquila[1,3], Emilia Middea[1], Mariaelena Gentile[2], Marcello Maggiolini[1], Fabrizia Mastroianni[1], Daniela Montanaro[1] and Sebastiano Andò*[,2]

[1]*Dipartimento Farmaco-Biologico, Università della Calabria, Arcavacata di Rende, Italy;* [2]*Dipartimento di Biologia Cellulare, Centro Sanitario, Università della Calabria, Arcavacata di Rende, Cosenza 87030, Italy*

The expression of estrogen receptor alpha (ERα) is generally associated with a less invasive and aggressive phenotype in breast carcinoma. In an attempt to understand the role of ERα in regulating breast cancer cells invasiveness, we have demonstrated that cell adhesion on fibronectin (Fn) and type IV Collagen (Col) induces ERα-mediated transcription and reduces cell migration in MCF-7 and in MDA-MB-231 cell lines expressing ERα. Analysis of deleted mutants of ERα indicates that the transcriptional activation function (AF)-1 is required for ERα-mediated transcription as well as for the inhibition of cell migration induced by cell adhesion on extracellular matrix (ECM) proteins. In addition, the nuclear localization signal region and some serine residues in the AF-1 of the ERα are both required for the regulation of cell invasiveness as we have observed in HeLa cells. It is worth noting that c-Src activation is coincident with adhesion of cells to ECM proteins and that the inhibition of c-Src activity by PP2 or the expression of a dominant-negative c-Src abolishes ERα-mediated transcription and partially reverts the inhibition of cell invasiveness in ERα-positive cancer cells. These findings address the integrated role of ECM proteins and ERα in influencing breast cancer cell motility through a mechanism that involves c-Src and seems not to be related to a specific cell type.
Oncogene advance online publication, 27 September 2004; doi:10.1038/sj.onc.1208098

Keywords: estrogen receptor alpha; extracellular matrix; fibronectin; type IV collagen; c-Src

Introduction

Several clinical studies have demonstrated that estrogen receptor alpha (ERα)-positive tumors have lower metastatic potential than ERα-negative tumors (Fraker *et al*., 1984; Osborne *et al*., 1985; McGuire, 1986; Price *et al*., 1990). Many reports correlate ERα expression to lower matrigel invasiveness and to a reduced metastatic potential of breast cancer cell lines (Liotta *et al*., 1991; Thompson *et al*., 1992; Rochefort *et al*., 1998); however, the molecular mechanisms that define this process are still unclear. The interaction of cells with the extracellular matrix (ECM) influences many aspects of cell behavior, including growth, morphology, migratory properties and differentiation (Hynes, 1990; Clark and Brugge, 1995; Giancotti and Ruoslahti, 1999). The adhesion to ECM is mediated by integrin receptors that are reported to control growth factor signaling pathways. Specifically, cells adherent to ECM show an enhanced activation of the p42 and p44 forms of the mitogen-activated protein kinase (MAPK) (Miyamoto *et al*., 1996; Lin *et al*., 1997; Renshaw *et al*., 1997; Aplin and Juliano, 1999). In addition, binding of the integrin receptor with ECM proteins causes a direct transient activation of MAP kinase in the absence of growth factors (Chen *et al*., 1994; Schlaepfer *et al*., 1994; Zhu and Assoian, 1995).

The transcriptional activation function (AF)-1 of the N-terminal ERα is a target of various protein kinases such as MAPK, PI3-k, Akt and c-Src, which are activated by growth factor pathways, either in the presence or in the absence of 17β-estradiol (E_2) (Power *et al*., 1991; Chalbos *et al*., 1993; Aronica *et al*., 1994; Kato *et al*., 1994; Couse *et al*., 1995; Ignar-Trowbridge *et al*., 1995; Bunone *et al*., 1996; Weigel, 1996; Joel *et al*., 1998). c-Src is also one of the first protein kinases activated by cell adhesion to ECM (Guan, 1997; Schlaepfer *et al*., 1997; Schaller *et al*., 1999) and it has been shown to play a significant role in several phases of outside–in signaling in many cell types (Kaplan *et al*., 1995; Lowell *et al*., 1996; Suen *et al*., 1999). The overexpression and activation of Src family kinases have been identified in a range of human cancers (Irby and Yeatman, 2000) and these have been indicated to contribute not only to the growth and survival of breast cancer cells but also to increase their metastatic potential (Summy and Gallick, 2003).

In this study, we have tested the hypothesis that cell adhesion on ECM modulates ERα transcriptional activity, producing a reduction of cell migration. Our results show that estrogen receptor activation function 1 (AF-1)/ERα is an effector of the adhesion protein signals. Cell adhesion on Fibronectin (Fn) and type IV collagen (Col) induces the transcriptional activation of

*Correspondence: S Andò; E-mail: sebastiano.ando@unical.it
[3]These authors contributed equally to this work
Received 27 January 2004; revised 21 May 2004; accepted 8 July 2004

ERα and the reduction of cell migration in MCF-7 cells, as well as in MDA-MB-231 and in HeLa cells both engineered to express ERα. In addition, we have found that c-Src is essential for ERα activation in response to cell adhesion. Focusing on the relationship between c-Src activity and ERα expression in breast cancer cells, we have shown that the transactivation of ERα upon cell adhesion on ECM proteins counteracts the action of c-Src on cell motility and invasiveness in cancerous cells.

Results

Cell adhesion on Fn or Col induces ERα translocation into the nuclear compartment

First, we determined whether cell adhesion on either Fn or Col may influence ERα expression. MCF-7 cells, serum-starved for 24 h, were plated onto Fn-, Col- and P-Lys- (negative control) coated dishes and incubated for 30 min, 1 h, 4 h and 8 h. Equal amounts of cytosolic and total (nuclear + cytosolic) protein lysates were resolved by SDS–PAGE and analysed by Western blot for ERα detection. Figure 1b shows a significant decrease of ERα content in the cytosol 30 min to 4 h after cell adhesion on Fn and Col with respect to the control reported in Figure 1a. No substantial changes in total ERα content were observed in our time course study (Figure 1b). These results support the conclusion that cell adhesion on either Fn or Col induced a translocation of ERα into the nuclear compartment. The observed compartmentalization of ERα was confirmed by immunocytochemistry using MCF-7 cells maintained in a serum-free medium for 96 h, then detached, plated onto Fn-, Col- and P-Lys-coated slides and incubated for 2 h (Figure 1c). No signal was detected in the control cells (P-Lys); this may be due to the binding of ERα with chaperon proteins that possibly mask the epitope for the ERα antibody.

Fn and Col induce estrogen-responsive element (ERE) transcription

Since Fn and Col were able to translocate ERα into the nuclear compartment, we evaluated their ability to induce ERα-mediated transcription. MCF-7 cells were transfected with the ERE responsive reporter plasmid (XETL) and the pRL-Tk plasmid expressing *Renilla luciferase*, as an internal control. The cells were then serum starved for 24 h and exposed to E_2, Fn, Col or P-Lys before luciferase assays. Figure 2a shows a significant increase in ERE-mediated transcription induced by both Fn and Col in the absence of ER ligand. In contrast, P-Lys failed to induce ERα-mediated transcription, showing that the observed effect is specifically due to the integrin substrates.

The same results were obtained in MDA-MB-231 cells transiently expressing ERα and the reporter gene, suggesting that the Fn/Col-induced transcriptional activation is specifically mediated by ERα (Figure 2c). A slight but significant increase in luciferase expression was observed in wild-type MDA-MB-231 treated with both Fn and Col (Figure 2b), probably due to the expression of ERβ (Lazennec *et al*., 2001), as we detected in the present study (data not shown). The antiestrogen ICI reversed this upregulatory effect induced by both ECM proteins in all the experimental conditions and in both cell lines.

In addition, no substantial differences were observed in luciferase expression when transfected MCF-7 and MDA-MB-231 were plated onto both Fn- and Col-coated dishes (data not shown).

ERE-mediated transcription induced by Fn and Col upregulates pS2 and cathepsin D mRNA

Owing to their ability to induce ERE-mediated transcription, Fn and Col were assessed for their capacity to regulate the expression of endogenous ERα-specific target genes as pS2 (Figure 3a) and cathepsin D (Figure 3b).

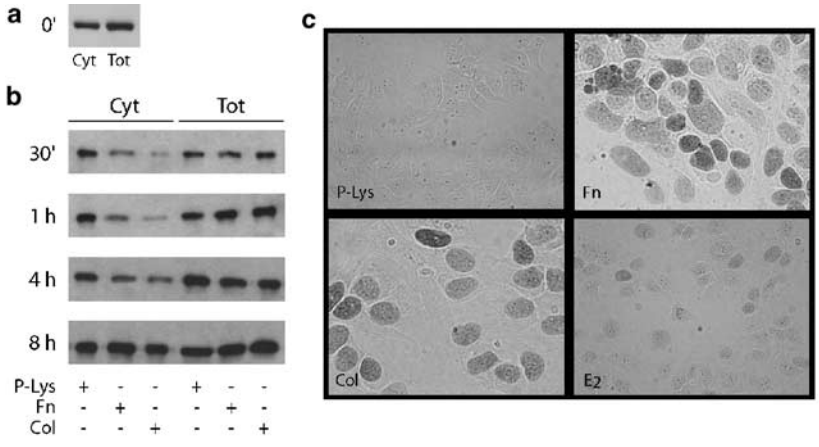

Figure 1 Cell adhesion on Fn or Col induces ERα translocation into the nuclear compartment. (**a**) MCF-7 cells serum-starved for 24 h were detached and an aliquot was lysed and used as control (time 0); (**b**) a further aliquot was plated in PRF-SFM on P-Lys- (2 μg/cm^2), Fn- (30 μg/ml) or Col- (30 μg/ml) coated dishes. After 30 min, 1 h, 4 h and 8 h of incubation, cytosolic (Cyt) and total (cytosolic and nuclear) (Tot) protein lysates were subjected to Western blotting with an anti-ERα monoclonal antibody. These results are representative of five independent experiments. (**c**) MCF-7 cells serum starved for 96 h were detached and plated in PRF-SFM on P-Lys- (2 μg/cm^2), Fn- (30 μg/ml) and Col- (30 μg/ml) coated slides or plated on culture-treated slide and incubated with E_2 (10 nM). After 2 h, cells were fixed, probed with anti-ERα antibody and stained as described in Materials and methods

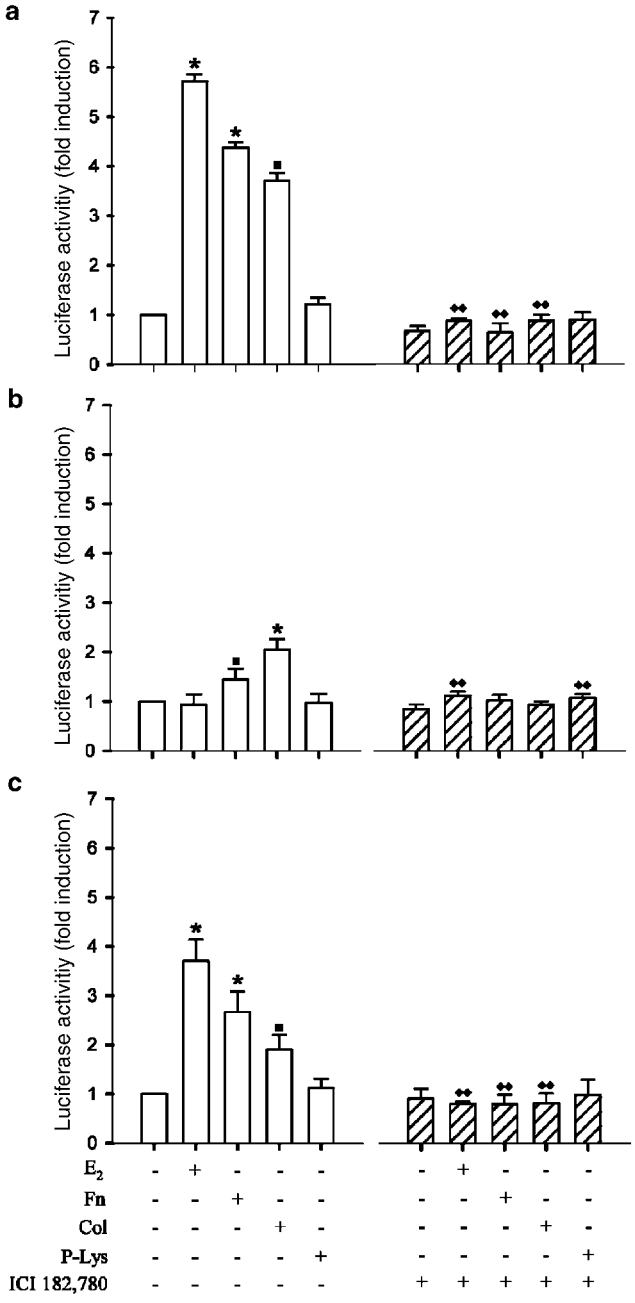

Figure 2 Fn and Col activate ERE-mediated transcription. MCF-7 (**a**) and MDA-MB-231 (**b**) cells were transfected with 0.3 μg/well of pSG5 and 0.6 μg/well of XETL by calcium phosphate method. MDA-MB-231 were also cotransfected with 0.3 μg/well HeG0 and 0.6 μg/well of XETL (**c**). Cells were incubated in the transfection cocktail for 6 h, serum starved for an additional 24 h and then incubated for 16 h in PRF-SFM (untreated) or in PRF-SFM containing either 10 nM estradiol (E_2), 30 μg/ml Fn, 30 μg/ml Col or 15 μg/ml P-Lys. The same treatments were also carried out in the presence of 100 nM ICI 182,780. Firefly luciferase activity was internally normalized to *R. luciferase* and expressed as fold of increase with respect to the PRF-SFM (untreated) sample. Results represent the mean $\pm$ s.d. of at least five independent experiments. $^{\star}P<0.001$ *vs* PRF-SFM; $^{\blacksquare}P<0.05$ *vs* PRF-SFM; $^{\blacklozenge\blacklozenge}P<0.001$ *vs* the homologues samples without ICI 182,780

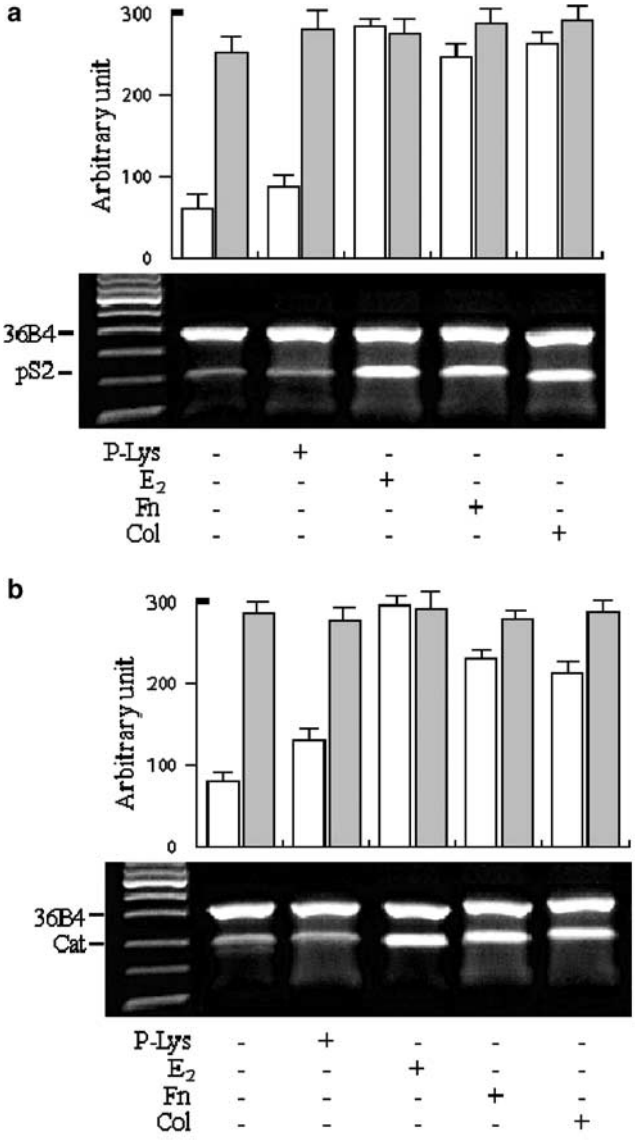

Figure 3 Adhesion of breast cancer cells on Fn and Col upregulates pS2 and cathepsin D mRNA levels. Semiquantitative RT–PCR of pS2 mRNA (**a**) and cathepsin D (**b**). Serum-starved MCF-7 cells were detached and plated, in PRF-SFM, on dishes previously coated with 2 μg/cm^2 P-Lys, 30 μg/ml Fn (Fn), 30 μg/ml or plated on uncoated dishes and treated with 10 nM estradiol (E_2). The 36B4 mRNA levels were determined in the same amplification tube as control. The quantitative representation of three independent experiments expressing the optical density of pS2 (□) and 36B4 (▩) RT–PCR products (**a**) and of cathepsin D (□) and 36B4 (▩) RT–PCR products (**b**) is reported in the histograms

The results show the ability of Fn and Col, but not of P-Lys, to upregulate both pS2 and cathepsin D mRNAs.

Fn and Col induce ERE-mediated transcription through AF-1 activation

Subsequently, we questioned which functional domain of ERα was affected by the adhesion protein signals. To exclude the influence of specific factors present in breast cancer cells, we transiently cotransfected HeLa cells with

the reporter plasmid XETL and with either HeG0 (data not shown) or HE15 (Figure 4a) or HE19 (Figure 4b) coding for the carboxyl-terminal and amino-terminal truncated receptor, respectively. The treatment with either E_2 or Fn and Col leads to an increase of luciferase activity in HeLa cells expressing ERα corresponding to that observed in MCF-7 (data not shown). Both ECM proteins induced ERE-mediated transcription only in HeLa cells transiently expressing the AF-1/DBD domains of ERα (Figure 4a), while the treatment with E_2 gave a significant increase of ERE-mediated transcription when the AF-2/DBD domains of ERα were expressed (Figure 4b). ICI abolished the upregulatory effects induced by Fn, Col and E_2, while 4-OH tamoxifen (4OH-Tam) treatment was able to negatively interfere only with E_2-induced activation in cells expressing either ERα (data not shown) or the AF-2/DBD domains of ERα. In summary, these data demonstrate that either Fn or Col is able to activate ERα by targeting the AF-1 domain.

Fn and Col activate ERα through c-Src

On the basis of previous findings demonstrating that c-Src is activated by Fn (Schlaepfer *et al*., 1997) and that ERα is activated in its AF-1 domain by signals transduced from c-Src (Feng *et al*., 2001), we questioned whether c-Src might be involved in ERα activation induced by cell adhesion/treatment to Fn and Col. We investigated the role of c-Src in MCF-7 cells transfected with pcDNA3 as control vector, c-Src(+) and c-Src(−) (dominant negative of c-Src) (Figure 5a). The overexpression of c-Src potentiates ERα transactivation both in basal condition as well as upon E_2, Fn and Col exposure. The expression of the dominant-negative c-Src as well as the treatment with PP2-abrogated ERE-mediated transcription induced by both Fn and Col, however, only attenuated the response to E_2. Altogether, these data suggest that c-Src is required for ERα activation by signals derived from cell adhesion to ECM. Under the same experimental conditions, we evaluated the autophosphorylation of c-Src and the phosphorylation of the exogenous substrate enolase (Figure 5b) after 5 min of exposure. The indicated time was chosen after a time course study (here not reported) performed at 0, 5, 10 and 20 min displaying the maximal enzymatic activity at 5 min. The results provide evidence that both E_2, Fn and Col activate c-Src, while either the expression of a dominant-negative c-Src or the presence of PP2 strongly reduces both the autophosphorylation of c-Src and the phosphorylation of enolase.

E_2, Fn and Col reduce cell motility

Since previous studies have shown that ERα expression leads to a lower matrigel invasiveness and to a reduced metastatic potential in breast cancer cells (Rochefort *et al*., 1998; Platet *et al*., 2000), we investigated whether

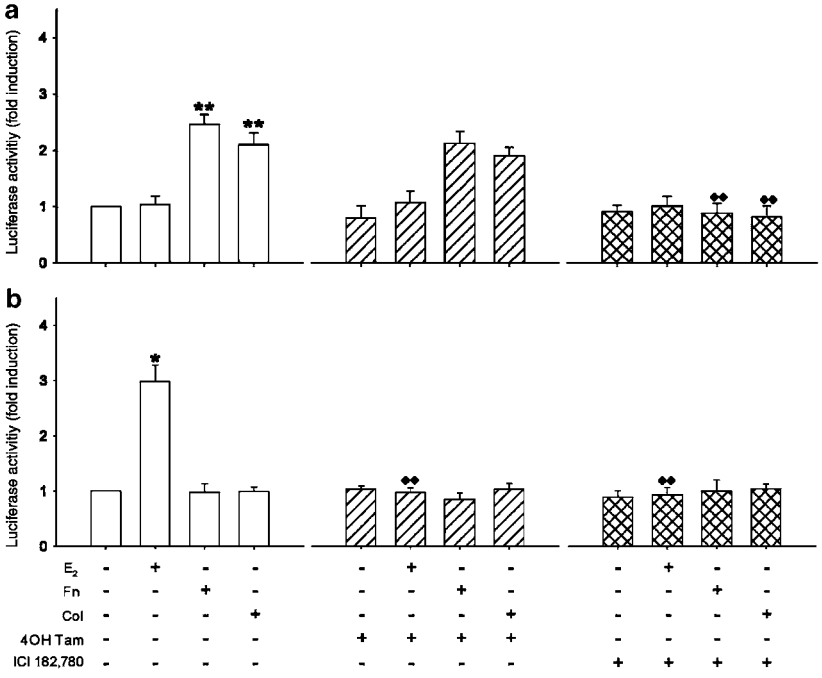

Figure 4 Fn and Col induce ligand-independent transcriptional activation of the ERα. HeLa cells were transfected with 0.3 μg/well HE15 and 0.6 μg/well XETL (**a**) or with 0.3 μg/well HE19 and 0.6 μg/well XETL (**b**). At 6 h after transfection cocktail addition, cells were shifted in PRF-SFM for 24 h and then incubated for 16 h in PRF-SFM containing either 15 μg/ml P-Lys, 10 nM estradiol (E_2), 30 μg/ml Fn or 30 μg/ml Col. The same treatments were also carried out in the presence of 100 nM 4-OH Tam and 100 nM ICI 182,780. Firefly luciferase activity was internally normalized to *R. luciferase* and expressed as fold of increase with respect to the PRF-SFM (untreated) samples. Results represent the mean ± s.d. of five independent experiments. $^{**}P<0.001$ and $^{*}P<0.01$ *vs* PRF-SFM (untreated); $^{\blacklozenge\blacklozenge}P<0.005$ *vs* the homologues samples without 4-OH Tam and ICI 182,780

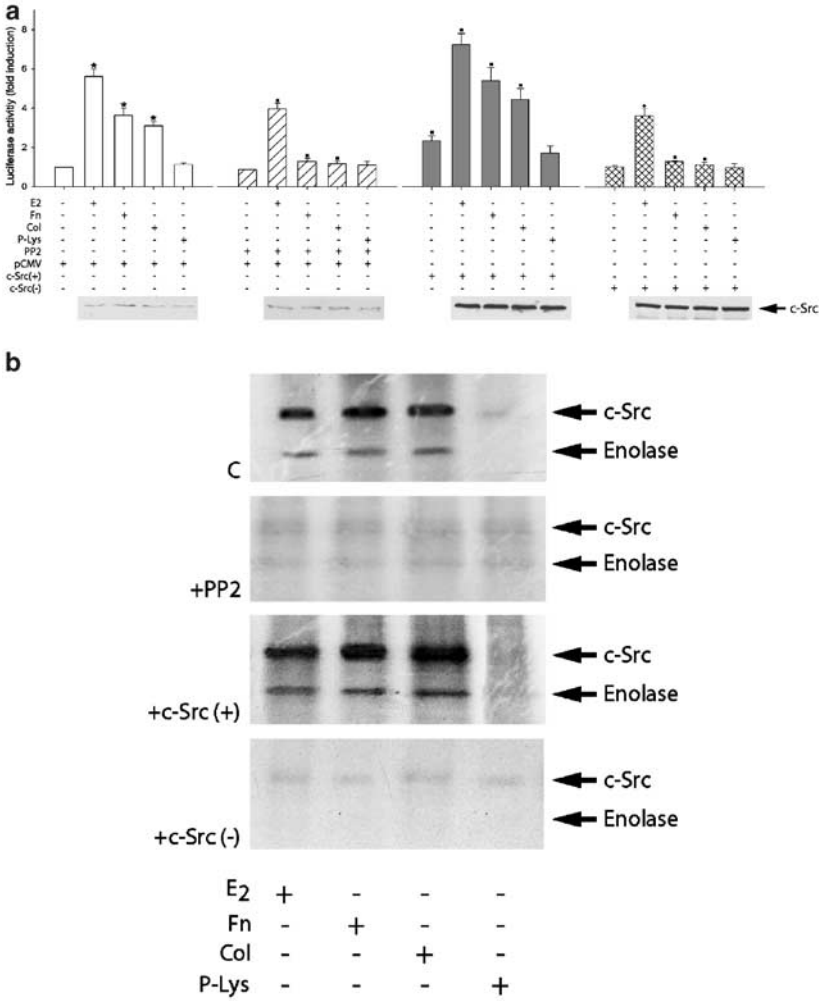

Figure 5 Fn and Col activate unliganded-ERα through c-Src. (**a**) MCF-7 cells were cotransfected with calcium phosphate precipitation method using 0.5 μg/well of XETL and 0.5 μg/well of pCMV empty vector or 0.5 μg/well of XETL plasmid with 0.5 μg/well of c-Src(+) or 0.5 μg/well of c-Src(−). At 6 h after transfection, cells were serum starved for 24 h and then incubated for 16 h in PRF-SFM (untreated) or PRF-SFM containing either 10 nM estradiol (E_2), 30 μg/ml Fn, 30 μg/ml Col or 15 μg/ml P-Lys. The same treatments were also carried out in the presence of 3 μM of PP2. Firefly luciferase activity was internally normalized to *R. luciferase* and expressed as fold of increase with respect to the PRF-SFM (untreated) sample. Results represent the mean ± s.d. of five independent experiments. The inset pictures present the expression of c-Src and were assessed by Western blotting as described in Materials and methods using 30 μg of total cell lysates. (**b**) MCF-7 cells, transfected and treated as before for 5 min, were lysed and immunoprecipitated with an anti c-Src antibody/protein A/G complex and assayed for c-Src-kinase activity using acid-treated enolase as described in Materials and methods. These results are representative of three independent experiments. ⋆$P<0.001$ *vs* the PRF-SFM (untreated); ■$P<0.01$ *vs* the homologues samples without PP2 and cSrc(−); ◆$P<0.05$ *vs* the homologues samples without PP2 and cSrc(−)

the activation of ERα by both ECM proteins was correlated with the motility of breast cancer cells. MCF-7, MDA-MB-231 and HeLa cells were used to evaluate cell invasion on Transwell chambers previously coated with Fn, Col or P-Lys and incubated overnight in PRF-SFM or in PRF-SFM containing E_2. In agreement with previous studies (Rochefort *et al*., 1998), E_2 treatment produced a marked reduction of cell migration in MCF-7 (Figure 6a) as well as in both MDA-MB-231 (data not shown) and HeLa cells expressing ERα (Figure 6b). Similar inhibition was observed after cell adhesion to either Fn or Col. To further clarify the contribution of the two ERα/AF domains in regulating cell motility, HeLa cells were transfected with either the AF-1- or AF-2-deleted constructs and plated onto transwells coated with both ECM proteins. Cells expressing the AF-1/DBD domains (Figure 6c) showed a strong reduction of cell invasion induced by both ECM proteins and reversed by ICI (data not shown). In contrast, only E_2 treatment reduced cell migration when the AF-2/DBD domains of the ERα were expressed (Figure 6d).

Fn and Col reduce cell motility through c-Src in breast cancer cells expressing ERα

Having established the role of c-Src in mediating ERα activation induced by cell adhesion to both Fn and Col, we examined its involvement in the regulation of breast

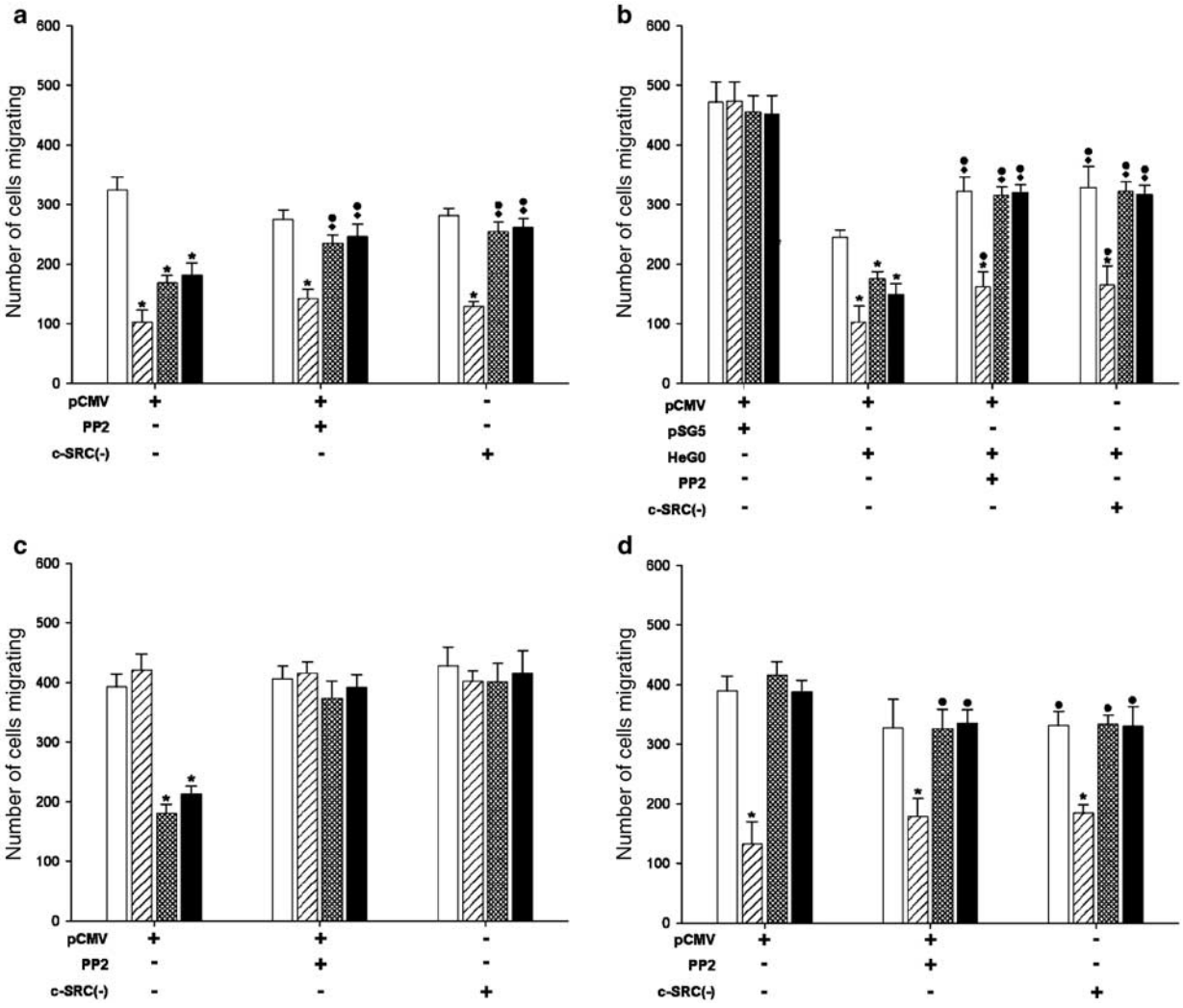

Figure 6 Cell adhesion on Fn and Col activate AF-1/ERα through c-Src reducing cell invasion. MCF-7 cells transiently transfected with 1 μg/well of c-Src(−) or pCMV (**a**) and HeLa cells transfected with 0.5 μg/well of the following plasmids; (**b**) pCMV and pSG5, pCMV and HeG0 or HeG0 and c-Src(−); (**c**) pCMV and pSG5, pCMV and HE15 or HE15 and c-Src(−); (**d**) pCMV and pSG5, pCMV and HE19 or HE19 and c-Src(−), after 6 h cells were serum starved for 24 h, detached, plated and allowed to migrate for 16 h on membranes coated either with 2 μg/cm² P-Lys (□) or 30 μg/ml Fn (⊠) or 30 μg/ml Col (■) or treated with 10 nM estradiol (▨). The effects induced by P-Lys, Fn, Col and E_2 on cell motility were also evaluated upon exposure to 3 μM PP2. Cells were then fixed, stained and the cells that migrated to the lower surface of the membranes were counted. The results represent the mean ± s.d. of four independent experiments. *$P<0.001$ *vs* P-Lys; •$P<0.001$ *vs* the homologues samples in vectors; ◆$P<0.05$ *vs* vectors/P-Lys

cancer cell motility. MCF-7, HeLa cells and HeLa expressing ectopic ERα as well as ERα deleted in the AF-1 or AF-2 domain were plated onto either Fn- or Col-coated membranes and incubated in the presence of PP2 or cotransfected with c-Src(−).

In MCF-7 (Figure 6a), the presence of either c-Src inhibitor or dominant-negative c-Src partially reverses the decrease in cell invasion caused by cell adhesion on both ECM proteins and, to a lesser extent, by E_2. In agreement with previous reports (reviewed in Summy and Gallick, 2003), the inhibition of c-Src elicits a slight decrease in both cell motility and invasiveness of about 20% ($P<0.05$) in wild-type HeLa cells (data not shown), while the ectopic expression of ERα induces a strong reduction in cell motility (Figure 6b), which appears emphasized by the adhesion on both ECM proteins, and is partially reversed by the inhibition of c-Src. Under the same circumstances, the dramatic reduction induced by E_2 still persists. Finally, the inhibition of c-Src with PP2 or the dominant-negative c-Src partially reverts the decrease on cell invasion induced by both ECM proteins in HeLa cells expressing the AF-1/DBD domains (Figure 6c). These data clearly show that c-Src is required for ligand-independent ERα-mediated reduction of breast cancer cell invasion.

Relationship between ERα and c-Src in mediating cell motility

It was previously demonstrated that elevated expression and/or activity of c-Src drastically increases motility, invasiveness and the metastatic potential of cancerous

cells (Summy and Gallick, 2003). To further clarify the role of ERα and c-Src in regulating cell motility, we transfected MDA-MB-231 with both HeG0 and Y527F, a constitutively active c-Src (Figure 7). The different levels of c-Src ectopically expressed in MDA-MB-231 cells does not induce substantial changes in cell motility, while the concomitant expression of ERα is sufficient to reduce cell motility. Namely, when ERα and active c-Src were expressed in a 4 : 1 ratio, a stronger reduction of cell motility was observed with respect to that obtained in cells expressing ERα alone. However, when MDA-MB-231 were transfected with ERα/c-Src using a 1 : 4 ratio, the reduction was partially reversed. These results indicate an opposite role for ERα and c-Src activity in regulating cell motility.

Nuclear localization of ERα is required to inhibit cell motility

Next, we questioned whether the nuclear localization of ERα is required for the reduction of cell invasion. With this aim, we tested cell invasion in HeLa cells transfected with either ERα or ERα in which serine 104, 106 and 118 were replaced by alanine residues (ER/Ser/A) and with the ERα lacking the NLS domain (E241G) in the presence of E_2, Fn and Col. In HeLa cells expressing the wild-type ERα E_2, Fn and Col induced a functional

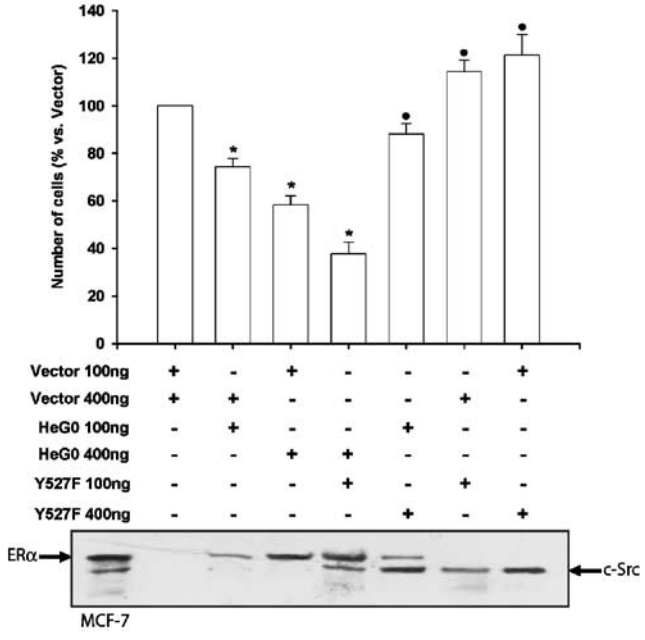

Figure 7 Relationship between ERα and c-Src in the regulation of cell motility. MDA-MB-231 cells were transfected, by calcium phosphate DNA co-precipitation method, using HeG0 and Y527F in a 4 : 1 or 1 : 4 ratio. The same plasmids were transfected either with pcDNA3 or pSG5 as vector of Y527F and HeG0, respectively. At 6 h after transfection, cells were serum starved for 24 h and then detached, counted and plated onto porous membranes in DMEM/F12 + 5% CS for 16 h. Cells were then fixed and stained, and cells which migrated to the lower surface of the filters were counted. The inset picture presents the expression of both ERα and c-Src in MDA-MB-231 cells after transfection. ERα and c-Src expression was assessed by Western blot as described in Materials and methods using 20 μg of total cell lysates. A measure of 20 μg MCF-7 cell lysates was used as positive control. The results represent the mean ± s.d. of three independent experiments. $^{*}P<0.01$ *vs* vectors, $^{\bullet}P<0.05$ *vs* vectors

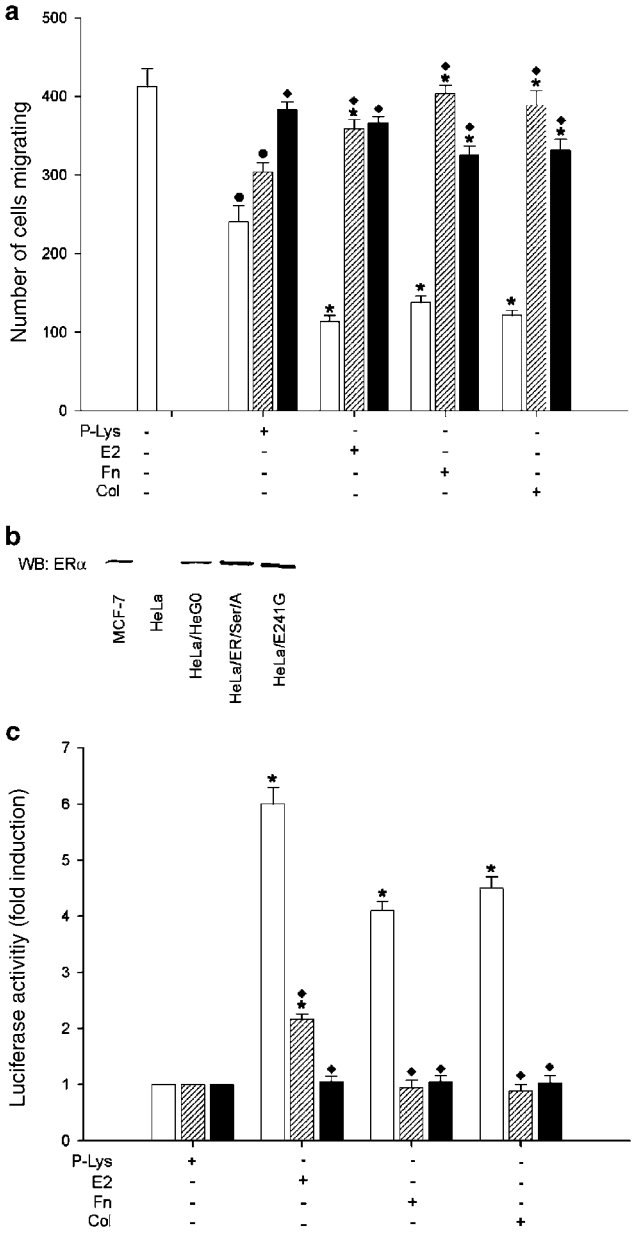

Figure 8 NLS and the AF-1 domain of ERα are required for ligand-dependent and -independent regulation of cell migration. HeLa cells were transfected with either HeG0 (□) or ER/Ser/A (▨) or E241G (■) by the calcium phosphate DNA co-precipitation method. After 6 h, cells were serum starved for 24 h and then detached and plated onto porous membranes coated either with 2 μg/cm² P-Lys, 30 μg/ml Fn (Fn), 30 μg/ml Col (Col) or treated with 10 nM estradiol (E_2) and incubated for 16 h, allowing cells to migrate. Cells were then fixed, stained and cells which migrated to the lower surface of the filters were counted (**a**). The inset picture presents the expression of ERα by Western blot after transfection (**b**). In the same experimental conditions, HeLa cells were co-transfected with either 0.3 μg/well HeG0, ER/Ser/A, E241G plus 0.6 μg/well of XETL (**c**). Firefly luciferase activity was internally normalized to *R. luciferase* and expressed as fold of increase with respect to the P-Lys samples. The results represent the mean ± s.d. of four independent experiments. $^{\bullet}P<0.01$ *vs* C0; $^{*}P<0.05$ *vs* the respective C; $^{\blacklozenge}P<0.01$ *vs* the respective treatment in HeG0

transactivation of ERα (Figure 8a) together with a dramatic reduction of cell invasiveness (Figure 8c). In the presence of ER/Ser/A, only E_2 induced a slight functional transactivation of ERα (Figure 8a), while none of the treatments produced substantial effects on cell invasiveness (Figure 8c). In HeLa cells expressing ERα deleted in the NLS region, the functional transactivation of ERα was abolished (Figure 8a), while just a slight decrease of cell invasiveness was observed after the cells adhesion on membranes coated with Fn and Col (Figure 8c).

Discussion

Several previous studies have indicated an important role for E_2 in decreasing '*in vitro*' invasiveness and motility of ERα-positive breast and ovarian cancer cells (Thompson *et al*., 1992; Hayashido *et al*., 1998; Rochefort *et al*., 1998). We found that cell adhesion on Fn and Col induces ERα translocation from the cytoplasm into the nucleus increasing the expression of estrogen-responsive genes, such as PS2 and cathepsin D, together with a downregulation of cell motility and invasion. Using ERα mutants lacking the AF-1 or the AF-2 region, we have provided evidence that both Fn and Col activate ERα in a ligand-independent manner as efficiently as the AF-2/ERα-mediated transcription induced by E_2.

It has been well documented that human ERα is phosphorylated by c-Src *in vitro* (Arnold *et al*., 1995) and that breast tumors, exhibiting an enhanced c-Src activity, frequently express a progesterone receptor. These findings raise the possibility that Src family kinases may contribute to the hormone dependence of tumor cell growth (Lehrer *et al*., 1989). In the same scenario, c-Src is able to transactivate the AF-1 domain of unliganded ERα partly through the ERK1/ERK2 signaling cascade and partly through the JNK signaling cascade (Feng *et al*., 2001).

Cell adhesion to ECM proteins induces the recruitment and activation of the FAK/c-Src kinase complex, which may be a crucial step in integrin-mediated signal transduction processes (Chen *et al*., 1994; Schlaepfer *et al*., 1994; Morino *et al*., 1995; Schlaepfer and Hunter, 1996). These findings well suit our data demonstrating that c-Src is activated by cell adhesion on both Fn and Col, leading to the functional transactivation of ERα with a concomitant reduction of cell invasion. Both ERα transactivation and the reduction of cell invasion, caused by both ECM proteins, were reversed by either PP2 or the expression of a dominant-negative c-Src. However, E_2 is still able to activate ERα with a reduction in cell invasion. These data strengthen previous findings demonstrating the existence of two distinct mechanisms through which ERα inhibits breast cancer cell motility according to its unliganded or liganded status (Platet *et al*., 2000). The ability of both ECM proteins to transactivate ERα via c-Src is not linked to specific factors present in breast cancer cells since it was reproduced in HeLa cells engineered to express ERα, ERβ (data not shown) and ERα deleted in the AF-2 domain. The expression of either ERα or AF-1/ERα is sufficient to reduce cell invasion that results enhanced by cell interactions with both Fn and Col. These data, taken together, address how A/B region of ERα is crucial for both ligand-independent transcriptional activation and the reduction of cell invasion induced by the two ECM proteins, thus confirming that the AF-2 domain may be dispensable for hormone-independent inhibition of cell invasiveness and motility (Platet *et al*., 2000).

C-Src is an effector of multiple protein tyrosine kinase signals, particularly active during the process of tumorigenesis (Summy and Gallick, 2003). For instance, the enhanced expression of c-Src in cells expressing elevated levels of EGF-R resulted in increased DNA synthesis, soft agar growth and tumor formation in nude mice (Maa *et al*., 1995). The sustained activation of c-Src, observed in mammary epithelial cells overexpressing Erb-B2 (Sheffield, 1998) and in TGF-α-induced mammary tumor cell line (Amundadottir and Leder, 1998), enhances the anchorage-independent growth of these cells. Activated c-Src in mammary tumors has been well studied in transgenic mice. Mice expressing viral polyoma middle T antigen under the control of the MMTV promoter produce highly metastatic mammary tumors with elevated c-Src kinase activity (Guy *et al*., 1994). Besides, mice overexpressing the *neu* oncogene also develop mammary tumors with 6–8-fold higher c-Src kinase activity than the adjacent normal tissue (Muthuswamy *et al*., 1994). Thus, it appears from the above reported findings that c-Src lies at the hub of a very complex network of signaling pathways, which integrate a variety of intracellular and extracellular events. Part of this network links the adhesion proteins to ERα, leading to the reduction of cell motility. The latter effect appears to be mediated at the nuclear level since it is abrogated in the presence of ERα deleted in the NLS. This strongly suggests that ERα may induce the expression of genes able to enhance cell adhesion and negatively control cell migration.

Importantly, it has been demonstrated that ERα activation upregulates fibulin-1, an Fn-binding ECM protein (Hayashido *et al*, 1998), while it decreases metalloproteinase 9 (Crowe and Brown, 1999) and type IV collagenase (Abbas Abidi *et al*., 1997), producing a decrease of cell migration. In other words, we have defined an autoregulatory loop linking ECM–integrin–FAK–c-Src signals to ERα. The output of this loop is dependent on the delicate balance between c-Src and ERα. However, this balance is distorted during tumorigenesis, resulting in a sustained marked activation of c-Src. When a continued activation on c-Src occurs, the balance of the autoregulatory loop between integrins–FAK–c-Src kinase and ERα may be over-ridden and the effect of constitutive active c-Src in enhancing cell migration and invasiveness becomes dominant. Indeed, we observed that the reduced cell migration induced by ectopic expression of ERα in MDA-MB-231 cells is reversed when c-Src content substantially exceeds that of ERα.

On the basis of our findings, it is reasonable to assume that a coordinate role between ECM proteins and ERα exists in controlling cell motility and cell metastatic potential in ERα-positive breast cancer cells. Even though several substrates of the FAK/c-Src complex have been recently identified (Cary *et al*., 1998; Klemke *et al*., 1998; Petit *et al*., 2000), the mechanisms whereby c-Src pathways regulate cell migration remain, however, to be fully elucidated.

Materials and methods

Cell lines and cell culture conditions

Two human breast cancer epithelial cell lines, MCF-7 (ER+) and MDA-MB-231 (ER−) and a *cervicae* carcinoma cell line HeLa (ER−) were used. MCF-7 and MDA-MB-231 cells were maintained in a monolayer culture in Dulbecco's modified Eagle's/Ham's F-12 medium (1 : 1) (DMEM/F12; Eurobio, F) supplemented with 5% calf serum (CS; Eurobio, F), 100 UI/ml penicillin (Eurobio, F), 100 μg/ml streptomycin (Eurobio, F) and 0.2 mM L-glutamine (Eurobio, F). HeLa cells were maintained in monolayer cultures in minimal essential medium (MEM) with Earle's salts (Eurobio, F) supplemented with 10% fetal bovine serum (Eurobio, F), 100 UI/ml penicillin, 100 μg/ml streptomycin and 0.2 mM L-glutamine. Cells were passed weekly using trypsin–EDTA (Eurobio, F) and media were changed every 2 days.

In all experiments, steroids and growth factors were withdrawn from cells, and were grown in phenol red-free DMEM (PRF-SFM; Eurobio, F) containing 0.5% BSA and 2 mM L-glutamine for 24 h.

Western blotting

To establish the influence of both ECM proteins on ERα protein expression, MCF-7 cells, serum starved for 24 h, were detached with versene (Eurobio, F), resuspended in PRF-SFM and plated for 30 min, 1 h, 4 h and 8 h on culture-coated wells with either 30 μg/ml Fn (Sigma, USA) in PBS or 30 μg/ml Col (Sigma, USA) in 10 mM acetic acid or 2 μg/cm^2 poly-L-lysine (P-Lys; Sigma, USA) in PBS. At the end of each incubation time, cells were washed with ice-cold PBS and lysed for 1 min at 4°C in Triton lysis buffer (50 mM HEPES (pH 7.5), 150 mM NaCl, 1.5 mM $MgCl_2$, 1 mM $CaCl_2$, 1% Triton X-100, 0.2 mM Na_3VO_4, 1% PMSF, 1% Aprotinin) for the cytosolic lysates and in SDS lysis buffer (62.5 mM Tris-HCl (pH 6.8), 50 mM dithiothreitol, 2% SDS, 10% glycerol, 0.2 mM Na_3VO_4, 1% phenylmethyl-sulfonylfluoride) for the total (cytosolic and nuclear) lysates. Cell lysates were cleared by centrifugation (14 000 r.p.m. for 10 min at 4°C) and the protein content was determined by the Bradford method. Cellular lysates (20 μg of protein/lane) were resolved by SDS–PAGE, then transferred to nitrocellulose membranes and probed with an ERα monoclonal antibody (F-10 clone; Santa Cruz Biotechnology, USA). The antigen–antibody complexes were detected by incubation of the membranes with peroxidase-coupled anti-mouse IgG and developed using the ECL Plus Western Blotting detection system (Amersham Pharmacia Biotech, UK).

Immunocytochemical staining

MCF-7 cells, serum starved for 96 h, were detached with versene, resuspended in PRF-SFM and plated either on 30 μg/ml Fn-, 30 μg/ml Col- or 2 μg/cm^2 P-Lys-coated wells, as described previously, or treated with 10 nM of E_2. After 2 h of incubation, the cells were fixed with paraformaldehyde (2% PFA for 30 min). Endogenous peroxidase activity was inhibited by hydrogen peroxide (3% in absolute methanol for 30 min) and nonspecific sites were blocked by normal horse serum (10% for 30 min). ERα immunostaining was then performed incubating the primary antibody (F-10 clone) overnight at 4°C, while a biotinylated horse-anti-mouse IgG was utilized at room temperature for 1 h as a secondary antibody. Avidin–biotin–horseradish peroxidase complex (ABC/HRP) was applied for 30 min and the chromogen 3-3′-diaminobenzidine tetrachloride dihydrate was then used as detection system for 5 min. TBS-T (0.05 M Tris-HCl plus 0.15 M NaCl (pH 7.6) containing 0.05% Triton X-100) served as a washing buffer. The primary antibody was replaced by normal mouse serum at the same concentration in control experiments on MCF-7-cultured cells (not shown).

Plasmids, transfections and ERE-luciferase assay

The reporter plasmid XETL drives the expression of luciferase by an ERE from the *Xenopus* vitellogenin promoter (Bunone *et al*., 1996). The SV40 promoter-based pSG5 vector encoding ERα (wild-type) pSG5-HeG0 (HeG0, Tora *et al*., 1989). The two deleted constructs of ERα, pSG5-HE15 and pSG5-HE19, code for a carboxyl-terminal truncated receptor (HE15, amino acids 1–281) and for the amino-terminal truncated receptor (HE19, amino acids 179–575), respectively (a gift from D Picard). The pcDNA3-ER-S104/S106/S118/A is an ERα derivative containing Ser 104, 106 and 118 mutated in Ala inserted in a pcDNA3 expression vector (ER/Ser/A; a gift from DA Lannigan). The pCMV-hE241G is a construct of ERα deleted in the nuclear localization signal (NLS) region (amino acids 250–303) and inserted in the pCMV expression plasmid (E241G; a gift from R Song). The empty expression vector, pCMV, and the same vector containing the c-DNA encoding the wild type of c-Src, pCMV-c-Src (c-Src(+)), and the dominant negative of c-Src, pCMV-cSrc-K295R,Y527F (c-Src(−)) were gifts from J Brugge and the active form of c-Src, pcDNA3-cSrc-Y527F, (Y527F) was a gift from DD Boyd. The *R. reniformis* luciferase expression vector used was pRL-Tk (Promega, USA).

To monitor the activation of ERα by ECMs, MCF-7 and MDA-MB-231 cells (5×10^4 density) were plated onto 24-well plates, grown in DMEM/F12 to an approximate confluence of 70–80% and then cotransfected with XETL and pRL-Tk (MCF-7) or XETL, HeG0 and pRL-Tk (MDA-MB-231). All the transfections were carried out using the calcium phosphate DNA co-precipitation method. Cells were transfected in a growing medium and 6 h after transfection were washed twice with PRF-SFM and switched to PRF-SFM for 24 h and then treated for 8 h either with 10 nM E_2, 30 μg/ml Fn, 30 μg/ml Col or 15 μg/ml P-Lys. The same treatments were carried out in the presence of either 100 nM ICI 182,780 (ICI; Zeneca, UK), 100 nM 4-OH-Tam (Sigma, USA) or 3 μM PP2, an inhibitor of c-Src (Calbiochem, USA). To evaluate which ERα functional domain was involved in ERα activation by ECMs, HeLa cells, cultured and treated as before, were cotransfected with pRL-Tk, XETL and HeG0, HE15 or HE19.

Firefly luciferase and *R. reniformis* luciferase activities were determined using the Dual Luciferase reporter assay system (Promega, USA) according to the manufacturer's instructions. Firefly luciferase activity was normalized to *R. reniformis* luciferase activity and expressed as relative luciferase units.

The influence of ERα and c-Src on cell motility was analysed in HeLa cells transfected with HeG0 and Y527F at different

concentrations (ratio 1:4 and 4:1). The same cells were transfected with HeG0 and pcDNA3 or Y527F and pSG5 using the same concentrations mentioned before. To evaluate if ERα acts at the nuclear level in mediating the induced effects of ECM/c-Src on cell motility, MDA-MB-231 cells cultured and treated as before were transfected, as described previously, with ERα mutated in some serine residues (ER/Ser/A, 10 μg/dish), or with ERα deleted in the NLS (E241G, 10 μg/dish).

RT–PCR

MCF-7 cells were incubated for 24 h in PRF-SFM and then detached and plated on coated or uncoated dishes with either 2 μg/cm² P-Lys, 30 μg/ml Fn or 30 μg/ml Col as described previously. The cells plated on uncoated dishes were treated both with and without 10 nM E_2. After 24 h, total cellular RNA was extracted using RNeasy (Quiagen, USA) and reverse transcribed using Moloney murine leukemia virus (M-MLV) reverse transcriptase (Promega, USA). Briefly, reverse transcription was performed on 1 μg of total RNA in a final volume of 10 μl by incubation at 37°C for 30 min with 200 U of M-MLV reverse transcriptase, 0.4 μg oligo-dT, 0.5 μM deoxynucleotidetriphosphate (dNTP) and 24 U RNAsin, followed by heat denaturation for 5 min at 95°C.

Subsequent PCR analysis was performed on 1 μl of the RT product in a final volume of 25 μl. The following pairs of primers were used to amplify the 210 bp of PS2: 5′-TTCTATCC-TAATACCATCGACG-3′ (PS2 forward) and 5′-TTTGAGTAGTCAAAGTCAGA-GC-3′ (PS2 reverse); the 304 bp of cathepsin D: 5′-AACAACAGGGTGGGCTTC-3′ (Cat forward) and 5′-ATGCACGAAACAGATCTGTGCT-3′ (Cat reverse). The amplification of the 408 bp of ribosomal RNA 36B4 was performed as control using the following primers: 5′-CTCAACA-TCTCCCCCTTCTC-3′ (36B4 forward) and 5′-CAAATCCCATATCCTCGTCC-3′ (36B4 reverse). The PCR mixture consisted of 1.25 U GoTaq DNA Polymerase (Promega, USA), 1 × PCR buffer (10 mM Tris-HCl, 50 mM KCl), 2.5 mM $MgCl_2$ and 0.2 mM each dNTP, 0.6 μM of each PS2 primer and 0.2 μM of each 36B4 primer and 0.6 μM of each cathepsin D primer and 0.2 μM of each 36B4 primer. PCR was performed for 20 cycles at 95°C/1 min, 59°C/2 min and 72°C/1 min. A measure of 10 μl of the PCR products were separated on a 1.2% agarose gel.

Immunoprecipitation and kinase activity of c-Src

To assay for c-Src kinase activity MCF-7 cells transfected, as reported in *plasmids and transfection* section, with c-Src(−), c-Src(+) or pcDNA3 were grown in PRF-SFM for 24 h and stimulated with either 15 μg/ml P-Lys, 30 μg/ml Fn, 30 μg/ml Col or E_2 10 nM for 5 min. Another set of cells, transfected with pcDNA3 and treated as before, were incubated with 3 μM PP2. Cells were then lysed with RIPA lysis buffer (500 mM Tris-HCl, 150 mM NaCl, 1% Triton X-100) containing 10 mM PMSF, 1.5 mg/ml aprotinin and 2 mg/ml leupeptin and immunoprecipitated. A Protein G–Agarose and an anti-c-Src antibody complex was prepared to immunopurify the lysates. A measure of 1 μg of mouse monoclonal anti-c-Src antibody (clone 327; Oncogene, USA) and 30 μl of protein G–agarose (Santa Cruz, Biotechnology, USA) were incubated at 4°C for 1 h in 500 μl of PBS with a tube rotator. The complexes were microfuged and washed with 1 ml of lysis buffer for three times. At the end, 500 μg of each cell lysates were added to the protein G–agarose/anti-c-Src antibodies and incubated at 4°C for 2 h rotating. The proteins/complexes were centrifuged and washed three times with the kinase buffer (200 mM PIPES, 100 mM $MnCl_2$). c-Src kinase activity was assayed by a standard *in vitro* kinase assay using acidified enolase as substrate. The incubation was performed in a total volume of 50 μl composed of the immunopurified c-Src protein and the kinase buffer containing 5 mM ATP, 1 μC of [γ^{32}P]ATP and 2.5 μg of acid denatured rabbit muscle enolase (Sigma, USA) as exogenous substrate. Samples were incubated at 30°C for 10 min then reduced with an equal volume of 2 × SDS Laemmli sample buffer (Sigma, USA) and aliquots of them (40 μl) were submitted to SDS–PAGE (acrylamide 11%). The dried gel was exposed to X-omat film (Kodak, USA) for 12 h. All gels were stained with Coomassie blue to ensure that an equal amount of enolase was present in all samples.

Motility assay

To evaluate the role of ERα on cell motility, the following cell lines were used: MCF-7, HeLa and MDA-MB-231 transfected as reported in *plasmids and transfections* section.

Cells maintained in PRF-SFM for 24 h were dispersed with versene (Eurobio, F), washed twice, resuspended in PRF-SFM and counted using a hemocytometer. The 24-well modified Boyden chambers, containing porous (8 μm) polycarbonate membranes (Costar, USA), were coated, on the internal surface, with either 30 μg/ml Fn, 30 μg/ml Col or 2 μg/cm² P-Lys by incubation at room temperature (Doerr and Jones, 1996). The lower chambers were loaded with 500 μl of PRF-SFM, while synchronized cells (2×10^4) suspended in 200 μl of PRF-SFM with or without 10 nM E_2 and/or 100 nM ICI were plated into upper chambers. Another set of cells, treated as before, was suspended in 200 μl of PRF-SFM with or without 10 nM E_2 and/or 3 μM PP2. After 16 h of incubation in 5% CO_2 at 37°C, the cells in the upper chamber were removed by a cotton swab, so that only cells that had migrated through the membrane remained. The membranes were then fixed and stained in Coomassie blue solution (0.25 g Coomassie blue, 45 ml water, 45 ml methanol, 10 ml glacial acetic acid) for 5 min, then each well was rinsed three times with distilled water. The migrated cells were determined using an inverted microscope.

Statistical analysis

All data were expressed as the mean ± s.d. (standard deviation) of at least three different experiments. Statistical significances were tested using Student's *t*-test or paired Student's *t*-test where appropriate.

Abbreviations

AF-1, estrogen receptor activation function 1; AF-2, estrogen receptor activation function 2; Col, type IV collagen; ECM, extracellular matrix; ERα, estrogen receptor alpha; ERβ, estrogen receptor beta; Fn, fibronectin; ERE, estrogen-responsive element; c-Src(+), c-Src; Src(−), dominant negative of c-Src.

Acknowledgements

We thank Dr Didier Picard for kindly providing XETL, pSG5-HeG0, pSG5-HE15 and pSG5-HE19 plasmids, Dr Joan Brugge for generously providing pCMV-cSrc-K295R, Y527F plasmid, Dr Douglas D Boyd for helpfully providing pcDNA3-c-Src/Y527F plasmid, Dr Deborah A Lannigan for kindly providing pcDNA3/ER-S104/S106/S118/A plasmid and Dr Robert XD Song for helpfully providing hE241G/pCMV plasmid. This work was supported by Grant 'AIRC 2001'.

References

Abbas Abidi SM, Howard EW, Dmytryk JJ and Pento JT. (1997). *Clin. Exp. Metast.*, **15,** 432–439.

Amundadottir LT and Leder P. (1998). *Oncogene*, **16,** 737–746.

Aplin AE and Juliano RL. (1999). *J. Cell Sci.*, **112,** 695–706.

Arnold SF, Vorojeikina DP and Notides AC. (1995). *J. Biol. Chem.*, **270,** 30205–30212.

Aronica SM, Kraus WL, Katzenellenbogen BS and Power RF. (1994). *Proc. Natl. Acad. Sci. USA*, **91,** 8517–8521.

Bunone G, Briand PA, Miksicek RJ and Picard D. (1996). *EMBO J.*, **15,** 2174–2183.

Cary LA, Han DC, Polte TR, Hanks SK and Guan JL. (1998). *J. Cell Biol.*, **140,** 211–221.

Chalbos D, Philips A, Galtier F and Rochefort H. (1993). *Endocrinology*, **133,** 571–576.

Chen Q, Kinch MS, Lin TH, Burridge K and Juliano RL. (1994). *J. Biol. Chem.*, **6,** 26602–26605.

Clark EA and Brugge JS. (1995). *Science*, **268,** 233–239.

Couse JF, Curtis SW, Washburn TF, Eddy EM, Schomberg DW and Korach KS. (1995). *Biochem. Soc. Trans.*, **23,** 929–935.

Crowe DL and Brown TN. (1999). *Neoplasia*, **1,** 368–372.

Doerr ME and Jones JI. (1996). *J. Biol. Chem.*, **271,** 2443–2447.

Feng W, Webb P, Nguyen P, Liu X, Li J, Karin M and Kushner PJ. (2001). *Mol. Endocrinol.*, **15,** 32–45.

Fraker LD, Halter SA and Forbes JT. (1984). *Cancer Res.*, **44,** 5757–5763.

Giancotti F and Ruoslahti E. (1999). *Science*, **285,** 1028–1032.

Guan JL. (1997). *Int. J. Biochem. Cell Biol.*, **29,** 1085–1096.

Guy CT, Muthuswamy SK, Cardiff RD, Soriano P and Muller WJ. (1994). *Genes Dev.*, **8,** 23–32.

Hayashido Y, Lucas A, Rougeot C, Godyna S, Argraves WS and Rochefort H. (1998). *Int. J. Cancer*, **75,** 654–658.

Hynes RO. (1990). *Fibronectins*. Springer: New York.

Ignar-Trowbridge DM, Pimentel M, Teng CT, Korach KS and McLachlan JA. (1995). *Environ. Health Perspect.*, **103,** 35–38.

Irby RB and Yeatman TJ. (2000). *Oncogene*, **19,** 5636–5642.

Joel PB, Traish AM and Lannigan DA. (1998). *J. Biol. Chem.*, **273,** 13317–13323.

Kaplan KB, Swedlow JR, Morgan DO and Varmus HE. (1995). *Genes Dev.*, **9,** 1505–1517.

Kato S, Endoh H, Masuhiro Y, Kitamoto T, Uchiyama S, Sasaki H, Masushige S, Gotoh Y, Nishida E, Kawashima H, Metzger D and Chambon P. (1994). *Science*, **270,** 1491–1494.

Klemke RL, Leng J, Molander R, Brooks PC, Vuori K and Cheresh DA. (1998). *J. Cell Biol.*, **140,** 961–972.

Lazennec G, Bresson D, Lucas A, Chauveau C and Vignon F. (2001). *Endocrinology*, **142,** 4120–4130.

Lehrer S, O'Shaughnessy J, Song HK, Levine E, Savoretti P, Dalton J, Lipsztein R, Kalnicki S and Bloomer WD. (1989). *Mt. Sinai. J. Med.*, **56,** 83–85.

Lin TH, Chen Q, Howe A and Juliano RL. (1997). *J. Biol. Chem.*, **272,** 8849–8852.

Liotta LA, Stracke ML, Aznavoorian SA, Beckner ME and Schiffmann E. (1991). *Semin. Cancer Biol.*, **2,** 111–114.

Lowell CA, Fumagalli L and Berton G. (1996). *J. Cell. Biol.*, **133,** 895–910.

Maa MC, Leu TH, McCarley DJ, Schatzman RC and Parsons SJ. (1995). *Proc. Natl. Acad. Sci. USA*, **92,** 6981–6985.

McGuire WL. (1986). *Cancer Surveys: Hormone Receptors Breast Cancer* Vol. 5. Bulbrook RD (ed). Oxford University Press: Oxford, pp. 527–536.

Miyamoto S, Teramoto H, Gutkind JS and Yamada KM. (1996). *J. Cell Biol.*, **135,** 1633–1642.

Morino N, Mimura T, Hamasaki K, Tobe K, Ueki K, Kikuchi K, Takehara K, Kadowaki T, Yazaki Y and Nojima Y. (1995). *J. Biol. Chem.*, **270,** 269–273.

Muthuswamy SK, Siegel PM, Dankort DL, Webster MA and Muller WJ. (1994). *Mol. Cell. Biol.*, **14,** 735–743.

Osborne CK, Hobbs K and Clark GM. (1985). *Cancer Res.*, **45,** 584–590.

Petit V, Boyer B, Lentz D, Turner CE, Thiery JP and Valles AM. (2000). *J. Cell Biol.*, **148,** 957–970.

Platet N, Cunat S, Chalbos D, Rochefort H and Garcia M. (2000). *Mol. Endocrinol.*, **14,** 999–1009.

Power RF, Mani SK, Codina J, Conneely OM and O' Malley BW. (1991). *Science*, **254,** 1636–1639.

Price JE, Polyzos A, Zhang RD and Daniels LM. (1990). *Cancer Res.*, **50,** 717–721.

Renshaw MW, Ren XD and Schwartz MA. (1997). *EMBO J.*, **16,** 5592–5599.

Rochefort H, Platet N, Hayashido Y, Derocq D, Lucas A, Cunat S and Garcia M. (1998). *J. Steroid Biochem. Mol. Biol.*, **65,** 163–168.

Schaller MD, Hildebrand JD and Parsons JT. (1999). *Mol. Cell. Biol.*, **10,** 3489–3505.

Schlaepfer DD, Broome MA and Hunter T. (1997). *Mol. Cell. Biol.*, **17,** 1702–1713.

Schlaepfer DD, Hanks SK, Hunter T and Van der Geer P. (1994). *Nature*, **372,** 786–791.

Schlaepfer DD and Hunter T. (1996). *Mol. Cell. Biol.*, **16,** 5623–5633.

Sheffield LG. (1998). *Biochem. Biophys. Res. Commun.*, **250,** 27–31.

Suen PW, Ilic D, Caveggion E, Berton G, Damsky CH and Lowell CA. (1999). *J. Cell Sci.*, **112,** 4067–4078.

Summy JM and Gallick GE. (2003). *Cancer Metast. Rev.*, **22,** 337–358.

Thompson EW, Paik S, Brunner N, Sommers CL, Zugmaier G, Clarke R, Shima TB, Torri J, Donahue S, Lippman ME, Martin GR and Dixon RB. (1992). *J. Cell. Physiol.*, **150,** 534–544.

Tora L, Mullick A, Metzger D, Ponglikitmongkol M, Park I and Chambon P. (1989). *EMBO J.*, **8,** 1981–1986.

Weigel N. (1996). *Biochem. J.*, **319,** 657–667.

Zhu X and Assoian RK. (1995). *Mol. Cell. Biol.*, **6,** 273–282.